Effects of Magnetic Field in Heavy-Ion Collision Phenomenology

By

ARITRA DAS

PHYS05201504023

Saha Institute of Nuclear Physics, Kolkata

A thesis submitted to the

Board of Studies in Physical Sciences

In partial fulfilment of requirements

For the Degree of

DOCTOR OF PHILOSOPHY

of

HOMI BHABHA NATIONAL INSTITUTE

March, 2021

Homi Bhabha National Institute

Recommendations of the Viva Voce Board

As members of the Viva Voce Board, we certify that we have read the dissertation prepared by **ARITRA DAS** entitled **Effects of Magnetic Field in Heavy-Ion Collision Phenomenology** and recommend that it may be accepted as fulfilling the dissertation requirement for the Degree of Doctor of Philosophy.

Date: 08.09.2021

Chair - Prof. Sukalyan Chattopadhyay

Pradip Kr. Roy

Date: 08.09.2021

Guide/Convener - Prof. Pradip Kr. Roy

Date: 08.09.2021

Co-Guide/Member 1 - Prof. Munshi Golam Mustafa

Date: 08.09.2021

Member 2 - Prof. Debasish Das

Date: 08.09.2021

Member 3 - Prof. Sourav Sarkar

Date: 08.09.2021

External Examiner - Prof. Saumen Datta

Final approval and acceptance of this dissertation is contingent upon the candidate's submission of the final copies of the dissertation to HBNI.

I hereby certify that I have read this dissertation prepared under my direction and recommend that it may be accepted as fulfilling the dissertation requirement.

Date: 08.09.2021
Place: Kolkata

Guide: Pradip Kr. Roy
Prof. Pradip Kr. Roy

STATEMENT BY AUTHOR

This dissertation has been submitted in partial fulfilment of requirements for an advanced degree at Homi Bhabha National Institute (HBNI) and is deposited in the Library to be made available to borrowers under rules of the HBNI.

Brief quotations from this dissertation are allowable without special permission, provided that accurate acknowledgement of source is made. Requests for permission for extended quotation from or reproduction of this manuscript in whole or in part may be granted by the Competent Authority of HBNI when in his or her judgement the proposed use of the material is in the interests of scholarship. In all other instances, however, permission must be obtained from the author.

Aritra Das

Aritra Das

Pradip Kr. Roy

Signature of the guide:

DECLARATION

I, hereby declare that the investigation presented in the thesis has been carried out by me. The work is original and has not been submitted earlier as a whole or in part for a degree / diploma at this or any other Institution / University.

Aritra Das

Aritra Das

Pradip Kr. Roy

Signature of the guide:

List of Publications Arising From This Thesis

Journal

1. "General structure of fermion two-point function and its spectral representation in a hot magnetised medium"

   Aritra Das, Aritra Bandyopadhyay, Pradip K. Roy, Munshi G. Mustafa

   Phys. Rev. D 97, 034024 (2018),

   [arXiv:1709.08365v2 [hep-ph]].

2. "Hard dilepton production from a weakly magnetized hot QCD medium"

   Aritra Das, Najmul Haque, Munshi G. Mustafa, Pradip K. Roy

   Phys. Rev. D 99, 094022 (2019),

   [arXiv:1903.03528v3 [hep-ph]].

Chapters in books and lectures notes N. A.

Conferences

- "Recent progresses in the "Dynamics of QCD Matter", Int. J. Mod. Phys. **E** 24 (2021) 2130001, [arXiv:2007.14959 [hep-ph]].

Others

3. "Neutral pion mass in the linear sigma model coupled to quarks at arbitrary magnetic field"

   Aritra Das, Najmul Haque

   Phys. Rev. D 101, 074033 (2020),

   [arXiv:1908.10323v2 [hep-ph]].

4. "Saha Ionization Equation in the Early Universe"

   Aritra Das, Ritesh Ghosh, S. Mallik

The Astrophysical Journal, Vol. 881, Page 40, (2019),
[arXiv:1812.10686v2 [hep-ph]].

Aritra Das

Aritra Das

Pradip Kr. Roy

Signature of the guide:

DEDICATIONS

Dedicated to my Mother and my Father

ACKNOWLEDGEMENTS

First of all, I would like to express my sincere gratitude to my supervisors Prof. Pradip Kr. Roy and Prof. Munshi Golam Mustafa, without their constant push and support it was not possible for me to complete this wonderful journey of five years and write this thesis. I would thank them for introducing me to this enriched field of heavy-ion collision and giving me all the freedom to explore the realms of this field. They were always there to bear my inconsistencies, foolishness and even audacities.

I acknowledge my senior Najmul Haque with whom I worked in a couple of projects. He trained me how to implement an idea successfully into a research paper and how to never lose hope during the time when things do not work. As we share a great personal bonding, I am always inspired by his hard work, dedication towards his duties not only in his academic life but also in his family. I am very grateful to him for teaching me numerical computations with Mathematica® and inviting me to NISER during those projects.

I sincerely thank my collaborator Prof. Samirnath Mallik for working with me and especially de-cluttering my concepts in thermal field theory. I am greatly motivated by witnessing his punctuality, honest dedication towards research and energetic nature even at his age.

I thank my seniors Aritra Bandyopadhyay, Chowdhury Aminul Islam, Arghya Mukherjee and Sovik Priyam Adhya. I learnt a lot about thermal field theory from Aritra Da. Aminul da was always there to boost my morale and helped me to broaden my views on life and to enrich my thoughts. I thank Arghya for patiently listening to my silly academic as well as non-academic questions. I am indebted to SPA for his warm welcome into his place when I visited Prague in 2018.

I would like to thank my junior Bithika and Ritesh for very good academic as well as non-academic discussions.

I cannot express how thankful I am to all the past and present scholars of 249, especially Suvankar da, Kuntal da, Shamik da, Arnab da, Biswarup da, Asim da, Rajarshi da, Wadut, Jhuma, Debabrata, Gourab, Pritam, Shamsul, for bearing my foolishness, stupidity, moody and touchy nature. We shared all sorts of emotion with each others that made our relationship to evolve beyond friendship. Without them, these years of my Ph.D life would be dull and boring. Those unending chatting of midnight, watching movies together, going out for dinner, celebration of birthdays, singing and dancing for no apparent reasons, playing guitar together helped me to relieve stress enormously. I shall always cherish Shamik da for motivating me in trying guitar, Pritam for cheering me up and giving me valuable advices, Gourab for helping me in emergency, Wadut for behaving like a crazy.

I would like to thank all the members of SINP, especially the members of HENPP division, with whom I have interacted directly or indirectly at some point of time. I expresses my deepest gratitude to all the members of MSA-1 hostel where I spent my entire PhD life. I shall always cherish those unending conversations, table tennis matches at midnight, watching movies together for the rest of my life. I would Like to thank Apurba, Bibhuti, Sajad, Rome da, Palash da, Biswajit da, Anshu da, Naosad da, Sukannya di, Shramana di, Maireyee di, Sudeshna di, Sourav da, Tapash da, Prashant, Snehal, Gourab, Arpita, Sangeeta, Moumita , Dibyashree, Satyabrata da.

I must thank my friend from my college life Bankim for the constant support when I was feeling low especially during the lock-down due to the outbreak of COVID-19 and for giving valuable advises. I am indebted to my friend Pallavi for supporting me and boost my morale during my PhD. Finally, I thank my parents for their constant love and support.

Aritra Das

Aritra Das

Contents

List of Tables

List of Figures

CHAPTER 1

Preliminaries of Heavy-Ion Collision

1.1 Introduction

Mankind were keen to find the answer of a simple but profound question from the beginning of human civilization— 'what are the basic states of matter?' In ancient times, it was believed that matter exists in four fundamental elements — earth, air, water and fire. As the advancement of science continued through different civilisations, the quest for the knowledge about the nature in a much more deeper level had been intensified progressively. As the science advanced, scientists and philosophers had identified basic thoughts regarding nature in a categorical manner as following

- What are the fundamental states and the constituents of matter?
- What are the fundamental interactions between them that govern their dynamics?

As per our current knowledge, the basic states of matter are — solid, liquid, gas and plasma. But there are plethora of others that are worth mentioning — conductors, insulators, superconductors, super-fluids, ferromagnets, spin-glasses and many more.

As of now, the fundamental interactions that governs the dynamics of matter are divided into four categories — electromagnetic, weak, strong and gravitational. The electromagnetic and weak interactions were later combined in the Standard model and called electroweak interaction. The most common interactions among the four is the electromagnetic interaction which is responsible for most of the phenomena, from contraction of muscle to explosion of dynamite, in our everyday life. It is the force felt by two electrically charged particle at some distance. The modern theory of electromagnetic interaction is quantum electrodynamics (QED). Next common one is the gravitational force which acts between the particles due to their masses. Other forces, e.g. weak and strong, have no role in our everyday life but are important deciders of various processes in nuclear and sub-atomic levels. Weak force is the force that is responsible for the beta decay and other phenomena. Strong force is the force that binds the constituents of nucleus together. The strong force is the strongest among them whereas the gravitational force is most feeble one.

So far, it is established that modern elementary particle physics deals with the constituents of matter and their interactions. The fundamental particles can be grouped together into two catagories based on their intrinsic spin— fermions (leptons and quarks with there corresponding anti-particles) with half-integer spin and bosons (gauge bosons like photons, gluons, $W^{\pm}$, Z and Higgs bosons) with integer spin. The fundamental constituents of matter are leptons (electron, muon, tau) and quarks (up, down, strange, charm, beauty and top) with their corresponding antiparticles which are all fermions. Their interactions are mediated through bosons which are called mediators. In table 1.1, we have listed the fundamental interactions with their corresponding mediators. Now, free quarks are not observed in nature. They are combined to form mesons (a pair of quarks and anti-quarks) and baryons (a combination of three quarks). In this dissertation, we shall focus on phenomena

Interaction	Theory	strength	Mediator
Strong	Quantum Chromodynamics	1	Gluons
Weak	Quantum Flavourodynamics	10^{-13}	$W^{\pm}$ & Z bosons
Electromagnetic	Quantum Electrodynamics	10^{-2}	Photons
Gravitational	Quantum Gravity	10^{-38}	Graviton

Table 1.1: Fundamental interactions with their corresponding theory strength and mediators

related to strong interactions. In the next section, some of the properties of strong interactions will be discussed in a nutshell.

1.2 Quantum Chromodynamics

The modern theory of strong interaction is quantum chromodynamics (QCD) [1, 2]. It describes the interactions between fundamental partonic degrees of freedoms (D.O..F), i.e., quarks and gluons. The Lagrangian of QCD for N_c colors and N_f flavours is written as

$$\mathcal{L}_{\mathsf{QCD}} = -\frac{1}{4}G_a^{\mu\nu}G^a_{\mu\nu} + \sum_f \bar{\psi}_f \left(i\not{D} - m\right)\psi_f \tag{1.1}$$

Here ψ_f is the $4N_c$ dimensional quark spinor, $G^a_{\mu\nu}$ is strength tensor defined as

$$G^a_{\mu\nu} = \partial_\mu A^a_\nu - \partial_\nu A^a_\mu + g f_{bca} A_{\mu^b} A^c_\nu, \tag{1.2}$$

$D_\mu = \partial_\mu - igT_a A^a_\mu$ is the covariant derivative, g is the strong coupling constant, A^a_μ's are non-abelian gauge fields with $a\big(=1,2,\cdots,N_c^2-1\big)$ being the color representation. T_a's are the generators of $SU(N_c)_c$ group satisfying the group algebra $[T_a, T_b] = if_{abc}T_c$. The third term on the right hand side in Eq. (1.2) is responsible for the interactions of gluons among themselves. Due to the self interactions of gluons, the vacuum of QCD behaves differently from that of QED. In QED, the vacuum fluctuations are responsible for screening of electric charge of electrons which is similar to the charge screening in dielectric medium. But due to the presence of gluon-gluon interactions, color charges get anti-screened. As a result, the QCD coupling constant decrease with the increase of probing energy (shown in Fig. 1.1). This unique phenomena is the *asymptotic freedom* [3–5].

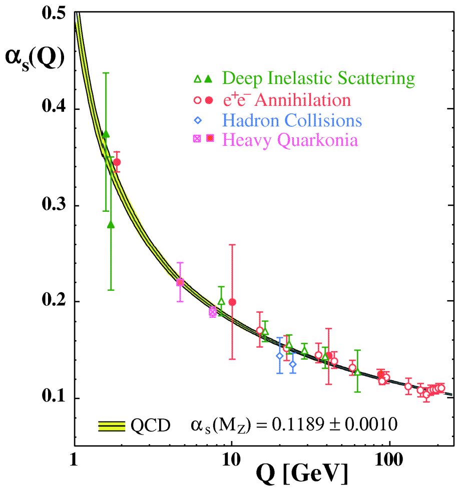

Figure 1.1: The strength of QCD coupling constant $\alpha_s(Q)$ with probing energy scale Q. The Fig. is taken from [7]

Another important property that strong interaction exhibits is color-confinement [8]. It is responsible for the fact that color charged particles are not directly observed in the nature. There is no analytical proof suggesting that QCD should be confining and the reason for this confinement is not yet understood completely. QCD provides a satisfactory description of strong interactions in high energy regime or short distances when the appropriate D.O.F are quarks and gluons. As coupling constant becomes very small due to the asymptotic freedom, perturbative formalisms can be employed in calculating various observables. But as coupling constant becomes large in the low energy limit, perturbative treatment completely breaks down. As a result, it cannot be predicted analytically how quarks and gluons can confine inside a hadron. In this situation, various effective models, which are based upon the underlying symmetries of QCD, are employed to understand confinement and low energy dynamics. Lattice quantum chromodynamics (LQCD) [6] is the first principle numerical calculations in non-perturbative regime both at zero and non-zero temperature. But it suffers from infamous sign problem at finite chemical potential [9, 10]. The infamous sign problem is related to the fact that the regular Monte Carlo simulation can be applied only when μ is either zero or purely imaginary. For real μ the fermion determinant is not real and the regular Monte Carlo fails. Also, it takes a substantial amount of computational power and time for execution.

1.3 What is Quark Gluon Plasma (QGP)?

The quarks and gluons are confined inside hadrons in ordinary matter. Their interaction is governed by the strong force. As discussed in the previous section, when the energy is increased the strength of the coupling constant decreases. Theoretically, if one increases the energy of a system comprising of hadrons, at one point quarks and gluons inside the hadrons will leave the hadronic volume and roam around a larger volume in quasi free state. This particular phenomena is called de-confinement and the created new state of matter is called Quark Gluon Plasma (QGP) [11, 12].

The QGP can be achieved in two possible ways — at high temperature and/or high density. If the QCD vacuum is gradually heated beyond a certain temperature, then the similar sized hadrons will start to overlap. After crossing a critical temperature, the constituents of the hadrons a.k.a quarks and gluons will no longer be confined inside the hadrons and will form QGP (shown in Fig. 1.2). Similarly, when the density of a hadronic system is increased beyond a critical baryon density via compression, the quarks and gluons are forced to lose their individual hadronic identity to form QGP (shown in Fig. 1.3).

Now, QGP is assumed to exist in the following cases:

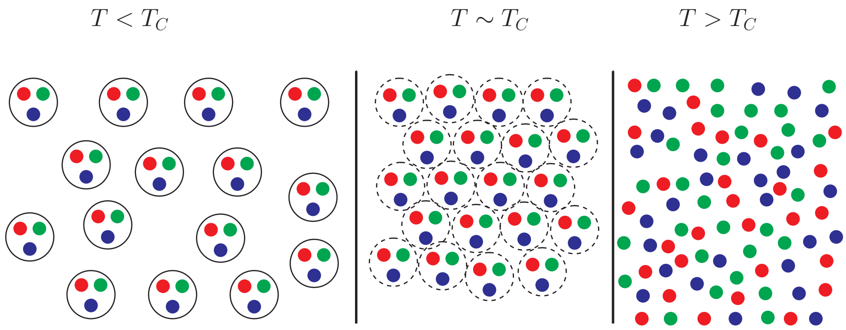

Figure 1.2: Creation of QGP at high temperature

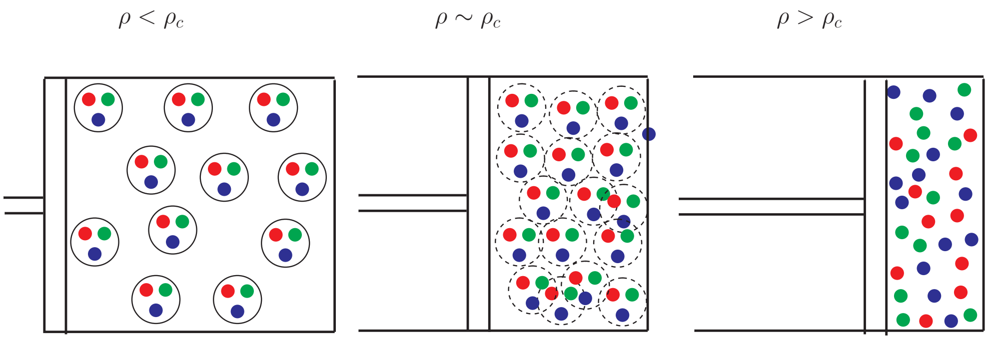

Figure 1.3: Creation of QGP at high densities

1. Few microseconds after the Big Bang, the temperature (estimated as 10^{12} K or 200 MeV) of the Universe was much greater than the critical temperature. Thus, in the 'Particle Era' during the evolution of the Universe, a transient QGP state was likely to be present.

2. In the core of the neutron stars, the density is believed to exceed 10^{15} gm/cm^3 (few times of that inside nucleus) with the temperature at the surface as low as 10^5 K or less.

3. In high energy collision between two heavy nuclei a transient state of QGP is predicted to be created.

The big bang is far remote in time and terrestrial 'laboratory' like neutron stars is far remote in space. So it is impossible to access to study the QGP properties. These situations make the high energy Heavy Ion Collisions (HIC) (also known as 'little bang') the only viable option to study QGP in the laboratory.

1.4 QCD Phase Diagram

The ultimate goal of high energy HIC is to explore the phase diagram of hot and dense strongly interacting matter. The first conjectured phase diagram [13] is depicted in Fig. 1.4(a). As time passed, it became very complicated with more investigations and looked like Fig. 1.4(b). The most general QCD phase diagram is drawn in the the space of all the possible parameters (temperature(T), baryon chemical potential (μ_B), isospin chemical potential (μ_I), quark masses ($m_u, m_d, \cdots$) and others) of the strongly interacting matter. But it is widely explored only in $T-\mu_B$ plane.

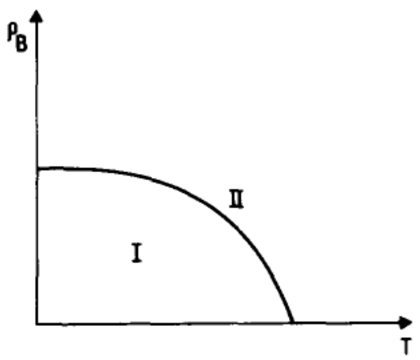

(a)

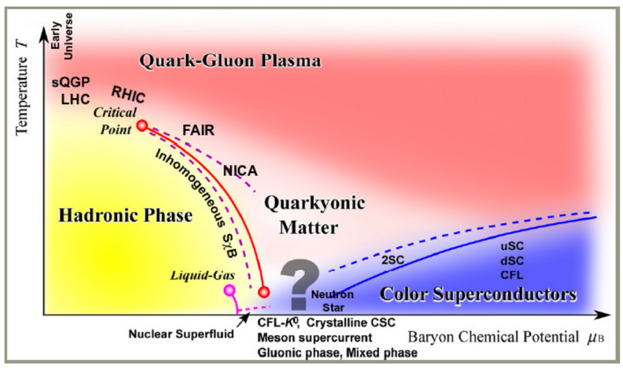

(b)

Figure 1.4: Schematic diagram of QCD phase transition — a) The initially conjectured diagram (taken from [13]), b) The modern version

The $\mu_B = 0$ is well explored by LQCD studies. The Early LQCD related the energy density (ε) to the pressure (p), i.e. the equation of state (EoS) at $\mu_B = 0$ in the temperature range $100 - 1000$ MeV. Around $T = 160$ MeV, both pressure and energy density were seen to rise (Fig. 1.5(a) and Fig. 1.5(b)) which indicated the change of effective D.O.F from hadrons to quarks and gluons. This phenomena is formally identified as *confinement-deconfinement* phase transition. With the advancement of LQCD studies, it has been established that confinement-deconfinement transition is not a phase transition in true sense but rather a rapid *cross-over* [14].

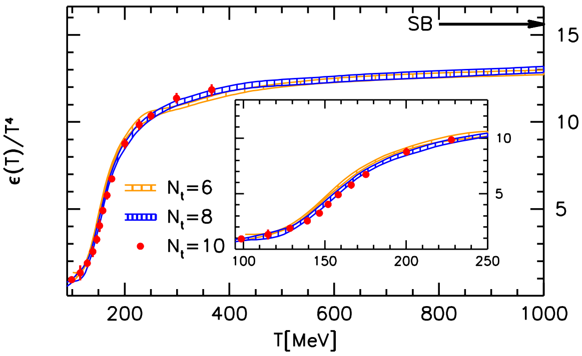

(a)

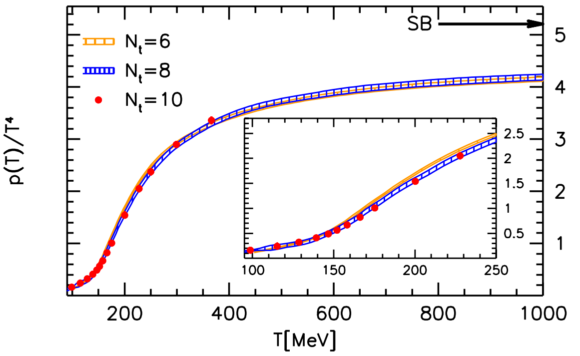

(b)

Figure 1.5: a) Energy density and b) pressure normalized by T^4 as a function of temperature (T) on $N_t = 6, 8$ and 10 lattices. N_t is the number of lattice points in the temporal direction. In the high temperature limit, the EoS approaches to $\varepsilon = 3P$ which is expected for massless particles. However, it is 20% less than ε_{SB} in the Stefan Boltzman (SB) limit of non-interacting ideal gas (Consistent with holography [15] based estimation for strongly coupled plasma). The arrows in the upper tight corner indicates SB limits. Figure is taken from [30].

Now, at finite baryo-chemical potential, LQCD suffers from systematic uncertainties and the infamous sign problem which restricts the standard Monte Carlo simulation to the case where either $\mu_B = 0$ or μ_B is purely imaginary. To circumvent this problem, a number of methods were employed. A Taylor series expansion [16–20] of the observables at $\mu_B = 0$ and an analytic continuation [21, 22] from imaginary to real μ_B are worth mentioning. From these, it can be concluded that the transition from Hadronic phase to QGP is crossover upto the region where $\mu_B/T \gtrsim 2$ [9]. But beyond this regime, LQCD cannot provide reliable information on phase transition. So the QCD phase diagram at high baryon density still vastly remains unexplored from first principle calculations. From the theory of effective models, there is a strong evidence of first order phase transition near high baryon density. The chiral models suggests a critical point (T_c, μ_c) in the phase diagram. When $\mu_B > \mu_c$, the crossover becomes first order chiral phase transition [23–26]. The first order phase boundary ends at another critical point at (T_F, μ_F). In very low temperature and high density region along the μ_B axis, there are strong theoretical evidences of color superconducting (CSC) phase [27–29] which occurs due to the attractive interactions between two quarks at the Fermi surface. Then, by Cooper's theorem, cooper pairs are formed by these quarks in the ground state of QCD. This phenomena is analogous to electrons in metals.

The current or bare mass of u and d quarks are as low as 5 MeV. But when they form the lowest mass hadrons, e.g. pions, the mass of the hadrons turns out to be of the order of 1 GeV. As a result, the constituent quark mass (obtained by dividing the hadron mass by number of valance quarks) $M_f \sim 300$ MeV is bigger than current or bare quark mass $m_f \sim 0$. The reason behind this phenomena is the dressing of quarks with gluons in QCD non-perturbative vacuum. Now, we know that the dynamical origin of mass is spontaneous symmetry breaking. QCD at $m_f = 0$ is chirally symmetric. So, $M_f \neq 0$ implies spontaneous breaking of chiral symmetry whereas, $M_f \to 0$ corresponds to the restoration of chiral symmetry. Thus, there appears a phase transition called *chiral phase transition* in going from a state of relatively heavy constituent quark phase to light bare or current quark phase at high temperature and/or density.

Some exotic phases, like quarkonic phase [31, 32], chirally symmetric but confined phase [33, 34], are believed to exist if the chiral and de-confinement phase transition does not coincide.

In this dissertation, we shall focus on the high temperature quark-gluon plasma phase.

1.5 Overview of Heavy Ion Collisions

The idea of creation of hot equilibrated nuclear matter in ultra-relativistic collision was first conveyed by Fermi [35], Landau [36] and Hagedron [37]. With time, technology developed and as a result high energy regions were accessible to the particle accelerator.

The first experimental heavy ion programme began at Bevelac facility in Lawrence Berkley National Laboratory (LBNL) around early seventies [38, 39] when collective phenomena were first observed [40]. Next, the energy of the colliding ions was increased at the Alternating Gradient Synchrotron (AGS) at Brookhaven and at Super-Proton Synchrotron (SPS) at European council for Nuclear Research or "Conseil Européen pour la Recherche Nucléeaire" (CERN). The measurements in low energy regime were performed at Schwerionensynchrotron (SIS) at Gesellschaft für Schwerionenforschung (GSI), Darmstadt. The experimental program at Relativistic Heavy Ion Collider (RHIC) has been initiated in the year 2000 which took data at $\sqrt{s_{NN}} = 8 - 200$ GeV. At $\sqrt{s_{NN}} = 200$ GeV, a large coherence in the created system was observed which was not achievable from mere one to one nucleon nucleon collision [41, 42]. The energy density ε overshoots $1\,\mathrm{GeV/fm^3}$ which is predicted by LQCD if QGP is formed [43]. The November-December month of the year 2010 marked the starting of a new era when lead-lead $(Pb + Pb)$ collisions at $\sqrt{s_{NN}} = 2.76$ TeV took place at Large Hardron Collider (LHC) at CERN. The LHC experiments provided improved statistics and larger kinematic range for observables. The highest energy achieved in HIC experiments at LHC was $\sqrt{s_{NN}} = 5.02$ TeV in $Pb + Pb$ collisions and $\sqrt{s_{NN}} = 5.44$ TeV in Xenon-Xenon $(Xe + Xe)$ collisions.

Two heavy ions are accelerated in ultra relativistic speed directed towards each other inside the beam pipeline. Each incident nucleus, which can be looked upon more precisely as color-glass-condensate [44], gets Lorentz contracted in the direction of their propagation. The diameter of the disc is roughly about 14 fm and its thickness is about $14/\gamma$ fm, where $\gamma = 1/\sqrt{1-\left(\frac{v}{c}\right)^2}$ is the relativistic factor, v is the speed of the nucleus for Au and Pb nucleus. The kinetic energies of the incoming nuclei are lost and deposited in the region where they overlap. The nucleons in this region take part in collisions and are called participant. The constituents of the nuclei that do not participate in collision are called spectators. The spectators play a crucial role in the creation of high magnetic field in HIC which will be explored later in section 1.7.

Depending on the the collisional energy $\sqrt{s_{NN}}$, there are two situations that arises.

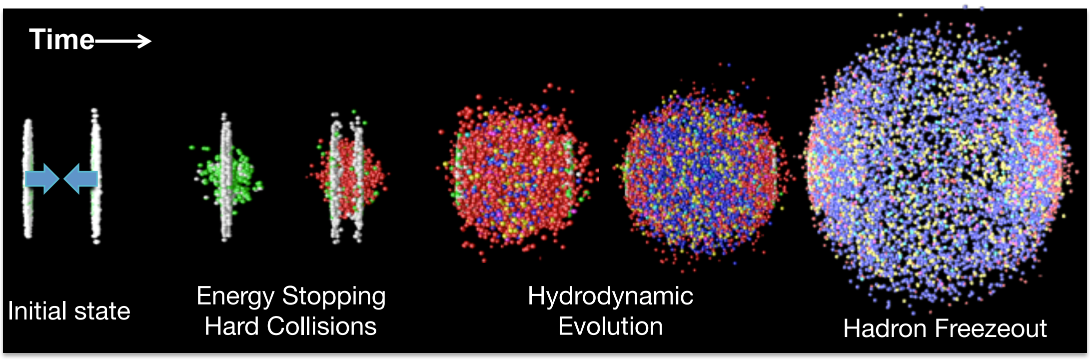

Figure 1.6: Evolution of a HIC. Figure is taken from [45]

- When the collisional energy $\sqrt{s_{NN}}$ is low ($\sim$ 10 GeV/ nucleon), the incoming nuclei lose almost all of their kinetic energy and the participating nuclei stop each other in the process of collision. As a result of this, nuclear matter with very high baryon density is created at the center. It mimics the conditions at the core of the neutron stars where the baryon density exceeds that of the nuclear density present in ordinary matter. The future Compressed Baryonic

Matter (CBM) [46] experiment at Facility for Anti-proton Ion Research (FAIR) at GSI, Darmstadt will explore the phase diagram of QCD at very high baryon density and low temperature.

- At larger energies, owing to the asymptotic freedom, the interactions between partons become weak and as a result the collision becomes transparent i.e. the nuclei pass through each other. In this case the density of the created medium becomes low but the temperature becomes very high.

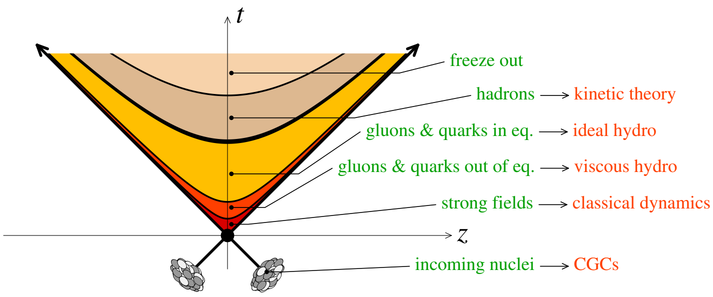

Figure 1.7: Schematic diagram of the different stages of HIC as a function of the coordinate z (the collision axis) and time t. The 'time' variable used is the proper time $\tau = \sqrt{t^2 - z^2}$ and it is constant along the hyperbolic curves separating different stages. Taken from [47]

In HIC, the system passes through different phases while colliding which are given below

1.5.0.0.1 Pre-equilibrium: At relativistic energies when the two nuclei collides with each other, a fireball is produced in highly excited state as a result of initial partonic collisions. It is evident that initially the fireball is in non-equilibrium state. The constituents of the fireballs collide with each other and reach thermal equilibrium state. The time taken to reach thermal equilibrium is called thermalization time. Models like color-glass condensates (CGC) [48, 49] are used to describe the states before thermal equilibrium.

1.5.0.0.2 Expansion: After the establishment of local thermal equilibrium stage, the constituents of the fireball, i.e., quarks and gluons are in deconfined state. After this, the system undergoes a collective expansion in all direction due to the thermal pressure that acts against the surrounding vacuum. This collective expansion of the system is surprisingly well described by hydrodynamic models [50–54]. As the system expands, it cools down and energy density decreases. When it goes below a critical temperature, a phase transition happens and the system eventually hadronizes.

1.5.0.0.3 Freeze-out: After hadronization, the constituents still collide with each other and maintain local thermal equilibrium. Eventually inelastic collisions between hadrons ceases and as a result the chemical compositions of produced hadrons do not change [55]. This stage is called *chemical freeze-out*. After attaining chemical freeze-out, the system further expands and cools with fixed hadron abundances. The local equilibrium can still be maintained after chemical freeze-out due to the occurrence of elastic collisions between hadrons. Then at one stage, the hadron gas becomes so dilute that even the mean free path between the constituents becomes greater than the dimension of the system. As a result, the local equilibrium cannot be maintained further and hydrodynamic description of the system completely breaks down. This stage is called *kinetic freeze-out*. Hadrons coming out from the kinetic freeze-out surface are detected in the detector. The particle yield can be described to a high degree of accuracy by thermal statistical models [56–59].

The pictorial representation of the evolution is schematically displayed in Fig. 1.6.

1.6 Probes of QGP

The production and most importantly the detection of QGP at RHIC and LHC is very formidable task. The acceleration of heavy nuclei taking part in collision at ultra-relativistic speed requires very high energy. Not all of the events in the collisions can produce QGP state. The production of QGP state depends on the depletion of energy in the central region of collision which in turn depends on impact parameter of the collision. The QGP state, if produced, is very transient in nature. So it is impossible to perform any direct measurement on it to gain informations about it's properties. The only data that is accessible to the experimentalists is the number of the clicks on the particle detector. In this circumstances, the information regarding the hot de-confined matter is extracted by observing the spectra of different particles that come out of the fireball. The probes can be broadly categorized as

- Anisotropic flow,
- Electromagnetic probes
- Quarkonia dissociations
- Jet-energy losses
- Strangeness enhancements and etc.

Below, we briefly outline the basic ideas behind exploiting the above phenomena to our advantages in gathering information about the hot and dense nuclear medium

1.6.1 Anisotropic Flow

After the collision and the confinement-deconfinement phase transition at $T_c \simeq 160 - 180$ MeV, when thermal medium hadronizes all the direct information about the initial stages are lost. But a global hydrodynamic flow [61, 62] is generated which gives an additional boost in overall momentum, if the early medium, formed after the collision, posses a very high energy density and can expand freely. The produced hadron spectra show a radial flow depending on the initial energy density of the medium. If, on the other hand, the collision is non-central between the participating nuclei, then a further directed (v_1), elliptic flow (v_2) and/or higher order harmonics ($v_3, v_4, \cdots$) are observed [63,64]. v_n echoes the re-scattering among the constituents after collision. The initial spatial anisotropy in the overlap zone creates an anisotropy in the pressure gradient in the transverse plane which, in turn, will cause momentum anisotropy in the produced particles. If the particles do not interact with each other, the azimuthal momentum distribution will be isotropic. Thus, the anisotropic flow coefficients v_n indicates the "degree of thermalization" of the QGP medium. So the bottom line is that the spatial anisotropy is converted into momentum anisotropy via rescattering of produced particles and it is these rescattering processes which thermalizes the system. For a comprehensive analysis of anisotropic flow in HIC and interpretations, see [65,66].

1.6.2 Electromagnetic Probes

Photons and lepton-antilepton pairs or dileptons(e^+-e^- and μ^+-μ^-) play prominent role as a probe of QGP. They interact with the system only electromagnetically and their mean free path is larger than the size of the fireball ($\sim$ 10 fm) [67,68]. Since electromagnetic fine-structure constant is much much less than strong coupling constant ($\alpha_{\mathsf{em}} \ll \alpha_s$), the photons and dileptons can escape the fireball with very negligible final state interaction [69]. The situation is different for the case of hadrons. Hadrons interact strongly with the system during its evolution and as a result they lose initial informations about the system. So looking at the spectrum of photons and dileptons, one can extract informations about the state of the medium at the space-time coordinate of their formation [70]. But there is a problem in extracting informations from the spectrum of electromagnetic radiations. The most prominent among them is the fact that photons and dileptons are produced in all stages of nuclear collision including initial hard scattering before the formation of the medium and in hadronic decays. So, all these background contributions has to be subtracted to gather informations about the hot deconfined media.

1.6.3 Quarkonia Dissociation

Quarkonia are essentially bound states of heavy quark and antiquark pair $\bar{Q}Q$. By the term heavy in this context, we usually indicate charm c and bottom b quark. The mass of charm and bottom quarks are given by $1.2-1.5$ GeV and $4.5-4.8$ GeV. The quarkonia J/ψ is the bound states of charm anti-charm ($\bar{c}c$) pair with mass $M_{J/\psi}=3.1$ GeV and Υ is the bound state of bottom anti-bottom ($\bar{b}b$) pair $M_{\Upsilon}=9.5$ GeV, respectively. In nucleus nucleus collisions, quarkonia are formed at the early stage of the collision before the formation of the deconfined QGP medium. In the medium, there is screening of color charge of quarks due to presence of quarks, antiquarks and gluons. It is called *color screening*. Similar to the Debye radius of QED plasma, there is a temperature dependent color screening radius $r_D(T)$. It decreases with the temperature. When $r_D(T)$ becomes less than the binding radius r_i of $\bar{Q}_iQ_i$, the quarkonium i dissociates as they can no longer bind together [73–76]. This phenomena leads to the suppression of quarkonium production in high energy nucleus nucleus $(A+A)$ collisions as compared to proton-nucleus $(p+A)$ or proton-proton $(p+p)$ collisions if the QGP is formed. This provides us with a first-hand signature of the deconfined hot medium. The quarkonium dissociation points T_i are determined through $r_D(T_i)\simeq r_i$. From this, a lower bound of the temperature and energy density of the deconfined medium can be extracted. In this way the quarkonium suppression acts as a signature and a thermometer of the QGP medium.

1.6.4 Jet Energy Loss

As mentioned previously, in HIC before thermalisation and formation of the medium, initial hard parton scattering processes take place. In $A + A$ collision where a thermal medium is formed, the scattered partons pass through the medium before converting into jets of hadrons that eventually reach the detector. In this process, the scattered partons lose their energy while traversing through the medium mainly via collisions with the quasi-particles of the medium and gluon radiations [77]. But in $p + p$ collisions, such energy loss processes do not occur. Thus, comparing the yields of $p + p$ and $A + A$ collisions and calculating the energy loss in medium field theoretically, one can get an estimates of different properties of the produced hot and dense medium. For an extensive review on this topic, please consult [78–82].

1.6.5 Strangeness Enhancement

The strangeness enhancement is a very important signature of QGP formation in heavy ion nuclear collision. Compared to *pp* data, the production of strange particles is expected to enhance. Since the initial colliding nuclei have no strange particles in it, any strange particle produced in the collision must be accompanied by its antiparticle. The main production mechanism of strange hadron in an equilibrated hadron gas proceeds via reactions like $N\,N \to S\,\bar{S}$, where N denotes the nucleons and S denotes the strange hadrons. The threshold of such a process to occur is $2m_S$, where m_S is the mass of any strange hadron. The lowest lying strange particle is Kaon whose mass m_K is around 493.7 MeV making the threshold energy of such process around 1 GeV. But if a hot and/or dense deconfined QGP medium is produced after collision, the strange quark antiquark pair will be generated mainly via $q\,\bar{q} \to s\,\bar{s}$ and $g\,g \to s\,\bar{s}$, with $q = u, d$. Since $m_s = 95$ MeV. The threshold energy of such process are $2m_s = 190$ MeV making it kinematically more favourable than production of strangeness via nucleon-nucleon interactions. Also, at the temperature as high as in QGP, the huge abundance of u and d quark-antiquarks makes the thermal production of $s\bar{s}$ pair much more energetically favourable. Since, the strange quark-antiquarks ultimately recombine to produce strange particles, a significant enhancement of strangeness signals the production of QGP medium.

1.7 Magnetic Field in Heavy Ion collision

1.7.1 Geometry of the Collision

Before going to the generation of magnetic field, let us briefly discuss the geometry of HIC shown in Fig. 1.8. As discussed earlier, two Lorentz contracted thin discs travelling towards each other in opposite direction along the beam pipe collides with each other. The plane perpendicular to the z-direction is called the *transverse plane*as shown in Fig. 1.9(a) and Fig. 1.9(b). The projection of the distance between

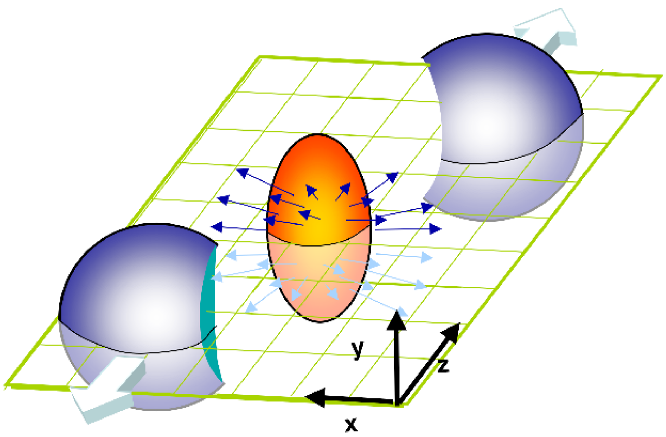

Figure 1.8: The schematic representation of non-central heavy ion collision: The spectator particles (in blue) are leaving the collision region (shown in orange). The magnetic field is generated in the collision region along the y-axis perpendicular to the reaction plane ($x - y$ plane)

the two discs on the transverse or $x - y$ plane is called *impact parameter* ($\boldsymbol{b}$) of collision. The impact parameter vector and the direction of motion of incoming nuclei z-direction together creates a plane which is called the *reaction plane*. The angle that the reaction plane creates with x-axis is denoted as Φ_R. The impact parameter vector's orientation in the transverse plane as well as the magnitude fluctuates from event to event.

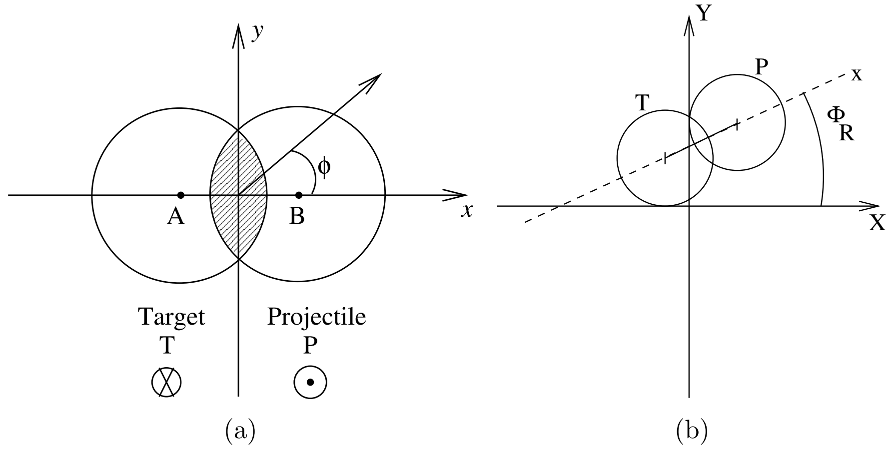

Figure 1.9: The transverse view of nuclear collision — the almond shaped shaded region contains the nucleons which take part in collision,

1.7.2 Magnitude and Profile of the Field

The participants in HIC carry electric charges. We know that moving charges produce electric currents. According to the classical electrodynamics, an electric current produces a magnetic field [88]. The magnitude of this magnetic field thus created can be obtained from a very beautiful and hand-waving argument by Tuchin [89]. Tuchin considered two heavy ions of radius R and electric charge Ze travelling towards each other at some impact parameter $\boldsymbol{b}$. Biot-Savart law tells us that the magnitude of the magnetic field goes as

$$B \sim \gamma Ze \frac{b}{R^3} \tag{1.3}$$

in the center of mass frame and the direction is perpendicular to the reaction plane. Here the factor $\gamma = \sqrt{s_{NN}}/2m_N$. At RHIC, for $Au + Au$ collision, using $\gamma = 100$, $Z = 79$, $b \sim R_A \sim 7$ fm, we get $B \sim 10^{18}$ Gauss or $eB \sim m_\pi^2$ as $\sqrt{s_{NN}} = 200$ GeV. A similar calculation reveals that $eB \sim 10m_\pi^2$ at LHC energies. Although this argument is purely classical in nature, the estimation coming from it is quite good.

It is a well known fact that in HIC a high magnetic field is generated. The highest magnitude of the field was roughly estimated to be $eB \sim 3m_\pi^2 = 3 \times 10^{18}$ Gauss at $\sqrt{s_{NN}} = 200$ GeV by Kharzeev *et.al.* in [90]. Later, this qualitative estimate was improved by Skokov *et. al.* [91] by considering properly several factors that can heavily influence it like impact parameter of collision, the total energy of incoming nuclei in center of mass reference frame. They have also done some very simple analytic calculation and matched them with UrQMD simulations (for detailed description of UrQMD see [92, 93]). According to their results, the magnetic field in the collision has non-zero component perpendicular to the reaction plane. It declines rapidly with time but is homogeneous to a high degree along the y-direction as well as the transverse plane. Technically, the magnetic field has both x and y components with comparable value in event by event basis [94]. But when the x-component is averaged over many events, it vanishes. So in conclusion according to this school of thought, the magnetic field generated in HIC at a particular time is directed along the y direction per event and decreases rapidly with time.

Tuchin proposed that when a medium is formed in the collision, the time dependence of the magnetic field is affected by the response of the medium via electrical conductivity [89, 95, 96]. The electrical conductivity of the medium is responsible for delaying the decay of the magnetic field. So the magnetic field lasts longer than expected. Tuchin considered essentially two cases where a) the medium is static, i.e., temperature of the medium is independent of time and b) the medium is expanding, i.e., the temperature is time dependent and solved Maxwell's equation with electrical conductivity. He found out that the relaxation time of the magnetic field to be larger in an expanding medium than in a static one. The magnetic field essentially freezes out due to the electrical conductivity of the medium.

1.7.3 Observable Effects of Magnetic Fields

The effects of magnetic field in the observables of heavy ion collision are gaining increasing attention recently. Some novel phenomena are believed to be exhibited due to the magnetic field. Below, we try to present some unprecedented effects accompanied by magnetic field.

1.7.3.1 Chiral Magnetic Effect (CME)

The phenomena of charge separation along the direction of magnetic field induced a by chirality imbalance is called *chiral magnetic effect* [98–101]. It is a topological effect arising because of the transitions between the topologically distinct states. This charge separation induces an electric current given as

$$\boldsymbol{j} = N_c \sum_f \frac{q_f^2 \mu_5}{2\pi^2} \boldsymbol{B}, \tag{1.4}$$

where N_c is the number of quark colors, q_f is charge of the quark with flavour f, μ_5 is the chiral chemical potential, $\boldsymbol{B}$ is the abelian magnetic field. The chiral chemical potential measures the asymmetry between total number of left handed and right handed quarks (with antiquarks substracted). CME was studied in numerical LQCD framework [102, 103] and in hydrodynamical approximation [104]. The experimental searches for CME [105–109] in HIC is being carried out from decades but the signature is still a topic of debate. For a detailed review on this fascinating subject, consult [110, 111, 113–115].

1.7.3.2 Chiral Vortical Effects (CVE)

In non-central relativistic HIC, a high angular momentum $\boldsymbol{J}_{\rm sys}$ of the order of $10^3\hbar$ is also generated at large impact parameter [116–118]. Also, a high vorticity is generated as a result of shear forces that arises when two inter penetrating nuclei pass each other. Mathematically vorticity $\boldsymbol{\omega}$ can be expressed in terms of local fluid velocity $\boldsymbol{v}$ as $\boldsymbol{\omega} = \frac{1}{2}\boldsymbol{\nabla} \times \boldsymbol{v}$ [119, 120]. A polarization in local fluid rest frame along the direction of vorticity is generated due to the spin orbit coupling describable by an effective interaction term $\sim \boldsymbol{\omega} \cdot \boldsymbol{S}$. When averaged over the entire system, this polarization becomes parallel to $\hat{\boldsymbol{J}}_{\rm sys}$. Now, if there is an imbalance in chirality, then there will be more right handed (RH) particles than left handed (LH) one (assuming $\mu_5 > 0$). On top of that, there are more RH quarks than anti-quark (assuming $\mu > 0$). So the net RH quarks move along the direction of $\hat{\omega}$ and contribute to the vector current

$$\boldsymbol{J} = \frac{1}{\pi^2}\mu_5\mu\boldsymbol{\omega}. \tag{1.5}$$

This phenomena of generation of current in a chiral medium along the direction of vorticity is called chiral vortical effects [111].

1.7.3.3 Magnetic Catalysis (MC)

The magnetic field induced enhancement of dynamical symmetry breaking is broadly called magnetic catalysis [122,123]. The order parameter of chiral phase transition is the thermal expectation value of $\langle\bar{q}q\rangle$. Now, in the chiral limit $m_f \to 0$ we have [124]

$$\begin{aligned} \langle\bar{q}q\rangle &= 0 \qquad \text{in the Wigner-Weyl phase,} \\ \langle\bar{q}q\rangle &\neq 0 \qquad \text{in the Nambu-Goldstone phase.} \end{aligned} \tag{1.6}$$

When the temperature increases, there is a phase transition from Nambu-Goldstone phase to Wigner phase around some temperature $T = T_c$. When there is a magnetic catalysis, T_c increases with the increase of B. The phenomena of magnetic catalysis was exhibited in different effective model calculations such as Nambu-Jona Laisiono(NJL) model [125–132], its Polyakov loop extended NJL model(PNJL) [133,134], chiral perturbation theory [135–137], quark-meson model [138,139] and its Polyakov loop extended counterpart [140], renormalization group method [141–146], Dyson-Schwinger equation [147] and from first principle numerical LQCD [148, 149, 151–154] simulations.

1.7.3.4 Inverse Magnetic Catalysis (IMC)

The inverse magnetic catalysis (IMC) effect is the opposite to that of magnetic catalysis where the quark condensate decreases with the strength of the magnetic field [155]. This phenomena first came to prominence in LQCD simulations of Bali et. al. with $N_f = 2 + 1$ extrapolating the continuum and using a lower value of quark mass corresponding to pion mass of $m_\pi = 140$ MeV [152, 153]. But for $N_f = 3$, increasing light quark masses to the strange mass, they found out a increasing trend of condensate at all T. This behaviour made them to conclude that the pseudo-critical temperature is dependent on quark mass used in the simulations. The mechanism behind this puzzling behaviour was sorted out subsequently within a framework developed from LQCD techniques according to which there is competition between valance and sea quark contribution to the quark condensation around pseudocritical temperature [156]. The absence of sea effect in model calculation was attributed to the exclusion of dynamical gauge field. Another explanation comes from the fact that strong coupling receives corrections from temperature as well as magnetic field which is responsible for the increase or decrease of quark condensate as a result of competition between thermal and magnetic effects. This scenario has been investigated in various effective QCD models [157–163], Dyson-Schwinger equation [147, 164] etc. For a fascinating review on IMC, see Ref. [165].

1.7.3.5 Superconductivity of the Vacuum

The QCD vacuum can be superconducting under very strong magnetic field in low temperature [166]. Under these conditions, the QCD vacuum obeys the basic conditions that are required to exhibit superconductivity namely the presence of electrical charge carriers, one-dimensional dynamics of those charge carriers and the presence of attractive interaction between those charge carriers [167, 168]. Under strong magnetic field, QCD vacuum produces u, $\overline{u}$ and d, $\overline{d}$ pair which condensate to form $\rho^+(u\overline{d})$, $\rho^-(\overline{u}d)$ mesons. These $\rho^\pm$ mesons play the role of the charge carriers analogous to cooper pairs in conventional superconductivity. Also in presence of strong magnetic field there is a phenomena of dimensional reduction from $(3+1)$D to $(1+1)$D. The presence of an attractive interaction is ensured by gluon exchange which binds the quark and anti-quark pair in ρ mesons. Although, the vacuum superconductivity is not destroyed by high magnetic field unlike the conventional superconductivity, it can be destroyed by thermal effects similar to that of normal superconductivity. The evidence of vacuum super conductivity was confirmed in Vector Dominace Model (VDM) [169], NJL model [170] and in lattice gauge theory [171].

These novel phenomena stimulated researchers to investigate the effects of magnetic field on various aspects of heavy ion collision. Apart from this, a lot of efforts have been made to understand the influence of magnetic field on QCD phase transitions, thermodynamics of the QGP phase, collective excitations, various probes from perturbative and non-perturbative QCD, effective field theory approaches.

1.8 Scope of this Thesis

In chapter 2, we shall discuss about the quantum field theory at non-zero temperature. The basic formulation of QFT at non-zero temperature can be formulated in three different formalisms — Imaginary time formalism, real time formalism and thermofield dynamics. In this chapter we adhere ourselves to imaginary time formalism which will be used to calculate the main portion of the calculation carried out in this thesis. Also we shall discuss the basic concepts of hard thermal loop approximation technique at finite temperature in a nutshell.

In chapter 3, the derivation of fermion propagator in an external magnetic field shall be discussed. Starting from the modified Dirac's equation in presence of background magnetic field, we shall employ Schwinger's proper time method to derive the expression of fermion propagator.

In chapter 4, we shall review properties of quark two-point function at non-zero temperature in hot de-confined medium. We shall employ HTL approximation to obtain the expression of quark self energy at non-zero temperatue. Then, Dyson-Schwinger equation was employed to get the quasi-quark propagator, collective modes and its thermal mass. Subsequently, we shall examine the behaviour of the spectral density of the effective quark propagator and discrete symmetries.

In chapter 5, we shall discuss quark two point function at non-zero temperature as well as non-zero magnetic field. In doing so, we shall derive one loop HTL quark self energy in weak field approximation of the propagator in background magnetic field. Applying Dyson-Schwinger equation, we shall obtain one loop effective quark propagator. The pole of the propagator will give the collective modes of excitation. We shall also investigate discrete symmetries, spectral functions etc.

In chapter 6, we shall compute hard dilepton rate in hot magnetised medium. In doing so, we take one of the quasi-quark mode to be soft and another one hard. The rate is obtained from imaginary part of photon polarization tensor. We shall see the dilepton rate will be consists of two contribution — pole-pole contributions which encodes the process involved in the dilepton production mechanism in quark sector and pole-cut contribution giving the Landau damping part.

In chapter 7, we summarise and discuss the outlook.

CHAPTER 2

Field Theory at Non-zero Temperature

2.1 Introduction

In this chapter, we shall discuss about the field theory at non-zero temperature. The field theory at zero temperature has been developed a long ago by pioneer work of Feynman, Schwinger, Tomonaga et al. It needs to be redefined to incorporate non-zero temperature. Technically, thermal field theory is all about an alternative description of quantum statistical mechanics of many particle system where the number of particles are not fixed.

Currently, in thermal field theory, there are three formalisms exists — imaginary-time formalism (ITF), real-time formalism (RTF) and thermofield dynamics(TFD). Details of each of these methods can be found in [178–180]. ITF is the most common and widely used formalism among these two which is used mainly in the case in equilibrium system [181]. However, ITF is not applicable for non-equilibrium situation but RTF [182–185] is. Lastly, thermofield dynamics [186, 187] is a framework that arose from RTF which can naturally describe nature of thermal vacuum, Goldstone states etc. We shall carry out all of our calculation in this thesis with ITF. It can be popularly introduced in two ways — the operator method and the path integral method. We shall present a brief outline of these two method.

2.2 Partition Function

The thermodynamic properties of a system in equilibrium with a heat bath can be extracted from the partition function. So the primary aim in statistical mechanical calculation is to evaluate the partition function of a quantum mechanical system in equilibrium.

Consider a system with Hamiltonian operator $\hat{H}$ and a set of conserved charge $\hat{N}_i$. The density matrix operator $\hat{\rho}$ is defined as

$$\hat{\rho}(\beta) = \exp\left[-\beta\left(\hat{H} - \sum_i \mu_i \hat{N}_i\right)\right], \tag{2.1}$$

where β represents the inverse of equilibrium temperature $\beta = 1/k_B T$.(Here k_B is Boltzmann constant which is taken to be 1 in natural units) and μ_i is the chemical potential of i^{th} conserved charge.
The partition function is defined as trace of density matrix operator in any complete set of basis as

$$Z(\beta) = \mathsf{Tr}\,\hat{\rho}(\beta). \tag{2.2}$$

The ensemble average of any observable $\hat{\mathcal{O}}$ can be defined via $\hat{\rho}$ as

$$\langle\hat{\mathcal{O}}\rangle_\beta = \frac{\mathsf{Tr}\left(\hat{\mathcal{O}}\,\hat{\rho}(\beta)\right)}{Z(\beta)}. \tag{2.3}$$

For an arbitrary Schrödinger operator $\hat{A}$, we can define its Heisenberg picture representation as

$$\hat{A}_h(t) = e^{iHt}\hat{A}e^{-iHt}, \tag{2.4}$$

At this point it is convenient to perform analytic continuation to Euclidean time $t \to -i\tau$. So any operator $\hat{A}_h(t)$ is analytically continued to $\hat{A}_h(-i\tau)$, which we write as $\hat{A}_h(\tau)$. So, in euclidean time, Eq. (2.4) takes the form

$$\hat{A}_h(\tau) = e^{\tau\hat{H}}\hat{A}e^{-\tau\hat{H}}. \tag{2.5}$$

Note that transformation defined in (2.5) is not unitary since $\hat{A}_h^\dagger(\tau) \neq e^{\tau\hat{H}}\hat{A}^\dagger e^{-\tau\hat{H}}$. Now, the thermal correlation function of two Heisenberg operators $A_h(t_a)$ and $B_h(t_b)$ can be written as

$$\begin{aligned}
\langle \hat{A}_h(t_a)\hat{B}_h(t_b)\rangle_\beta &= \frac{1}{Z(\beta)}\mathsf{Tr}\left[e^{-\beta\hat{H}}\hat{A}_h(t_a)\hat{B}_h(t_b)\right] \\
&= \frac{1}{Z(\beta)}\mathsf{Tr}\left[\hat{A}_h(t_a)e^{-\beta\hat{H}}e^{\beta\hat{H}}\hat{B}_h(t_b)e^{-\beta\hat{H}}\right] \\
&= \frac{1}{Z(\beta)}\mathsf{Tr}\left[e^{-\beta\hat{H}}e^{\beta\hat{H}}\hat{B}_h(t_b)e^{-\beta\hat{H}}\hat{A}_h(t_a)\right] \\
&= \frac{1}{Z(\beta)}\mathsf{Tr}\left[e^{-\beta\hat{H}}\hat{B}_h(t_b - i\beta)\hat{A}_h(t_a)\right]
\end{aligned} \tag{2.6}$$

In the second step of the above derivation, we have inserted the resolution of identity operator $\hat{\mathbb{1}} = e^{-\beta\hat{H}}e^{\beta\hat{H}}$ and in the last step cyclic property of trace has been used. Thus, we have an important identity

$$\langle \hat{A}_h(t_a)\hat{B}_h(t_b)\rangle_\beta = \langle \hat{B}_h(t_b - i\beta)\hat{A}_h(t_a)\rangle_\beta. \tag{2.7}$$

The identity in Eq. (2.7) is called **Kubo-Martin-Schwinger** or KMS relation. It holds for *both bosonic and fermionic* operators. It is useful for obtaining the periodicity properties of Green's function. Here we note that $i\beta$ is connected to the time variable. The KMS relation can be analytically continued to Euclidean time as

$$\langle \hat{A}_h(\tau_a)\hat{B}_h(\tau_b)\rangle_\beta = \langle \hat{B}_h(\tau_b+\beta)\hat{A}_h(\tau_a)\rangle_\beta. \tag{2.8}$$

We shall see in section 2.4 that the KMS relation in Eq. (2.8) is useful in deriving Matsubara frequencies of boson and fermion Green's function in ITF.

2.3 Imaginary Time Formalism

In general, partition function can hardly be evaluated because we have to perform the summation over expectation values of $e^{-\beta\hat{H}}$ with all possible states of Fock space. To circumvent this situation, we shall not work with states but with operators. In this section, we shall discuss ITF first introduced by Matsubara [188] in nutshell using operator as well as path integral method.

2.3.1 Operational Method

Let us write the total Hamiltonian operator $\hat{H}$ into two parts — the free part $\hat{H}_0$ and the interaction part $\hat{H}^{\mathsf{int}}$ as follows

$$\hat{H} = \hat{H}_0 + \hat{H}_{\mathsf{int}}. \tag{2.9}$$

The density matrix is given as

$$\hat{\rho}(\beta) = e^{-\beta\left(\hat{H}-\mu\hat{N}\right)}. \tag{2.10}$$

Here for simplicity, we take only one conserved charge as opposed to Eq. (2.1). Now, the $\hat{\rho}(\beta)$ can also be written as

$$\hat{\rho}(\beta) = \hat{\rho}_0(\beta)\hat{S}(\beta), \tag{2.11}$$

where

$$\hat{\rho}_0(\beta) = e^{-\beta\left(\hat{H}_0 - \mu\hat{N}\right)} \tag{2.12}$$

is the density matrix of free theory and $\hat{S}$ is an operator playing a role analogous to the S-matrix QFT at $T = 0$. The density matrices can be easily seen to satisfy the following equations

$$\frac{\partial\hat{\rho}_0(\tau)}{\partial\tau} = -\hat{\mathcal{H}}_0\hat{\rho}_0(\tau), \tag{2.13}$$

$$\frac{\partial\hat{\rho}(\tau)}{\partial\tau} = -(\hat{\mathcal{H}}_0 + \hat{H}')\,\hat{\rho}(\tau), \tag{2.14}$$

where $\hat{\mathcal{H}}_0 \equiv \hat{H}_0 - \mu$ and τ is bounded in the region $0 \leq \tau \leq \beta$. From Eq. (2.11), (2.13) and (2.14), it is a matter of a few steps of simple algebra to show that

$$\frac{\partial\hat{S}(\tau)}{\partial\tau} = \hat{H}_I'(\tau)\hat{S}(\tau), \tag{2.15}$$

where the interaction Hamiltonian H' is evolved with free hamiltonian $\mathcal{H}_0$ in τ to define H_I' as

$$\hat{H}_I'(\tau) = \exp\left(-\hat{\mathcal{H}}_0\tau\right)\hat{H}_I'\exp\left(\hat{\mathcal{H}}_0\tau\right). \tag{2.16}$$

Note that such a transformation in Eq. (2.16) is not a unitary for real τ because the adjoint of an operator does not coincide with the transformed adjoint operator. Now we can get a solution of Eq. (2.16), like in the case of zero temperature field theory, as

$$\hat{S}(\beta) = T_\tau \left[\exp\left(- \int_0^\beta d\tau \, \hat{H}'_I(\tau) \right) \right], \tag{2.17}$$

where T_τ is the ordering operator in τ. It is analogues to time ordered product in zero temperature field theory with the exception that in this case the range of τ is bounded in the region $[0, \beta]$.

Furthermore, if we define

$$\hat{S}(\tau_1, \tau_2) = T_\tau \left[\exp\left(- \int_{\tau_1}^{\tau_2} d\tau \hat{H}'_I(\tau) \right) \right], \tag{2.18}$$

then it can be seen to satisfy

$$\hat{S}^{-1}(\tau_1, \tau_2) = \hat{S}(\tau_2, \tau_1), \tag{2.19}$$

$$\hat{S}(\tau_1, \tau')\hat{S}(\tau', \tau_2) = \hat{S}(\tau_1, \tau_2) \quad \text{for} \quad \tau_1 \leq \tau' \leq \tau_2, \tag{2.20}$$

$$\hat{S}(\tau, \tau) = \mathbb{1}. \tag{2.21}$$

2.3.2 Path Integral Formulation

The path integral formalism is very intuitive way to introduce finite temperature field theory. The basic idea is to write the partition function $\mathcal{Z}(\beta)$ as a sum over all posible routes between two states. In this section, we demonstrate how the identification of temperature with euclidean time, as hinted in section 2.2, is manifested in a very natural way in path integral formalism. For simplicity, we demonstrate the basic concept with the quantum field theory in $(0 + 1)$ dimension which is essentially ordinary quantum mechanics. It is straightforward to generalise the case of quantum field theory in $(3 + 1)$ dimension.

The quantum mechanical amplitude of a particle going from position x_i at euclidean time τ_i to a position x_f at time τ_f in potential $V(x)$ is written as

$$\langle x_f(\tau_f)|x_i(\tau_i)\rangle = \langle x_f|\, e^{-(\tau_f-\tau_i)\hat{H}}\, |x_i\rangle = \int \mathcal{D}x(\tau)\; e^{-S[x]/\hbar}, \tag{2.22}$$

Here $S[x]$ is the euclidean action functional defined as

$$S[x] = \int\limits_{\tau_i}^{\tau_f} d\tau\, L\big(x(\tau), \partial_\tau x(\tau)\big), \tag{2.23}$$

where L is the Lagrangian

$$L\big(x(\tau), \partial_\tau x(\tau)\big) = \frac{1}{2} m \big(\partial_\tau x(\tau)\big)^2 + V\big(x(\tau)\big). \tag{2.24}$$

The partition function, defined in Eq. (2.1) and Eq. (2.2), can be casted in the following form

$$\mathcal{Z}(\beta) = \int dx\, \langle x|\, e^{-\beta\hat{H}}\, |x\rangle\,, \tag{2.25}$$

where $|x\rangle$ is position eigenket with $\hat{X}\,|x\rangle = x\,|x\rangle$.

Now, we can put the terms $\langle x_f|\, e^{-(\tau_f-\tau_i)\hat{H}}\, |x_i\rangle$ and $\langle x|\, e^{-\beta\hat{H}}\, |x\rangle$ in a one to one correspondence by identifying both x_f and x_i as x and setting $\tau_f = \beta$, $\tau_i = 0$. Therefore, we can write

$$\mathcal{Z}(\beta) = \int\limits_{x(\beta)=x(0)} \mathcal{D}x(\tau)\;\; \exp\left[-\frac{1}{\hbar}\int\limits_{0}^{\beta} d\tau\;\, L\Big(x(\tau), \partial_\tau x(\tau)\Big)\right], \tag{2.26}$$

where $\mathcal{D}x(\tau) = \prod_\tau dx(\tau)$ is the functional integral measure. Note that, the domain of euclidean time is bounded as $\tau \in [0, \beta]$ and x must satisfy periodicity condition $x(0) = x(\beta)$. Surprisingly, the inverse temperature β is traded of as euclidean time. For any observable $\mathcal{O}(\tau_0)$ in Heisenberg picture, the thermal expectation value can be written in functional integral form as

$$\langle \mathcal{O}(\tau_0) \rangle_\beta = \frac{1}{\mathcal{Z}(\beta)} \int \mathcal{D}x(\tau)\ \mathcal{O}(\tau_0) \exp\left[-\frac{1}{\hbar} \int_0^\beta d\tau\, L\Big(x(\tau), \partial_\tau x(\tau)\Big)\right]. \tag{2.27}$$

Now, in (3+1)D, there are uncountably infinite degrees of freedom (D.O.F) labelled by position $\boldsymbol{x} = (x, y, z)$ as opposed to the case of single particle quantum mechanics. We denote the D.O.F at position $\boldsymbol{x}$ or the field as $\phi(\boldsymbol{x})$. Thus, the expression of partition function in Eq. (2.26) takes the following form for a quantum field theory at finite temperature

$$\mathcal{Z}(\beta) = \int\limits_{\phi(\boldsymbol{x},0)=\phi(\boldsymbol{x},\beta)} \mathcal{D}\phi(\boldsymbol{x}, \tau) \exp\left(-\int_0^\beta d\tau \int d^3x\ \ \mathcal{L} \right). \tag{2.28}$$

where $\mathcal{D}\phi(\boldsymbol{x}, \tau) = \prod\limits_{\boldsymbol{x},\tau} d\phi(\boldsymbol{x}, \tau)$ is the measure of functional integral which is just the product of $d\phi(\boldsymbol{x}, \tau)$ at each space-time point where the field is defined and

$$\mathcal{L} = \frac{1}{2} m \left(\partial_\tau^2 + \boldsymbol{\nabla}^2\right) \phi(\boldsymbol{x}, \tau) + V\left(\phi(\boldsymbol{x}, \tau)\right) \tag{2.29}$$

is the euclidean Lagrangian density.

The potential $V(\phi)$ contains the mass term and the interaction term. For ϕ^4 theory, it looks like

$$V\left(\phi(\boldsymbol{x}, \tau)\right) = \frac{1}{2} m^2 \phi^2(\boldsymbol{x}, \tau) + \frac{\lambda}{4!} \phi^4(\boldsymbol{x}, \tau). \tag{2.30}$$

In the absence of interaction the functional integration can be evaluated analytically.

But when the interaction is turned on the partition function can be written as a perturbation series in λ for $\lambda < 1$. The same conclusion is applied for N point function. The two point function is defined as

$$G(\boldsymbol{x}_a - \boldsymbol{x}_b, \tau_a - \tau_b) = \frac{1}{\mathcal{Z}(\beta)} \int \mathcal{D}\phi(\boldsymbol{x}, \tau)\ T_\tau\{\phi(\boldsymbol{x}_a, \tau_a)\phi(\boldsymbol{x}_b, \tau_b)\} \exp\left(- \int_0^\beta d\tau \int d^3x\ \mathcal{L} \right). \tag{2.31}$$

The rest of the computation is similar to the euclidean field theory at zero temperature.

2.4 Green's Function at Non-Zero Temperature — Matsubara Modes

In quantum field theory at zero temperature, the two-point Green's function or propagator is defined as

$$\begin{aligned} \langle 0| T\left\{\Phi(t, \boldsymbol{x})\phi(t', \boldsymbol{x}')\right\} |0\rangle = \Theta\left(t - t'\right) \langle 0| \Phi(t, \boldsymbol{x})\Phi(t', \boldsymbol{x}') |0\rangle \\ \pm\, \Theta\left(t' - t\right) \langle 0| \Phi(t', \boldsymbol{x}')\Phi(t, \boldsymbol{x}) |0\rangle \,. \end{aligned} \tag{2.32}$$

The state $|0\rangle$ is the ground state of interacting theory. The plus sign and minus sign in Eq. (2.32) is used when Φ is bosonic and fermionic field, respectively.

Let us consider for simplicity the case of real scalar field. The definition of Green's function in non-zero temperature involves all the states in the Fock space. So, it is defined in ITF of thermal field theory as

$$\mathcal{G}_\beta(\tau-\tau',\boldsymbol{x}-\boldsymbol{x}') = \frac{1}{\mathcal{Z}(\beta)}\mathsf{Tr}\left[e^{-\beta H}T_\tau\left\{\phi(\tau,\boldsymbol{x})\phi(\tau',\boldsymbol{x}')\right\}\right]. \tag{2.33}$$

Consider, the case $\beta > \tau > \tau' > 0$

$$\begin{aligned}\mathcal{G}_\beta(\tau-\tau',\boldsymbol{x}-\boldsymbol{x}') &= \frac{1}{\mathcal{Z}(\beta)}\mathsf{Tr}\left[e^{-\beta H}\phi(\tau,\boldsymbol{x})\phi(\tau',\boldsymbol{x}')\right] \\ &= \frac{1}{\mathcal{Z}(\beta)}\mathsf{Tr}\left[e^{-\beta H}\phi(\tau'+\beta,\boldsymbol{x}')\phi(\tau,\boldsymbol{x})\right] \\ &= \frac{1}{\mathcal{Z}(\beta)}\mathsf{Tr}\left[e^{-\beta H}T_\tau\left\{\phi(\tau,\boldsymbol{x})\phi(\tau'+\beta,\boldsymbol{x}')\right\}\right] \\ &= \mathcal{G}_\beta(\tau-\tau'-\beta,\boldsymbol{x}-\boldsymbol{x}'). \end{aligned}\tag{2.34}$$

Here we used KMS condition in Eq. (2.8) and the definition of euclidean time ordered product for the case of $\tau > \tau'$. Likewise, for the case $\beta > \tau' > \tau > 0$, we get

$$\begin{aligned}\mathcal{G}_\beta(\tau-\tau',\boldsymbol{x}-\boldsymbol{x}') &= \frac{1}{\mathcal{Z}(\beta)}\mathsf{Tr}\left[e^{-\beta H}\phi(\tau',\boldsymbol{x}')\phi(\tau,\boldsymbol{x})\right] \\ &= \frac{1}{\mathcal{Z}(\beta)}\mathsf{Tr}\left[e^{-\beta H}\phi(\tau+\beta,\boldsymbol{x})\phi(\tau',\boldsymbol{x}')\right] \\ &= \frac{1}{\mathcal{Z}(\beta)}\mathsf{Tr}\left[e^{-\beta H}T_\tau\left\{\phi(\tau+\beta,\boldsymbol{x})\phi(\tau',\boldsymbol{x}')\right\}\right] \\ &= \mathcal{G}_\beta(\tau+\beta-\tau',\boldsymbol{x}-\boldsymbol{x}'). \end{aligned}\tag{2.35}$$

Thus, we have

$$\mathcal{G}^B_\beta(\tau-\tau',\boldsymbol{x}-\boldsymbol{x}') = \begin{cases}\mathcal{G}^B_\beta(\tau-\tau'-\beta,\boldsymbol{x}-\boldsymbol{x}') & \text{for } \tau>\tau', \\ \mathcal{G}^B_\beta(\tau-\tau'+\beta,\boldsymbol{x}-\boldsymbol{x}') & \text{for } \tau<\tau', \end{cases}\tag{2.36}$$

where the superscript B indicates bosonic Green function. Since we have periodicity property in time argument of Green's function at finite temperature, we can have the following Fourier expansion

$$\mathcal{G}^B_\beta(\tau-\tau',\boldsymbol{x}-\boldsymbol{x}') = \frac{T}{V}\sum_{n=-\infty}^{\infty}\int\frac{d^3k}{(2\pi)^3}e^{-i\omega^B_n\tau+i\boldsymbol{k}.\boldsymbol{x}}\widetilde{\mathcal{G}}^B_n(\boldsymbol{k}). \tag{2.37}$$

The consequence of the periodicity property of Green's function is the appearance of the discrete spectrum of frequency

$$\omega^B_n = 2n\pi T \qquad \text{with } n = 0, \pm 1, \pm 2, \cdots . \tag{2.38}$$

For the case of fermionic field, a similar analysis leads to the conclusion that the position space Green's function is anti-periodic

$$\mathcal{G}^F_\beta(\tau-\tau',\boldsymbol{x}-\boldsymbol{x}') = \begin{cases} -\mathcal{G}^F_\beta(\tau-\tau'-\beta,\boldsymbol{x}-\boldsymbol{x}') & \text{for } \tau > \tau' \\ -\mathcal{G}^F_\beta(\tau-\tau'+\beta,\boldsymbol{x}-\boldsymbol{x}') & \text{for } \tau < \tau'. \end{cases} \tag{2.39}$$

As a result of this, we can write an expansion similar to that shown in Eq. (2.37) with ω_n taking values

$$\omega^F_n = (2n+1)\pi T \qquad \text{with } n = 0, \pm 1, \pm 2, \cdots . \tag{2.40}$$

2.5 Feynman Rules at Finite Temperature

Some of the rules for computing Feynman diagrams get modified in ITF but others remain the same as in the case of zero temperature. Below, we outline the modified rules

- **Vertex:**

  Same as in the case of zero temperature.

- **Momentum space propagator:**

Same as in the case of zero temperature but $k_0 \to i\omega_n$, where

$$\omega_n = \begin{cases} 2n\pi T & \text{for Bosons,} \\ (2n+1)\pi T & \text{for Fermions,} \end{cases} \tag{2.41}$$

with T being the temperature of the system in equilibrium and $n = 0, \pm 1, \pm 2, \cdots$

- **Loops**

  The four momentum integration is replaced by sum-integral. The spatial three momentum integration is left unchanged. The k_0 integration is replaced by frequency sum as follows

$$\int_{-\infty}^{\infty} \frac{dk_0}{2\pi} f(k_0, \boldsymbol{k}) \to T \sum_{n=-\infty}^{\infty} f(i\omega_n, \boldsymbol{k}), \tag{2.42}$$

  where ω_n is defined in Eq. (2.41).

- **External line**

  The rules remain the same as in zero temperature field theory.

As an application of above mentioned Feynman rule, we wish to evaluate one loop correction mass correction of a real scalar field theory with ϕ^4 interaction. The Lagrangian is written as

$$\mathcal{L} = \frac{1}{2}\partial^\mu \phi \partial_\mu \phi - \frac{1}{2} m^2 \phi^4 - \frac{\lambda}{4!}\phi^4. \tag{2.43}$$

The scalar field propagator is written as

$$\Delta_F(K) = \frac{1}{k_0^2 - E_k^2}, \tag{2.44}$$

where $k_0 = i\omega_n = i2\pi nT$ and $E_k = \sqrt{|\boldsymbol{k}|^2 + m^2}$. The interaction term in the Lagrangian is $\mathcal{L}_{\mathsf{int}} = -\dfrac{\lambda}{4!}\phi^4$. So, the interaction vertex is given as $-i\lambda$. The expression of the self energy is written down applying the Feynman rule to the diagram as

$$\Pi_1(T) = \lambda T \sum_{n=-\infty}^{\infty} \int \frac{d^3k}{(2\pi)^3} \Delta_F(K) = -\lambda T \sum_{n=-\infty}^{\infty} \int \frac{d^3k}{(2\pi)^3} \frac{1}{4\pi^2 n^2 T^2 + E_k^2}. \quad (2.45)$$

We isolate the frequency sum part as

$$T \sum_{n=-\infty}^{\infty} \frac{1}{4\pi^2 n^2 T^2 + E_k^2} = \frac{1}{2E_k} \left(1 + 2n(E_k)\right), \quad (2.46)$$

where $n(E_k) = \dfrac{1}{\exp(E_k/T) - 1}$ is the Bose-Einstein distribution function. Thus, we are left with the three momentum integration

$$\Pi_1(T) = \lambda \int \frac{d^3k}{(2\pi)^3} \frac{1}{2E_k} \left(1 + 2n(E_k)\right). \quad (2.47)$$

Note that the self energy has two parts. The first part does not involve distribution function and the second part does. It turns out that the first part is exactly equal to the expression of Π_1 at zero temperature. Therefore we identify the second part as the thermal correction to the one loop boson self energy and write $\Pi_1(T) = \Pi_1^{\text{vac}} + \Pi_1^{\text{th}}(T)$ where

$$\Pi_1^{\text{vac}} = \lambda \int \frac{d^3k}{(2\pi)^3} \frac{1}{2E_k}, \quad (2.48)$$

$$\Pi_!^{\text{th}}(T) = \lambda \int \frac{d^3k}{(2\pi)^3} \frac{n(E_k)}{E_k}. \quad (2.49)$$

The vacuum part is ultraviolet (UV) divergent and it drops out after conventional zero-temperature renormalization. The thermal part is UV finite due to the presence of distribution function associated with it. The integrand in both Eq. (2.48) and Eq. (2.49) is spherically symmetric. So, to compute the thermal part, we can write the integration measure in spherical polar coordinate. For $m = 0$ case the k

integration can be performed analytically and the result is

$$\Pi_1(T, m = 0) = \frac{\lambda T^2}{12}. \tag{2.50}$$

For $m \neq 0$, we make a a change in variable $x = \sqrt{|\boldsymbol{k}|^2 + m^2}/T$ and obtain

$$\Pi(T, m) = \frac{\lambda T^2}{2\pi^2} \int\limits_{m/T}^{\infty} dx \, \frac{\sqrt{x^2 - (m/T)^2}}{e^x - 1}. \tag{2.51}$$

Note that the dependence of m and T come in the form of a dimensionless quantity m/T. This implies that when the temperature is very much higher than all the mass scales, i.e. $T >> m$, we can approximate $\Pi(T)$ as that in the case of massless scalar $\Pi(T, m) \simeq \lambda T^2/12$. Therefore, the thermal mass acquired by the particle is given as $m_T^2 = \lambda T^2/12$.

2.6 HTL Resumation

To demonstrate the essence of HTL resummation method, we consider the simple case of real massless scalar field theory with ϕ^4 interaction. The lagrangian is obtained by setting $m = 0$ in Eq. (2.43). The one loop correction to the self energy is given as

$$\Pi_1(T) = \frac{\lambda T^2}{12}. \tag{2.52}$$

The correction due to the thermal fluctuations are incorporated into the effective propagator. It is given from the resumation as

$$\Delta_1^*(k) = \frac{1}{k_0^2 - |\boldsymbol{k}|^2 - m_T^2}. \tag{2.53}$$

According to the standard perturbation theory, the ϕ^4 self energy Π, which is the sum of all 1PI diagram, is expected to have the perturbative expansion $\Pi = \lambda T^2 [1 + \mathcal{O}(\lambda)]$. But this naive expectation breaks down due to the presence of infrared (IR) divergence in the thermal part of the diagram containing more than one loops. But it turns out that if we resum all the higher order diagram into the effective propagator in Eq. (2.53), then we get the following advantages

1. The theory is saved from the infrared divergence by the thermal mass which is of the order of $m_T \sim \sqrt{\lambda}T$. It acts as a infrared cutoff to the theory and plays an analogous role of Debye mass in QED plasma.

2. The effects of thermal fluctuations are taken into account through the thermal mass.

The one loop tadpole diagram is given as

$$\Pi_1^\star = \lambda \sum\!\!\!\!\!\!\!\!\int_K \frac{1}{K^2 + m_T^2}. \tag{2.54}$$

It is simplified after performing the frequency sum and angular integration to

$$\Pi_1^\star = \lambda \int_0^\infty dk \frac{k^2}{\omega_T^2} \left[1 + 2n\left(\omega_T\right)\right], \tag{2.55}$$

where $\omega_T = \sqrt{k^2 + m_T^2}$. The integration in Eq. (2.55) cannot be performed exactly but it can be approximated by introducing a separation in the scale $p^\star$ such that $\sqrt{\lambda}T << p^\star << T$. In this scenario, we approximate $k, m_T << T$ below $p^\star$ and $k >> m_T$ above $p^\star$ to get

$$\Pi_1^\star = \lambda T^2 \left[1 - \frac{3}{\pi}\sqrt{\lambda} + \mathcal{O}(\lambda)\right]. \tag{2.56}$$

The effective tadpole $\Pi_1^\star$ is IR divergence free in spite of containing the summation of infinitely many IR divergent diagrams. This result is not perturbative as the correction is not multiple of the coupling constant λ. The reason of this surprising behaviour is the use of effective propagator containing the thermal mass as IR regulator. As a result, significant contribution from small momentum comes up in the integral in Eq. (2.56) and successive order of the coupling constant is reduced. The above steps motivates us to employ the following method in massless scalar theory at finite temperature

1. The diagram that contribute to λT^2 is isolated. It is the tadpole diagram Π_1 in this case.
2. Next, construction of effective propagator $\Delta^\star(K)$ by resummation of the tadpole diagram is carried out.
3. Depending on the circumstance, bare or effective propagator is used as in ordinary perturbation theory.

If the momentum and energies flowing through the Green's function is *hard*, i.e., of the order of T, bare propagator $\Delta(K)$ is sufficient for the calculation as can be seen from the example since m_T^2 can be neglected if $K^2 \gtrsim T^2$. But if they are soft, i.e. of the order of $\sqrt{\lambda}T$, then the effective propagator $\Delta^\star(K)$ must be used because higher order diagram contributes to the lower order in the coupling constant [189]. These higher order diagrams are called hard thermal loops (HTL) [190]. This method of effective perturbation theory was developed by Pisarsky and it is called HTL perturbation theory. Now, the whole argument of HTL perturbation theory is based on the assumption that the coupling constant λ is much smaller than 1, i.e., $\lambda << 1$.

In case of gauge theory, there is an additional complication that arises from bare perturbation theory. The gluon damping rate calculated using naive perturbative method is not gauge invariant and it turned out to be negative in some gauges.

This problem is traced to the fact that in bare perturbation expansion, higher order diagram contribute to lower order in coupling constant. Also in gauge theory, the self energy has dependencies on external momentum P. Now the diagrams that contribute to the Green's function at the same order in gauge coupling constant g depend on the external momentum P. Loop corrections are g^2T^2/P^2 times the corresponding tree level amplitude. Therefore, when the external momentum is soft ($P \sim gT$), the loop correction is of the same order in g as tree level. But when P is hard ($P \sim T$) the loop correction is suppressed by a factor of g^2 from the tree level amplitude. The gluon damping rate was recalculated with these resummation technique in [191] which turned out to be gauge independent displaying the triumph of this proposed method.

2.7 Conclusion

In conclusion, we briefly outlined the techniques necessary for theoretical calculation in quantum field theory at finite temperature in the most popular imaginary time formalism in this chapter. As an example, we demonstrated a simple evaluation of self-interacting scalar boson self energy using Feynman rules in presence of thermal medium in equilibrium. We also introduced the basic recipes and underlying concepts of hard thermal loop perturbation theory in a nutshell. The important takeaway from this chapter is the discreteness of frequency in modified Green's function. These technicality will be useful in calculations in upcoming chapters.

CHAPTER 3

Fermion Propagator in External Magnetic field

3.1 Introduction

In this chapter, we shall derive the fermion propagator in the presence of background magnetic field. We know from elementary quantum mechanics that there are some notable changes that are observed in the system under consideration in presence of background magnetic field. The most prominent one is the modification of the energy spectrum of the particle moving in the field and the alteration of density of states. The rotational invariance of the system is broken in presence of magnetic field as the system picks up a preferred direction $\hat{\boldsymbol{n}}$ along the magnetic field. The energy level of a particle gets quantised in *Landau Levels* on the plane perpendicular to the field

$$E_\ell(k_n) = \begin{cases} \sqrt{k_n^2 + (2\ell+1)|qB| + m^2} & \text{for bosons,} \\ \sqrt{k_n^2 + 2\ell|qB| + m^2} & \text{for fermions,} \end{cases} \tag{3.1}$$

where k_n is the momentum of the particle along the direction of the field $\boldsymbol{B} = B\hat{\boldsymbol{n}}$, $\ell = 0, 1, 2, \cdots$ is the Landau levels, q is the charge of the particle and m is the mass.

In the language of quantum field theory, any process from a specific initial state to final states is accompanied by the creation and destruction of off-shell or virtual particles. The propagation of the virtual particles are represented by two-point functions called propagators. In the presence of a magnetic field, the structure of the propagator of virtual or intermediate *charged* particles are modified which, in turn, influence the S-matrix elements. Thus, it is necessary to examine propagator of charged particles in external background field.

The problem of fermion propagator in the presence of background electromagnetic field was first considered by the seminal work of Julian Schwinger [192] in 1951. Schwinger employed proper time method in which the spacetime coordiantes were parametrised by a quantity called proper time $s \in [0, \infty]$. Later, Ritus [193] derived the fermionic field propagator in a simplistic and innovative way by diagonalising the Dirac operator in energy the eigenfunction basis. Apart from these two widely used methods, in Ref. [194, 195], author solved the Dirac equation in background field and derived the expression of fermionic propagator.

In this chapter, we shall employ the Schwinger's proper time method in deriving the expression of propagator.

3.2 Green's Function

In this section, we look at the concept of Green's function in a different perspective. The Green's function associated with a differential operator can be defined as the matrix element of its inverse. To justify this, we shall work with just one variable to demonstrate in this section.

Suppose, we have a differential equation of the form

$$\mathcal{O}_x f(x) = g(x), \tag{3.2}$$

where $\mathcal{O}_x$ is a differential operator involving derivatives of various orders with respect to x. Here $g(x)$ is some given function and $f(x)$ is the function which we need to determine. Let us define this equation in abstract form in some appropriate linear vector space. Let $|f\rangle$ and $|g\rangle$ are the elements of a linear vector space which are represented by $f(x)$ and $g(x)$ in function space. Then, we can write $\langle x|f\rangle = f(x)$ and $\langle x|g\rangle = g(x)$. So, in the abstract linear vector space, the differential equation takes the following form

$$\hat{\mathcal{O}} \left|f\right\rangle = \left|g\right\rangle, \tag{3.3}$$

where $\hat{\mathcal{O}}$ is the abstract operator that is represented by $\mathcal{O}_x$ in function space. Formally, the general solution of this operator equation is given by

$$\left|f\right\rangle = \hat{\mathcal{O}}^{-1} \left|g\right\rangle + \sum_i c_i \left|h_i\right\rangle, \tag{3.4}$$

where c_i's are the constants and $|h_i\rangle$ are linearly independent solution of the homogeneous equation

$$\hat{\mathcal{O}} \left|h_i\right\rangle = 0 \quad \text{or,} \quad \mathcal{O}_x h_i(x) = 0. \tag{3.5}$$

We take the inner product of the above equation with $\langle x|$ to get

$$\begin{aligned}\langle x|f\rangle = f(x) &= \langle x|\,\hat{\mathcal{O}}^{-1}\,|g\rangle + \sum_i c_i \langle x|h_i\rangle \\ &= \int dx' \,\langle x|\,\hat{\mathcal{O}}^{-1}\,|x'\rangle \langle x'|g\rangle + \sum_i c_i h_i(x) \\ &= \int dx' \mathcal{G}(x,x') g(x') + \sum_i c_i h_i(x), \end{aligned} \tag{3.6}$$

where we have defined

$$\mathcal{G}(x,x') = \langle x|\,\hat{\mathcal{O}}^{-1}\,|x'\rangle\,. \tag{3.7}$$

Here $\mathcal{G}(x,x')$ is called Green's function of the differential operator $\mathcal{O}_x$. It is just a 'matrix' element of the operator $\hat{\mathcal{O}}$ between $\langle x|$ and $|x'\rangle$.

Now

$$\hat{\mathcal{O}}\hat{\mathcal{O}}^{-1} = \hat{\mathbb{1}} \qquad \Rightarrow \qquad \langle x|\,\hat{\mathcal{O}}\hat{\mathcal{O}}^{-1}\,|x'\rangle = \langle x|\,\hat{\mathbb{1}}\,|x'\rangle = \delta(x-x'). \tag{3.8}$$

But

$$\begin{aligned}\langle x|\,\hat{\mathcal{O}}\hat{\mathcal{O}}^{-1}\,|x'\rangle &= \int dy\, \langle x|\,\hat{\mathcal{O}}\,|y\rangle \langle y|\,\hat{\mathcal{O}}^{-1}\,|x'\rangle \\ &= \int dy \delta(x-y)\mathcal{O}_y \mathcal{G}(y,x') \\ &= \mathcal{O}_x \mathcal{G}(x,x') \end{aligned} \tag{3.9}$$

Thus, the Green's function obeys the following differential equation

$$\mathcal{O}_x \mathcal{G}(x,x') = \delta(x-x'). \tag{3.10}$$

3.3 Fermion Propagator

The fermion Green's function in external electromagnetic field reads

$$(i\partial\!\!\!/ - q\mathcal{A}\!\!\!/(x) - m)\mathcal{G}(x, x') = \delta^{(4)}(x - x'), \tag{3.11}$$

where $\partial\!\!\!/ \equiv \gamma^\mu \partial_\mu$ which is similar to the Feynman slash notation applied to a four-vector. Here, $\mathcal{A}_\mu(x)$ is the vector potential associated with background electromagnetic field, q is the electric charge of the particle including its magnitude as well as sign. As an example, for electron $q = -e$, $q = +e$ for positron and so on. Also, m is the mass of the particle. Now, as we have discussed in section 3.2, we can cast Eq. (3.11) in the operator form. Green's function is defined as an operator equation as

$$(\hat{\Pi\!\!\!/} - m\hat{\mathbb{1}})\hat{G} = \hat{\mathbb{1}}, \tag{3.12}$$

where

$$\hat{\Pi}_\mu \equiv \hat{P}_\mu - q\mathcal{A}_\mu(\hat{X}). \tag{3.13}$$

From now on, we shall not write explicitly the unit operator $\hat{\mathbb{1}}$ where it is multiplied with some number.

Inverting Eq. (3.12), we get

$$\mathcal{G}(x, x') = \langle x| (\hat{\Pi\!\!\!/} - m)^{-1} |x'\rangle \,. \tag{3.14}$$

We can cast $(\hat{\Pi\!\!\!/} - m)^{-1}$ as

$$(\hat{\Pi\!\!\!/} - m)^{-1} = \left(\hat{\Pi\!\!\!/}^2 - m^2\right)^{-1} \left(\hat{\Pi\!\!\!/} + m\right). \tag{3.15}$$

Now, for any operator $\hat{A}$, we can write the identity

$$(\hat{A} + i\epsilon)^{-1} = -i \int_0^\infty ds \, \exp\left[is(\hat{A} + i\epsilon)\right], \tag{3.16}$$

where $\epsilon \to 0^+$ is incorporated to ensure the convergence of the integration at $s = \infty$. Applying this identity to Eq. (3.14), we arrive at

$$\begin{aligned}
\mathcal{G}(x, x') &= -i \int_0^\infty ds \, \langle x| \exp\left[is\left(\hat{\not{\Pi}}^2 - m^2\right)\right]\left(\hat{\not{\Pi}} + m\right)|x'\rangle \\
&= -i \int_0^\infty ds \, e^{-ism^2} \langle x| \, e^{is\hat{\not{\Pi}}^2}\left(\hat{\not{\Pi}} + m\right)|x'\rangle \\
&= -i \int_0^\infty ds \, e^{-ism^2} \langle x(s)|\left(\hat{\not{\Pi}} + m\right)|x'\rangle .
\end{aligned} \tag{3.17}$$

We define $\hat{U}(s) = e^{-is\hat{H}}$, where $\hat{H} = -\hat{\not{\Pi}}^2$ and write $\langle x(s)| = \langle x| \, \hat{U}(s)$. Here s is a parameter which is loosely called proper time variable and likewise $\hat{U}(s)$ is identified as time-evolution operator. The coordinate space manifestation of $\hat{U}(s)$ is $\langle x|e^{-is\hat{H}}|x'\rangle = U(x, x'; s)$. So, we have

$$\mathcal{G}(x, x) = -i \int_0^\infty ds \, e^{-ism^2}\left[\langle x(s)| \, \hat{\not{\Pi}} \, |x'\rangle + mU(x, x'; s)\right]. \tag{3.18}$$

Now, we write down two important commutators as

$$\begin{aligned}
\left[\hat{\Pi}_\mu, \hat{X}_\nu\right] &= ig_{\mu\nu}, \\
\left[\hat{\Pi}_\mu, \hat{\Pi}_\nu\right] &= -iq\mathcal{F}_{\mu\nu},
\end{aligned} \tag{3.19}$$

where $\mathcal{F}_{\mu\nu} = \partial_\mu \mathcal{A}_\nu - \partial_\nu \mathcal{A}_\mu$ is the electromagnetic field strength tensor. In the case of constant background field, $\mathcal{F}_{\mu\nu}$ does not have any dependence on space-time coordinate. We can write

$$\begin{aligned}\hat{H} &= -\hat{\not{\Pi}}^2 = -\gamma^\mu\gamma^\nu\hat{\Pi}_\mu\hat{\Pi}_\nu = -\gamma^\mu\gamma^\nu\left(\hat{\Pi}_\nu\hat{\Pi}_\mu - iq\mathcal{F}_{\mu\nu}\right)\\ &= -\gamma^\mu\gamma^\nu\hat{\Pi}_\nu\hat{\Pi}_\mu + iq\gamma^\mu\gamma^\nu\mathcal{F}_{\mu\nu} = \left(\gamma^\nu\gamma^\mu - 2g^{\mu\nu}\right)\hat{\Pi}_\nu\hat{\Pi}_\mu + iq\mathcal{F}_{\mu\nu}\left(g^{\mu\nu} - i\sigma^{\mu\nu}\right)\\ &= \hat{\not{\Pi}}^2 - 2\hat{\Pi}^2 + q\mathcal{F}_{\mu\nu}\sigma^{\mu\nu} = -H - 2\hat{\Pi}^2 + q\mathcal{F}_{\mu\nu}\sigma^{\mu\nu},\end{aligned} \tag{3.20}$$

where $\sigma^{\mu\nu} \equiv \frac{i}{2}\left(\gamma^\mu\gamma^\nu - \gamma^\nu\gamma^\mu\right)$, $\gamma^\mu\gamma^\nu = g^{\mu\nu} - i\sigma^{\mu\nu}$ and $\{\gamma_\mu, \gamma_\nu\} = 2g^{\mu\nu}$. So, we obtain

$$\hat{H} = \frac{q}{2}\mathcal{F}_{\mu\nu}\sigma^{\mu\nu} - \hat{\Pi}^2. \tag{3.21}$$

Now, we can write the equation of motion

$$i\frac{\partial}{\partial s}U(x, x'; s) = H(x, \partial)U(x, x'; s). \tag{3.22}$$

Here $H(x, \partial)$ is the function space manifestation of the operator $\hat{H}$. Now, the equations governing the evolution of $\hat{X}(s)$ and $\hat{\Pi}(s)$ are given as

$$\frac{d}{ds}\hat{X}^\mu(s) = i\left[\hat{H}, \hat{X}^\mu(s)\right], \tag{3.23}$$

$$\frac{d}{ds}\hat{\Pi}^\mu(s) = i\left[\hat{H}, \hat{\Pi}^\mu(s)\right]. \tag{3.24}$$

Now, we need to solve the equation of motions (3.23) and (3.24). Using $\left[\hat{\Pi}^\mu, \hat{X}^\nu\right] = ig^{\mu\nu}$, it is just a matter of few steps of operator algebra to show that

$$i\left[\hat{H}, \hat{X}^\mu\right] = 2\Pi^\mu, \tag{3.25}$$

$$i\left[\hat{H}, \hat{\Pi}^\mu\right] = 2\mathcal{F}^{\mu\nu}\Pi_\nu. \tag{3.26}$$

Thus, the equation of motions in Eq. (3.23) and Eq. (3.24) become

$$\frac{d}{ds}\hat{X}^{\mu}(s) = 2\hat{\Pi}^{\mu}(s), \tag{3.27}$$
$$\frac{d}{ds}\hat{\Pi}^{\mu}(s) = 2\mathcal{F}^{\mu\nu}\hat{\Pi}_{\nu}(s). \tag{3.28}$$

Note that Eq. (3.28) and Eq. (3.27) are valid for the case of constant electromagnetic field. Now, we consider the field to be directed along the +ve z direction in space. In this case, only the components $\mathcal{F}_{12}$ and $\mathcal{F}_{21}$ survive and are given as

$$\mathcal{F}_{12} = -\mathcal{F}_{21} = -B. \tag{3.29}$$

In this case, we arrange Eq. (3.28) and Eq. (3.27) in matrix form to solve them in a convenient manner. For this purpose, we arrange the parallel and perpendicular components of $\hat{X}$ and $\hat{\Pi}$ in a two by two matrix form as given below

$$\hat{X}_{\shortparallel} = \begin{pmatrix} \hat{X}^0 \\ \hat{X}^3 \end{pmatrix}, \qquad \hat{X}_{\perp} = \begin{pmatrix} \hat{X}^1 \\ \hat{X}^2 \end{pmatrix}, \tag{3.30}$$
$$\hat{\Pi}_{\shortparallel} = \begin{pmatrix} \hat{\Pi}^0 \\ \hat{\Pi}^3 \end{pmatrix}, \qquad \hat{\Pi}_{\perp} = \begin{pmatrix} \hat{\Pi}^1 \\ \hat{\Pi}^2 \end{pmatrix}. \tag{3.31}$$

So, the equation of motions become

$$\frac{d}{ds}\hat{X}_{\shortparallel}(s) = 2\Pi_{\shortparallel}(s), \qquad \frac{d}{ds}\hat{X}_{\perp}(s) = 2\Pi_{\perp}(s), \tag{3.32}$$
$$\frac{d}{ds}\hat{\Pi}_{\shortparallel}(s) = 0, \qquad \frac{d}{ds}\hat{\Pi}_{\perp}(s) = 2qB\mathbb{F}\hat{\Pi}_{\perp}(s). \tag{3.33}$$

Here $\mathbb{F} = i\sigma_y$, where we denote the $i^{\rm th}$ component of Pauli spin matrix as σ_i with $i = x, y, z$. The solutions of Eq. (3.32) and Eq. (3.33) are given as

$$\hat{X}_{\shortparallel}(s) = \hat{X}_{\shortparallel}(0) + 2s\hat{\Pi}_{\shortparallel}(0), \qquad \hat{X}_{\perp}(s) = \hat{X}_{\perp}(0) + \frac{i\sigma_y}{qB}\left(e^{i2qBs\sigma_y} - 1\right)\hat{\Pi}_{\perp}(0), \tag{3.34}$$

$$\hat{\Pi}_{\shortparallel}(s) = \hat{\Pi}_{\shortparallel}(0), \qquad \hat{\Pi}_{\perp}(s) = \hat{\Pi}_{\perp}(0)e^{i2qBs\sigma_y}. \tag{3.35}$$

The expression of $\hat{X}_{\perp}(s)$ in Eq. (3.35) can be further simplified by applying the identity

$$e^{i\boldsymbol{\sigma}.\boldsymbol{a}} = \cos(|\boldsymbol{a}|) + i\boldsymbol{\sigma}.\boldsymbol{a}\frac{\sin(|\boldsymbol{a}|)}{|\boldsymbol{a}|} \tag{3.36}$$

to obtain

$$\hat{X}_{\perp}(s) = \hat{X}_{\perp}(0) - 2\frac{\sin(|qB|s)}{|qB|}e^{iqBs\sigma_y}\hat{\Pi}_{\perp}(0). \tag{3.37}$$

Note that $\hat{\not{\Pi}}$ operator is sandwiched between $\langle x(s)|$ and $|x'\rangle$. So using Eq. (3.34) and (3.35), we write $\hat{\Pi}$ in terms of $\hat{X}$ and apply $\hat{X}^{\mu}(0)\,|x'\rangle = x'^{\mu}\,|x'\rangle$ and $\langle x(s)|\,\hat{X}^{\mu}(s) = \langle x(s)|\,x^{\mu}$ to get

$$\langle x(s)|\,\hat{\not{\Pi}}_{\shortparallel}\,|x'\rangle = \frac{1}{2s}\left(\not{x}_{\shortparallel} - \not{x}'_{\shortparallel}\right)U(x, x'; s) \tag{3.38}$$

and

$$\begin{aligned}\langle x(s)|\,\hat{\not{\Pi}}_{\perp}\,|x'\rangle = \frac{|qB|}{2\sin(|qB|s)}&\left[\cos(|qB|s) + \mathsf{sgn}(qB)\sin(|qB|s)\gamma^1\gamma^2\right]\\ &\left(\not{x} - \not{x}'_{\perp}\right)U(x, x'; s).\end{aligned} \tag{3.39}$$

So, we have

$$\langle x(s)|\,\hat{\not{\Pi}}\,|x'\rangle = \frac{1}{2}\left\{\frac{1}{s}\left(\not{x}_{\shortparallel} - \not{x}'_{\shortparallel}\right) - \frac{|qB|}{\sin(|qB|s)}\left[\cos(|qB|s) + \mathsf{sgn}(qB)\sin(|qB|s)\right]\right.$$
$$\left.\left(\not{x}_{\perp} - \not{x}'_{\perp}\right)\right\} U(x,x';s). \quad (3.40)$$

Now, we are left to determine $U(x,x';s) = \langle x|\, e^{-is\hat{H}}\,|x'\rangle$. Note that

$$i\frac{\partial}{\partial s}U(x,x';s) = \langle x|\, e^{-is\hat{H}}\hat{H}\,|x'\rangle = \langle x(s)|\,\hat{H}\,|x'\rangle\,. \quad (3.41)$$

Unlike evaluating by inserting directly the complete set of eigenkets of $\hat{H}$ between $e^{-is\hat{H}}$ and $|x'\rangle$ in the expression of $U(x,x';s)$, the trick is to first compute $\langle x(s)|\,\hat{H}\,|x'\rangle$ and solve the obtained differential equation to get $U(x,x';s)$. So, we have

$$\begin{aligned}\langle x(s)|\,H\,|x'\rangle &= -\Big(\langle x(s)|\,\hat{\Pi}^2\,|x'\rangle + iqB\gamma^1\gamma^2\,\langle x(s)|x'\rangle\Big)\,,\\ &= -\Big(\langle x(s)|\,\hat{\Pi}^2_{\shortparallel}\,|x'\rangle - \langle x(s)|\,\hat{\Pi}^2_{\perp}\,|x'\rangle + iqB\gamma^1\gamma^2\,\langle x(s)|x'\rangle\Big)\,. \end{aligned} \quad (3.42)$$

For the parallel part, the matrix element becomes

$$\langle x(s)|\,\hat{\Pi}^2_{\shortparallel}\,|x'\rangle = \left[\frac{1}{4s^2}\left(x_{\shortparallel} - x'_{\shortparallel}\right)^2 + \frac{i}{s}\right]U(x,x';s). \quad (3.43)$$

Here we used commutation relations

$$\left[\hat{X}^0(0), \hat{X}^0(s)\right] = 2is, \qquad \left[\hat{X}^3(0), \hat{X}^3(s)\right] = -2is, \quad (3.44)$$

which is obtained by expressing $\hat{X}_{\shortparallel}(s)$ in terms of $\hat{X}_{\shortparallel}(0)$ and $\hat{\Pi}_{\shortparallel}(0)$ from the first relation shown in Eq. (3.34). Now the calculation of the perpendicular part is a little bit involved than its parallel counterpart. Firstly, we compute the commutation relation

$$s\left[\hat{X}^i(0),\hat{X}^j(s)\right]=-2\frac{\sin(|qB|s)}{|qB|}\left(\mathcal{R}^{-1}\right)^{jk}\left[\hat{X}^i(0),\hat{\Pi}^k(0)\right]=2i\frac{\sin(|qB|s)}{|qB|}\left(\mathcal{R}^{-1}\right)^{jk}\delta^{ik}$$
$$=2i\frac{\sin(|qB|s)}{|qB|}\left(\mathcal{R}^{-1}\right)^{ji}, \tag{3.45}$$

with $i=1,2$, where

$$\mathcal{R}=e^{-iqBs\sigma_y}=\begin{pmatrix}\cos(|qB|s) & -\mathsf{sgn}(qB)\sin(|qB|s)\\ \mathsf{sgn}(qB)\sin(|qB|s) & \cos(|qB|s)\end{pmatrix}. \tag{3.46}$$

So we have

$$\langle x(s)|\,\hat{\Pi}_\perp^2\,|x'\rangle=\sum_{i=1,2}\langle x(s)|\,\hat{\Pi}^i\hat{\Pi}_\perp^i\,|x'\rangle$$
$$=\frac{|qB|^2}{4\sin^2(|qB|s)}\sum_{i,j,k}\delta^{jk}\left[\left(x-x'\right)^j\left(x-x'\right)^k-2i\frac{\sin(|qB|s)}{|qB|}\left(\mathcal{R}^{-1}\right)^{jj}\right]. \tag{3.47}$$

Using the unitary property of $\mathcal{R}$, we use $\mathcal{R}^{ij}\mathcal{R}^{ik}=\left(\mathcal{R}^T\right)^{ji}\mathcal{R}^{ik}=\delta^{jk}$ and $\sum_{j=1,2}\left(\mathcal{R}^{-1}\right)^{jj}=2\cos(|qB|s)$ to get the last line of the last equation and we arrive at

$$\langle x(s)|\,\hat{\Pi}_\perp^2\,|x'\rangle=\left[\frac{|qB|^2}{4\sin^2(|qB|s)}\left(x-x'\right)^2-i\frac{|qB|}{\tan(|qB|s)}\right]U(x,x';s). \tag{3.48}$$

Putting Eq. (3.43) and Eq. (3.48) in Eq. (3.42), we get

$$\langle x(s)|\,\hat{H}\,|x'\rangle=-f(x,x',s)U(x,x';s), \tag{3.49}$$

where

$$f(x,x',s)=\frac{1}{4s^2}\left(x-x'\right)_\parallel^2-\frac{|qB|^2}{4\sin^2(|qB|s)}\left(x-x'\right)_\perp^2+i\left(\frac{1}{s}+\frac{|qB|}{\tan(|qB|s)}\right)+i\gamma^1\gamma^2qB. \tag{3.50}$$

So from Eq. (3.41), we get the differential equation satisfied by $U(x, x'; s)$ as

$$i\frac{\partial}{\partial s}U(x, x', s) = -f(x, x', s)U(x, x', s). \tag{3.51}$$

Eq. (3.51) can be solved as

$$U(x, x'; s) = C(x, x') \exp\left[i\int^{s} ds' f(x, x', s')\right]. \tag{3.52}$$

Here $C(x, x')$ is the constant of integration which is independent of s. Thus, we get the expression of $U(x, x'; s)$ as

$$U(x, x'; s) = C(x, x')\frac{1}{s\ \sin(|qB|s)} \exp\left[-\frac{i}{4}\left(\frac{1}{s}(x-x')^2_{\shortparallel} - \frac{|qB|}{\tan(|qB|s)} (x-x')^2_{\perp}\right) - qBs\gamma^1\gamma^2\right]. \tag{3.53}$$

Substituting Eq. (3.53) and Eq. (3.40) in Eq. (3.18) we get

$$\mathcal{G}(x, x') = -iC(x, x')\int_0^\infty ds\frac{e^{-ism^2}}{s\ \sin(|qB|s)}\left[\frac{1}{2}\left\{\frac{1}{s}\left(\not{x}_{\shortparallel} - \not{x}'_{\shortparallel}\right) - \frac{|qB|}{\sin(|qB|s)}\right.\right.$$
$$\left.\left.\left[\cos(|qB|s) + \mathsf{sgn}(qB)\sin(|qB|s)\gamma^1\gamma^2\right]\left(\not{x}_{\perp} - \not{x}'_{\perp}\right)\right\} + m\right]$$
$$\times \exp\left[-\frac{i}{4}\left(\frac{(x-x')^2_{\shortparallel}}{s} - \frac{|qB|}{\tan(|qB|s)}(x-x')^2_{\perp}\right)\right] e^{-qBs\gamma^1\gamma^2}. \tag{3.54}$$

We define $r^\mu = x^\mu - x'^\mu$. So Green function can be written as $\mathcal{G}(x, x') = C(x, x')G(r)$, where

$$G(r) = -i\int_0^\infty \frac{ds}{s\ \sin(|qB|s)}\left[\left(\frac{1}{2s}\not{r}_{\shortparallel} + m\right)e^{-qBs\gamma^1\gamma^2} - \frac{|qB|}{2\sin(|qB|s)}\not{r}_{\perp}\right]$$
$$\times \exp\left[-i\left(\frac{r^2_{\shortparallel}}{4s} - \frac{|qB|}{4\tan(|qB|s)}r^2_{\perp} + s\,m^2\right)\right]. \tag{3.55}$$

We note that the Green's function do have a translational invariant part $G(r)$.

Now we wish to evaluate momentum space representation of $\mathcal{G}(x,x')$. But as discussed earlier, the factor $C(x,x')$ is gauge dependent and in general breaks translational symmetry of the propagator which is clear from Eq. (3.54). So, unlike in zero background field case, it is not convenient to define the Fourier transformation of $\mathcal{G}(x,x')$ without choosing a gauge for the vector potential of the background field. Therefore, we can choose a gauge in which $C(x,x') = 1$ for convenience. In this circumstance, translational invariance is restored. This allows us to define the momentum space Green function $\mathcal{G}(p)$ via Fourier transformation of $\mathcal{G}(x,x')$ as $\widetilde{G}(p) = \int d^4 r e^{ip.r} G(r)$. To evaluate the r integral, we analytically continue the expression of $G(r)$ to the Euclidean space-time achieved through a series of transformation $s \to -is_E$, $r_0 \to -i\tau_r$. So, the propagator takes the following form

$$G(r) = \int_0^\infty \frac{ds_E}{s_E \sinh(|qB|s_E)} \left[\left(-\frac{i}{2s}\not{r}^E_{\shortparallel} + m\right) e^{iqBs_E\gamma^1\gamma^2} - i\frac{|qB|}{2\sinh(|qB|s_E)}\not{r}_\perp\right] \exp\left[-\left(\frac{\tau_r^2 + r_3^2}{4s} + \frac{|qB|}{4\tanh(|qB|s)}(r_1^2 + r_2^2) + sm^2\right)\right], \quad (3.56)$$

where we define $\not{r}^E_{\shortparallel} = \gamma^3 r^3 + \gamma^4 \tau_r$ with $\gamma^4 = i\gamma^0$.

In Euclidean space, the Fourier transformation of a function f is defined as

$$\tilde{f}(\omega, \boldsymbol{p}) = \int_{-\infty}^{\infty} d\tau \int d^3x \exp\left[-i(\boldsymbol{p}.\boldsymbol{x} + \omega\tau)\right] f(\tau, \boldsymbol{x}). \quad (3.57)$$

To compute the Fourier transformation, we have to tackle the following r integrals

$$\mathcal{I} = \int d^4r_{_E}\ e^{-i(\omega\tau_r + \boldsymbol{p}.\boldsymbol{r})} \exp\left[-\left(\frac{r_3^2+\tau_r^2}{4s_{_E}} + \frac{|qB|}{\tanh(|qB|s_{_E})}(r_1^2+r_2^2)\right)\right], \tag{3.58}$$

$$\mathcal{I}_{\shortparallel} = \int d^4r_{_E}\ e^{-i(\omega\tau_r + \boldsymbol{p}.\boldsymbol{r})} \not{r}^E_{\shortparallel} \exp\left[-\left(\frac{r_3^2+\tau_r^2}{4s_{_E}} + \frac{|qB|}{\tanh(|qB|s_{_E})}(r_1^2+r_2^2)\right)\right], \tag{3.59}$$

$$\mathcal{I}_{\perp} = \int d^4r_{_E}\ e^{-i(\omega\tau_r + \boldsymbol{p}.\boldsymbol{r})} \not{r}^E_{\perp} \exp\left[-\left(\frac{r_3^2+\tau_r^2}{4s_{_E}} + \frac{|qB|}{\tanh(|qB|s_{_E})}(r_1^2+r_2^2)\right)\right], \tag{3.60}$$

where $\int d^4r_{_E} \equiv \int\limits_{-\infty}^{\infty} d\tau_r \int d^3r$. These can be done by using the following basic Gaussian integral

$$\int\limits_{-\infty}^{\infty} dx\ e^{-ibx}e^{-ax^2} = \sqrt{\frac{\pi}{a}}e^{-\frac{b^2}{4a}}, \tag{3.61}$$

$$\int\limits_{-\infty}^{\infty} dx\ x\, e^{-ibx}e^{-ax^2} = -i\frac{b}{2a}\sqrt{\frac{\pi}{a}}e^{-\frac{b^2}{4a}} \tag{3.62}$$

and the result is quoted below

$$\mathcal{I} = \frac{(4\pi)^2}{|qB|}\frac{s\tanh(|qB|s_{_E})}{|qB|}\exp\left[-s_{_E}(p_4^2+p_3^2) - \frac{\tanh(|qB|s_{_E})}{|qB|}(p_1^2+p_2^2)\right], \tag{3.63}$$

$$\mathcal{I}_{\shortparallel} = 2is_{_E}\mathcal{I}, \tag{3.64}$$

$$\mathcal{I}_{\perp} = -2i\frac{\tanh(|qB|s_{_E})}{|qB|}\mathcal{I}. \tag{3.65}$$

Using the results of integrations shown in Eq. (3.63)-(3.65), we get $\widetilde{\mathcal{G}}(p)$ as

$$\widetilde{G}(p) = \frac{(4\pi)^2}{|qB|}\int\limits_0^{\infty} ds_{_E}\ \Big[\big(\gamma_4p_4 - \gamma^3p^3 + m\big)\left(\mathbb{1} + i\mathsf{sgn}(qB)\tanh(|qB|s_{_E})\gamma^1\gamma^2\right) - \frac{1}{\cosh^2(|qB|s_{_E})}\left(\gamma^1p^1+\gamma^2p^2\right)\Big] \times \exp\left[-s_{_E}\left(p_{\shortparallel}^2 + \frac{\tanh(|qB|s_{_E})}{|qB|s_{_E}}p_\perp^2 + m^2\right)\right]. \tag{3.66}$$

Now, we go back to the Minkowski space and finally write the momentum space propagator as [1]

$$\widetilde{G}(p) = i\frac{(4\pi)^2}{|qB|}\int\limits_0^\infty ds\,\Big\{\big(p^0\gamma^0 - p^3\gamma^3 + m\big)\left[\mathbb{1} - \mathsf{sgn}(qB)\tan(|qB|s)\gamma^1\gamma^2\right] - \sec^2(|qB|s)\left(p^1\gamma^1 + p^2\gamma^2\right)\Big\} \times \exp\left[is\left(p_0^2 - (p^3)^2 - \frac{\tanh(|qB|s)}{|qB|s}\left[(p^1)^2 + (p^2)^2\right] - m^2\right)\right]. \tag{3.67}$$

This happened due to the sign difference in the expression of D_μ.

3.4 The Phase Factor

The term $C(x,x')$ do not have any s dependence as indicated in previous section. It satisfies the following differential equations

$$\left[i\,\partial_\mu - q\,\mathcal{A}_\mu(x) + \frac{1}{2}\,q\,\mathcal{F}_{\mu\nu}\,(x'-x)^\nu\right] C\,(x,x') = 0, \tag{3.68}$$

$$\left[-i\,\partial'_\mu - q\,\mathcal{A}_\mu\,(x') - \frac{1}{2}\,q\,\mathcal{F}_{\mu\nu}\,(x'-x)^\nu\right] C\,(x,x') = 0. \tag{3.69}$$

Integrating Eq. (3.68) and Eq. (3.69), we get

$$C(x,x') = C'(x',x')\,\exp\left[-i\,q\int_{x'}^{x} d\xi^\mu\left(\mathcal{A}_\mu(\xi) + \frac{1}{2}\mathcal{F}_{\mu\nu}(\xi - x')^\nu\right)\right] \tag{3.70}$$

$$C(x,x') = C'(x,x)\,\exp\left[-i\,q\int_{x'}^{x} d\xi^\mu\left(\mathcal{A}_\mu(\xi) + \frac{1}{2}\mathcal{F}_{\mu\nu}(\xi - x)^\nu\right)\right]. \tag{3.71}$$

Equating (3.70) and (3.71), we have $C'(x',x') = C'(x,x)$. It follows from the fact that, since $\mathcal{F}_{\mu\nu}$ is antisymmetric, $(x-x')^\mu\mathcal{F}_{\mu\nu}(x-x')^\nu = 0$. Thus we conclude from the last line that $C'(x,x)$ is just a constant. Note that the integral in

[1] In this chapter, we denote the complete momentum four-vector in Minkowsky space in small letter, i.e., $p^\mu = (p_0, \boldsymbol{p})$. For the parallel and the perpendicular components we adopt $\not{p}_{_\shortparallel} = p_0\gamma_0 - p^3\gamma^3$, $\not{p}_{_\perp} = p^1\gamma^1 + p^2\gamma^2$ and $p_{_\shortparallel}^2 = (p_0)^2 - (p^3)^2$ and $p_{_\perp}^2 = (p^1)^2 + (p^2)^2$

(3.71) is independent of the integration path connecting the points x and x' as the curl of the term $\mathcal{A}_\mu(\xi) + \frac{1}{2}\mathcal{F}_{\mu\nu}(\xi - x)^\nu$ vanishes. Now the curl of a four-vector is not a four-vector like ordinary three-vector but a 2nd rank tensor. For any four-vector $V_\mu(x)$, the curl is proportional to the term $\frac{\partial}{\partial x^\mu}V_\nu(x) - \frac{\partial}{\partial x^\nu}V_\mu(x)$. In our case $V_\mu(\xi) = \mathcal{A}_\mu(\xi) + \frac{1}{2}\mathcal{F}_{\mu\nu}(\xi - x)^\nu$ and we can show that $\frac{\partial}{\partial \xi^\mu}V_\nu(\xi) - \frac{\partial}{\partial \xi^\nu}V_\mu(\xi) = 0$.

Proof:

$$
\begin{aligned}
&\frac{\partial}{\partial \xi^\mu}V_\nu(\xi) - \frac{\partial}{\partial \xi^\nu}V_\mu(\xi)\\
&= \frac{\partial}{\partial \xi^\mu}\mathcal{A}_\nu(\xi) - \frac{\partial}{\partial \xi^\nu}\mathcal{A}_\mu(\xi) + \frac{1}{2}\left[\mathcal{F}_{\nu\alpha}\frac{\partial}{\partial \xi^\mu}\left(\xi^\alpha - x'^\alpha\right) - \mathcal{F}_{\mu\alpha}\frac{\partial}{\partial \xi^\nu}\left(\xi^\alpha - x'^\alpha\right)\right]\\
&= \mathcal{F}_{\mu\nu} + \frac{1}{2}\left[\mathcal{F}_{\nu\alpha}\delta_\mu{}^\alpha - \mathcal{F}_{\mu\alpha}\delta_\nu{}^\alpha\right]\\
&= \mathcal{F}_{\mu\nu} + \frac{1}{2}\left[\mathcal{F}_{\nu\mu} - \mathcal{F}_{\mu\nu}\right]\\
&= \mathcal{F}_{\mu\nu} + \mathcal{F}_{\nu\mu}\\
&= 0 \qquad\qquad\qquad\qquad (QED)
\end{aligned}
$$

This gives us freedom to choose the path connecting x' and x as a straight line. The straight line is parameterized by t as follows

$$
\xi^\mu(t) = x'^\mu + t\left(x^\mu - x'^\mu\right) \qquad \text{with } \; t \in [0,1] \tag{3.72}
$$

This choice is consistent as can be seen by noting that $\xi^\mu(1) = x'^\mu$ and $\xi^\mu(0) = x^\mu$. In symmetric gauge $\mathcal{A}^\mu(x) = \frac{B}{2}(0, -y, x, 0)$ leading to

$$
\int_{x'}^{x} d\xi^\mu\, \mathcal{A}_\mu(\xi) = \frac{B}{2}\left(x'^1 x^2 - x'^2 x^1\right). \tag{3.73}
$$

The term

$$\int_{x'}^{x} d\xi^{\mu}\,\frac{1}{2}\mathcal{F}_{\mu\nu}\,(\xi-x)^{\nu} = \int_{0}^{1} dt\,(x^{\mu}-x'^{\mu})\frac{1}{2}\mathcal{F}_{\mu\nu}\,(x^{\nu}-x'^{\nu})(t-1) \tag{3.74}$$

$$= (x^{\mu}-x'^{\mu})\frac{1}{2}\mathcal{F}_{\mu\nu}\,(x^{\nu}-x'^{\nu}) \int_{0}^{1} dt\ (t-1) \tag{3.75}$$

$$= 0. \tag{3.76}$$

So, in the symmetric gauge, $\Phi(x,x') \equiv \exp\left[-i\,q\,\int_{x'}^{x} d\xi^{\mu}\,\left(\mathcal{A}_{\mu}(\xi)+\frac{1}{2}\mathcal{F}_{\mu\nu}\,(\xi-x)^{\nu}\right)\right] = \exp\left[\frac{-i\,q\,B}{2}\left(x'^{1}x^{2}-x'^{2}x^{1}\right)\right]$. The four-vector potential enjoys gauge symmetry. So for the same field configuration, we can choose another four-vector potential defined by

$$\mathcal{A}'_{\mu}(\xi) \equiv \mathcal{A}_{\mu}(\xi) + \frac{\partial}{\partial\xi^{\mu}}\Lambda(\xi), \tag{3.77}$$

where $\Lambda(\xi)$ is a function of ξ which we choose as

$$\Lambda(\xi) = \frac{B}{2}\left(y\ \xi^{1} - x\ \xi^{2}\right). \tag{3.78}$$

So, in the $\mathcal{A}'$ gauge

$$\begin{aligned}
\Phi(x,x') &= \exp\left[-i\,q\,\int_{x'}^{x} d\xi^{\mu}\,\left(\mathcal{A}'_{\mu}(\xi)+\frac{1}{2}\mathcal{F}_{\mu\nu}\,(\xi-x)^{\nu}\right)\right] \\
&= \exp\left[-i\,q\,\int_{x'}^{x} d\xi^{\mu}\,\left(\mathcal{A}_{\mu}(\xi)+\frac{1}{2}\mathcal{F}_{\mu\nu}\,(\xi-x)^{\nu}\right) - i\,q\,\int_{x}^{x'} d\xi^{\mu}\,\Lambda(\xi)\right] \\
&= \exp\left[-i\,q\,\int_{x'}^{x} d\xi^{\mu}\,\left(\mathcal{A}_{\mu}(\xi)+\frac{1}{2}\mathcal{F}_{\mu\nu}\,(\xi-x)^{\nu}\right)\right] \exp\left[-i\,q\,\int_{x}^{x'} d\xi^{\mu}\,\frac{\partial}{\partial\xi^{\mu}}\Lambda(\xi)\right] \\
&= \exp\left[\frac{-i\,q\,B}{2}\left(x'^{1}x^{2}-x'^{2}x^{1}\right)\right] \exp\left[-i\,q\,\left(\Lambda(x')-\Lambda(x)\right)\right] \\
&= \exp\left[\frac{-i\,q\,B}{2}\left(x'^{1}x^{2}-x'^{2}x^{1}\right)\right] \exp\left[\frac{i\,q\,B}{2}\left(x'^{1}x^{2}-x'^{2}x^{1}\right)\right] \\
&= \exp\left(0\right) \\
&= 1.
\end{aligned} \tag{3.79}$$

So, essentially in this special special gauge, $C(x, x')$ is just a constant C and we can choose it to be $C = -\frac{|qB|}{(4\pi)^2}$. Also note that C is exactly the same as the degeneracy associated with LLL. Finally, the expression of the momentum space fermion propagator in presence of time independent uniform background magnetic field is given as

$$\begin{aligned}\widetilde{G}(p) = -i\int_0^\infty ds \Big\{ &\left(p^0\gamma^0 - p^3\gamma^3 + m\right)\left[\mathbb{1} - \mathsf{sgn}(qB)\tan(|qB|s)\gamma^1\gamma^2\right] - \sec^2(|qB|s) \\ &\times \left(p^1\gamma^1 + p^2\gamma^2\right)\Big\} \times \exp\left[is\left(p_0^2 - (p^3)^2 - \frac{\tanh(|qB|s)}{|qB|s}\left[(p^1)^2 + (p^2)^2\right]\right.\right. \\ &\left.\left. -m^2 + i\epsilon\right)\right],\end{aligned} \tag{3.80}$$

where the $i\epsilon$ with $\epsilon \to 0^+$ is introduced to make the integral finite at $s \to \infty$.

3.5 Landau Level Representation

In this section, we derive an alternative representation of the expression of fermion propagator $\mathcal{G}(p)$ shown in Eq. (3.80) [196]. The propagator is essentially written as a sum over the contribution coming from all the *Landau levels*. To do this, we start by performing the s integration in Eq. (3.80) by employing the following identity of generalised Laguerre polynomial

$$\sum_{\ell=0}^{\infty} L_\ell^{(\alpha)}(x)t^\ell = \frac{\exp\left(-\frac{t\,x}{1-t}\right)}{(1-t)^{\alpha+1}} \qquad (|t| \leq 1) \tag{3.81}$$

Setting $\alpha = 0$ and rearranging the sum, i is easy to show

$$\exp\left(-\frac{xt}{1-t}\right) = \sum_{\ell=0}^{\infty}\left[L_\ell(x) - L_{\ell-1}(x)\right]t^\ell, \tag{3.82}$$

where $L_\ell^{(0)}(x) \equiv L_\ell(x)$ and also $L_{-1}(x) = 0$ by definition. We can rearrange $\tan(|qB|s)$ in the exponential to get

$$e^{-i\frac{p_\perp^2}{|qB|}\tan(|qB|s)} = \exp\left(\frac{\alpha_p}{2}\frac{v+1}{v-1}\right) = \exp\left(-\frac{\alpha_p}{2}\right)\exp\left(-\frac{\alpha_p v}{1-v}\right), \tag{3.83}$$

where $v \equiv -e^{-i2|qB|s}$ and $\alpha_p \equiv \frac{2p_\perp^2}{|qB|}$. With the help of identity in Eq. (3.82) and Eq. (3.83), we can write

$$\exp\left(-i\frac{p_\perp^2}{|qB|}\tan(|qB|s)\right) = \exp\left(-\frac{\alpha_p}{2}\right)\sum_{\ell=0}^{\infty}(-1)^\ell\big[L_\ell(\alpha_p) - L_{\ell-1}(\alpha_p)\big]e^{-i2\ell|qB|s}. \tag{3.84}$$

Now, we can cast the integral in Eq. (3.80) as

$$\mathcal{G}(p) = \left(\not{p}_{_\shortparallel} + m\right)\left[I_0 - \mathsf{sgn}(qB)\gamma^1\gamma^2 I_1\right] - \not{p}_{_\perp} I_3, \tag{3.85}$$

where

$$I_0 = \int_0^\infty ds\, e^{-i\frac{p_\perp^2}{|qB|}\tan(|qB|s)} e^{is(p_\shortparallel^2 - m^2 + i\epsilon)}, \tag{3.86}$$

$$I_1 = \int_0^\infty ds\, \tan(|qB|s) e^{-i\frac{p_\perp^2}{|qB|}\tan(|qB|s)} e^{is(p_\shortparallel^2 - m^2 + i\epsilon)}, \tag{3.87}$$

$$I_3 = \int_0^\infty ds\, \sec^2(|qB|s) e^{-i\frac{p_\perp^2}{|qB|}\tan(|qB|s)} e^{is(p_\shortparallel^2 - m^2 + i\epsilon)}. \tag{3.88}$$

Now, it is easy to see that I_1 and I_2 can be expressed in terms of I_0 as

$$I_1 = 2\,i\,\mathsf{sgn}(qB)\,\frac{\partial I_0}{\partial \alpha_p}\,, \tag{3.89}$$

$$I_2 = I_0 - 4\,\frac{\partial^2 I_0}{\partial \alpha_p^2}\,. \tag{3.90}$$

From Eq. (3.84), we can perform the I_0 integral very easily and obtain

$$I_0 = ie^{-\frac{p_\perp^2}{|qB|}} \sum_{\ell=0}^{\infty} (-1)^\ell \frac{L_\ell(\alpha_p) - L_{\ell-1}(\alpha_p)}{p_\shortparallel^2 - 2\ell|qB| - m^2 + i\epsilon}. \tag{3.91}$$

Now, putting Eq. (3.91) in Eq. (3.89) and Eq. (3.90), we get the expression of I_1 and I_2. Lastly, substituting the resulting expression of I_0, I_1 and I_2 written in terms of infinite sum over ℓ in Eq. (3.85), we arrive at Landau level representation of the fermion propagator in background magnetic field as

$$\mathcal{G}(p) = \exp\left(-\frac{p_\perp^2}{|qB|}\right) \sum_{\ell=0}^{\infty} (-1)^\ell \frac{D_\ell(p, qB)}{p_\shortparallel^2 - 2\ell|qB| - m^2 + i\epsilon}, \tag{3.92}$$

where the factor $D_\ell(p, qB)$ in the numerator is defined as

$$D_\ell(p, qB) \equiv \left(\not{p}_\shortparallel + m\right) \left\{ \left[\mathbb{1} + i\mathsf{sgn}(qB)\gamma^1\gamma^2\right] L_\ell\left(\frac{2p_\perp^2}{|qB|}\right) - \left[\mathbb{1} - i\mathsf{sgn}(qB)\gamma^1\gamma^2\right] L_{\ell-1}\left(\frac{2p_\perp^2}{|qB|}\right) \right\} + \not{p}_\perp L_{\ell-1}^{(1)}\left(\frac{2p_\perp^2}{|qB|}\right). \tag{3.93}$$

It is evident from the expression of Eq. (3.92), the propagator has a simple pole at $p_0 = \pm E_{\ell,p}$ for $\ell = 0, 1, 2, \cdots$ where

$$E_{\ell,p} = \sqrt{k_z^2 + 2\ell|qB| + m^2}. \tag{3.94}$$

3.6 The Strong and the Weak Field Limit of the Propagator

Calculations with the propagators in Eq. (3.92) and (3.67) are very cumbersome. So, we can make approximations when the field is strong or weak.

In the limit of very high background magnetic field (ideally in $|qB| \to \infty$ limit), the contributions coming from the $\ell \geq 1$ terms to the fermion propagator $S^B(p)$[2] becomes very substantial and thus can be neglected but in this circumstance $\ell = 0$ term survives as there is no $|qB|$ dependence in the denominator. It is called *strong field* or lowest Landau level (LLL) approximation. In this case the propagator becomes

$$S^B_{LLL}(p) = e^{-\frac{p_\perp^2}{|qB|}} \frac{\not{p}_{\shortparallel} + m}{p^2 - m^2 + i\epsilon} \left[\mathbb{1} + i\, \mathsf{sgn}(qB)\, \gamma^1\gamma^2\right]. \quad \textit{Strong field approximation (SFA)} \tag{3.95}$$

In the weak field limit, the full propagator can be written as a series in powers of qB as

$$S^B(p) = S^{(0)}(p) + qB\, S^{(1)}(p) + (qB)^2\, S^{(1)}(p) + \cdots \tag{3.96}$$

Here $S^{(0)}(p)$ part of the propagator is the exactly the same as that in absence of background field

$$S^{(0)}(p) = \frac{\not{p} + m}{p^2 - m^2}. \tag{3.97}$$

The expansion procedure is a bit involved. It can be performed step by step analytically as shown in Chyi et al [211]. Since it is sufficient to obtain the series in Eq. (3.96) upto $(qB)^1$, we employ Mathematica to get our job done. Starting from the proper time representation in Eq. (3.80), we obtain

$$S^B_{\mathsf{WFA}}(p) = \frac{\not{p} + m}{p^2 - m^2 + i\epsilon} - \frac{\not{p}_{\shortparallel} + m}{(p^2 - m^2 + i\epsilon)^2}\gamma^1\gamma^2\, qB + \mathcal{O}(qB)^2 \quad \text{Weak field approximation (WFA).} \tag{3.98}$$

[2]From now on, the fermion propagator will be denoted by the symbol S and B in the superscript or subscript will indicate the presence of background magnetic field

Note that the denominator of each term in the expansion has the structure $(p^2 - m^2)^n$ with n being positive integer.

3.7 Conclusion

In this chapter, we have explicitly derived fermion propagator in the presence of background magnetic field. We have also written down the strong and weak field limit of the propagator. Due to the presence of the phase factor $C(x, x')$, the propagator breaks gauge invariance as well as translational symmetry. But the latter can be restored by going to a particular gauge as discussed in section. It is important to note that the cancellation of phase factor to is no longer possible in complicated processes like in triangle diagram where there is three fermion propagators are multiplied together. In this situation, one is compelled to start the work in position space. In the rest of the thesis, we shall work in weak field approximation.

CHAPTER 4

Collective Behaviour of Quarks at High Temperature QGP

4.1 Introduction

At non-zero temperature, many physical quantities are modified as compared to zero-temperature field theory. As an example, quarks gain an temperature dependent effective mass. Also, they get dressed by the medium and behaves collectively in the plasma. Technically, they develop a quasi-particle or collective modes and exhibit some of the collective properties which are absent at zero temperature.

The collective modes are is generally characterised by their dependecies of energy on momentum encoded in dispersion law $\omega(\boldsymbol{p})$. Contrary to stable particle, collective modes posses a finite lifetime in the plasma which urge their decay rate $\Gamma(\boldsymbol{p})$ to be considered as a relevant parameter. Mathematically, the real part of the pole of the resummed propagator gives dispersion law whereas the imaginary part gives decay rate. The temperature T along with the strong coupling constant g introduces an energy scale of the hot medium. Since at high temperature the QCD coupling constant $g \ll 1$, the medium effects can vastly be studied by the method of pQCD.

Now, the phenomena which are important at soft energy scale gT are encoded in the behaviour of the collective excitations of quarks, gluons and photons.

In this chapter, we shall investigate the medium induced collective properties of quasi-quarks in hot QGP medium.

4.2 Covariant Description

At non-zero temperature, one of the most intriguing issue that arises is associated with Lorentz covariance and definition of temperature. The question that comes up is that in which frame, among the rest frame of the particle and the rest frame of plasma, the particle's motion should be described. It was addressed first by Planck and Einstein and later by Tolman [197], Pauli [198] and Ott [199]. Finally, Israel [200, 201] settled this issue by characterizing a fluid in thermodynamic equilibrium by a Lorentz invariant parameter T and the four-velocity vector u^μ of the heat bath. T is the temperature of the fluid in its own rest frame.

Consider a particle moving with momentum P^μ in medium. The higher order radiative correction will also involve the four-vector u^μ. Now, we have to construct Lorentz scalar variables of the theory from P^μ and u^μ. They are P^2, $P.u$ and u^2. But we have the constraint on u^μ that $u^2 = 1$. So, we have two Lorentz scalars variables. We choose these two variables as $P.u$ and $P.u - P^2$ for convenience. In this bin the rest frame of heat bath, we have $u^\mu = (1, 0, 0, 0)$ and

$$P.u = p_0, \qquad (P.u)^2 - P^2 = |\boldsymbol{p}|^2. \tag{4.1}$$

Thus, $P.u$ and $(P.u)^2 - P^2$ can be interpreted as energy and magnitude of three-momentum vector squared of particle in the rest frame of heat bath, respectively.

Since we will be working with the magnitude of three-vector, we drop the boldface notation, i.e., for any three vector $\boldsymbol{a}$, we shall denote its magnitude by a.

4.3 Structure of Quark Self Energy

The quark self energy has, apart from the dependence on four vectors P^μ and u^μ, a 4×4 matrix structure. Any 4×4 matrix can be written as a linear combination of 16 linearly independent basis matrices. In quantum field theory, one of the convenient choice of these basis is the set of gamma matrices $\Gamma = \left\{1, \gamma^5, \gamma^\mu, \gamma^\mu\gamma^5, \gamma^{[\mu}\gamma^{\nu]}\right\}$, namely, the identity matrix, γ^5 matrix, four γ^μ matrices, four $\gamma^\mu\gamma^5$ matrices and six $\gamma^{[\mu}\gamma^{\nu]}$ matrices. Here $\gamma^{[\mu}\gamma^{\nu]}$ denotes the anti-symmetric combination of γ^μ and γ^ν, i.e., $\gamma^\mu\gamma^\nu - \gamma^\nu\gamma^\mu$. So the general form of quark self energy reads

$$\Sigma = -a\mathbb{1} - a_5\gamma_5 - \left(bP^\mu + b'u^\mu\right)\gamma^\mu - \left(b_5P^\mu + b_5'u^\mu\right)\gamma^\mu\gamma_5 - f\left(P^\mu u^\nu + P^\nu u^\mu\right)\sigma^{\mu\nu}, \tag{4.2}$$

where $\sigma^{\mu\nu} = \dfrac{i}{2}\left(\gamma^\mu\gamma^\nu - \gamma^\nu\gamma^\mu\right)$. Here the coefficients associated with various basis matrices are analytic functions of Lorentz scalars $P.u$ and $P.u - P^2$.

In our context, Eq. (4.2) gets further simplified based on the following assumptions

- At high temperature, chiral symmetry of the plasma gets restored. So, the self energy is chirally symmetric. As a result, it anti-commutes with γ_5, i.e., $\{\gamma_5, \Sigma\} = 0$. This implies that the coefficients of $\mathbb{1}$, γ_5 are zero. The parity invariance of the theory does not allow $\gamma^\mu\gamma_5$ to appear in the self-energy Σ.

- Also, in one loop order, the terms involving $\sigma^{\mu\nu}$ will be absent.

Thus, the structure of self energy reads in one loop order as

$$\Sigma(P) = -\left(bP^{\mu} + b' u^{\mu}\right)\gamma^{\mu}. \tag{4.3}$$

We change the notation from b to a and b' to b in Eq. (4.3) and get

$$\Sigma(P) = -a\not{P} - b\not{u}. \tag{4.4}$$

From Eq. (4.4), we can extract the coefficients a, b as

$$\begin{aligned} a &= \frac{\mathrm{Tr}(\not{P}\Sigma) - (P.u)\mathrm{Tr}(\not{u}\Sigma)}{4\left[(P.u)^2 - P^2\right]}, \\ b &= \frac{P^2\mathrm{Tr}(\not{u}\Sigma) - (P.u)\mathrm{Tr}(\not{P}\Sigma)}{4\left[(P.u)^2 - P^2\right]}. \end{aligned} \tag{4.5}$$

In the rest frame of heat bath, Eq. (4.5) reduces to

$$\begin{aligned} a(p_0, p) &= \frac{1}{4p^2}\left[\mathrm{Tr}(\not{P}\Sigma) - p_0\mathrm{Tr}(\not{u}\Sigma)\right], \\ b(p_0, p) &= \frac{1}{4p^2}\left[P^2\mathrm{Tr}(\not{u}\Sigma) - p_0\mathrm{Tr}(\not{P}\Sigma)\right]. \end{aligned} \tag{4.6}$$

4.4 Quark Self Energy at Non-Zero Temperature

In this section, we shall evaluate the structure functions $a(p_0, p)$ and $b(p_0, p)$ up to one loop order in the strong coupling constant. The Feynman diagram relevant for this computation is depicted in Fig. 4.1. The quark propagator of flavour f takes

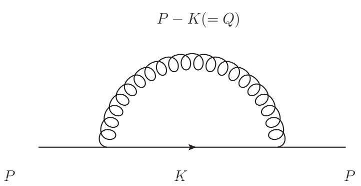

Figure 4.1: One loop Feynman diagram to compute quark self energy

the form

$$S_f(K) = \frac{\not{K} + m_f}{K^2 - m_f^2}, \tag{4.7}$$

where m_f is the current quark mass. The gluon propagator

$$iD^{ab}_{\mu\nu}(P - K) = \frac{-ig^{\mu\nu}\delta_{ab}}{(P - K)^2}. \tag{4.8}$$

The quark gluon vertex term is obtained from the interaction term in the Lagrangian as $ig\gamma^\mu T^a$. So, the expression of one-loop quark self energy of flavour f reads from Fig. 4.1 as

$$-i\Sigma(P) = \int \frac{d^4K}{(2\pi)^4}(ig\gamma^\mu T^a)\, iS_f(K)\, (ig\gamma^\nu T^b)\, iD^{ab}_{\mu\nu}(P - K). \tag{4.9}$$

Substituting Eq. (4.7) and Eq. (4.8) in Eq. (4.9), we obtain

$$\Sigma(P) = -ig^2 C_F \int \frac{d^4K}{(2\pi)^4} \frac{\gamma^\mu \left(\not{K} + m_f\right)\gamma_\mu}{\left(K^2 - m_f^2\right)\left[(P - K)^2 + i\epsilon\right]}. \tag{4.10}$$

Here, we define $C_F = (N_c^2 - 1)/2N_c$ which comes from the identity as

$$\sum_{a=1}^{N_c^2-1} T^a T^a = \frac{(N_c^2 - 1)}{2N_c}. \tag{4.11}$$

Simplifying Eq. (4.10), we get

$$\Sigma(P) = -i2g^2 C_F \int \frac{d^4K}{(2\pi)^4} \frac{2m_f - \not{K}}{\left(K^2 - m_f^2\right)\left[(P - K)^2 + i\epsilon\right]}. \tag{4.12}$$

At of non-zero temperature, we replace the k_0 integral by discrete sum over frequencies $k_0 = i(2n+1)\pi T + \mu$ as shown below

$$\int_{-\infty}^{\infty} \frac{dk_0}{2\pi} \to i\,T \sum_{n=-\infty}^{\infty} . \tag{4.13}$$

So, the self energy of fermion with flavour f is written in sum-integral as

$$\Sigma_f(P) = 2g^2 C_F T \sum_{k_0} \int \frac{d^3k}{(2\pi)^3} \frac{2m_f - \not{K}}{\left(K^2 - m_f^2\right)\left[(P-K)^2 + i\epsilon\right]}. \tag{4.14}$$

At this stage, we define the frequency sums as

$$\mathcal{F}^{(0,0)}_{(F,B)} = T \sum_{k_0} \frac{1}{\left(k_0^2 - E_k^2\right)\left(q_0^2 - \boldsymbol{q}^2\right)}, \tag{4.15}$$

$$\mathcal{F}^{(1,0)}_{(F,B)} = T \sum_{k_0} \frac{k_0}{\left(k_0^2 - E_k^2\right)\left(q_0^2 - \boldsymbol{q}^2\right)}. \tag{4.16}$$

The summations are performed Appendix A. Here we quote the results.

$$\mathcal{F}^{(0,0)}_{(F,B)} = \frac{1}{4E_k q}\left[\frac{1-\widetilde{n}_-(E_k)+n(q)}{p_0+E_k+q} - \frac{1-\widetilde{n}_+(E_k)+n(q)}{p_0-E_k-q} + \frac{\widetilde{n}_-(E_k)+n(q)}{p_0+E_k-q} - \frac{\widetilde{n}_+(E_k)+n(q)}{p_0-E_k+q}\right], \tag{4.17}$$

$$\mathcal{F}^{(1,0)}_{(F,B)} = -\frac{1}{4E_k}\left[\frac{1-\widetilde{n}_+(E_k)+n(q)}{p_0-E_k-q} + \frac{1-\widetilde{n}_-(E_k)+n(q)}{p_0+E_k+q} + \frac{\widetilde{n}_+(E_k)+n(q)}{p_0-E_k+q} + \frac{\widetilde{n}_-(E_k)+n(q)}{p_0+E_k-q}\right], \tag{4.18}$$

where $\widetilde{n}_\pm(E) = \dfrac{1}{e^{\beta(E\mp\mu)}+1}$. Our goal is to compute the coefficients $a(p_0,p)$ and $b(p_0,p)$. To do so, first it is convenient to compute the traces, $T_P \equiv \mathsf{Tr}\left[\not{P}\Sigma(P)\right]$ and $T_u \equiv \mathsf{Tr}\left[\gamma_0\Sigma(P)\right]$, and replace the result in Eq. (4.6). This leads to

$$T_P = 8g^2 C_F \int \frac{d^3k}{(2\pi)^3}\left[\boldsymbol{p}.\boldsymbol{k}\mathcal{F}^{(0,0)}_{(F,B)} - p_0\mathcal{F}^{(1,0)}_{(F,B)}\right],$$

$$T_u = -8g^2 C_F \int \frac{d^3k}{(2\pi)^3}\mathcal{F}^{(1,0)}_{(F,B)}. \tag{4.19}$$

From Eq. (4.6), we have

$$a(p_0,p) = 2g^2C_F\int\frac{d^3k}{(2\pi)^3}\frac{\boldsymbol{k}.\hat{\boldsymbol{p}}}{p}\mathcal{F}^{(0,0)}_{(F,B)},$$
$$b(p_0,p) = 2g^2C_F\int\frac{d^3k}{(2\pi)^3}\left[\mathcal{F}^{(1,0)}_{(F,B)} - p_0\frac{\boldsymbol{k}.\hat{\boldsymbol{p}}}{p}\mathcal{F}^{(0,0)}_{(F,B)}\right]. \tag{4.20}$$

The three-momentum integration is performed, for convenience, in the spherical polar coordinates. Also, we choose the z direction along the direction of external momentum $\hat{\boldsymbol{p}}$ which allows us to write $\hat{\boldsymbol{k}}.\hat{\boldsymbol{p}} = \cos\theta$, where θ is the angle between $\hat{\boldsymbol{p}}$ and $\hat{\boldsymbol{k}}$. So we have $q = |\boldsymbol{p}-\boldsymbol{k}| = \sqrt{k^2+p^2-2pk\cos\theta}$. Now, we can perform the theta integration analytically [202]. To do this, we need to remove the θ dependence from the distribution function. The θ dependence comes from $q = \sqrt{p^2+k^2-2kp\cos\theta}$ which is eliminated by a change of variable $\boldsymbol{k}' = \boldsymbol{p}-\boldsymbol{k}$. After that, the k integration is performed numerically to get the exact one loop self energy. It is performed in ref. [202]. We shall obtain the expression of a and b in HTL approximation.

As discussed before, the hard thermal loop approximation we assume that the momentum flowing through the external legs are of the order of gT, i.e., soft and that flowing through the loop are of the order of T, i.e., hard. We can simplify the calculation of $a(p_0,p)$ and $b(p_0,p)$ by invoking the following approximations [203]

1. The current quark mass m_f is very small compared to the relevant momentum scale. So we can safely drop it and write $E_k \cong k$.

2. Also, the following approximation can be made on the momentum flowing through the gluon line in the figure

$$q = |\boldsymbol{p}-\boldsymbol{k}| = \sqrt{k^2+p^2-2\,\boldsymbol{k}.\boldsymbol{p}} \simeq \sqrt{k^2-2\,\boldsymbol{k}.\boldsymbol{p}} \simeq k - \hat{\boldsymbol{k}}.\boldsymbol{p} \tag{4.21}$$

In the last line, we ignored p^2 since it is of the order of g^2T^2. It is smallest among k^2 and $\boldsymbol{k}.\boldsymbol{p}$ which are of the order of T^2 and gT^2, respectively.

3. We can drop the term $p_0 \pm (k+q)$ since it contributes to linear in T and is small compared to $p_0 \pm (k-q)$ which is of the order of gT.

4. In the light of approximation described in point no 1, we can write

$$n(q) \simeq n(k) - \hat{\boldsymbol{k}}.\boldsymbol{p}\frac{\partial}{\partial k}n(k) \simeq n(k). \tag{4.22}$$

Here in the last line, the second term which is associated with derivative of $n(k)$ is suppressed by a factor of g compared to the first one. Thus we drop the 2nd term.

In this case, it is convenient to evaluate T_u and T_P first and substitute that in Eq. (4.6) to obtain HTL approximated result of $a(p_0, p)$ and $b(p_0, p)$. We drop the vacuum contribution, i.e., the term that does not involves distribution functions. The vacuum part is divergent which is eliminated using zero temperature renormalization. Employing the approximations listed above, we arrive at

$$T_u = \mathsf{Tr}\left[\gamma_0 \Sigma(P)\right] = 2g^2 C_F \int \frac{d^3k}{(2\pi)^3}\frac{1}{k}\left[\frac{\widetilde{n}_+(k)+n(k)}{p_0 - \boldsymbol{p}.\hat{\boldsymbol{k}}} + \frac{\widetilde{n}_-(|k)+n(k)}{p_0 + \boldsymbol{p}.\hat{\boldsymbol{k}}}\right] \tag{4.23}$$

and

$$\begin{aligned} T_P = \mathsf{Tr}\left[\not{P}\Sigma(P)\right] = 2C_F g^2 \int \frac{d^3k}{(2\pi)^3}\frac{1}{k}\Bigg(\boldsymbol{p}.\hat{\boldsymbol{k}}\left[\frac{\widetilde{n}_-(k)+n(k)}{p_0 + \boldsymbol{p}.\hat{\boldsymbol{k}}} - \frac{\widetilde{n}_+(k)+n(k)}{p_0 - \boldsymbol{p}.\hat{\boldsymbol{k}}}\right] \\ +p_0\left[\frac{\widetilde{n}_+(k)+n(k)}{p_0 - \boldsymbol{p}.\hat{\boldsymbol{k}}} + \frac{\widetilde{n}_-(k)+n(k)}{p_0 + \boldsymbol{p}.\hat{\boldsymbol{k}}}\right]\Bigg). \end{aligned} \tag{4.24}$$

Now, we have $\hat{\boldsymbol{k}}$ varying in all direction in the space.

$$\begin{aligned} \int \frac{d\Omega}{4\pi}\frac{1}{p_0 - \boldsymbol{p}.\hat{\boldsymbol{k}}} &= \int \frac{d\Omega}{4\pi}\frac{1}{p_0 + \boldsymbol{p}.\hat{\boldsymbol{k}}}, \\ \int \frac{d\Omega}{4\pi}\frac{\boldsymbol{p}.\hat{\boldsymbol{k}}}{p_0 - \boldsymbol{p}.\hat{\boldsymbol{k}}} &= -\int \frac{d\Omega}{4\pi}\frac{\boldsymbol{p}.\hat{\boldsymbol{k}}}{p_0 + \boldsymbol{p}.\hat{\boldsymbol{k}}}. \end{aligned} \tag{4.25}$$

We decompose the measure $d^3k = k^2\, dk\, d\Omega$ to perform the integral. So, we have

$$
\begin{aligned}
T_u &= \frac{g^2 C_F}{\pi^2} \left(\int\limits_0^\infty dk\, k\, [\widetilde{n}_+(k) + n(k)] \int \frac{d\Omega}{4\pi} \frac{1}{p_0 - \boldsymbol{p}.\hat{\boldsymbol{k}}} \right. \\
&\qquad \left. + \int\limits_0^\infty dk\, k\, [\widetilde{n}_-(k) + n(k)] \int \frac{d\Omega}{4\pi} \frac{1}{p_0 + \boldsymbol{p}.\hat{\boldsymbol{k}}} \right) \\
&= \frac{g^2 C_F}{\pi^2} \int\limits_0^\infty dk\, k \Big(\widetilde{n}_+(k) + \widetilde{n}_-(k) + 2n(k) \Big) \int \frac{d\Omega}{4\pi} \frac{1}{p_0 - \boldsymbol{p}.\hat{\boldsymbol{k}}}. \qquad (4.26)
\end{aligned}
$$

The integral over k is performed analytically as

$$
\int\limits_0^\infty dk\, k \Big(\widetilde{n}_+(k) + \widetilde{n}_-(k) + 2n(k) \Big) = \frac{\pi^2}{2} \left(T^2 + \frac{\mu^2}{\pi^2} \right). \qquad (4.27)
$$

Let us define a vector $\hat{K}^\mu = (1, \hat{\boldsymbol{k}})$ and quantity defined through that vector

$$
\mathcal{T}^\mu(p_0, p) = \int \frac{d\Omega}{4\pi} \frac{\hat{K}^\mu}{P \cdot \hat{K}} = \left\langle \frac{\hat{K}^\mu}{P.\hat{K}} \right\rangle_{\hat{\boldsymbol{k}}}. \qquad (4.28)
$$

This leads to

$$
T_u = \frac{1}{2} g^2 C_F \left(T^2 + \frac{\mu^2}{\pi^2} \right) \mathcal{T}^0(p_0, p) = 4 m_{\mathsf{th}}^2 \mathcal{T}^0(p_0, p). \qquad (4.29)
$$

Here m_{th} is the thermal mass of quark which is a pure medium effect and it is defined as

$$
m_{\mathsf{th}}^2 = \frac{1}{8} C_F g^2 \left(T^2 + \frac{\mu^2}{\pi^2} \right). \qquad (4.30)
$$

The angular dependence of the integral from the expression of T_P goes away.

$$T_P = 2g^2C_F\int\frac{d^3k}{(2\pi)^3}\frac{1}{k} = \frac{g^2C_F}{\pi^2}\int_0^\infty dk\, k\Big(\widetilde{n}_+(k)+\widetilde{n}_-(k)+2n(k)\Big)\int\frac{d\Omega}{4\pi}$$
$$= \frac{1}{2}g^2C_F\left(T^2+\frac{\mu^2}{\pi^2}\right) = 4m_{\mathsf{th}}^2. \tag{4.31}$$

So, $a(p_0,p)$ and $b(p_0,p)$ is written in terms of $\mathcal{T}^0$ as

$$a(p_0,p) = \frac{m_{\mathsf{th}}^2}{p^2}\left[1-p_0\mathcal{T}^0(p_0,p)\right], \tag{4.32}$$
$$b(p_0,p) = \frac{m_{\mathsf{th}}^2}{p^2}\left[P^2\mathcal{T}^0\left(p_0,p\right)-p_0\right], \tag{4.33}$$

where $\mathcal{T}^0(p_0,p)$ can be written in closed form as

$$\mathcal{T}^0(p_0,p) = \frac{1}{2p}\log\left(\frac{p_0+p}{p_0-p}\right). \tag{4.34}$$

4.5 Modified Quark Propagator

In the language of field theory, the effective propagator is obtained from Dyson-Schwinger equation. So, the quark propagator takes the form [204]

$$S_f^*(P) = \frac{(1+a(p_0,p))\,\not{P}+b(p_0,p)\not{u}}{D(p_0,p)}, \tag{4.35}$$

where we have

$$D(p_0,p) = \left[1+a(p_0,p)\right]^2P^2+2\,a(p_0,p)\,\left[1+b(p_0,p)\right]\,P.u+b^2(p_0,p). \tag{4.36}$$

Now, the quasi-particle modes are obtained from pole of the effective propagator obtained by solving $D(p_0,p) = [(1+a)p_0+b]^2-(1+a)^2p^2 = 0$. It has two quasi-particle modes $D_\pm(p_0, p)$ [179]

$$D_\pm(p_0, p) = [1 + a(p_0, p)]\,(p_0 \mp p) + b(p_0, p) = 0. \tag{4.37}$$

$D_+(p_0, p) = 0$ has two solutions

$$p_0 = \omega_+(p), \qquad\qquad p_0 = -\omega_-(p), \tag{4.38}$$

whereas $D_-(p_0, p) = 0$ has the solutions

$$p_0 = \omega_-(p), \qquad\qquad p_0 = -\omega_+(p). \tag{4.39}$$

The plasmino mode is a consequence of breaking of Lorentz symmetry due to the presence of heat bath. The plus sign corresponds to normal propagating mode and the minus sign corresponds to plasmino mode.

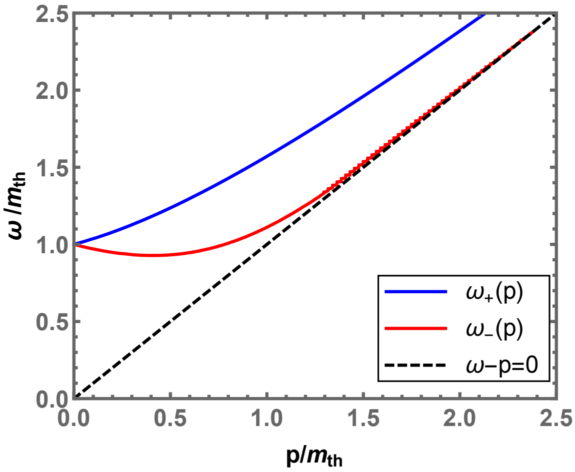

Figure 4.2: The dispersion relation of quasi-quark in HTL approximation. ω_+ is the normal quasi-quark mode and ω_- is the plasmino mode which emerges as a result of non-zero temperature. Both modes are time-like and starts from thermal mass $\left(\omega_\pm(p \to 0) = m_{\rm th}\right)$. The plasmino mode exhibits a minimum which is related to Van-Hove singularity.

4.6 Spectral Representation

The physical interpretation of any calculation will be clear if the propagator can be casted in a simpler form

$$S_f^*(P) = \frac{\gamma_0 - \boldsymbol{\gamma}\cdot\hat{\boldsymbol{p}}}{2\,D_+(p_0,p)} + \frac{\gamma_0 + \boldsymbol{\gamma}\cdot\hat{\boldsymbol{p}}}{2\,D_-\,(p_0,p)}, \tag{4.40}$$

where

$$D_\pm(p_0,p) = p_0 \mp \left(p + \frac{m_{\mathsf{th}}^2}{p}\right) - \frac{m_{\mathsf{th}}^2}{2p}\left(1 \mp \frac{p_0}{p}\right)\log\left(\frac{p_0+p}{p_0-p}\right). \tag{4.41}$$

The spectral representation of $D_\pm$ is defined via

$$\frac{1}{D_\pm(p_0,p)} = \int_{-\infty}^{\infty} ds\, \frac{\rho_\pm(s,p)}{s-p_0}. \tag{4.42}$$

As quoted in section 4.5, the effective propagator has four poles at $p_0 = \omega_\pm(p), -\omega_\pm(p)$ in complex p_0 plane above lightcone $p_0 > p$ and below the lightcone, i.e., in the region $p_0 < p$, it has branch-cut singularity.

So the structure of spectral function can be written in the following form

$$\begin{aligned}\mathsf{Im}\frac{1}{D_\pm(p_0,p)} \equiv \rho_\pm(p_0,p) = Z_\pm(p)\delta\big(p_0-\omega_\pm(p)\big) + Z_\mp(p)\delta\big(p_0+\omega_\mp(p)\big) \\ + \beta_\pm(p_0,p)\Theta(p^2-p_0^2),\end{aligned} \tag{4.43}$$

where $Z_\pm(p)$ are the residue at the pole of the propagator and $\beta_\pm$ are the cut-part. Notice that the theta function is incorporated with argument $p^2 - p_0^2$ to indicate that the cut part contributes only below the light-cone. The expressions of $Z_\pm$ can be written in terms of the modes $\omega_\pm$ as

$$Z_\pm(p) = \frac{\omega_\pm^2(p) - p^2}{2m_{\text{th}}^2} \tag{4.44}$$

and the cut part is written as

$$\beta_\pm(x,y) = \frac{1}{2}\frac{y \mp x}{\left[y(x \mp y) - \frac{1}{2}\left(1 \mp \frac{x}{y}\right)\log\left|\frac{x+y}{x-y}\right| \mp 1\right]^2 + \left[\frac{1}{2}\pi\left(1 \mp \frac{x}{y}\right)\right]^2}, \tag{4.45}$$

where $x = p_0/m_{\text{th}}$ and $y = p/m_{\text{th}}$.

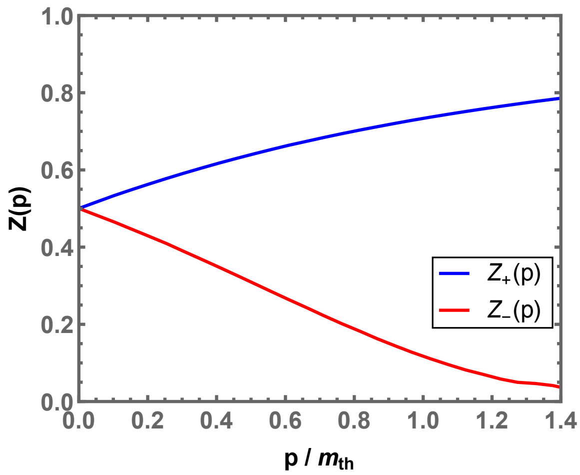

Figure 4.3: Plot of residue of effective quark propagator in HTL approximation

4.7 Asymptotic Form of Dispersion Relation

The analytical expression of the modes $\omega_\pm(p)$ can be found in the small and large momentum limit.

For small momentum limit ($p << m_{\text{th}}$)

$$\omega_\pm(p) \simeq m_{\text{th}} \pm \frac{p}{3} \tag{4.46}$$

and for large momentum

$$\omega_+(p) = p + \frac{m_{\text{th}}^2}{p}, \tag{4.47}$$

$$\omega_-(p) = p + 2p \exp\left(-\frac{2p^2 + m_{\text{th}}^2}{m_{\text{th}}^2}\right). \tag{4.48}$$

4.8 Modified Dirac Equation

We get a new Dirac equation corresponding to the effective propagator

$$\left[(1+a)\not{P} + b\gamma_0\right] U = 0, \tag{4.49}$$

where U is the modified Dirac spinor. In the rest frame of the heat bath, Eq. (4.49) takes the form

$$\{[(1+a)p_0 + b]\,\gamma_0 - (1+a)\boldsymbol{\gamma}.\boldsymbol{p}\}\, U = 0 \tag{4.50}$$

We solve the Eq. (4.50) by writing the gamma matrices in the chiral or Weyl basis. In this basis, Eq. (4.50) becomes

$$\begin{pmatrix} 0 & [(1+a)p_0 + b] - (1+a)\boldsymbol{\sigma}.\boldsymbol{p} \\ [(1+a)p_0 + b] - (1+a)\boldsymbol{\sigma}.\boldsymbol{p} & 0 \end{pmatrix} U = 0. \tag{4.51}$$

Setting the determinant of Eq. (4.51), we get the following equations

$$[(1 + a(p_0, p)]\,(p_0 - p) + b(p_0, p) = 0, \tag{4.52}$$

$$[(1 + a(p_0, p)]\,(p_0 + p) + b(p_0, p) = 0. \tag{4.53}$$

Note that, these two equations are precisely the dispersion equations for quark. Now, we note that if ω is a solution of Eq. (4.52), then $-\omega$ is the solution of Eq. (4.53).

When Eq. (4.52) is satisfied, we get a non-trivial solution of Eq. (4.51) which takes the following form

$$\begin{pmatrix} 0 & 1-\boldsymbol{\sigma}.\hat{\boldsymbol{p}} \\ 1+\boldsymbol{\sigma}.\hat{\boldsymbol{p}} & 0 \end{pmatrix} U = 0 \tag{4.54}$$

and likewise we get

$$\begin{pmatrix} 0 & 1+\boldsymbol{\sigma}.\hat{\boldsymbol{p}} \\ 1-\boldsymbol{\sigma}.\hat{\boldsymbol{p}} & 0 \end{pmatrix} U = 0, \tag{4.55}$$

when Eq. (4.53) is satisfied.

We write the components of Dirac spinor U explicitly as $U = (U_1, U_2, U_3, U_4)$. Now, the solution of the eigenvalue problem reduces the same as the solutions of ordinary Dirac equation.

$$U_-^{(1)} = \begin{pmatrix} -\frac{\hat{p}_x - i\hat{p}_y}{1+\hat{p}_z} \\ 1 \\ 0 \\ 0 \end{pmatrix}, \qquad U_-^{(2)} = \begin{pmatrix} 0 \\ 0 \\ 1 \\ \frac{\hat{p}_x + i\hat{p}_y}{1+\hat{p}_z} \end{pmatrix}, \qquad \text{when} \quad p_0 = \omega_+(p), -\omega_-(p), \tag{4.56}$$

$$U_+^{(1)} = \begin{pmatrix} 1 \\ \frac{\hat{p}_x + i\hat{p}_y}{1+\hat{p}_z} \\ 0 \\ 0 \end{pmatrix}, \qquad U_+^{(2)} = \begin{pmatrix} 0 \\ 0 \\ -\frac{\hat{p}_x - i\hat{p}_y}{1+\hat{p}_z} \\ 1 \end{pmatrix}, \qquad \text{when} \quad p_0 = \omega_-(p), -\omega_+(p), \tag{4.57}$$

where $\hat{p}_i$ is the i^{th} component of unit vector $\hat{\boldsymbol{p}}$.

The chirality operator is defined as $\chi = \gamma = -\begin{pmatrix} 1 & 0 \\ 0 & -1 \end{pmatrix}$.

The helicity operator is defined in chiral basis $\mathcal{H}_{\boldsymbol{p}} = \begin{pmatrix} \boldsymbol{\sigma}.\boldsymbol{p} & 0 \\ 0 & \boldsymbol{\sigma}.\boldsymbol{p} \end{pmatrix}$. The $U_{\pm}^{(1,2)}$ satisfies the helicity eigenvalue equations

$$\mathcal{H}_{\boldsymbol{p}} U_{-}^{(1)} = -U_{-}^{(1)}, \qquad \mathcal{H}_{\boldsymbol{p}} U_{-}^{(2)} = U_{-}^{(2)}, \tag{4.58}$$

$$\mathcal{H}_{\boldsymbol{p}} U_{+}^{(1)} = U_{+}^{(1)}, \qquad \mathcal{H}_{\boldsymbol{p}} U_{+}^{(2)} = -U_{+}^{(2)} \tag{4.59}$$

and chirality eigenvalue equations

$$\chi U_{-}^{(1)} = -U_{-}^{(1)}, \qquad \chi U_{-}^{(2)} = U_{-}^{(2)}, \tag{4.60}$$

$$\chi U_{+}^{(1)} = -U_{+}^{(1)}, \qquad \chi U_{+}^{(2)} = U_{+}^{(2)}. \tag{4.61}$$

We note that the chirality and helicity ratio for normal modes is = +1 whereas for the plasmino modes it is = -1.

4.9 Discrete Symmetries

In this section, we list some of the properties of effective propagator with respect to the discrete symmetries. We denote the effective propagator with a superscript eff instead of $*$ to avoid the clash with the notation of complex conjugation.

1. **Parity**:

$$\mathcal{P}: \qquad S_f^{\mathsf{eff}}(p_0, \boldsymbol{p}) = \gamma_0 S_f^{\mathsf{eff}}(p_0, -\boldsymbol{p})\gamma_0 \tag{4.62}$$

2. **Chirality**:

$$\mathcal{Q}_5: \qquad S_f^{\mathsf{eff}}(p_0, \boldsymbol{p}) = -\gamma_5 S_f^{\mathsf{eff}}(p_0, -\boldsymbol{p})\gamma_5 \tag{4.63}$$

3. **Time reversal symmetry**

$$\mathcal{T}: \qquad S_f^{\mathsf{eff}}(p_0, \boldsymbol{p}) = \mathfrak{T}\gamma_0 \left[S_f^{\mathsf{eff}}(p_0, -\boldsymbol{p})\right]^T \gamma_0 \mathfrak{T} \tag{4.64}$$

   where $\mathfrak{T} = i\gamma^1\gamma^3$ and T denotes transposition.

4. **Charge conjugation**

$$\mathcal{C}: \qquad S_f^{\mathsf{eff}}(p_0, \boldsymbol{p}) = \mathfrak{C}\gamma_0 \left[S_f^{\mathsf{eff}}(-p_0^*, -\boldsymbol{p})\right]^* \gamma_0 \mathfrak{C}, \tag{4.65}$$

   where $\mathfrak{C} = i\gamma^2\gamma_0$.

5. **CPT symmetry** All physical interactions must obey the combined $\theta = CPT$ symmetry.

$$\mathcal{CPT}: \qquad S_f^{\mathsf{eff}}(p_0, \boldsymbol{p}) = \gamma_5\gamma_0 S_f^{\mathsf{eff}}(-p_0^*, -\boldsymbol{p})\gamma_0\gamma_5 \tag{4.66}$$

If we test our effective propagator against these symmetries, it will be seen to satisfy all of these [205]. So, our propagator in Eq. (4.40) is *parity, chirality, time reversal and charge conjugation invariant.*

4.10 Conclusion

The properties of quasi-quark modes in hot deconfined medium are discussed in this chapter. We observed that the structure of the quark self energy is modified. Due to the presence of thermal medium, the Lorentz covariance of the system is broken. As a result the energy and three-momentum have acquired unequal footing unlike in the case of zero temperature. Consequently, a new collective quasi-particle mode called plasmino has emerged with chirality over helicity ratio equal to -1. The spectral representation of effective propagator is obtained which is employed in calculation of dilepton rate.

CHAPTER 5

General Structure and Properties of Quark Two-point Function in Hot Magnetised Medium

5.1 Introduction

In the last chapter, we discuss various properties of collective modes in hot QGP medium. Introduction of magnetic field heavily alters the existing dynamics and properties of the collective excitation. The magnetic field introduces a new energy scale $|eB|$ in the system apart from the temperature T and gT. Also it breaks the rotational invariance of the space. In this scenario, a systemic study of the collective excitation is in order since a magnetic field causes a non-trivial effects on the collective excitations on thermalised media [206–209]. In this chapter, we derived dispersion relations of the collective modes in the weak field approximation which is relevent in the study of QGP.

This chapter is based on *General structure of fermion two-point function and its spec-*

tral representation in a hot magnetized medium by Aritra Das, Aritra Bandyopadhyay, Pradip K. Roy, Munshi G. Mustafa, **Phys.Rev.D 97 (2018) 3, 034024** [210].

5.2 General Structure of the Fermion Self-Energy

The quark propagator in presence of the background magnetic field $\boldsymbol{B} = B\hat{\boldsymbol{z}}$ pointing in z-direction was derived in weak field approximation in chapter 3. It is given as

$$S(P) = \frac{\not{P} + m_f}{P^2 - m_f^2 + i\epsilon} - \frac{\not{P}_{\shortparallel} + m_f}{(P^2 - m_f^2 + i\epsilon)^2}\gamma^1\gamma^2\, q_f B + \mathcal{O}(qB)^2 \tag{5.1}$$

In presence of magnetic field, an additional vector space-like $n^\mu = (0, \boldsymbol{n})$ must be taken into account whose space part specifies the direction of the magnetic field. It is related to the electromagnetic field strength tensor given as

$$n^\mu = \frac{1}{2B}\epsilon^{\mu\nu\lambda\rho}u_\nu F_{\lambda\rho} = \frac{1}{B}u_\nu \widetilde{F}^{\mu\nu}, \tag{5.2}$$

where the $\widetilde{F}_{\mu\nu}$ is the dual strength tensor defined by

$$\widetilde{F}^{\mu\nu} = \frac{1}{2}\epsilon^{\mu\nu\lambda\rho}F_{\lambda\rho}, \tag{5.3}$$

$u^\mu = (1, \boldsymbol{u})$ is the four-velocity of the heat bath. So the general structure of the self energy involves an additional four vector n^μ to the existing P^μ and u^μ. Following the same procedure in chapter 4, we can write the most general structure of the quark self energy as

$$\begin{aligned}\Sigma(P) = &-\alpha\mathbb{1} - \beta\gamma_5 - a\not{P} - b\not{u} - c\not{n} - a'\gamma_5\not{P} - b'\gamma_5\not{u} - c'\gamma_5\,\not{n} \\ &- h\,\sigma_{\mu\nu}P^\mu P^\nu - h'\sigma_{\mu\nu}u^\mu u^\nu - \kappa\,\sigma_{\mu\nu}n^\mu n^\nu - d\sigma_{\mu\nu}P^\mu u^\nu - d'\sigma_{\mu\nu}n^\mu P^\nu - \kappa'\sigma_{\mu\nu}u^\mu n^\nu\,,\end{aligned} \tag{5.4}$$

where various coefficients are known as structure functions. Now the term $\slashed{P}_{\shortparallel} i\gamma^1\gamma^2$ can be rearranged as

$$\slashed{P}_{\shortparallel} i\gamma^1\gamma^2 = \gamma_5 \left[(P\cdot u)\slashed{n} - (P\cdot n)\slashed{u}\right] \tag{5.5}$$

The last Eq. suggests that in the structure of quark two point function there will be terms involving γ_5. We note that the combinations involving $\sigma_{\mu\nu}$ do not appear due to antisymmetric nature of it in any loop order of self-energy. Also in a chirally invariant theory, the terms $\alpha\mathbb{1}$ and $\gamma_5\beta$ will not appear as they would break the chiral symmetry. The term $\gamma_5\slashed{P}$ would appear in the self-energy if fermions interact with an axial vector[1]. By dropping those in (5.4) for chirally symmetric theory, one can now write

$$\Sigma(P) = -a\,\slashed{P} - b\,\slashed{u} - c\,\slashed{n} - b'\gamma_5\,\slashed{u} - c'\gamma_5\,\slashed{n}. \tag{5.6}$$

Now we point out that some important information is encoded into the fermion propagator in (3.98) for a hot magnetised medium. This suggests that $c\slashed{n}$ should not appear in the fermion self-energy [2] and the most general form of the fermion self-energy for a hot magnetised medium becomes

$$\Sigma(P) = -a\,\slashed{P} - b\slashed{u} - b'\gamma_5\,\slashed{u} - c'\gamma_5\,\slashed{n}. \tag{5.7}$$

When a fermion propagates in a vacuum, then $b = b' = c' = 0$ and $\Sigma(P) = -a\slashed{P}$. But when it propagates in a background of pure magnetic field without any heat bath, then $a \neq 0$, $b = 0$ and the structure functions, b' and c', will depend only on the background magnetic field as we will see later. When a fermion propagates in a

[1] The presence of an axial gauge coupling leads to chiral or axial anomaly and a chirally invariant theory does not allow this. Other way, the preservation of both chiral and axial symmetries is impossible, a choice must be made which one should be preserved. For a chirally invariant theory this term drops out. Also the presence of γ_5 in a Lagrangian violates parity invariance.

[2] We have checked that even if one keeps $c\,\slashed{n}$, the coefficient c becomes zero in one-loop order in the weak field approximation.

heat bath, then $a \neq 0$, $b \neq 0$ but both b' and c' vanish because there would not be any thermo-magnetic corrections as can also be seen later.

We now write down the *right chiral* projection operator, $\mathcal{P}_+$ and the *left chiral* projection operator $\mathcal{P}_-$, respectively, defined as:

$$\mathcal{P}_+ = \frac{1}{2}\left(\mathbb{1} + \gamma_5\right), \tag{5.8a}$$

$$\mathcal{P}_- = \frac{1}{2}\left(\mathbb{1} - \gamma_5\right), \tag{5.8b}$$

which satisfy the usual properties of projection operator:

$$\mathcal{P}_\pm^2 = \mathcal{P}_\pm, \quad \mathcal{P}_+\mathcal{P}_- = \mathcal{P}_-\mathcal{P}_+ = 0, \quad \mathcal{P}_+ + \mathcal{P}_- = \mathbb{1}, \quad \mathcal{P}_+ - \mathcal{P}_- = \gamma_5. \tag{5.9}$$

Using the chirality projection operators, the general structure of the self-energy in (5.7) can be casted in the following form

$$\Sigma(P) = -\mathcal{P}_+ \not{C}\, \mathcal{P}_- - \mathcal{P}_- \not{D}\, \mathcal{P}_+, \tag{5.10}$$

where $\not{C}$ and $\not{D}$ are defined as

$$\not{C} = a \not{P} + (b + b')\not{u} + c' \not{n}, \tag{5.11a}$$

$$\not{D} = a \not{P} + (b - b')\not{u} - c' \not{n}. \tag{5.11b}$$

From (5.7) one obtains the general form of the various structure functions as

$$a = \frac{1}{4}\,\frac{\mathrm{Tr}\left(\Sigma\not{P}\right) - (P.u)\ \mathrm{Tr}\left(\Sigma\not{u}\right)}{(P.u)^2 - P^2}, \tag{5.12a}$$

$$b = \frac{1}{4}\,\frac{-(P.u)\ \mathrm{Tr}\left(\Sigma\not{P}\right) + P^2\ \mathrm{Tr}\left(\Sigma\not{u}\right)}{(P.u)^2 - P^2}, \tag{5.12b}$$

$$b' = -\frac{1}{4}\ \mathrm{Tr}\left(\not{u}\Sigma\gamma_5\right), \tag{5.12c}$$

$$c' = \frac{1}{4}\ \mathrm{Tr}\left(\not{n}\Sigma\gamma_5\right), \tag{5.12d}$$

which are also Lorentz scalars . Beside T and B, they would also depend on three Lorentz scalars defined by

$$\omega \equiv P^\mu u_\mu, \tag{5.13a}$$

$$p^3 \equiv -P^\mu n_\mu = p_z\,, \tag{5.13b}$$

$$p_\perp \equiv \left[(P^\mu u_\mu)^2 - (P^\mu n_\mu)^2 - (P^\mu P_\mu)\right]^{1/2}. \tag{5.13c}$$

Since $P^2 = \omega^2 - p_\perp^2 - {p_z}^2$, we may interpret ω, $p_\perp$, p_z as Lorentz invariant energy, transverse momentum, longitudinal momentum respectively.All these structure functions for 1-loop order in a weak field and HTL approximations have been computed in section 5.3 and quoted here [3] as

$$a(p_0,p) \;=\; -\frac{m_{\mathsf{th}}^2}{p^2}Q_1\left(\frac{p_0}{|\boldsymbol{p}|}\right), \tag{5.14a}$$

$$b(p_0,p) \;=\; \frac{m_{\mathsf{th}}^2}{p}\left[\frac{p_0}{p}Q_1\left(\frac{p_0}{p}\right) - Q_0\left(\frac{p_0}{p}\right)\right], \tag{5.14b}$$

$$b'(p_0,p) \;=\; 4C_F g^2 M^2(T,m_f,q_f B)\frac{p_z}{p^2}Q_1\left(\frac{p_0}{p}\right), \tag{5.14c}$$

$$c'(p_0,p) \;=\; 4C_F g^2 M^2(T,m_f,q_f B)\frac{1}{p}Q_0\left(\frac{p_0}{p}\right). \tag{5.14d}$$

We note that the respective vacuum contributions in a, b, b' and c' have been dropped by the choice of the renormalisation prescription.

[3] In weak field approximation the domain of applicability becomes $m_{\mathsf{th}}^2(\sim g^2T^2) < q_f B < T^2$ instead of $m^2 < q_f B < T^2$ as discussed in Appendix 5.3.

5.3 Computations of Structure Functions in One-loop in a Weak Field Approximation for Hot Magnetised QCD Medium:

Here, we present the computations of the various structure functions in ((5.12a)) to ((5.12d)) in 1-loop order (Fig.5.1) in a weak field and HTL approximations following the imaginary time formalism. In Fig.5.1, the modified quark propagator (bold line)

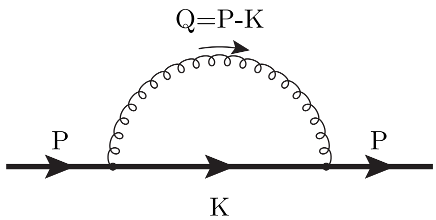

Figure 5.1: One loop quark self-energy in a hot magnetized medium.

due to background magnetic field is given in (5.17). Since glouns are chargeless, their propagators do not change in presence of magnetic field. The gluon propagator in Feynman gauge, is given as [211]

$$D^{\mu\nu}_{ab}(Q) = -i\delta_{ab}\frac{g^{\mu\nu}}{Q^2}. \tag{5.15}$$

We note that we would like to explore the fermion spectrum in a hot magnetised background in the limit $m_f^2 < q_fB < T^2$. We apply Eq. (5.5) to Eq. (3.98) and get

$$S(K) = i\frac{\not{K}}{K^2-m_f^2} - \frac{\gamma_5\left[(K.n)\not{u} - (K.u)\not{n}\right]}{(K^2-m_f^2)^2}(q_fB) + \mathcal{O}[(q_fB)^2] \tag{5.16}$$

$$= S_0^{B=0}(K) + S_1^{B\neq 0}(K) + \mathcal{O}\left[(q_fB)^2\right], \tag{5.17}$$

where the fermion mass in the numerator has been neglected in the weak field domain, $m_f^2 < (q_fB) < T^2$.

The one-loop quark self-energy upto $\mathcal{O}(|q_f B|)$ can be written as

$$\Sigma(P) = g^2\, C_F\, T \sum\!\!\!\!\!\!\!\int_K \gamma_\mu \left(\frac{\not{K}}{K^2 - m_f^2} - \frac{\gamma_5\left[(K.n)\,\not{u} - (K.u)\,\not{n}\right]}{(K^2-m_f^2)^2}\, q_f B \right) \gamma^\mu\, \frac{1}{(P-K)^2} \tag{5.18}$$

$$\simeq \Sigma^{B=0}(P,T) + \Sigma^{B\neq 0}(P,T) \equiv \Sigma^0 + \Sigma^B, \tag{5.19}$$

where g is the QCD coupling constant, $C_F = 4/3$ is the Casimir invariant of $SU(3)$ group, T is the temperature of the system. The first term is the thermal bath contribution in absence of magnetic field ($B = 0$) whereas the second one is from the magnetised thermal bath.

Using (5.19) in ((5.12a)) and ((5.12b)), the structure functions a and b, respectively, become

$$a(p_0,p) = \frac{1}{4}\, \frac{\mathsf{Tr}\left(\Sigma^0 \not{P}\right) - (P.u)\ \mathsf{Tr}\left(\Sigma^0 \not{u}\right)}{(P.u)^2 - P^2}, \tag{5.20a}$$

$$b(p_0,p) = \frac{1}{4}\, \frac{-(P.u)\ \mathsf{Tr}\left(\Sigma^0 \not{P}\right) + P^2\ \mathsf{Tr}\left(\Sigma^0 \not{u}\right)}{(P.u)^2 - P^2}, \tag{5.20b}$$

where the contributions coming from Σ^B vanish due to the trace of odd number of γ-matrices. Following the well known results in Ref. [204], one can write

$$a(p_0,p) = -\frac{m_{\mathsf{th}}^2}{p^2} Q_1\left(\frac{p_0}{p}\right), \tag{5.21a}$$

$$b(p_0,p) = \frac{m_{\mathsf{th}}^2}{p}\left[\frac{p_0}{p} Q_1\left(\frac{p_0}{p}\right) - Q_0\left(\frac{p_0}{p}\right)\right], \tag{5.21b}$$

where the Legendre functions of the second kind read as

$$Q_0(x) = \frac{1}{2}\ln\left(\frac{x+1}{x-1}\right), \tag{5.22a}$$

$$Q_1(x) = x\, Q_0(x) - 1 = \frac{x}{2}\ln\left(\frac{x+1}{x-1}\right) - 1, \tag{5.22b}$$

and the thermal mass [179, 204] of the quark is given as

$$m_{\text{th}}^2 = C_F \frac{g^2 T^2}{8}. \tag{5.23}$$

The thermal part of the self-energy in (5.19) becomes

$$\Sigma^{B=0}(P,T) \equiv \Sigma^0(P,T) = g^2\, C_F\, T \sum\!\!\!\!\!\!\int_K \gamma_\mu \frac{\not{K}}{K^2 - m^2} \gamma^\mu \frac{1}{(P-K)^2} \tag{5.24}$$

$$= -a(p_0,p)\not{P} - b(p_0,p)\not{u}. \tag{5.25}$$

Again using (5.19) in (5.12c) and (5.12d), the structure functions b' and c', respectively, become

$$b' = -\frac{1}{4}\ \mathsf{Tr}(\not{u}\gamma_5 \Sigma^B), \tag{5.26}$$

$$c' = \frac{1}{4}\ \mathsf{Tr}(\not{n}\gamma_5 \Sigma^B), \tag{5.27}$$

where the contributions coming from Σ^0 vanish due to the trace of odd number of γ-matrices. For computing the above thermo-magnetic structure functions, one needs to use the following two traces:

$$\mathsf{Tr}\left[\not{u}\gamma_5\gamma_\mu\gamma_5\left[(K.n)\not{u} - (K.u)\not{n}\right]\gamma^\mu\right] = 8\,(K.n)\,, \tag{5.28}$$

$$\mathsf{Tr}\left[\not{n}\gamma_5\gamma_\mu\gamma_5\left[(K.n)\not{u} - (K.u)\not{n}\right]\gamma^\mu\right] = 8\,(K.u)\,. \tag{5.29}$$

With this one can obtain

$$b' = 2\, g^2\, C_F\, T\, q_f\, B \sum\!\!\!\!\!\!\!\int_K (K.n)\, \widetilde{\Delta}^2(K)\Delta(P-K), \tag{5.30}$$

$$c' = -2\, g^2\, C_F\, T\, q_f\, B \sum\!\!\!\!\!\!\!\int_K (K.u)\, \widetilde{\Delta}^2(K)\, \Delta(P-K), \tag{5.31}$$

where the boson propagator in Saclay representation [212] is given by

$$\Delta(K) = -\int_0^\beta d\tau e^{k_0\tau}\Delta(\tau,k)$$

and

$$\begin{aligned}\Delta(\tau,k) &= \sum_{k_0} e^{-k_0\tau}\Delta(K)\\ &= \frac{1}{2\omega_k}\left\{\left[1+n(\omega_k)\right]e^{-\omega_k\tau}+n(\omega_k)e^{\omega_k\tau}\right\}\end{aligned}$$

where the sum is over $k_0 = 2\pi i n T$ and $\omega_k^2 = k^2 + m_f^2$. Also the fermion propagator in Saclay representation reads

$$\widetilde{\Delta}(K) = -\int_0^\beta d\tau e^{k_0\tau}\widetilde{\Delta}(\tau,k)$$

and

$$\begin{aligned}\widetilde{\Delta}(\tau,k) &= \sum_{k_0} e^{-k_0\tau}\widetilde{\Delta}(K)\\ &= \frac{1}{2\omega_k}\left\{\left[1-\widetilde{n}(\omega_k)\right]e^{-\omega_k\tau}-\widetilde{n}(\omega_k)e^{\omega_k\tau}\right\}\end{aligned}$$

where the sum above is over $k_0 = (2n+1)\pi i T$. Now following HTL approximation in presence of magnetic field [213, 214] the (5.30) and (5.31) are simplified as

$$b' = -4\, g^2\, C_F\, M^2(T, m_f, q_f B) \int \frac{d\Omega}{4\pi} \frac{\hat{K}\cdot n}{P\cdot \hat{K}}\,,$$
$$c' = 4\, g^2\, C_F\, M^2(T, m_f, q_f B) \int \frac{d\Omega}{4\pi} \frac{\hat{K}\cdot u}{P\cdot \hat{K}}\,.$$

Using the results of the HTL angular integrations [215]

$$\int \frac{d\Omega}{4\pi} \frac{\hat{K}\cdot u}{P\cdot \hat{K}} = \frac{1}{p}\, Q_0\left(\frac{p^0}{p}\right), \tag{5.32}$$
$$\int \frac{d\Omega}{4\pi} \frac{\hat{K}\cdot n}{P\cdot \hat{K}} = -\frac{p^3}{p^2} Q_1\left(\frac{p^0}{p}\right), \tag{5.33}$$

the thermo-magnetic structures functions become

$$b' = 4g^2\, C_F\, M^2(T, m_f, q_f B)\, \frac{p^3}{p^2} Q_1\left(\frac{p^0}{p}\right), \tag{5.34}$$
$$c' = 4g^2\, C_F\, M^2(T, m_f, q_f B)\, \frac{1}{p}\, Q_0\left(\frac{p^0}{p}\right), \tag{5.35}$$

with the magnetic mass is obtained as

$$M^2(T, m_f, q_f B) = \frac{q_f B}{16\pi^2}\left[\ln(2) - \frac{T}{m_f}\frac{\pi}{2}\right]. \tag{5.36}$$

We note here that for $m_f \to 0$, the magnetic mass diverges but it can be regulated by the the thermal mass m_{th} in (5.23) as is done in Refs. [213, 215]. Then the domain of applicability becomes $m_{\mathsf{th}}^2(\sim g^2T^2) < q_f B < T^2$ instead of $m_f^2 < q_f B < T^2$.

The thermo-magnetic part of the self-energy in (5.19) becomes

$$\Sigma^{B\neq 0}(P,T) \equiv \Sigma^B(P,T) = -\, g^2\, C_F\, T\, q_f\, B \sum_K \gamma_\mu \frac{\gamma_5\left[(K.n)\not{u} - (K.u)\not{n}\right]}{(K^2 - m_f^2)^2} \gamma^\mu \frac{1}{(P-K)^2} \tag{5.37}$$

$$= -b'(p_0, p)\gamma_5 \not{u} - c'(p_0, p)\gamma_5 \not{n}. \tag{5.38}$$

Now combining (5.25), (5.38) and (5.19), the general structure of quark self-energy in hot magnetised QCD becomes

$$\Sigma(p_0, p) = -a(p_0, p)\slashed{P} - b(p_0, p)\slashed{u} - \gamma_5 b'(p_0, p)\slashed{u} - \gamma_5 c'(p_0, p)\slashed{n}\,. \tag{5.39}$$

which agrees quite well with the general structure as discussed in (5.7) and also with results directly calculated in Refs. [213–215].

5.4 Effective Fermion Propagator

The effective fermion propagator is given by Dyson-Schwinger equation which reads as

$$S^*(P) = \frac{1}{\slashed{P} - \Sigma(P)}\,, \tag{5.40}$$

and the inverse fermion propagator reads as

$$S^{*-1}(P) = \slashed{P} - \Sigma(P)\,. \tag{5.41}$$

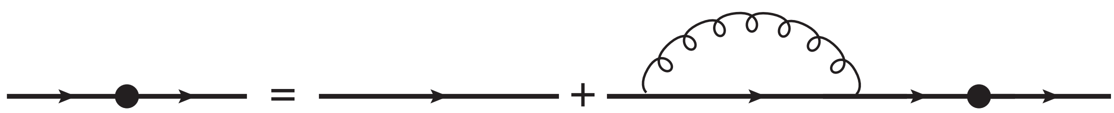

Figure 5.2: Diagramatic representation of the Dyson-Schwinger equation for one-loop effective fermion propagator.

Using (5.10) the inverse fermion propagator can be written as

$$S^{*-1}(P) = \mathcal{P}_+ \left[(1+a(p_0,p))\slashed{P} + (b(p_0,p) + b'(p_0,p_\perp,p_z))\,\slashed{u} + c'(p_0,p)\slashed{n}\right]\mathcal{P}_- \\ + \mathcal{P}_- \left[(1+a(p_0,p))\slashed{P} + (b(p_0,p) - b'(p_0,p_\perp,p_z))\,\slashed{u} - c'(p_0,p)\slashed{n}\right]\mathcal{P}_+ \tag{5.42}$$

$$= \mathcal{P}_+\,\slashed{L}\,\mathcal{P}_- + \mathcal{P}_-\,\slashed{R}\,\mathcal{P}_+\,, \tag{5.43}$$

where $\slashed{L}$ and $\slashed{R}$ can be obtained from two four vectors given by

$$L^\mu(p_0,p_\perp,p_z) = \mathcal{A}(p_0,p)\,P^\mu + \mathcal{B}_+(p_0,p_\perp,p_z)\,u^\mu + c'(p_0,p)\,n^\mu, \tag{5.44a}$$

$$R^\mu(p_0,p_\perp,p_z) = \mathcal{A}(p_0,p)\,P^\mu + \mathcal{B}_-(p_0,p_\perp,p_z)\,u^\mu - c'(p_0,p)\,n^\mu\,, \tag{5.44b}$$

with

$$\mathcal{A}(p_0,p) = 1 + a(p_0,p), \tag{5.45a}$$

$$\mathcal{B}_\pm(p_0,p_\perp,p_z) = b(p_0,p) \pm b'(p_0,p_\perp,p_z)\ . \tag{5.45b}$$

Using (5.43) in (5.40), the propagator can now be written as

$$S^*(P) = \mathcal{P}_-\frac{\slashed{L}}{L^2}\mathcal{P}_+ + \mathcal{P}_+\frac{\slashed{R}}{R^2}\mathcal{P}_-\,, \tag{5.46}$$

where we have used the properties of the projection operators $\mathcal{P}_\pm\gamma^\mu = \gamma^\mu\mathcal{P}_\mp$, $\mathcal{P}_\pm^2 = \mathcal{P}_\pm$, and $\mathcal{P}_+\mathcal{P}_- = \mathcal{P}_-\mathcal{P}_+ = 0$. It can be checked that $S^*(P)S^{*-1}(P) = \mathcal{P}_+ + \mathcal{P}_- = \mathbb{1}$. Also we have

$$L^2 = L^\mu L_\mu = (\mathcal{A}p_0 + \mathcal{B}_+)^2 - \left[(\mathcal{A}p_z + c')^2 + \mathcal{A}^2 p_\perp^2\right] = L_0^2 - |\boldsymbol{L}|^2\,, \tag{5.47a}$$

$$R^2 = R^\mu R_\mu = (\mathcal{A}p_0 + \mathcal{B}_-)^2 - \left[(\mathcal{A}p_z - c')^2 + \mathcal{A}^2 p_\perp^2\right] = R_0^2 - |\boldsymbol{R}|^2\,, \tag{5.47b}$$

where we have used $u^2 = 1$, $n^2 = -1$, $u\cdot n = 0$, $P\cdot u = p_0$, and $P\cdot n = -p_z$.

Note that we have suppressed the functional dependencies of L, R, $\mathcal{A}$, $\mathcal{B}_\pm$ and c' and would bring them back whenever necessary.

For the lowest Landau Level (LLL), $l = 0 \Rightarrow p_\perp = 0$, and these relations reduce to

$$L^2_{LLL} = (\mathcal{A}p_0 + \mathcal{B}_+)^2 - (\mathcal{A}p_z + c')^2 = L_0^2 - L_z^2\,, \tag{5.48a}$$

$$R^2_{LLL} = (\mathcal{A}p_0 + \mathcal{B}_-)^2 - (\mathcal{A}p_z - c')^2 = R_0^2 - R_z^2\,. \tag{5.48b}$$

The poles of the effective propagator, $L^2 = 0$ and $R^2 = 0$, give rise to quasi-particle dispersion relations in a hot magnetised medium. There will be four collective modes with positive energies: two from $L^2 = 0$ and two from $R^2 = 0$. Nevertheless, we will discuss dispersion properties later.

5.5 Transformation Properties of Structure Functions and Propagator

First, we outline some transformation properties of the various structure functions as obtained in (5.14a), (5.14b), (5.14c) and (5.14d).

1. Under the transformation $\boldsymbol{p} \to -\boldsymbol{p} = (p_\perp, -p_z)$:

$$a(p_0, |-\boldsymbol{p}|) = a(p_0, p), \tag{5.49a}$$

$$b(p_0, |-\boldsymbol{p}|) = b(p_0, p), \tag{5.49b}$$

$$b'(p_0, p_\perp, -p_z) = -b'(p_0, p_\perp, p_z), \tag{5.49c}$$

$$c'(p_0, |-\boldsymbol{p}|) = c'(p_0, p). \tag{5.49d}$$

2. For $p_0 \to -p_0$:

$$a(-p_0, p) = a(p_0, p), \tag{5.50a}$$

$$b(-p_0, p) = -b(p_0, p), \tag{5.50b}$$

$$b'(-p_0, p_\perp, p_z) = b'(p_0, p_\perp, p_z), \tag{5.50c}$$

$$c'(-p_0, p) = -c'(p_0, p). \tag{5.50d}$$

3. For $P \to -P = (-p_0, -\boldsymbol{p})$:

$$a(-p_0, |-\boldsymbol{p}|) = a(p_0, p), \tag{5.51a}$$

$$b(-p_0, |-\boldsymbol{p}|) = -b(p_0, p), \tag{5.51b}$$

$$b'(-p_0, p_\perp, -p_z) = -b'(p_0, p_\perp, p_z), \tag{5.51c}$$

$$c'(-p_0, |-\boldsymbol{p}|) = -c'(p_0, p). \tag{5.51d}$$

We have used the fact that $Q_0(-x) = -Q_0(x)$ and $Q_1(-x) = Q_1(x)$.

Now based on the above we also note down the transformation properties of those quantities appearing in the propagator: .

1. For $\mathcal{A}$:

$$\mathcal{A}(p_0, p_\perp, p_z) \xrightarrow{\boldsymbol{p} \to -\boldsymbol{p}} \mathcal{A}(p_0, p_\perp, p_z), \tag{5.52a}$$

$$\mathcal{A}(p_0, p_\perp, p_z) \xrightarrow{p_0 \to -p_0} \mathcal{A}(p_0, p_\perp, p_z), \tag{5.52b}$$

$$\mathcal{A}(p_0, p_\perp, p_z) \xrightarrow[\boldsymbol{p} \to -\boldsymbol{p}]{p_0 \to -p_0} \mathcal{A}(p_0, p_\perp, p_z). \tag{5.52c}$$

2. For $\mathcal{B}_\pm$:

$$\mathcal{B}_\pm(p_0,p_\perp,p_z) \xrightarrow{\boldsymbol{p}\to-\boldsymbol{p}} \mathcal{B}_\mp(p_0,p_\perp,p_z), \tag{5.53a}$$

$$\mathcal{B}_\pm(p_0,p_\perp,p_z) \xrightarrow{p_0\to-p_0} -\mathcal{B}_\mp(p_0,p_\perp,p_z), \tag{5.53b}$$

$$\mathcal{B}_\pm(p_0,p_\perp,p_z) \xrightarrow[\boldsymbol{p}\to-\boldsymbol{p}]{p_0\to-p_0} -\mathcal{B}_\pm(p_0,p_\perp,p_z). \tag{5.53c}$$

Using the above transformation properties, it can be shown that $\not{L}$, $\not{R}$, L^2 and R^2, respectively given in (5.44a), (5.44b), (5.47a) and (5.47b) transform as

$$\not{L}(p_0,p_\perp,p_z) \xrightarrow{\boldsymbol{p}\to-\boldsymbol{p}} \mathcal{A}(p_0,p)(p_0\gamma^0+\boldsymbol{p}\cdot\boldsymbol{\gamma})+\mathcal{B}_-(p_0,p_\perp,p_z)\not{u}+c'(p_0,p)\not{n}\,, \tag{5.54a}$$

$$\not{R}(p_0,p_\perp,p_z) \xrightarrow{\boldsymbol{p}\to-\boldsymbol{p}} \mathcal{A}(p_0,p)(p_0\gamma^0+\boldsymbol{p}\cdot\boldsymbol{\gamma})+\mathcal{B}_+(p_0,p_\perp,p_z)\not{u}-c'(p_0,p)\not{n}\,, \tag{5.54b}$$

$$L^2(p_0,p_\perp,p_z) \xrightarrow{\boldsymbol{p}\to-\boldsymbol{p}} R^2(p_0,p_\perp,p_z)\,, \tag{5.54c}$$

$$R^2(p_0,p_\perp,p_z) \xrightarrow{\boldsymbol{p}\to-\boldsymbol{p}} L^2(p_0,p_\perp,p_z)\,, \tag{5.54d}$$

$$\tag{5.54e}$$

and

$$\not{L}(p_0,p_\perp,p_z) \xrightarrow[\boldsymbol{p}\to-\boldsymbol{p}]{p_0\to-p_0} -\not{L}(p_0,p_\perp,p_z), \tag{5.55a}$$

$$\not{R}(p_0,p_\perp,p_z) \xrightarrow[\boldsymbol{p}\to-\boldsymbol{p}]{p_0\to-p_0} -\not{R}(p_0,p_\perp,p_z), \tag{5.55b}$$

$$L^2(p_0,p_\perp,p_z) \xrightarrow[\boldsymbol{p}\to-\boldsymbol{p}]{p_0\to-p_0} L^2(p_0,p_\perp,p_z), \tag{5.55c}$$

$$R^2(p_0,p_\perp,p_z) \xrightarrow[\boldsymbol{p}\to-\boldsymbol{p}]{p_0\to-p_0} R^2(p_0,p_\perp,p_z). \tag{5.55d}$$

Now we are in a position to check the transformation properties of the effective propagator under some of the discrete symmetries:

5.5.1 Chirality

Under chirality the fermion propagator transform as [205]

$$S(p_0, \boldsymbol{p}) \longrightarrow -\gamma_5\, S(p_0, \boldsymbol{p})\, \gamma_5. \tag{5.56}$$

The effective propagator, $S^*(p_0, p_\perp, p_z)$, in (5.46) transforms under chirality as

$$\begin{aligned}
-\gamma_5\, S^*(p_0, p_\perp, p_z)\, \gamma_5 &= -\gamma_5 \mathcal{P}_- \frac{\not{L}(p_0, p_\perp, p_z)}{L^2(p_0, p_\perp, p_z)} \mathcal{P}_+ \gamma_5 - \gamma_5 \mathcal{P}_+ \frac{\not{R}(p_0, p_\perp, p_z)}{R^2(p_0, p_\perp, p_z)} \mathcal{P}_- \gamma_5 \\
&= \mathcal{P}_+ \frac{\not{L}(p_0, p_\perp, p_z)}{L^2(p_0, p_\perp, p_z)} \mathcal{P}_+ + \mathcal{P}_- \frac{\not{R}(p_0, p_\perp, p_z)}{R^2(p_0, p_\perp, p_z)} \mathcal{P}_-
\end{aligned} \tag{5.57}$$

$$= S^*(p_0, p_\perp, p_z), \tag{5.58}$$

which satisfies (5.56) and indicates that it is chirally invariant.

5.5.2 Reflection

Under reflection the fermion propagator transforms [205] as

$$S(p_0, \boldsymbol{p}) \longrightarrow S(p_0, -\boldsymbol{p}). \tag{5.59}$$

The effective propagator, $S^*(p_0, p_\perp, p_z)$, in (5.46) transforms under reflection as

$$
\begin{aligned}
S^*(p_0, p_\perp, -p_z) &= \mathcal{P}_- \frac{\slashed{L}(p_0, p_\perp, -p_z)}{L^2(p_0, p_\perp, -p_z)} \mathcal{P}_+ + \mathcal{P}_+ \frac{\slashed{R}(p_0, p_\perp, -p_z)}{R^2(p_0, p_\perp, -p_z)} \mathcal{P}_- \\
&= \mathcal{P}_- \frac{\mathcal{A}(p_0, p)(p_0\gamma^0 + \boldsymbol{p}\cdot\boldsymbol{\gamma}) + \mathcal{B}_-(p_0, p_\perp, p_z)\slashed{u} + c'(p_0, p)\slashed{n}}{R^2(p_0, p_\perp, p_z)} \mathcal{P}_+ \\
&\quad + \mathcal{P}_+ \frac{\mathcal{A}(p_0, p)(p_0\gamma^0 + \boldsymbol{p}\cdot\boldsymbol{\gamma}) + \mathcal{B}_+(p_0, p_\perp, p_z)\slashed{u} - c'(p_0, p)\slashed{n}}{L^2(p_0, p_\perp, p_z)} \mathcal{P}_- \\
&\neq S^*(p_0, p_\perp, p_z). \qquad (5.60)
\end{aligned}
$$

However, now considering the rest frame of the heat bath, $u^\mu = (1, 0, 0, 0)$, and the background magnetic field along z-direction, $n^\mu = (0, 0, 0, 1)$, one can write (5.60) as

$$
\begin{aligned}
S^*(p_0, p_\perp, -p_z) &= \mathcal{P}_- \frac{\mathcal{A}(p_0, p)(p_0\gamma^0 + \boldsymbol{p}\cdot\boldsymbol{\gamma}) + \mathcal{B}_-(p_0, p_\perp, p_z)\gamma_0 - c'(p_0, p)\gamma^3}{R^2(p_0, p_\perp, p_z)} \mathcal{P}_+ \\
&\quad + \mathcal{P}_+ \frac{\mathcal{A}(p_0, p)(p_0\gamma^0 + \boldsymbol{p}\cdot\boldsymbol{\gamma}) + \mathcal{B}_+(p_0, p_\perp, p_z)\gamma_0 + c'(p_0, p)\gamma^3}{L^2(p_0, p_\perp, p_z)} \mathcal{P}_- \\
&\neq S^*(p_0, p_\perp, p_z). \qquad (5.61)
\end{aligned}
$$

As seen in both cases the reflection symmetry is violated as we will see later while discussing the dispersion property of a fermion.

5.5.3 Parity

Under parity a fermion propagator transforms [205] as

$$
S(p_0, \boldsymbol{p}) \longrightarrow \gamma_0\, S(p_0, -\boldsymbol{p})\, \gamma_0 . \qquad (5.62)
$$

The effective propagator, $S^*(p_0, p_\perp, p_z)$, in (5.46) under parity transforms as

$$\begin{aligned}
\gamma_0\, S^*(p_0, p_\perp, -p_z)\,\gamma_0 &= \gamma_0 \mathcal{P}_- \frac{\slashed{L}(p_0, p_\perp, -p_z)}{L^2(p_0, p_\perp, -p_z)} \mathcal{P}_+ \gamma_0 + \gamma_0 \mathcal{P}_+ \frac{\slashed{R}(p_0, p_\perp, -p_z)}{R^2(p_0, p_\perp, -p_z)} \mathcal{P}_- \gamma_0 \\
&= \mathcal{P}_+ \gamma_0 \frac{\slashed{L}(p_0, p_\perp, -p_z)}{R^2(p_0, p_\perp, p_z)} \gamma_0 \mathcal{P}_- + \mathcal{P}_- \gamma_0 \frac{\slashed{R}(p_0, p_\perp, -p_z)}{L^2(p_0, p_\perp, p_z)} \gamma_0 \mathcal{P}_+ \\
&\neq S^*(p_0, p_\perp, p_z)\,,
\end{aligned} \tag{5.63}$$

which does not obey (5.62), indicating that the effective propagator in general frame of reference is not parity invariant due to the background medium.

However, now considering the rest frame of the heat bath, $u^\mu = (1, 0, 0, 0)$, and the background magnetic field along z-direction, $n^\mu = (0, 0, 0, 1)$, one can write (5.63) by using (5.54a), (5.54b) and $\gamma_0\,\gamma^i = -\gamma^i\,\gamma_0$ as

$$\begin{aligned}
\gamma_0\, S^*(p_0, p_\perp, -p_z)\,\gamma_0 &= \mathcal{P}_+ \frac{\slashed{R}(p_0, p_\perp, p_z)}{R^2(p_0, p_\perp, p_z)} \mathcal{P}_- + \mathcal{P}_- \frac{\slashed{L}(p_0, p_\perp, p_z)}{L^2(p_0, p_\perp, p_z)} \mathcal{P}_+ \\
&= S^*(p_0, p_\perp, p_z),
\end{aligned} \tag{5.64}$$

which indicates that the propagator is parity invariant in the rest frame of the magnetised heat bath. We note that other discrete symmetries can also be checked but leave them on the readers.

5.6 Modified Dirac Equation

5.6.1 For the General Case

The effective propagator that satisfy the modified Dirac equation with spinor U is given by

$$\left(\mathcal{P}_+ \slashed{L}\, \mathcal{P}_- + \mathcal{P}_- \slashed{R}\, \mathcal{P}_+\right) U = 0. \tag{5.65}$$

Using the chiral basis

$$\gamma_0 = \begin{pmatrix} 0 & \mathbb{1} \\ \mathbb{1} & 0 \end{pmatrix}, \qquad \boldsymbol{\gamma} = \begin{pmatrix} 0 & \boldsymbol{\sigma} \\ -\boldsymbol{\sigma} & 0 \end{pmatrix}, \qquad \gamma_5 = \begin{pmatrix} -\mathbb{1} & 0 \\ 0 & \mathbb{1} \end{pmatrix}, \qquad U = \begin{pmatrix} \psi_L \\ \psi_R \end{pmatrix}, \tag{5.66}$$

one can write (5.65) as

$$\begin{pmatrix} 0 & \sigma \cdot R \\ \bar{\sigma} \cdot L & 0 \end{pmatrix} \begin{pmatrix} \psi_L \\ \psi_R \end{pmatrix} = 0\,, \tag{5.67}$$

where ψ_R and ψ_L are two component Dirac spinors with $\sigma \equiv (1, \boldsymbol{\sigma})$ and $\bar{\sigma} \equiv (1, -\boldsymbol{\sigma})$, respectively. One can obtain nontrivial solutions with the condition

$$\begin{aligned} \det \begin{pmatrix} 0 & \sigma \cdot R \\ \bar{\sigma} \cdot L & 0 \end{pmatrix} &= 0 \\ \det[L \cdot \bar{\sigma}]\, \det[R \cdot \sigma] &= 0 \\ L^2 R^2 &= 0\,. \end{aligned} \tag{5.68}$$

We note that for a given p_0 $(= \omega)$, either $L^2 = 0$, or $R^2 = 0$, but not both of them are simultaneously zero. This implies that i) when $L^2 = 0$, $\psi_R = 0$; ii) when $R^2 = 0$, $\psi_L = 0$. These dispersion conditions are same as obtained from the poles of the effective propagator in (5.46) as obtained in subsec. 5.4.

1. For $R^2 = 0$ but $L^2 \neq 0$, the right chiral equation is given by

$$(R \cdot \sigma)\ \psi_R = 0. \tag{5.69}$$

Again $R^2 = 0 \quad \Rightarrow \quad R_0 = \pm|\boldsymbol{R}| = \pm\sqrt{R_x^2 + R_y^2 + R_z^2}$ and the corresponding dispersive modes are denoted by $R^{(\pm)}$. So the solutions of (5.69) are

$$\text{(i) } R_0 = |\boldsymbol{R}|; \qquad \text{mode } R^{(+)}; \qquad U_{R^{(+)}} = \sqrt{\frac{|\boldsymbol{R}|+R_z}{2|\boldsymbol{R}|}} \begin{pmatrix} 0 \\ 0 \\ 1 \\ \frac{R_x+iR_y}{|\boldsymbol{R}|+R_z} \end{pmatrix} = \begin{pmatrix} 0 \\ \psi_R^{(+)} \end{pmatrix}, \tag{5.70a}$$

$$\text{(ii) } R_0 = -|\boldsymbol{R}|; \quad \text{mode } R^{(-)}; \quad U_{R^{(-)}} = -\sqrt{\frac{|\boldsymbol{R}|+R_z}{2|\boldsymbol{R}|}} \begin{pmatrix} 0 \\ 0 \\ \frac{R_x-iR_y}{|\boldsymbol{R}|+R_z} \\ -1 \end{pmatrix} = \begin{pmatrix} 0 \\ \psi_R^{(-)} \end{pmatrix}. \tag{5.70b}$$

2. For $L^2 = 0$ but $R^2 \neq 0$, the left chiral equation is given by

$$(L \cdot \bar{\sigma})\, \psi_L = 0, \tag{5.71}$$

where $L^2 = 0$ implies two conditions; $L_0 = \pm|\boldsymbol{L}| = \pm\sqrt{L_x^2 + L_y^2 + L_z^2}$ and the corresponding dispersive modes are denoted by $L^{(\pm)}$. The two solutions of

(5.71) are obtained as

$$\text{(i) } L_0 = |\boldsymbol{L}|; \qquad \text{mode } L^{(+)}; \qquad U_{L^{(+)}} = -\sqrt{\frac{|\boldsymbol{L}|+L_z}{2|\boldsymbol{L}|}} \begin{pmatrix} \frac{L_x - iL_y}{|\boldsymbol{L}|+L_z} \\ -1 \\ 0 \\ 0 \end{pmatrix} = \begin{pmatrix} \psi_L^{(+)} \\ 0 \end{pmatrix}, \tag{5.72a}$$

$$\text{(i) } L_0 = -|\boldsymbol{L}|; \qquad \text{mode } L^{(-)}; \qquad U_{L^{(-)}} = \sqrt{\frac{|\boldsymbol{L}|+L_z}{2|\boldsymbol{L}|}} \begin{pmatrix} 1 \\ \frac{L_x + iL_y}{|\boldsymbol{L}|+L_z} \\ 0 \\ 0 \end{pmatrix} = \begin{pmatrix} \psi_L^{(-)} \\ 0 \end{pmatrix}. \tag{5.72b}$$

We note here that $\psi_L^{(\pm)}$ and $\psi_R^{(\pm)}$ are only chiral eigenstates but neither the spin nor the helicity eigenstates.

5.6.2 For the Lowest Landau level (LLL)

1. For $R^2_{LLL} = 0$ in (5.48b) indicates that $R_0 = \pm R_z$, $R_x = R_y = 0$. The two solutions obtained, respectively, in (5.87) and (5.88) in subsec 5.6.3 are given

as

$$\text{(i) } R_0 = R_z; \qquad \text{mode } R^{(+)}; \qquad U_{R^{(+)}} = \begin{pmatrix} 0 \\ 0 \\ 1 \\ 0 \end{pmatrix} = \begin{pmatrix} 0 \\ \chi_+ \end{pmatrix} . \tag{5.73a}$$

$$\text{(ii) } R_0 = -R_z; \qquad \text{mode } R^{(-)}; \qquad U_{R^{(-)}} = \begin{pmatrix} 0 \\ 0 \\ 0 \\ 1 \end{pmatrix} = \begin{pmatrix} 0 \\ \chi_- \end{pmatrix} , \tag{5.73b}$$

where $\chi_+ = \begin{pmatrix} 1 \\ 0 \end{pmatrix}$ and $\chi_- = \begin{pmatrix} 0 \\ 1 \end{pmatrix}$.

2. For LLL, $L^2_{LLL} = 0$ in (5.48a) indicates that $L_0 = \pm L_z$, $L_x = L_y = 0$. The two solutions obtained, respectively, in (5.89) and (5.90) in subsec 5.6.3 are given as

$$\text{(i) } L_0 = L_z; \qquad \text{mode } L^{(+)}; \qquad U_{L^{(+)}} = \begin{pmatrix} 0 \\ 1 \\ 0 \\ 0 \end{pmatrix} = \begin{pmatrix} \chi_- \\ 0 \end{pmatrix} , \tag{5.74a}$$

$$\text{(i) } L_0 = -L_z; \qquad \text{mode } L^{(-)}; \qquad U_{L^{(-)}} = \begin{pmatrix} 1 \\ 0 \\ 0 \\ 0 \end{pmatrix} = \begin{pmatrix} \chi_+ \\ 0 \end{pmatrix} . \tag{5.74b}$$

The spin operator along the z direction is given by

$$\Sigma^3 = \sigma^{12} = \frac{i}{2}\left[\gamma^1, \gamma^2\right] = i\,\gamma^1\gamma^2 = \begin{pmatrix} \sigma^3 & 0 \\ 0 & \sigma^3 \end{pmatrix}, \tag{5.75}$$

where σ with single index denotes Pauli spin matrices whereas that with double indices denote generator of Lorentz group in spinor representation. Now,

$$\Sigma^3\, U_{R(\pm)} = \begin{pmatrix} \sigma^3 & 0 \\ 0 & \sigma^3 \end{pmatrix} \begin{pmatrix} 0 \\ \chi_\pm \end{pmatrix} = \begin{pmatrix} 0 \\ \sigma^3\,\chi_\pm \end{pmatrix} = \pm \begin{pmatrix} 0 \\ \chi_\pm \end{pmatrix} = \pm\, U_{R(\pm)}, \tag{5.76}$$

$$\Sigma^3\, U_{L(\pm)} = \begin{pmatrix} \sigma^3 & 0 \\ 0 & \sigma^3 \end{pmatrix} \begin{pmatrix} \chi_\mp \\ 0 \end{pmatrix} = \begin{pmatrix} \sigma^3\,\chi_\mp \\ 0 \end{pmatrix} = \mp \begin{pmatrix} \chi_\mp \\ 0 \end{pmatrix} = \mp\, U_{L(\pm)}. \tag{5.77}$$

So, the modes $L^{(-)}$ and $R^{(+)}$ have spins along the direction of magnetic field whereas $L^{(+)}$ and $R^{(-)}$ have spins opposite to the direction of magnetic field. Now we discuss the helicity eigenstates of the various modes in LLL. The helicity operator is defined as

$$\mathcal{H}_{\boldsymbol{p}} = \hat{\boldsymbol{p}} \cdot \boldsymbol{\Sigma}\,. \tag{5.78}$$

When a particle moves along $+z$ direction, $\hat{\boldsymbol{p}} = \hat{\mathbf{z}}$ and when it moves along $-z$ direction, $\hat{\boldsymbol{p}} = -\hat{\mathbf{z}}$.

Thus

$$\mathcal{H}_{\boldsymbol{p}} = \begin{cases} \Sigma^3, & \text{for} \quad p_z > 0, \\ -\Sigma^3, & \text{for} \quad p_z < 0. \end{cases} \tag{5.79}$$

Thus,

$$\mathcal{H}_{\boldsymbol{p}}\, U_{R(\pm)} = \begin{cases} \pm U_{R(\pm)}, & \text{for} \quad p_z > 0, \\ \mp U_{R(\pm)}, & \text{for} \quad p_z < 0. \end{cases} \tag{5.80}$$

and

$$\mathcal{H}_{\boldsymbol{p}}\, U_{L(\pm)} = \begin{cases} \mp U_{L(\pm)}, & \text{for} \quad p_z > 0\,, \\ \pm U_{L(\pm)}, & \text{for} \quad p_z < 0\,. \end{cases} \tag{5.81}$$

5.6.3 Solution of the Modified Dirac equation at Lowest Landau Level (LLL)

At LLL, $l \to 0 \;\Rightarrow\; p_\perp = 0$ and the effective Dirac equation becomes

$$\begin{aligned} &\left(\mathcal{P}_+ \not{L} + \mathcal{P}_- \not{R}\right) U = 0 \\ &\begin{pmatrix} 0 & R_0 - \sigma^3 R_z \\ L_0 + \sigma^3 L_z & 0 \end{pmatrix} U = 0, \end{aligned} \tag{5.82}$$

where $U = \begin{pmatrix} \psi_L \\ \psi_R \end{pmatrix}$ with $\psi_{L(R)}$ are 2×1 blocks. Now, the condition for the non-trivial solution to exist is given as

$$\begin{aligned} \det \begin{pmatrix} 0 & R_0 - \sigma^3 R_z \\ L_0 + \sigma^3 L_z & 0 \end{pmatrix} &= 0 \\ \left[(R_0)^2 - (R_z)^2\right]\left[(L_0)^2 - (L_z)^2\right] &= 0 \\ \text{or,}\;\; R_0 = \pm R_z,\;\; L_0 = \pm L_z, & \end{aligned} \tag{5.83}$$

- Case-I: For $R_0 = R_z$ one can write (5.82) as

$$\begin{pmatrix} 0 & 0 & 0 & 0 \\ 0 & 0 & 0 & 2R_z \\ L_0 + L_z & 0 & 0 & 0 \\ 0 & L_0 - L_z & 0 & 0 \end{pmatrix} \cdot \begin{pmatrix} \psi_L^{(1)} \\ \psi_L^{(2)} \\ \psi_R^{(1)} \\ \psi_R^{(2)} \end{pmatrix} = 0, \tag{5.84}$$

which leads to the following conditions:

$$\begin{aligned} 2R_z\, \psi_R^{(2)} &= 0, \\ (L_0 + L_z)\, \psi_L^{(1)} &= 0, \\ (L_0 - L_z)\, \psi_L^{(2)} &= 0, \end{aligned} \tag{5.85}$$

$$\psi_R^{(1)} = \text{Arbitrary}. \tag{5.86}$$

For normalisation, we choose only non-zero component, $\psi_R^{(1)} = 1$ which leads to

$$U_R^{(+)} = \begin{pmatrix} 0 \\ 0 \\ 1 \\ 0 \end{pmatrix}. \tag{5.87}$$

Now, for $R_0 = -R_z$, similarly one can obtain as

$$U_R^{(-)} = \begin{pmatrix} 0 \\ 0 \\ 0 \\ 1 \end{pmatrix}. \tag{5.88}$$

- Case-II: For $L_0 = L_z$, one gets

$$U_L^{(+)} = \begin{pmatrix} 0 \\ 1 \\ 0 \\ 0 \end{pmatrix}, \tag{5.89}$$

whereas for $L_0 = -L_z$, one finds

$$U_L^{(-)} = \begin{pmatrix} 1 \\ 0 \\ 0 \\ 0 \end{pmatrix}. \tag{5.90}$$

5.7 Dispersion

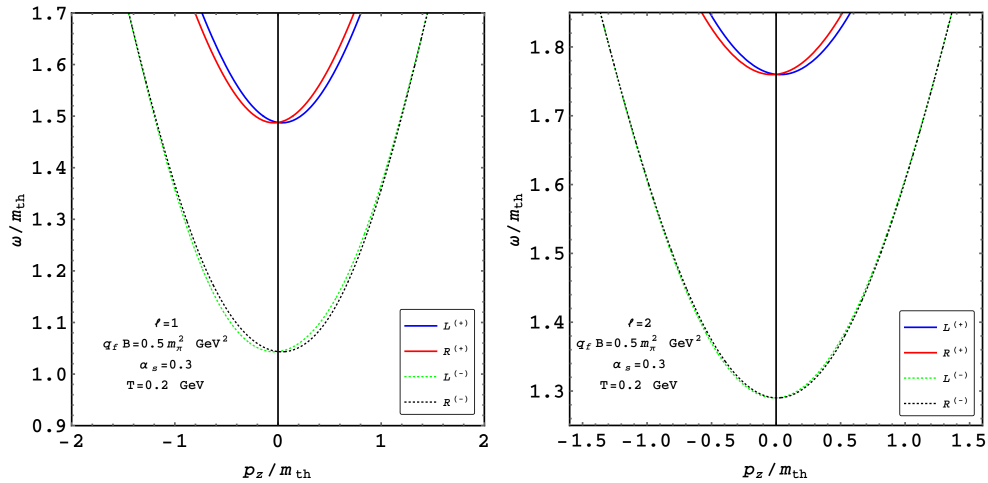

Figure 5.3: Dispersion plots for higher Landau level, $l \neq 0$. The energy ω is scaled with the thermal mass m_{th} for convenience

In presence of magnetic field, the component of momentum transverse to the magnetic field is Landau quantised and takes discrete values given by $p_\perp^2 = 2l|q_f B|$, where l is a given Landau levels. In presence of pure background magnetic field and no heat bath ($T = 0$), the Dirac equation gives rise a dispersion relation

$$E^2 = p_z^2 + m_f^2 + (2\,\nu + 1)\, q_f\, |Q| B - q_f\, Q\, B\, \sigma\,, \tag{5.91}$$

where $\nu = 0, 1, 2, \cdots$, $Q = \pm 1$, $\sigma = +1$ for spin up and $\sigma = -1$ for spin down. The solutions are classified by energy eigenvalues

$$E_l^2 = p_z^2 + m_f^2 + 2\, l\, q_f\, B\ . \tag{5.92}$$

where one can define

$$2\, l = (2\,\nu + 1)\, |Q| - Q\, \sigma\,. \tag{5.93}$$

Now we discuss the dispersion properties of a fermions in a hot magnetised medium. For general case (for higher LLs, $l \neq 0$) the dispersion curves obtained by solving, $L^2 = 0$ and $R^2 = 0$ given in (5.47a) and (5.47b), numerically. We note that the roots of $L_0 = \pm|\boldsymbol{L}| \Rightarrow L_0 \mp |\boldsymbol{L}| = 0$ are represented by $L^{(\pm)}$ with energy $\omega_{L^{(\pm)}}$ whereas those for $R_0 = \pm|\boldsymbol{R}| \Rightarrow R_0 \mp |\boldsymbol{R}| = 0$ by $R^{(\pm)}$ with energy $\omega_{R^{(\pm)}}$. The corresponding eigenstates are obtained in (5.72a), (5.72b), (5.70a) and (5.70b) in subsection 5.6.1. We have chosen $T = 0.2$ GeV, $\alpha_s = 0.3$ and $q_f B = 0.5 m_\pi^2$, where m_π is the pion mass. In Fig. 5.3 the dispersion curves for higher Landau levels are shown where all four modes can propagate for a given choice of Q. This is because the corresponding states for these modes are neither spin nor helicity eigenstates as shown in subsec. 5.6.1. We also note that there will be negative energy modes which are not displayed here but would be discussed in the analysis of the spectral representation of the effective propagator section 5.10.

At LLL $l = 0 \rightarrow p_\perp = 0$ and the roots of $R_0 = \pm R_z$ give rise to two right handed modes $R^{(\pm)}$ with energy $\omega_{R^{(\pm)}}$ whereas those for $L_0 = \pm L_z$ produce [4] two

[4]We make a general note here for left handed modes at LLL. At small p_z, L_z itself is negative for LLL and becomes positive after a moderate value of p_z. This makes the left handed modes

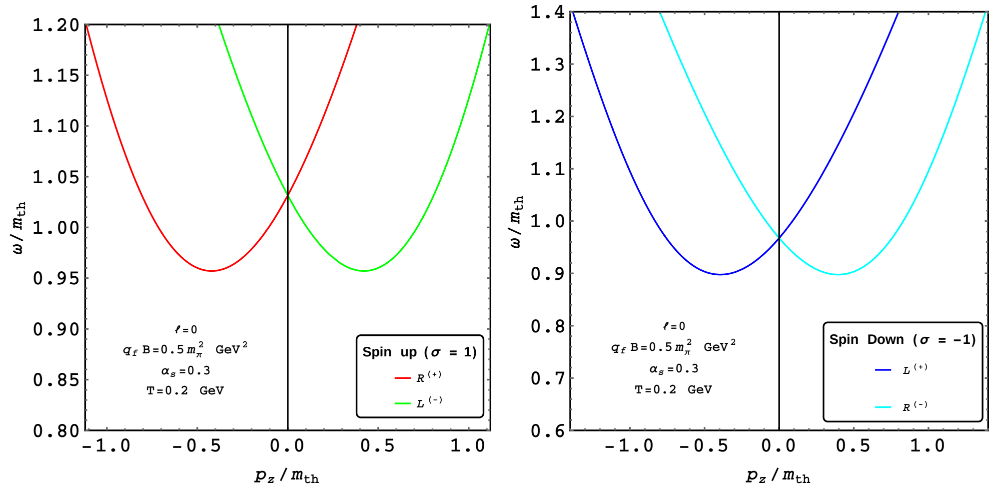

Figure 5.4: Dispersion plots for LLL, $l = 0$. The energy ω is scaled with the thermal mass m_{th} for convenience. For details see the text.

left handed modes $L^{(\pm)}$ with energy $\omega_{L^{(\pm)}}$. In section 5.9 the analytic solutions for the dispersion relations in LLL are presented which show four different modes and the corresponding eigenstates are obtained in subsec. 5.6.2. Now at LLL we discuss two possibilities below:

(i) for positively charged fermion $Q = 1$, $\sigma = 1$ implies $\nu = 0$ and $\sigma = -1$ implies $\nu = -1$. Now we note that ν can never be negative. This implies that the modes with $Q = 1$ and $\sigma = -1$ (spin down) cannot propagate in LLL. Now, the right handed mode $R^{(+)}$ and the left handed mode $L^{(-)}$ have spin up as shown in subsec. 5.6.2, will propagate in LLL for $p_z > 0$. The $R^{(+)}$ mode has helicity to chirality ratio $+1$ is a quasiparticle whereas the mode $L^{(-)}$ left handed has that of -1 known as plasmino (hole). However, for $p_z < 0$, the right handed mode flips to plasmino (hole) as its chirality to helicity ratio becomes -1 whereas the left handed mode becomes particle as its chirality to helicity ratio becomes $+1$. The dispersion behaviour of the two modes are shown in the left panel of Fig. 5.4 which begins at mass $m^{*-}_{LLL}\big|_{p_z=0}$ as given in (5.126).

$L^{(+)}$ and $L^{(-)}$ to flip in LLL than those in higher Landau levels. For details see section 5.9.

(ii) for negatively charged fermion $Q = -1$, $\sigma = 1$ implies $\nu = -1$ and $\sigma = -1$ implies $\nu = 0$. Thus, the modes with $Q = -1$ and $\sigma = +1$ (spin up) cannot propagate in LLL. However, the modes $L^{(+)}$ and $R^{(-)}$ have spin down as found in subsec. 5.6.2 will propagate in LLL. Their dispersion are shown in the right panel of Fig. 5.4 which begin at mass m^{*+}_{LLL} as given in (5.126). For $p_z > 0$ the mode $L^{(+)}$ has helicity to chirality ratio $+1$ whereas $R^{(-)}$ has that of -1 and vice-versa for $p_z < 0$.

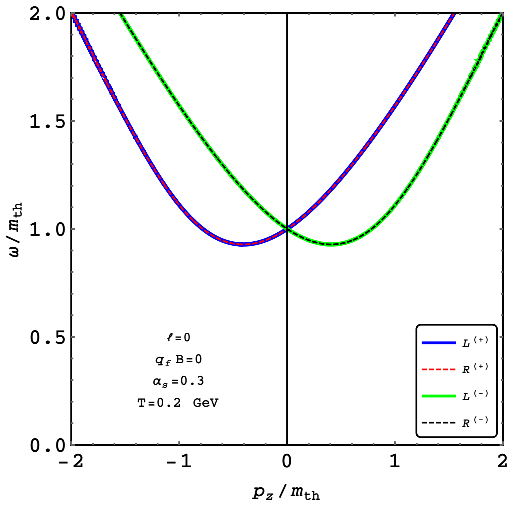

Figure 5.5: The dispersion plots corresponding to HTL propagator in absence of magnetic field, *i.e.*, $B = 0$.

In the absence of the background magnetic field ($B = 0$), the two modes, the left handed $L^{(+)}$ and the right handed $R^{(+)}$ fermions, merge together whereas the other two modes, the left handed $L^{(-)}$ and the right handed $R^{(-)}$ fermions, also merge together. This leads to degenerate (chirally symmetric) modes for which the dispersion plots start at $m_{\rm th}$ and one gets back the usual HTL result [216] with quasiparticle and plasmino modes in presence of heat bath as shown in Fig. 5.5.

As evident from the dispersion plots (Figs. 5.3 and 5.4) both left and right handed modes are also degenerate at $p_z = 0$ in presence of magnetic field but at non-zero $|p_z|$ both left and right handed modes get separated from each others, causing a chiral asymmetry without disturbing the chiral invariance (subsec. 5.5.1) in the system.

Also in subsec. 5.5.2, it was shown that the fermion propagator does not obey the reflection symmetry in presence of medium, which is now clearly evident from all dispersion plots as displayed above.

5.8 Three Point Function

The $(N+1)$-point functions are related to the N-point functions through Ward-Takahashi (WT) identity. The 3-point function is related to the 2-point function as

$$Q_\mu \Gamma^\mu(P,K;Q) = S^{-1}(P) - S^{-1}(K) = \not{P} - \not{K} - \Sigma(P) + \Sigma(K) \tag{5.94}$$

$$= \underbrace{(\not{P} - \not{K})}_{\text{Free}} - \underbrace{\left(\Sigma^{B=0}(P,T) - \Sigma^{B=0}(K,T)\right)}_{\text{Thermal or HTL correction}} - \underbrace{\left(\Sigma^{B\neq 0}(P,T) - \Sigma^{B\neq 0}(K,T)\right)}_{\text{Thermo-magnetic correction}} \tag{5.95}$$

$$= \not{Q} + a(p_0,|\boldsymbol{p}|)\not{P} + b(p_0,|\boldsymbol{p}|)\not{u} - a(k_0,|\boldsymbol{k}|)\not{K} - b(k_0,|\boldsymbol{k}|)\not{u} + b'(p_0,p_\perp,p_z)\gamma_5\not{u} \tag{5.96}$$

$$+ c'(p_0,p_\perp,p_z)\gamma_5\not{n} - b'(k_0,k_\perp,k_z)\gamma_5\not{u} - c'(k_0,k_\perp,k_z)\gamma_5\not{n}\,, \tag{5.97}$$

where $Q = P - K$. We note that recently the general form of the thermo-magnetic corrections for 3-point [213, 215] and 4-point [215] functions have been given in terms of the involved angular integrals, which satisfy WT identies. Nevertheless, to validate the general structure of the self-energy in (5.7) vis-a-vis the inverse propagator in (5.41), we obtain below the temporal component of the 3-point function at $\boldsymbol{q} = 0$; $\boldsymbol{p} = \boldsymbol{k}$ and $p = k$.

Using (5.14a), (5.14b), (5.14c) and (5.14d), we can obtain

$$\Gamma^0(P,K;Q)\big|_{\boldsymbol{q}=0} = \gamma_0 \underbrace{- \frac{m_{\mathsf{th}}^2}{pq_0}\,\delta Q_0\,\gamma^0 + \frac{m_{\mathsf{th}}^2}{pq_0}\,\delta Q_1\,(\hat{p}\cdot\boldsymbol{\gamma})}_{\text{Thermal or HTL correction}} \tag{5.98}$$

$$\underbrace{- \frac{M'^2}{pq_0}\left[\delta Q_0\,\gamma_5 \,+\, \frac{p_z}{p}\,\delta Q_1\,\left(i\gamma^1\gamma^2\right)\right]\gamma^3}_{\text{Thermo-magnetic correction}} \tag{5.99}$$

$$= \gamma^0 \,+ \delta\Gamma^0_{\rm HTL}(P,K;Q) \,+\, \delta\Gamma^0_{\rm TM}(P,K;Q)\;, \tag{5.100}$$

with

$$\gamma_5\gamma^0 = -i\gamma^1\gamma^2\gamma^3\,, \tag{5.101}$$

$$M'^2 = 4\,C_F\,g^2\,M^2(T,m,q_fB)\,, \tag{5.102}$$

$$\delta Q_j = Q_j\left(\frac{p_0}{p}\right) - Q_j\left(\frac{k_0}{p}\right)\,. \tag{5.103}$$

where Q_j are the Legendre functions of the second kind given in (5.22a) and (5.22b). Important to note that the thermo-magnetic (TM) correction $\delta\Gamma^0_{\rm TM}$ matches exactly with that from direct calculation in (5.113) in Appendix 5.8.1. The result also agrees with the HTL 3-point function [213, 215] in absence of background magnetic field by setting $B=0 \Rightarrow M'=0$ as

$$\Gamma^0_{\rm HTL}(P,K;Q)\big|_{\boldsymbol{q}=0} = \left[1 \,-\, \frac{m_{\mathsf{th}}^2}{pq_0}\,\delta Q_0\right]\gamma^0 \,+ \frac{m_{\mathsf{th}}^2}{pq_0}\,\delta Q_1\,(\hat{p}\cdot\boldsymbol{\gamma}) \tag{5.104}$$

$$= \gamma^0 + \delta\Gamma^0_{\rm HTL}(P,K;Q)\,, \tag{5.105}$$

where all components, *i.e.*, $(0,1,2,3)$, are relevant for pure thermal background.

Now in absence of heat bath, setting $T=0 \Rightarrow m_{\sf th}=0$ and $M'^2 = 4\,C_F\,g^2\,M^2(T=0,m,q_f,B)$, the temporal 3-point function in (5.100) reduces to

$$\Gamma^0_B(P,K;Q)\big|_{\boldsymbol{q}=0} = \gamma^0 \underbrace{-\frac{M'^2}{pq_0}\left[\delta Q_0\,\gamma_5 + \frac{p_z}{p}\,\delta Q_1\,(i\gamma^1\gamma^2)\right]\gamma^3}_{\text{Pure magnetic correction}} \tag{5.106}$$

$$= \gamma^0 + \delta\Gamma^0_{\rm M}(P,K;Q)\,. \tag{5.107}$$

We now note that the 3-point function with pure background magnetic field but no heat bath, the gauge boson is oriented along the field direction and there is no polarisation in the transverse direction. Thus, only the longitudinal components (*i.e*, (0,3)-components) of the 3-point function would be relevant for pure background magnetic field in contrast to that of (5.105) for pure thermal background.

5.8.1 Verification of the Three Point Function from Direct Calculation

In this section, we would verify the general structure of the temporal 3-point function as obtained in sec. 5.8 using the general structure of the self-energy.

We begin with the one-loop level 3-point function in a hot magnetised medium in [215] within HTL approximation [190, 217] as

$$\Gamma^\mu(P,K;Q) = \gamma^\mu + \delta\Gamma^\mu_{\rm HTL}(P,K) + \delta\Gamma^\mu_{\rm TM}(P,K), \tag{5.108}$$

where the external four-momentum $Q=P-K$. The HTL correction part [216–218] is given as

$$\delta\Gamma^{\mu}_{\text{HTL}}(P,K) = m^2_{\mathsf{th}} G^{\mu\nu}\gamma_\nu = m^2_{\mathsf{th}} \int \frac{d\Omega}{4\pi} \frac{\hat{Y}^\mu \hat{Y}^\nu}{(P\cdot\hat{Y})(K\cdot\hat{Y})}\gamma_\nu = \delta\Gamma^{\mu}_{\text{HTL}}(-P,-K), \tag{5.109}$$

where $\hat{Y}_\mu = (1, \hat{\boldsymbol{y}})$ is a light like four vector and the thermo-magnetic (TM) correction part [213, 215] is given

$$\delta\Gamma^{\mu}_{\text{TM}}(P,K) = 4\gamma_5 g^2 C_F M^2 \int \frac{d\Omega}{4\pi} \frac{1}{(P\cdot\hat{Y})(K\cdot\hat{Y})}\left[(\hat{Y}\cdot n)\not{u} - (\hat{Y}\cdot u)\not{n}\right]\hat{Y}^\mu \tag{5.110}$$

Now, choosing the temporal component of the thermo-magnetic correction part of the 3-point function and external three momentum $\boldsymbol{q} = 0$, we get

$$\delta\Gamma^{0}_{\text{TM}}(P,K)\big|_{\boldsymbol{q}=0} = \gamma_5 M'^2 \int \frac{d\Omega}{4\pi} \frac{1}{(P\cdot\hat{Y})(K\cdot\hat{Y})}\left[(\hat{Y}\cdot n)\not{u} - (\hat{Y}\cdot u)\not{n}\right] = \gamma_5 M'^2 \int \frac{d\Omega}{4\pi} \frac{1}{(P\cdot\hat{Y})(K\cdot\hat{Y})}\left[(\hat{Y}\cdot n)\gamma_0 + (\hat{Y}\cdot u)\gamma^3\right] \tag{5.111}$$

Along with this following identity:

$$\left(\frac{1}{K\cdot\hat{Y}} - \frac{1}{P\cdot\hat{Y}}\right) = \frac{Q\cdot\hat{Y}}{(P\cdot\hat{Y})(K\cdot\hat{Y})} = \frac{q_0}{(P\cdot\hat{Y})(K\cdot\hat{Y})}, \tag{5.112}$$

and, Eq. (5.32) and Eq. (5.33), we one finally obtain

$$\delta\Gamma^{0}_{\text{TM}}(P,K)\big|_{\boldsymbol{q}\to 0} = \frac{M'^2 p_z}{p^2 q_0}\delta Q_1 \gamma_5\gamma^0 - \frac{M'^2}{p q_0}\delta Q_0 \gamma_5 \gamma^3 = -\frac{M'^2}{p q_0}\left[\delta Q_0\,\gamma_5 + \frac{p_z}{p}\,\delta Q_1\,(i\gamma^1\gamma^2)\right]\gamma^3, \tag{5.113}$$

where $\delta Q_n = Q_n\left(\frac{p_0}{p}\right) - Q_n\left(\frac{k_0}{p}\right)$. We note that this expression matches exactly with the expression obtained in (5.107) from the general structure of fermion self-energy.

5.9 Analytical Solution of the Dispersion Relations and the Effective Mass in LLL

The dispersion relations at LLL can be written the equations (5.48a) and (5.48b) as

$$L^2_{LLL} = (\mathcal{A}p_0 + \mathcal{B}_+)^2 - (\mathcal{A}p_z + c')^2 = L_0^2 - L_z^2 = 0\,, \tag{5.114a}$$

$$R^2_{LLL} = (\mathcal{A}p_0 + \mathcal{B}_-)^2 - (\mathcal{A}p_z - c')^2 = R_0^2 - R_z^2 = 0\,, \tag{5.114b}$$

each of which leads to two modes, respectively, as

$$L_0 = \pm L_z \tag{5.115a}$$

$$\mathcal{A}p_0 + \mathcal{B}_+ = \pm\left(\mathcal{A}p_z + c'\right)\,, \tag{5.115b}$$

and

$$R_0 = \pm R_z \tag{5.116a}$$

$$\mathcal{A}p_0 + \mathcal{B}_- = \pm\left(\mathcal{A}p_z - c'\right)\,. \tag{5.116b}$$

Below we try to get approximate analytical solution of these equations at small and high p_z limits.

5.9.1 Low p_z limit

In the low p_z region, one needs to expand $a(p_0,|p_z|)$, $b(p_0,|p_z|)$, $b'(p_0,0,p_z)$ and $c'(p_0,|p_z|)$ defined in (5.14a), (5.14b), (5.14c) and (5.14d), respectively, which depend on Legendre function of second kind $Q_0(x)$ and $Q_1(x)$ as given in equations (5.22a) and (5.22b), respectively. The Legendre function Q_0 and structure coefficients are expanded in powers of $\dfrac{|p_z|}{p_0}$ as

$$Q_0\left(\frac{p_0}{|p_z|}\right) = \frac{|p_z|}{p_0} + \frac{1}{3}\frac{|p_z|^3}{p_0^3} + \frac{1}{5}\frac{|p_z|^5}{p_0^5} + \cdots \tag{5.117}$$

$$a(p_0,|p_z|) = -\frac{m_{\rm th}^2}{p_0^2}\left(\frac{1}{3} + \frac{1}{5}\frac{|p_z|^2}{p_0^2} + \cdots\right), \tag{5.118}$$

$$b(p_0,|p_z|) = -2\,\frac{m_{\rm th}^2}{p_0}\left(\frac{1}{3} + \frac{1}{15}\frac{|p_z|^2}{p_0^2} + \cdots\right), \tag{5.119}$$

$$b'(p_0,0,p_z) = 4\,g^2\,C_F\,M^2(T,m,qB)\,p_z\left(\frac{1}{3\,p_0^2} + \frac{|p_z|^2}{5\,p_0^4} + \cdots\right), \tag{5.120}$$

$$c'(p_0,|p_z|) = 4\,g^2\,C_F\,M^2(T,m,qB)\left(\frac{1}{p_0} + \frac{|p_z|^2}{p_0^3} + \cdots\right). \tag{5.121}$$

Now retaining the terms that are *upto the order of* p_z in (5.118), (5.119), (5.120), (5.121), we obtain the following expressions for the dispersion relation of various modes:

1. $L_0 = L_z$ leads to a mode $L^{(+)}$ as

$$\omega_{L^{(+)}}(p_z) = m^{*+}_{LLL} + \frac{1}{3}\,p_z\,. \tag{5.122}$$

2. $L_0 = -L_z$ leads to a mode $L^{(-)}$ as

$$\omega_{L^{(-)}}(p_z) = m^{*-}_{LLL} - \frac{1}{3}\,p_z\,. \tag{5.123}$$

3. $R_0 = R_z$ leads to a mode $R^{(+)}$ as

$$\omega_{R^{(+)}}(p_z) = m^{*-}_{LLL} + \frac{1}{3}\, p_z \,. \tag{5.124}$$

4. $R_0 = -R_z$ leads to a mode $R^{(-)}$ as

$$\omega_{R^{(-)}}(p_z) = m^{*+}_{LLL} - \frac{1}{3}\, p_z \,. \tag{5.125}$$

where the effective masses of various modes are given as

$$m^{*\pm}_{LLL} = \begin{cases} \sqrt{m^2_{\text{th}} + 4g^2 C_F M^2(T, M, q_f B)}, & \text{for} \quad L^{(+)} \,\&\, R^{(-)}, \\ \\ \sqrt{m^2_{\text{th}} - 4g^2 C_F M^2(T, M, q_f B)}, & \text{for} \quad R^{(+)} \,\&\, L^{(-)}. \end{cases} \tag{5.126}$$

5.9.2 High p_z limit

We note that p_z can be written as

$$p_z = \begin{cases} |p_z|, & \text{for } \ p_z > 0 \\ -|p_z|. & \text{for } \ p_z < 0 \end{cases}$$

In high p_z limit, we obtain

1.

$$\begin{aligned} &[1 + a(p_0, |p_z|)]\,(p_0 - p_z) + b(p_0, |p_z|) \\ &= \begin{cases} p_0 - |p_z| - \frac{m^2_{\text{th}}}{|p_z|}, & \text{for } \ p_z > 0 \\ 2\,|p_z| + \frac{m^2_{\text{th}}}{|p_z|} - \frac{m^2_{\text{th}}}{|p_z|}\, \ln\left(\frac{2\,|p_z|}{p_0 - |p_z|}\right), & \text{for } \ p_z < 0 \end{cases} \end{aligned} \tag{5.127}$$

2.

$$
\begin{aligned}
&[1+a(p_0,|p_z|)]\,(p_0+p_z)+b(p_0,|p_z|) \\
&=\begin{cases}
2\,|p_z|+\frac{m_{\rm th}^2}{|p_z|}-\frac{m_{\rm th}^2}{|p_z|}\,\ln\left(\frac{2\,|p_z|}{p_0-|p_z|}\right), & \text{for } p_z>0 \\
p_0-|p_z|-\frac{m_{\rm th}^2}{|p_z|}, & \text{for } p_z<0
\end{cases}
\end{aligned}
\tag{5.128}
$$

3.

$$
\begin{aligned}
&b'(p_0,0,p_z)+c'(p_0,|p_z|) \\
&=\begin{cases}
\frac{4g^2C_FM^2}{|p_z|}\,\ln\left(\frac{2|p_z|}{p_0-|p_z|}\right)-\frac{4g^2C_FM^2}{|p_z|}, & \text{for } p_z>0 \\
\frac{4g^2C_FM^2}{|p_z|} & \text{for } p_z<0
\end{cases}
\end{aligned}
\tag{5.129}
$$

4.

$$
\begin{aligned}
&b'(p_0,0,p_z)-c'(p_0,|p_z|) \\
&=\begin{cases}
-\frac{4g^2C_FM^2}{|p_z|} & \text{for } p_z>0 \\
-\frac{4g^2C_FM^2}{|p_z|}\,\ln\left(\frac{2|p_z|}{p_0-|p_z|}\right)+\frac{4g^2C_FM^2}{|p_z|}. & \text{for } p_z<0
\end{cases}
\end{aligned}
\tag{5.130}
$$

1. $L_0=L_z$ leads to a mode $L^{(+)}$:

   For $p_z>0$,

$$
\omega_{L^{(+)}}(p_z)=|p_z|+\frac{(m^{*+}_{LLL})^2}{|p_z|}. \tag{5.131}
$$

   For $p_z<0$,

$$
\omega_{L^{(+)}}(p_z)=|p_z|+\frac{2\,|p_z|}{e}\,\exp\left(-\frac{2\,p_z^2}{(m^{*+}_{LLL})^2}\right). \tag{5.132}
$$

2. $L_0=-L_z$ leads to a mode $L^{(-)}$:

For $p_z > 0$,

$$\omega_{L^{(-)}}(p_z) = |p_z| + \frac{2\,|p_z|}{e}\, \exp\left(-\frac{2\,p_z^2}{(m^{*-}_{LLL})^2}\right) . \tag{5.133}$$

For $p_z < 0$,

$$\omega_{L^{(-)}}(p_z) = |p_z| + \frac{(m^{*-}_{LLL})^2}{|p_z|} . \tag{5.134}$$

3. $R_0 = R_z$ leads to a mode $R^{(+)}$:

For $p_z > 0$,

$$\omega_{R^{(+)}}(p_z) = |p_z| + \frac{(m^{*-}_{LLL})^2}{|p_z|} . \tag{5.135}$$

For $p_z < 0$,

$$\omega_{R^{(+)}}(p_z) = |p_z| + \frac{2\,|p_z|}{e}\, \exp\left(-\frac{2\,p_z^2}{(m^{*-}_{LLL})^2}\right) . \tag{5.136}$$

4. $R_0 = -R_z$ leads to a mode $R^{(-)}$:

For $p_z > 0$,

$$\omega_{R^{(-)}}(p_z) = |p_z| + \frac{2\,|p_z|}{e}\, \exp\left(-\frac{2\,p_z^2}{(m^{*+}_{LLL})^2}\right) . \tag{5.137}$$

For $p_z < 0$,

$$\omega_{R^{(-)}}(p_z) = |p_z| + \frac{(m^{*+}_{LLL})^2}{|p_z|} . \tag{5.138}$$

Note that In the high momentum limit the above dispersion relations are given in terms of absolute values of p_z, i.e. $|p_z|$.

We further note that the above dispersion relations in the absence of the magnetic field reduce to HTL results, where left and right handed are degenerate.

5.10 Spectral Function Representation of the Effective Quark Propagator

The effective propagator as obtained in (5.46) is given by

$$S^* = \mathcal{P}_- \frac{\not{L}}{L^2}\mathcal{P}_+ + \mathcal{P}_+ \frac{\not{R}}{R^2}\mathcal{P}_- \,, \tag{5.139}$$

where $\not{L}$ and $\not{R}$ can be written in the rest frame of the heat bath and the magnetic field in the z-direction following (5.44a) and (5.44b), respectively, as

$$\begin{aligned}
\not{L} &= \left[(1+a(p_0,p))p_0 + b(p_0,p) + b'(p_0,p_\perp,p_z)\right]\gamma^0 \\
&\qquad\qquad - \left[(1+a(p_0,p))p_z + c'(p_0,p_\perp,p_z)\right]\gamma^3 - (1+a(p_0,p))(\gamma\cdot p)_\perp \\
&= \left[(1+a(p_0,p))p_0 + b(p_0,p) + b'(p_0,p_\perp,p_z)\right]\gamma^0 - \left[p(1+a(p_0,p))\right](\boldsymbol{\gamma}\cdot\hat{\boldsymbol{p}}) \\
&\qquad\qquad\qquad\qquad\qquad\qquad\qquad\qquad - c'((p_0,p_\perp,p_z)\gamma^3 \\
&= g_L^1(p_0,p_\perp,p_z)\gamma^0 - g_L^2(p_0,p_\perp,p_z)(\boldsymbol{\gamma}\cdot\hat{\boldsymbol{p}}) - g_L^3(p_0,p_\perp,p_z)\gamma^3,
\end{aligned} \tag{5.140}$$

$$\begin{aligned}
\not{R} &= \left[(1+a(p_0,p))p_0 + b(p_0,p) - b'(p_0,p_\perp,p_z)\right]\gamma^0 \\
&\qquad\qquad - \left[(1+a(p_0,p))p_z - c'(p_0,p_\perp,p_z)\right]\gamma^3 - (1+a(p_0,p))(\boldsymbol{\gamma}\cdot\hat{\boldsymbol{p}})_\perp \\
&= \left[(1+a(p_0,p))p_0 + b(p_0,p) - b'(p_0,p_\perp,p_z)\right]\gamma^0 - \left[p(1+a(p_0,p))\right](\boldsymbol{\gamma}\cdot\hat{\boldsymbol{p}}) \\
&\qquad\qquad\qquad\qquad\qquad\qquad\qquad\qquad + c'(p_0,p_\perp,p_z)\gamma^3 \\
&= g_R^1(p_0,p_\perp,p_z)\gamma^0 - g_R^2(p_0,p_\perp,p_z)(\boldsymbol{\gamma}\cdot\hat{\boldsymbol{p}}) + g_R^3(p_0,p_\perp,p_z)\gamma^3\,,
\end{aligned} \tag{5.141}$$

where $\hat{\boldsymbol{p}} = \mathbf{p}/p$ and, p_z and $p_\perp$ are given, respectively, in (5.13b) and (5.13c). We also note that though $g_L^2 = g_R^2$; $g_L^3 = g_R^3$, but they are treated separately for the sake of notations that we would be using, for convenience, as g_L^i and g_R^i.

The effective propagator in Eq. (5.46) can be decomposed into six parts by separating out the γ matrices as

$$\begin{aligned} S^*(p_0,p_\perp,p_z) &= \mathcal{P}_-\gamma^0\mathcal{P}_+\ \frac{g_L^1(p_0,p_\perp,p_z)}{L^2} - \mathcal{P}_-(\boldsymbol{\gamma}\cdot\hat{\boldsymbol{p}})\mathcal{P}_+\ \frac{g_L^2(p_0,p_\perp,p_z)}{L^2} \\ &- \mathcal{P}_-\gamma^3\mathcal{P}_+\ \frac{g_L^3(p_0,p_\perp,p_z)}{L^2} + \mathcal{P}_+\gamma^0\mathcal{P}_-\ \frac{g_R^1(p_0,p_\perp,p_z)}{R^2} - \mathcal{P}_+(\boldsymbol{\gamma}\cdot\hat{\boldsymbol{p}})\mathcal{P}_-\ \frac{g_R^2(p_0,p_\perp,p_z)}{R^2} \\ &+ \mathcal{P}_+\gamma^3\mathcal{P}_-\ \frac{g_R^3(p_0,p_\perp,p_z)}{R^2}. \end{aligned} \tag{5.142}$$

It was discussed earlier that $L^2=0$ yields four poles, giving four modes with positive and negative energy, $\omega_{L(\pm)}(p_\perp,p_z)$ and $-\omega_{R(\pm)}(p_\perp,p_z)$. Similarly, $R^2=0$ also gives four poles, namely $\omega_{R(\pm)}(p_\perp,p_z)$ and $-\omega_{L(\pm)}(p_\perp,p_z)$. With this information, the spectral representation [179,216,218,219] is obtained for the effective propagator in Eq. (5.142) as

$$\begin{aligned} \rho &= \left(\mathcal{P}_-\gamma^0\mathcal{P}_+\right)\ \rho_L^1 - \left(\mathcal{P}_-(\boldsymbol{\gamma}\cdot\hat{\boldsymbol{p}})\mathcal{P}_+\right)\ \rho_L^2 - \left(\mathcal{P}_-\gamma^3\mathcal{P}_+\right)\ \rho_L^3 \\ &+ \left(\mathcal{P}_+\gamma^0\mathcal{P}_-\right)\ \rho_R^1 - \left(\mathcal{P}_+(\boldsymbol{\gamma}\cdot\hat{\boldsymbol{p}})\mathcal{P}_-\right)\ \rho_R^2 + \left(\mathcal{P}_+\gamma^3\mathcal{P}_-\right)\ \rho_R^3, \end{aligned} \tag{5.143}$$

where the spectral functions corresponding to each of the terms can be written as

$$\begin{aligned} \rho_L^i &= \frac{1}{\pi}\ \mathrm{Im}\left(\frac{g_L^i}{L^2}\right) = \frac{1}{\pi}\ \mathrm{Im}\left(F_L^i\right) \\ &= Z_{L(+)}^{i+}(p_\perp,p_z)\delta(k_0-\omega_{L(+)}(p_\perp,p_z)) + Z_{L(-)}^{i+}(p_\perp,p_z)\delta(p_0-\omega_{L(-)}(p_\perp,p_z)) \\ &+ Z_{R(-)}^{i-}(p_\perp,p_z)\delta(p_0+\omega_{R(-)}(p_\perp,p_z)) + Z_{R(+)}^{i-}(p_\perp,p_z)\delta(p_0+\omega_{R(+)}(p_\perp,p_z)) + \beta_L^i\,, \end{aligned} \tag{5.144}$$

$$\begin{aligned} \rho_R^i &= \frac{1}{\pi}\ \mathrm{Im}\left(\frac{g_R^i}{R^2}\right) = \frac{1}{\pi}\ \mathrm{Im}\left(F_R^i\right) \\ &= Z_{R(+)}^{i+}(p_\perp,p_z)\delta(p_0-\omega_{R(+)}(p_\perp,p_z)) + Z_{R(-)}^{i+}(p_\perp,p_z)\delta(p_0-\omega_{R(-)}(p_\perp,p_z)) \\ &+ Z_{L(-)}^{i-}(p_\perp,p_z)\delta(p_0+\omega_{L(-)}(p_\perp,p_z)) + Z_{L(+)}^{i-}(p_\perp,p_z)\delta(p_0+\omega_{L(+)}(p_\perp,p_z)) + \beta_R^i\,, \end{aligned} \tag{5.145}$$

where $i = 1, 2, 3$. The delta functions are originated from the timelike domain ($p_0^2 > p^2$) whereas the cut parts $\beta^i_{L(R)}$ are involved with the Landau damping originating from the space-like domain ($p_0^2 < p^2$) of the propagator. The residues $Z^i_{L(R)}$ are determined at the various poles as

$$Z^{i\ \text{sgn of pole}}_{L(R)}(p_\perp, p_z) = g^i_{L(R)}(p_0, p_\perp, p_z) \left|\frac{\partial L^2(R^2)}{\partial p_0}\right|^{-1}_{p_0 = \text{ pole}}, \tag{5.146}$$

where the expressions of residues can be written in terms of the structure coefficients a, b, b', and c' and their derivatives.

5.11 Conclusions

In this chapter, the general structure of fermionic self-energy for a chirally invariant theory has been formulated for a hot and magnetised medium. Using this we have obtained a closed form of the general structure of the effective fermion propagator. The collective excitations in such a non-trivial background has been obtained for a time-like momenta in the weak field and HTL approximation in the domain $m^2_{\mathsf{th}}(\sim g^2T^2 < |eB| < T^2)$. We found that the left and right handed modes get separated and become asymmetric in presence of magnetic field which were degenerate and symmetric otherwise. The transformation of the effective propagator in a hot magnetised medium under some of the discrete symmetries have been studied and its consequences are also reflected in the collective fermion modes in the Landau levels. We have also obtained the Dirac spinors of the various collective modes by solving the Dirac equation with the effective two-point function. Further, we checked the general structure of the two-point function by obtaining the three-point function using the Ward-Takahashi identity, which agrees with the direct calculation of one-loop order in weak field approximation. We also found that only the longitudinal component of the vertex would be relevant when there is only background magnetic field. The spectral function corresponding to the effective propagator is explicitly obtained for a hot magnetised medium which will be extremely useful for studying the spectral properties, *e.g.*, photon/dilepton production, damping rate, transport coefficients for a hot magnetised medium. This has pole contribution due to the various collective modes originating from the time-like domain and a Landau cut contribution appearing from the space-like domain. It has explicitly been shown that the spectral function reduces to that obtained for thermal medium in absence of the magnetic field. Our formulation is in general applicable to both QED and QCD with nontrivial background like hot magnetised medium.

CHAPTER 6

Hard Dilepton Production in Hot Magnetised QGP Medium

6.1 Introduction

The electromagnetic probes is among the most important ones. As Discussed in Chapter 1, dileptons are very powerful and efficient probes to study the evolution of the heavy ion collision and the medium created in the collision owing to the fact that they interact only electromagnetically. The dileptons are massive unlike real photons. So by tuning their invariant mass M and transverse momentum p_T to investigate various stages of expanding medium [220]. Depending on the invariant mass, the lepton pairs can be broadly classified in three distinct regimes [69,221,222]

1. **Low-Mass Region (LMR)** In this region, we have $M \leq M_\phi (= 1.024\text{MeV})$ and the domination source of dilepton emission are vector meson (e.g. ρ, ω, ϕ) decays.

2. **Intermediate-Mass Region (IMR)** Radiations from QGP dominates the intermediate mass region with $M_\phi < M < M_{J/\psi} (= 3.1\text{GeV})$.

3. **High-Mass Region (HMR)** Lastly in HMR, i.e. $M \geq M_{J/\psi}$, heavy quarkonia (such as J/ψ, Υ) suppression and primordial emission are the source of dileptons.

For a current phenomenological and experimental understanding of dilepton emission from thermalised QCD matter, see [223].

The background magnetic field influences particle production in heavy-ion collision. This conclusion is motivated by the challenges thrown at the existing theories of electromagnetic radiation by recent experimental results. A significant underestimation of electromagnetic spectrum was observed in low momentum region [224,225]. Thus, it is necessary to take into account the effect of a magnetic field in the calculations of dilepton production rate (DPR). Tuchin [226] first considered the magnetic contribution to dilepton rate using equivalent photon approximation. In refs. [227–230], authors have carried out field theoretical calculation in this direction. The presence of magnetic field influences the general characteristics of the medium. As a result, the properties of the quarks also get modified which in turn governs the DPR. But none of the aforementioned work had taken the effect of quasi-quark mode in DPR into account. In our work, we attempt to fill this gap.

In this chapter, we shall discuss about dilepton production rate (DPR) from weakly magnetised QGP medium. This discussion is based on *Hard dilepton production from a weakly magnetized hot QCD medium*, Aritra Das, Najmul Haque, Munshi G. Mustafa, Pradip K. Roy, **Phys.Rev.D 99 (2019) 9, 094022** [231].

6.2 Formulation of Dilepton Production Rate

In this section, we derive the rate equation for the dilepton production. This was derived by McLarren-Toimela [232] and later reformulated by Weldon [233] in thermal field theoretical approach. We follow the work of Weldon to derive the rate equation. Consider a process (Fig. 6.1) in which an initial asymptotic state $|I\rangle$ con-

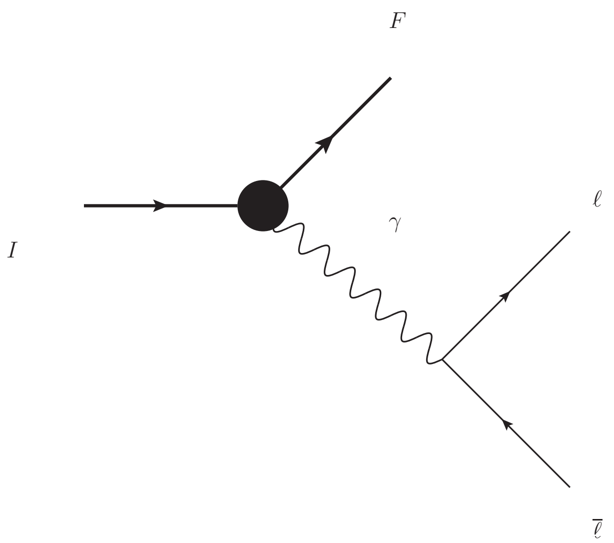

Figure 6.1: Dilepton production amplitude

taining two nuclei converts into a final state $|F\ell(\boldsymbol{k},\sigma)\overline{\ell}(\boldsymbol{k}',\sigma')\rangle$ containing hadronic species F along with lepton anti-lepton pair $\ell\overline{\ell}$ with momenta and z-component of spin P, σ and P', σ', respectively. The S-matrix element for the transition is $\langle F,\ell(\boldsymbol{k},\sigma)\overline{\ell}(\boldsymbol{k}',\sigma')|\, S\,|I\rangle$ where

$$S = T\exp\left(i\int d^4X\mathcal{L}_{\mathsf{int}}(X)\right). \tag{6.1}$$

with T being time ordering operator. So, the probability of the transition from a particular initial state $|I\rangle$ to a final state $|F,\ell(\boldsymbol{k},\sigma)\overline{\ell}(\boldsymbol{k}',\sigma')\rangle$

is $\left|\langle F, \ell(\boldsymbol{k},\sigma)\bar{\ell}(\boldsymbol{k}',\sigma')|\, S\, |I\rangle\right|^2$. The interaction Lagrangian is given as

$$\mathcal{L}_{\mathsf{int}}(X) = -e\left(j^\mu_\ell(X) + j^\mu_{\mathsf{h}}(X).\right)A_\mu(X), \tag{6.2}$$

In Eq. (6.2), the leptonic current $j^\mu_\ell(X)$ is given as

$$j^\mu_\ell(X) = \overline{\psi}(X)\gamma^\mu\psi(X). \tag{6.3}$$

The specific form of the hadronic current $j^\mu_{\mathsf{h}}(X)$ depends on the stage of the collision under consideration. To evaluate the total rate, we note the following points

- Since the spin polarization (σ and σ') of the final states of dileptons $\ell\bar{\ell}$ are not being observed, they are summed over.

- Since we are considering a thermalized medium, all the informations about the initial states $|I\rangle$ are erased. As a result, we take the ensemble average over all the initial states. This amounts to multiply a factor of $\exp\left(-\beta E_I\right)/\mathcal{Z}(\beta)$ with $\left|\langle F, \ell(\boldsymbol{k},\sigma)\bar{\ell}(\boldsymbol{k}',\sigma')|\, S\, |I\rangle\right|^2$. Here E_I is the energy of the state $|I\rangle$, i.e., $\mathcal{H}\,|I\rangle = E_I\,|I\rangle$ with $\mathcal{H}$ being the total hamiltonian of the system and $\mathcal{Z}(\beta) = \sum_I \exp\left(-\beta E_I\right) = \mathsf{Tr}\left(e^{-\beta\mathcal{H}}\right)$ being the partition function.

- Also, analogous to the spin, we sum up all the final states $|F\rangle$ as the final states are not observed except the leptons with momentum $\boldsymbol{k}$ and $\boldsymbol{k}'$.

Thus, the inclusive probability of the transition, where the final state hadrons are not observed, is given as

$$\mathcal{R} = \sum_F \sum_I \sum_{\sigma,\sigma'} \frac{\exp\left(-\beta E_I\right)}{\mathcal{Z}(\beta)} \left|\langle F, \ell(\boldsymbol{k},\sigma)\bar{\ell}(\boldsymbol{k}',\sigma')|\, S\, |I\rangle\right|^2. \tag{6.4}$$

The S matrix element, defined in Eq. (6.1), is written, to the second order in the interaction, as

$$\langle F,\ell(\boldsymbol{k},\sigma)\overline{\ell}(\boldsymbol{k}',\sigma')|\,S^{(2)}\,|I\rangle = -e^2\int d^4X d^4Y \,\langle \ell(\boldsymbol{k},\sigma)\overline{\ell}(\boldsymbol{k}',\sigma')|\,j^{\mu}_{\ell}(Y)\,|0\rangle\,\langle F|\,j^{\mu}_{\mathsf{h}}(X)\,|I\rangle \\ \langle 0|\,T\Big(A_\mu(X)A_\nu(Y)\Big)\,|0\rangle\,. \tag{6.5}$$

Here, the photon propagator is defined as

$$\langle 0|\,T\Big(A_\mu(X)A_\nu(Y)\Big)\,|0\rangle = \int \frac{d^4P'}{(2\pi)^4}e^{-iP'\cdot(X-Y)}\,\frac{-ig_{\mu\nu}}{P'^2}. \tag{6.6}$$

Also, the matrix element of the leptonic current is calculated as

$$\langle \ell(\boldsymbol{k},\sigma)\overline{\ell}(\boldsymbol{k}',\sigma')|\,j^{\mu}_{\ell}(Y)\,|0\rangle = \overline{u}(\boldsymbol{k},\sigma)\gamma^\mu v(\boldsymbol{k}',\sigma')e^{i(K+K').Y}. \tag{6.7}$$

Here u and v are the Dirac spinors and $k_0' = \sqrt{\boldsymbol{k}'^2+m^2}$ and $k_0 = \sqrt{\boldsymbol{k}^2+m^2}$. Using (6.7) and (6.6), the R.H.S of Eq (6.5) is written as

$$\langle F,\ell(\boldsymbol{k},\sigma)\overline{\ell}(\boldsymbol{k}',\sigma')|\,S^{(2)}\,|I\rangle = ie^2\overline{u}(\boldsymbol{k},\sigma)\gamma_\mu v(\boldsymbol{k}',\sigma')\int d^4X e^{-iP'\cdot X}\,\langle F|\,j^{\mu}_{\mathsf{h}}(X)\,|I\rangle \\ \int\frac{d^4P'}{(2\pi)^4}\frac{1}{P'^2}\int d^4Y e^{i(P'+K+K')\cdot Y}. \tag{6.8}$$

To further simplify (6.8), we first do the y integration which yields $\delta^{(4)}(P'+P)$. Then, the P' integral is performed to get

$$\langle F,\ell(\boldsymbol{k},\sigma)\overline{\ell}(\boldsymbol{k}',\sigma')|\,S^{(2)}\,|I\rangle = ie^2\frac{\overline{u}(\boldsymbol{k},\sigma)\gamma_\mu v(\boldsymbol{k}',\sigma')}{P^2}\int d^4X e^{iP\cdot X}\,\langle F|\,j^{\mu}_{\mathsf{h}}(x),|I\rangle\,, \tag{6.9}$$

where $P^\mu = K^\mu + K'^\mu$ being the total four-momentum of the lepton-antilepton pair. The complex conjugation of Eq. (6.9) leads to

$$\begin{aligned}
&\left(\langle F, \ell(\boldsymbol{k},\sigma)\bar{\ell}(\boldsymbol{k}',\sigma')|\, S^{(2)}\,|I\rangle\right)^* \\
&= \langle I|\, S^{(2)}\,|F, \ell(\boldsymbol{k},\sigma)\bar{\ell}(\boldsymbol{k}',\sigma')\rangle = -ie^2 \frac{\overline{v}(\boldsymbol{k}',\sigma')\gamma_\nu u(\boldsymbol{k},\sigma)}{P^2} \int d^4Z e^{-iP\cdot Z} \langle I|\, j^\nu_{\mathsf{h}}(Z)\,|F\rangle\,.
\end{aligned} \tag{6.10}$$

The leptonic spinor factor in front of Eq. (6.10) is obtained as follows

$$[\overline{u}(\boldsymbol{k},\sigma)\gamma_\nu v(\boldsymbol{k}',\sigma')]^\dagger = v^\dagger(\boldsymbol{k}',\sigma')\gamma_\nu^\dagger \overline{u}^\dagger(\boldsymbol{k},\sigma) = \overline{v}(\boldsymbol{k}',\sigma')\gamma_\nu u(\boldsymbol{k},\sigma) \tag{6.11}$$

by using the properties of conjugation $\overline{\psi} = \psi^\dagger\gamma_0$ and $\gamma^{\nu\dagger} = \gamma_0\gamma^\mu\gamma_0$. So, we get

$$\begin{aligned}
\mathcal{R} = &\sum_F\sum_I\sum_{\sigma,\sigma'} \frac{\exp\left(-\beta E_I\right)}{\mathcal{Z}(\beta)} \frac{e^4}{P^4} \overline{u}(\boldsymbol{k},\sigma)\gamma_\mu v(\boldsymbol{k}',\sigma')\overline{v}(\boldsymbol{k}',\sigma')\gamma_\nu u(\boldsymbol{k},\sigma) \\
&\qquad\times \int d^4X d^4Z e^{iP\cdot(X-Z)} \langle F|\, j^\mu_{\mathsf{h}}(X)\,|I\rangle \langle I|\, j^\nu_{\mathsf{h}}(Z)\,|F\rangle \\
= &\frac{e^4}{P^4}\ell_{\mu\nu}W_+^{\mu\nu}.
\end{aligned} \tag{6.12}$$

Here, the leptonic tensor $\ell_{\mu\nu}$ is computed as

$$\begin{aligned}
\ell_{\mu\nu} &= \sum_{\sigma,\sigma'} \overline{v}(\boldsymbol{k}',\sigma')\gamma_\mu u(\boldsymbol{k},\sigma)\overline{u}(\boldsymbol{k},\sigma)\gamma_\nu v(\boldsymbol{k}',\sigma') \\
&= \sum_{\sigma,\sigma'} \mathsf{Tr}\left[\overline{v}(\boldsymbol{k}',\sigma')\gamma_\mu u(\boldsymbol{k},\sigma)\overline{u}(\boldsymbol{k},\sigma)\gamma_\nu v(\boldsymbol{k}',\sigma')\right] \\
&= \sum_{\sigma,\sigma'} \mathsf{Tr}\left[v(\boldsymbol{k}',\sigma')\overline{v}(\boldsymbol{k}',\sigma')\gamma_\mu u(\boldsymbol{k},\sigma)\overline{u}(\boldsymbol{k},\sigma)\gamma_\nu\right] \\
&= \mathsf{Tr}\left[\left(\sum_{\sigma'} v(\boldsymbol{k}',\sigma')\overline{v}(\boldsymbol{k}',\sigma')\right)\gamma_\mu \left(\sum_\sigma u(\boldsymbol{k},\sigma)\overline{u}(\boldsymbol{k},\sigma)\right)\gamma_\nu\right] \\
&= \mathsf{Tr}\left[\left(\not{K}' - m\right)\gamma_\mu\left(\not{K}+m\right)\gamma_\nu\right] \\
&= 4\left[K_\mu K'_\nu + K'_\mu K_\nu - \left(K\cdot K' + m_\ell^2\right)g^{\mu\nu}\right],
\end{aligned} \tag{6.13}$$

where m_ℓ is the mass of the lepton. Analogously, the hadronic tensor part is defined as

$$W_+^{\mu\nu} = \sum_F \sum_I \frac{\exp\left(-\beta E_I\right)}{\mathcal{Z}(\beta)} \int d^4X d^4Z e^{iP\cdot(X-Z)} \left\langle F\right| j_{\mathsf{h}}^{\mu}(X) \left|I\right\rangle \left\langle I\right| j_{\mathsf{h}}^{\nu}(Z) \left|F\right\rangle . \quad (6.14)$$

To perform one of the position integral in R.H.S of Eq. (6.14), we make a change of variable $X' = X$, $\Xi = X - Z$. Thus

$$W_+^{\mu\nu} = \sum_F \sum_I \frac{\exp\left(-\beta E_I\right)}{\mathcal{Z}(\beta)} \int d^4X' d^4\Xi e^{iP\cdot\Xi} \left\langle F\right| j_{\mathsf{h}}^{\mu}(X') \left|I\right\rangle \left\langle I\right| j_{\mathsf{h}}^{\nu}(X'-\Xi) \left|F\right\rangle . \quad (6.15)$$

Now, the initial and final states are asymptotic states which are the simultaneous eigenstates of Hamiltonian and momentum operator. Combining this fact and the identity $j_{\mathsf{h}}^{\mu}(X') = e^{i\mathcal{P}.X'} j_{\mathsf{h}}^{\mu}(0) e^{-i\mathcal{P}.X'}$, we arrive at

$$\begin{aligned} W_+^{\mu\nu} &= \sum_F \sum_I \frac{\exp\left(-\beta E_I\right)}{\mathcal{Z}(\beta)} \int d^4\Xi e^{iP.\Xi} \int d^4X' e^{i(P_F-P_I).X'} \left\langle F\right| j_{\mathsf{h}}^{\mu}(0) \left|I\right\rangle e^{i(P_I-P_F).(X'-\Xi)} \\ &\qquad \times \left\langle I\right| j_{\mathsf{h}}^{\nu}(0) \left|F\right\rangle \\ &= \sum_F \sum_I \frac{\exp\left(-\beta E_I\right)}{\mathcal{Z}(\beta)} \int d^4\Xi e^{i(P+P_F-P_I).\xi} \int d^4X' \left\langle F\right| j_{\mathsf{h}}^{\mu}(0) \left|I\right\rangle \left\langle I\right| j_{\mathsf{h}}^{\nu}(0) \left|F\right\rangle , \end{aligned} \quad (6.16)$$

where P_I^{μ} and P_F^{μ} are the total four-momentum of the initial and final hadronic states. Note that the integrand in Eq. (6.16) is independent of X' and the integral is formally infinity. But, before performing it, we assume that the system is enclosed in some large but finite volume $\mathcal{V}$ and the interaction is turned on for a large finite time interval $\mathcal{T}$. So, the X' integration is just the total spacetime volume $\mathcal{V}\mathcal{T}$ of the system. Moreover, the Ξ integral gives delta function

$$W_+^{\mu\nu} = (2\pi)^4 \mathcal{V}\mathcal{T} \sum_F \sum_I \frac{\exp(-\beta E_I)}{\mathcal{Z}(\beta)} \delta^{(4)}(P + P_F - P_I) \langle F| j_{\mathsf{h}}^\mu(0) |I\rangle \langle I| j_{\mathsf{h}}^\nu(0) |F\rangle \,. \tag{6.17}$$

Since $p_F^0 = E_F$ and $p_I^0 = E_I$, we use the delta function to replace E_I with $E_F + p_0$ in $\exp(-\beta E_I)$ in Eq. (6.17) and get

$$\begin{aligned} W_+^{\mu\nu} &= (2\pi)^4 \mathcal{V}\mathcal{T} e^{-\beta p_0} \sum_F \sum_I \frac{\exp(-\beta E_F)}{\mathcal{Z}(\beta)} \delta^{(4)}(P + P_F - P_I) \langle F| j_{\mathsf{h}}^\mu(0) |I\rangle \langle I| j_{\mathsf{h}}^\nu(0) |F\rangle \\ &= \mathcal{V}\mathcal{T} e^{-\beta p_0} \sum_F \sum_I \frac{\exp(-\beta E_F)}{\mathcal{Z}(\beta)} \int d^4X e^{i(P+P_F-P_I).X} \langle F| j_{\mathsf{h}}^\mu(0) |I\rangle \langle I| j_{\mathsf{h}}^\nu(0) |F\rangle \\ &= \mathcal{V}\mathcal{T} e^{-\beta p_0} \sum_F \sum_I \frac{\exp(-\beta E_F)}{\mathcal{Z}(\beta)} \int d^4X e^{iP.X} \langle F| j_{\mathsf{h}}^\mu(X) |I\rangle \langle I| j_{\mathsf{h}}^\nu(0) |F\rangle \,. \end{aligned} \tag{6.18}$$

Now, using the completeness relation of the states $|I\rangle \langle I| = \mathbb{1}$, we arrive at

$$\begin{aligned} W_+^{\mu\nu} &= \mathcal{V}\mathcal{T} e^{-\beta p_0} \sum_F \frac{\exp(-\beta E_F)}{\mathcal{Z}(\beta)} \int d^4X e^{iP.X} \langle F| j_{\mathsf{h}}^\mu(X) j_{\mathsf{h}}^\nu(0) |F\rangle \\ &= \mathcal{V}\mathcal{T} e^{-\beta p_0} \sum_F \frac{1}{\mathcal{Z}(\beta)} \int d^4X e^{iP.X} \langle F| \exp(-\beta\mathcal{H}) j_{\mathsf{h}}^\mu(X) j_{\mathsf{h}}^\nu(0) |F\rangle \\ &= \mathcal{V}\mathcal{T} e^{-\beta p_0} \sum_F \int d^4X \, \langle j_{\mathsf{h}}^\mu(X) j_{\mathsf{h}}^\nu(0)\rangle_\beta \end{aligned} \tag{6.19}$$

From the definition of thermal expectation value, we finally arrive at the compact form of the hadronic tensor $W_+^{\mu\nu}$ as

$$W_+^{\mu\nu} = \mathcal{V}\mathcal{T} e^{-\beta q_0} \int d^4X \, \langle j_{\mathsf{h}}^\mu(X) j_{\mathsf{h}}^\nu(0)\rangle_\beta \,. \tag{6.20}$$

Now the joint probability that the one lepton in momentum $\boldsymbol{k}$ and anti-plepton in momentum state $\boldsymbol{k'}$ per unit volume and per unit time is $= \frac{\mathcal{R}}{\mathcal{V}\mathcal{T}} \frac{d^3k}{(2\pi)^3 2E_k} \frac{d^3k'}{(2\pi)^3 2E'_k}$. So the total number of dilepton in the four momentum range d^4P per unit volume and per unit time is given as

$$d^4P\int\frac{d^3k}{(2\pi)^3 2k_0}\int\frac{d^3k'}{(2\pi)^3 2k'_0}\int\delta^{(4)}(P-K-K')\frac{e^4}{(K+K')^4}e^{-\beta p_0}\ell_{\mu\nu}\mathcal{W}_+^{\mu\nu}, \quad (6.21)$$

where

$$\mathcal{W}_+^{\mu\nu}=\int d^4Xe^{iP\cdot X}\left\langle j_{\mathsf{h}}^{\mu}(X)j_{\mathsf{h}}^{\nu}(0)\right\rangle_\beta . \quad (6.22)$$

So, the total differential multiplicity

$$\frac{dR}{d^4Xd^4P}=e^4\int\frac{d^3k}{(2\pi)^3 2E_k}\int\frac{d^3k'}{(2\pi)^3 2E'_k}\delta^{(4)}(P-K-K')\frac{e^{-\beta p_0}}{(K+K')^4}\ell_{\mu\nu}\mathcal{W}_+^{\mu\nu}(K+K'). \quad (6.23)$$

It can be evidently simplified as using the delta function

$$\frac{d\mathcal{N}}{d^4q}=e^{-\beta p_0}\frac{e^4}{P^4}L_{\mu\nu}\mathcal{W}_+^{\mu\nu}(Q), \quad (6.24)$$

where

$$L_{\mu\nu}=\int\frac{d^3k}{(2\pi)^3 2E_k}\int\frac{d^3k'}{(2\pi)^3 2E'_k}\delta^{(4)}(P-K-K')\ell_{\mu\nu}. \quad (6.25)$$

The $L_{\mu\nu}$ is calculated by integrating over $\boldsymbol{k}$ and $\boldsymbol{k}'$ as

$$L_{\mu\nu}=\frac{1}{(2\pi)^6}\frac{2\pi}{3}\left(1+\frac{2m_\ell^2}{P^2}\right)\sqrt{1-\frac{4m^2}{P^2}}(P_\mu P_\nu-P^2g_{\mu\nu}), \quad (6.26)$$

which upon neglecting the mass m_ℓ^2 with respect to P^2 and noting that $\mathcal{W}_+^{\mu\nu}$ is conserved, Eq. (6.23) becomes

$$\frac{dR}{d^4Xd^4P}=-\frac{\alpha^2}{6\pi^3q^2}e^{-\beta p_0}g_{\mu\nu}\mathcal{W}_+^{\mu\nu}, \quad (6.27)$$

where $\alpha \equiv e^2/(4\pi)$ is the electromagnetic fine structure constant. Now, $\mathcal{W}_+^{\mu\nu}$ can be written in terms of Fourier transformation of current-current commutator as

$$\mathcal{W}_+^{\mu\nu}(P) = \frac{e^{\beta p_0}}{e^{\beta p_0} - 1}\mathcal{W}^{\mu\nu}(P), \tag{6.28}$$

with

$$\mathcal{W}^{\mu\nu}(P) = \int d^4X e^{iP\cdot X} \left\langle [j_{\mathsf{h}}^{\mu}(X), j_{\mathsf{h}}^{\nu}(0)] \right\rangle_\beta . \tag{6.29}$$

Using the expression of hadronic current, we finally arrive at the expression of differential DPR per unit volume

$$\frac{dR}{d^4Xd^4P} = \frac{\alpha}{12\pi^4}\frac{1}{P^2}\frac{1}{e^{\beta p_0} - 1}\mathsf{Im}\Pi^{\mu}_{\mu}(p_0 + i\epsilon, \boldsymbol{p}), \tag{6.30}$$

where $\Pi^{\mu\nu}$ is the photon polarisation tensor.

6.3 DPR at Vanishing Magnetic Field

In this section, we first discuss the DPR from deconfined QGP medium without any external magnetic field. In this stage, the dominant process to the lowest order is the annihilation of a quark and an antiquark to produce a virtual photon which subsequently decays into a lepton and and antilepton pair.

6.3.1 Born Rate

The Born rate is obtained from the annihilation of bare quarks and anti-quarks. It is calculated from the imaginary part of the photon self energy as shown in Fig 6.2.

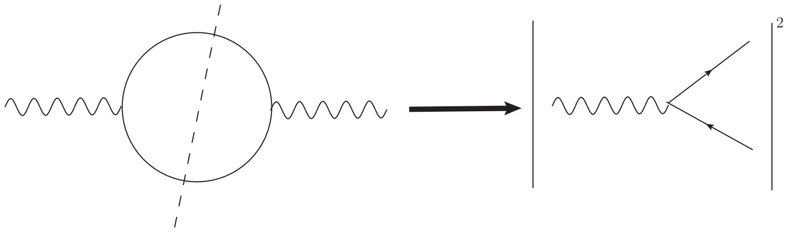

Figure 6.2: Born rate follows from the imaginary part of photon polarisation tensor which is obtained by cutting the one loop photon self energy

In the case of massless two flavour up and down quarks, Born rate takes the form

$$\frac{dR}{d^4Xd^4P} = \sum_f \left(\frac{q_f}{e}\right)^2 \frac{\alpha^2}{4\pi^4} \frac{n(p_0)}{\beta p_0} \ln \frac{\left(x_2 + e^{-\beta(p_0+\mu)}\right)\left(x_1 + e^{-\beta\mu}\right)}{\left(x_1 + e^{-\beta(p_0+\mu)}\right)\left(x_2 + e^{-\beta\mu}\right)}, \tag{6.31}$$

where $x_2 = \exp\left[-\beta(p_0 - p)\right]$, $x_1 = \exp\left[-\beta(p_0 + p)\right]$ and $n(y) = \left(e^{\beta y} - 1\right)^{-1}$ with μ being the chemical potential of the medium. For $\mu = 0$, Eq. (6.31) becomes

$$\frac{dR}{d^4Xd^4P} = \sum_f \frac{\alpha^2}{2\pi^4} \left(\frac{q_f}{e}\right)^2 \frac{n(p_0)}{\beta p_0} \ln \frac{\cosh\left[\frac{\beta}{4}(p_0 + p)\right]}{\cosh\left[\frac{\beta}{4}(p_0 + p)\right]}. \tag{6.32}$$

In the center of mass of the dilepton where the total three momentum becomes zero $\boldsymbol{p} = 0$, Eq. (6.31) becomes

$$\frac{dR}{d^4Xd^4P} = \sum_f \frac{\alpha^2}{4\pi^4} \left(\frac{q_f}{e}\right)^2 \widetilde{n}\left(\frac{p_0}{2} - \mu\right) \widetilde{n}\left(\frac{p_0}{2} + \mu\right), \tag{6.33}$$

where $\widetilde{n}(y) = \left(e^{\beta y} + 1\right)^{-1}$.

6.3.2 Hard DPR at B = 0

We know that it is unwise to judge the reliability of the lowest order result of DPR without considering the higher order correction into account. But infrared singularity and gauge dependent result in higher order calculation is the inevitable consequence of using bare perturbation theory. This problem can be circumvented partially by using HTL resummation method as discussed in chapter 1. This scenario compels us to take into account one more possibility even if the momentum flowing through the photon line is hard($\sim T$). Since in this case, the momentum flowing through one of the quark propagator can be hard while the other one can be soft, it is sufficient to dress only one quark propagator and leaving the other one and the vertices bare following the rule of HTLpt [235]. For this purpose, we use

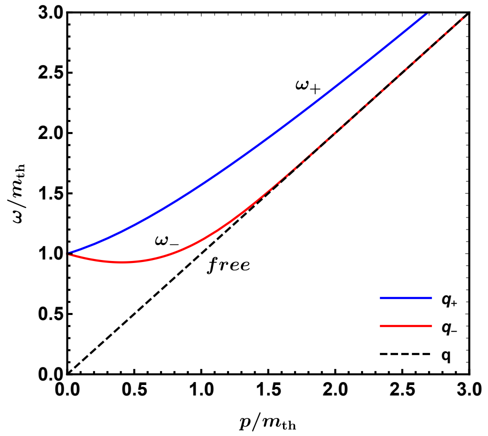

Figure 6.3: Soft (HTL) and hard (free) quark dispersion relation. q_+ and q_- are soft quarks coming from HTL resummed propagator and q is hard quark coming from free propagator.

one hard quark propagator and Hard Thermal Loop (HTL) resummed soft quark propagator with two modes [179] : one quasi-quark mode q_+ with energy ω_+ and other a plasmino mode q_- with energy ω_-. The free hard quark is represented by q with energy k. The corresponding dispersion is shown in Fig. 6.3. Now, in this case the allowed dilepton production processes coming from pole-pole part are annihilation processes $qq_+ \longrightarrow \gamma^* \longrightarrow l^+l^-$ and soft decay process $q_- \longrightarrow q\gamma^* \longrightarrow ql^+l^-$. There will also be other processes which are not allowed by energy conservation and kinematic restriction with the photon momentum, $\boldsymbol{p} = 0$. In addition, there will also be pole-cut contributions, as will be discussed below in detail. We also note that there is no cut-cut contribution as the spectral function for the hard propagator has only pole contributions. Now, the one-loop photon self-energy Π^μ_μ with one hard propagator S_0 and one resummed HTL propagator $S_{\rm HTL}$ can be written as

$$
\begin{aligned}
\Pi^\mu_\mu &= -N_c e^2 \sum_f \left(\frac{q_f}{e}\right)^2 \sum\!\!\!\!\!\!\!\int_K \mathsf{Tr}\left[\gamma^\mu S_0(K)\gamma_\mu S_{\rm HTL}(Q)\right] \\
&= 2N_c e^2 T \sum_f \left(\frac{q_f}{e}\right)^2 \sum_{k_0} \int \frac{d^3k}{(2\pi)^3} \left[\frac{1}{D_+(k)}\left(\frac{1-\hat{\boldsymbol{k}}\cdot\hat{\boldsymbol{q}}}{d_+(q)} + \frac{1+\hat{\boldsymbol{k}}\cdot\hat{\boldsymbol{q}}}{d_-(q)}\right)\right. \\
&\qquad \left. + \frac{1}{D_-(k)}\left(\frac{1+\hat{\boldsymbol{k}}\cdot\hat{\boldsymbol{q}}}{d_+(q)} + \frac{1-\hat{\boldsymbol{k}}\cdot\hat{\boldsymbol{q}}}{d_-(q)}\right)\right],
\end{aligned}
\tag{6.34}
$$

with

$$
d_\pm(q_0, q) = q_0 - q \tag{6.35}
$$

$$
D_\pm(k_0, k) = k_0 \mp k - \frac{m_{\rm th}^2}{2k}\left[\left(1 \mp \frac{k_0}{k}\right)\log\frac{k_0+k}{k_0-k} \pm 2\right]. \tag{6.36}
$$

Now, the imaginary part of Eq. (6.34) is obtained as

$$
\begin{aligned}
\mathsf{Im}\Pi^\mu_\mu &= 2N_c e^2 T \sum_f \left(\frac{q_f}{e}\right)^2 \left(e^{E/T}-1\right) \\
&\times \int \frac{d^3k}{(2\pi)^3} \int_{-\infty}^{\infty} d\omega \int_{-\infty}^{\infty} d\omega' \delta(E-\omega-\omega')\widetilde{n}(\omega)\widetilde{n}(\omega')\pi \left[(1-\hat{\boldsymbol{k}}\cdot\hat{\boldsymbol{q}})(\rho_+ r_- + \rho_- r_+)\right. \\
&\qquad \left. + (1+\hat{\boldsymbol{k}}\cdot\hat{\boldsymbol{q}})(\rho_+ r_+ + \rho_- r_-)\right],
\end{aligned}
\tag{6.37}
$$

which at $\boldsymbol{p} = 0$ reads as

$$
\begin{aligned}
\mathsf{Im}\Pi^\mu_\mu &= 2N_c e^2 T \pi \sum_f \left(\frac{q_f}{e}\right)^2 \left(e^{E/T}-1\right) \\
&\times \int \frac{d^3k}{(2\pi)^3} \int_{-\infty}^{\infty} d\omega \int_{-\infty}^{\infty} d\omega' \delta(E-\omega-\omega')\widetilde{n}(\omega)\widetilde{n}(\omega') 2(\rho_+ r_+ + \rho_- r_-).
\end{aligned}
\tag{6.38}
$$

The spectral representations of soft and hard propagator read [179], respectively, as

$$\rho_\pm(\omega,k) = \frac{\omega^2-k^2}{2m_{\rm th}^2}\left[\delta(\omega-\omega_\pm(k))+\delta(\omega+\omega_\mp(k))\right] + \beta_\pm(\omega,k)\Theta(k^2-\omega^2), \quad (6.39)$$

$$r_\pm(\omega',k) = \delta(\omega'\mp k), \quad (6.40)$$

with

$$\beta_\pm(x,y) = \frac{1}{2}\frac{y\mp x}{\left[y(x\mp y)-\frac{1}{2}\left(1\mp\frac{x}{y}\right)\log\left|\frac{x+y}{x-y}\right|\mp 1\right]^2+\left[\frac{1}{2}\pi\left(1\mp\frac{x}{y}\right)\right]^2}, \quad (6.41)$$

where $x=\omega/m_{\rm th}$ and $y=k/m_{\rm th}$. The soft spectral function contains the pole part coming from the poles of the HTL propagator and Landau cut contribution from the space-like domain, $k^2<\omega^2$, of the HTL propagator. The hard spectral function has only pole parts. So, there will be four energy conserving δ functions from the pole-pole part, namely, $\delta(E+\omega_++k)$, $\delta(E-\omega_-+k)$, $\delta(E-\omega_++k)$ and $\delta(E-\omega_+-k)$. But two processes $qq_+\gamma^*\longrightarrow$ nothing and $q\longrightarrow q_-\gamma^*\longrightarrow q_-l^+l^-$ coming, respectively, from $\delta(E+\omega_++k)$ and $\delta(E+\omega_--k)$ are not allowed by the energy conservation. The remaining two allowed processes coming from $\delta(E-\omega_+-k)$ and $\delta(E-\omega_-+k)$ lead to the respective processes $qq_+\longrightarrow\gamma^*\longrightarrow l^+l^-$ and $q_-\longrightarrow q\gamma^*\longrightarrow ql^+l^-$ as discussed earlier. The resulting pole-pole part of the dilepton rate is

$$\begin{aligned}
\left.\frac{dR}{d^4x d^4P}\right|_{\rm pole-pole} &= \frac{\alpha}{12\pi^4}\frac{1}{E^2}\frac{1}{e^{\beta E}-1}12\pi e^2\sum_f\left(\frac{q_f}{e}\right)^2\left(e^{E/T}-1\right)\int\frac{d^3k}{(2\pi)^3}\\
&\times\left[\frac{\omega_+^2-k^2}{2m_{\rm th}^2}\widetilde{n}(\omega_+)\widetilde{n}(k)\delta(E-\omega_+-k)+\frac{\omega_-^2-k^2}{2m_{\rm th}^2}\widetilde{n}(\omega_-)\widetilde{n}(-k)\delta(E-\omega_-+k)\right]\\
&= \frac{2\alpha^2}{\pi^4E^2}\sum_f\left(\frac{q_f}{e}\right)^2\int k^2dk\\
&\times\left[\frac{\omega_+^2-k^2}{2m_{\rm th}^2}\widetilde{n}(\omega_+)\widetilde{n}(k)\delta(E-\omega_+-k)+\frac{\omega_-^2-k^2}{2m_{\rm th}^2}\widetilde{n}(\omega_-)\widetilde{n}(-k)\delta(E-\omega_-+k)\right].
\end{aligned} \quad (6.42)$$

Scaling $\omega_\pm, k$ with $m_{\sf th}$ as $x_\pm = \omega_\pm/m_{\sf th}$, $E_s = E/m_{\sf th}$ and we get

$$\left.\frac{dR}{d^4xd^4P}\right|_{\rm pole-pole} = \frac{\alpha^2}{\pi^4 E_s^2}\sum_f\left(\frac{q_f}{e}\right)^2\int y^2dy\Bigg[\left(x_+^2-y^2\right)\frac{1}{e^{\beta m_{\sf th}x_+}+1}\frac{1}{e^{\beta m_{\sf th}y}+1}$$
$$\times\,\delta\left(E_s-x_+-y\right)+\left(x_-^2-y^2\right)\frac{1}{e^{\beta m_{\sf th}x_-}+1}\frac{1}{e^{-\beta m_{\sf th}y}+1}\delta\left(E_s-x_-+y\right)\Bigg]. \tag{6.43}$$

Now, the pole-cut part of the rate is obtained as

$$\left.\frac{dR}{d^4xd^4P}\right|_{\rm pole-cut} = \frac{\alpha}{12\pi^4}\frac{1}{E^2}\frac{1}{e^{\beta E}-1}12\pi e^2\sum_f\left(\frac{q_f}{e}\right)^2\left(e^{E/T}-1\right)\int\frac{d^3k}{(2\pi)^3}\int_{-k}^{k}d\omega$$
$$\times\left[\beta_+(\omega,k)\widetilde{n}(\omega)\widetilde{n}(k)\delta(E-\omega-k)+\beta_-(\omega,k)\widetilde{n}(\omega)\widetilde{n}(-k)\delta(E-\omega+k)\right]$$
$$= \frac{2\alpha^2}{\pi^4E_s^2}\sum_f\left(\frac{q_f}{e}\right)^2\int y^2dy\int_{-y}^{y}dx$$
$$\times\left[\beta_+(x,y)\widetilde{n}(x)\widetilde{n}(y)\delta(E_s-x-y)+\beta_-(x,y)\widetilde{n}(x)\widetilde{n}(-y)\delta(E_s-x+y)\right]. \tag{6.44}$$

We note that the second term of the pole-cut rate will vanish as the delta function gives the condition $x = E_s + y$, which lies outside of the domain $-y \leq x \leq y$ and the pole-cut contribution becomes

$$\left.\frac{dR}{d^4xd^4P}\right|_{\rm pole-cut} = \frac{2\alpha^2}{\pi^4E_s^2}\sum_f\left(\frac{q_f}{e}\right)^2\int y^2dy\ \beta_+(E_s-y,y)\widetilde{n}(E_s-y)\widetilde{n}(y)\Theta(2y-E_s). \tag{6.45}$$

It is worth it to write the Born rate [234] by setting $\mu = 0$ in Eq. (6.33) as

$$\left.\frac{dR}{d^4xd^4P}\right|_{\rm Born} = \sum_f\left(\frac{q_f}{e}\right)^2\frac{\alpha^2}{4\pi^4}\widetilde{n}^2(E/2). \tag{6.46}$$

In Fig. 6.4, we display the dilepton rate in the absence of magnetic field. For $E = 0$ the dilepton rate begins with the transition process $q_- \longrightarrow q\gamma^* \longrightarrow ql^+l^-$. This rate

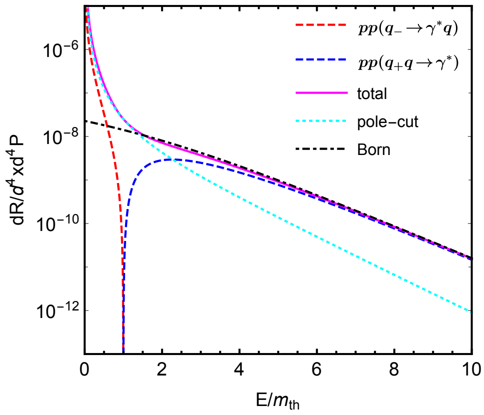

Figure 6.4: Dilepton rate for vanishing magnetic field

begins with a divergence as all plasmino, q_-, modes with higher energy (Fig. 6.3) prefer to make the transition to a free quark mode with lower energy and thus the density of states diverges. However, this rate decays very first because the plasmino mode q_- is exponentially suppressed and merges with the free hard quark mode as shown in Fig. 6.3. Then the annihilation of one soft (q_+) and one hard (q) mode, $qq_+ \longrightarrow \gamma^* \longrightarrow l^+l^-$, begins when $E = m_{\rm th}$ (as the mass of the hard mode is zero). It then grows with E and matches with the Bonn rate at large E. The dilepton rate coming from pole-cut part dominates at low E and falls off below the Bonn rate at large E. The net rate dominates the Bonn rate at low energy.

6.4 DPR at Non-Zero Magnetic Field

The dispersion solutions [210] are noted as a function of $p_\perp$ and p_z as

$$L_+ = 0 \Longrightarrow p_0 = \Big(\omega_{L(+)}, -\omega_{R(-)}\Big), \tag{6.47}$$

$$L_- = 0 \Longrightarrow p_0 = \Big(\omega_{L(-)}, -\omega_{R(+)}\Big), \tag{6.48}$$

$$R_+ = 0 \Longrightarrow p_0 = \Big(\omega_{R(+)}, -\omega_{L(-)}\Big), \tag{6.49}$$

$$R_- = 0 \Longrightarrow p_0 = \Big(\omega_{R(-)}, -\omega_{L(+)}\Big). \tag{6.50}$$

The corresponding dispersion of various quark modes $q_{L(+)}$, $q_{L(-)}$, $q_{R(+)}$ and $q_{R(-)}$ with respective frequencies $\omega_{L(+)}$, $\omega_{L(-)}$, $\omega_{R(+)}$ and $\omega_{R(-)}$ are displayed in Fig. 5.3. The free dispersion of hard quark q with energy $\omega = \sqrt{p_z^2 + p_\perp^2}$ is displayed in Fig. 6.3. It is clear from Fig. 5.3 that the processes that we expect will involve one hard and one soft quark since we are using one free (hard) quark propagator in the presence of magnetic field and one resummed thermomagnetic quark (soft) propagator in Fig. 6.5. Now, one can write the various dilepton production processes from the dispersion plot as $qq_{L(+)} \longrightarrow \gamma^* \longrightarrow l^+l^-$, $qq_{L(-)} \longrightarrow \gamma^* \longrightarrow l^+l^-$, $qq_{R(+)} \longrightarrow \gamma^* \longrightarrow l^+l^-$, and $qq_{R(-)} \longrightarrow \gamma^* \longrightarrow l^+l^-$. There could also be soft decay processes like $q_{L(+)} \longrightarrow q\gamma^* \longrightarrow ql^+l^-$, $q_{L(-)} \longrightarrow q\gamma^* \longrightarrow ql^+l^-$, $q_{R(+)} \longrightarrow q\gamma^* \longrightarrow ql^+l^-$, and $q_{R(-)} \longrightarrow q\gamma^* \longrightarrow ql^+l^-$. We will see below that all of them may not be allowed due to kinematic restrictions. Also, besides these processes there will be soft processes from Landau cut contributions.

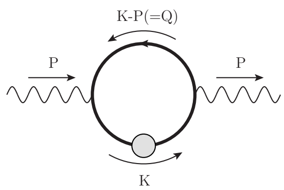

Figure 6.5: Feynman diagram for the production of the hard dileption in presence of weak background magnetic field

In this section, we shall investigate dilepton production in the presence of weak homogeneous background magnetic field. We are concerned on the dilepton whose momenta are of the order of T, i.e., $p_0, p \sim T$. In that case, as discussed, we need to dress just one quark propagator [235] as in Fig. 6.5. The bare propagator in the weak magnetic field approximation is given as

$$\begin{aligned} S_F(K) &= \frac{\not{K} + m_f}{K^2 - m_f^2} + i\gamma^1\gamma^2 \frac{\not{K}_\parallel + m_f}{(K^2 - m_f^2)^2} q_f B + \mathcal{O}[(q_f B)^2] \\ &= S_F^{(0)}(K) + S_F^{(1)}(K) + \mathcal{O}[(q_f B)^2], \end{aligned} \tag{6.51}$$

where $S_F^{(0)}$ is the $\mathcal{O}[(q_fB)^0]$ and $S_F^{(1)}$ is the $\mathcal{O}[(q_fB)]$ part of the propagator S_F. The dressed propagator is given as

$$S^*(K) = \mathcal{P}_- \frac{\not{L}(K)}{L(K)^2}\mathcal{P}_+ + \mathcal{P}_+ \frac{\not{R}(K)}{R(K)^2}\mathcal{P}_-, \tag{6.52}$$

which, for convenience, is decomposed into two parts as

$$S^*(K) = S_L^*(K) + S_R^*(K), \tag{6.53}$$

where

$$S_L^*(K) = \mathcal{P}_- \frac{\not{L}}{L^2}\mathcal{P}_+, \qquad S_R^*(K) = \mathcal{P}_+ \frac{\not{R}}{R^2}\mathcal{P}_-. \tag{6.54}$$

Now, using Eqs. (6.51) and (6.53), the one-loop photon polarization tensor corresponding to Fig. 6.5 can be obtained as

$$\begin{aligned}
\Pi^\mu{}_\mu(p_0,\mathbf{p}) &= -N_c e^2 \sum_f \left(\frac{q_f}{e}\right)^2 \sum\!\!\!\!\!\!\!\int_K \mathsf{Tr}\big[\gamma^\mu S^*(K)\gamma_\mu S_F(Q)\big] \\
&= -N_c e^2 \sum_f \left(\frac{q_f}{e}\right)^2 \sum\!\!\!\!\!\!\!\int_K \mathsf{Tr}\big[\gamma^\mu S_L^*(K)\gamma_\mu S_F^{(0)}(Q)\big] - N_c e^2 \sum_f \left(\frac{q_f}{e}\right)^2 \sum\!\!\!\!\!\!\!\int_K \mathsf{Tr}\big[\gamma^\mu S_R^*(K)\gamma_\mu S_F^{(0)}(Q)\big] \\
&\quad - N_c e^2 \sum_f \left(\frac{q_f}{e}\right)^2 \sum\!\!\!\!\!\!\!\int_K \mathsf{Tr}\big[\gamma^\mu S_L^*(K)\gamma_\mu S_F^{(1)}(Q)\big] - N_c e^2 \sum_f \left(\frac{q_f}{e}\right)^2 \sum\!\!\!\!\!\!\!\int_K \mathsf{Tr}\big[\gamma^\mu S_R^*(K)\gamma_\mu S_F^{(1)}(Q)\big].
\end{aligned} \tag{6.55}$$

The result of the Dirac trace is

$$\begin{aligned}
\mathsf{Tr}\big[\gamma^\mu S^*(K)\gamma_\mu S_F(Q)\big] = -4\Bigg[\frac{L^\mu Q_\mu}{L^2(Q^2-m_f^2)} + \frac{R^\mu Q_\mu}{R^2(Q^2-m_f^2)} + q_fB\Bigg\{\frac{Q^0L^3 - Q^3L^0}{L^2(Q^2-m^2)^2} \\
- \frac{Q^0R^3 - Q^3R^0}{R^2(Q^2-m^2)^2}\Bigg\}\Bigg],
\end{aligned} \tag{6.56}$$

where m_f is the current quark mass. The components of $L^\mu = (L^0, L^1, L^2, L^3)$ and

$R^\mu = (R^0, R^1, R^2, R^3)$ are given by

$$\begin{aligned}
L^0 &= [1 + a(k_0, k)]\, k_0 + b(k_0, k) + b'(k_0, k_\perp, k_z),\\
L^i &= [1 + a(k_0, k)]\, k^i; \qquad\qquad i = 1, 2\\
L^3 &= [1 + a(k_0, k)]\, k_z + c'(k_0, k),\\
R^0 &= [1 + a(k_0, k)]\, k_0 + b(k_0, k) - b'(k_0, k_\perp, k_z),\\
R^i &= (1 + a(k_0, k))k^i; \qquad\qquad i = 1, 2\\
R^3 &= (1 + a(k_0, k))k_z - c'(k_0, k).
\end{aligned} \tag{6.57}$$

Now Eq. (6.57) can be expressed in terms of $g^i_{L,R}$ $(i = 1, 2, 3)$ as

$$\begin{aligned}
L^0 &= g^1_L(k_0, k_\perp, k_z),\\
L^i &= g^2_L(k_0, k)\hat{k}^i; \qquad\qquad i = 1, 2\\
L^3 &= g^2_L(k_0, k)\hat{k}^3 + g^3_L(k_0, k),\\
R^0 &= g^1_R(k_0, k_\perp, k_z),\\
R^i &= g^2_R(k_0, k)\hat{k}^i; \qquad\qquad i = 1, 2\\
R^3 &= g^2_R(k_0, k)\hat{k}^3 - g^3_R(k_0, k).
\end{aligned} \tag{6.58}$$

As discussed in the previous subsection, we will investigate the case in which the virtual photon is at rest in the plasma rest frame, i.e., $\boldsymbol{p} = \mathbf{0}$, $P^\mu = (p_0, \mathbf{0})$. In this case, $Q^\mu = K^\mu - P^\mu = (k_0 - p_0, \boldsymbol{k})$. Thus, Eq. (6.55) becomes

$$
\begin{aligned}
\Pi^{\mu}{}_{\mu}(p_0,\mathbf{0}) &= 12e^2\sum_f\left(\frac{q_f}{e}\right)^2 \sum\!\!\!\!\!\!\!\int_K\Bigg[\frac{L_0(k_0-p_0)-\boldsymbol{L}\cdot\boldsymbol{k}}{L^2[(k_0-p_0)^2-\omega_k^2]}+\frac{R_0(k_0-p_0)-\boldsymbol{R}\cdot\boldsymbol{k}}{R^2[(k_0-p_0)^2-\omega_k^2]}\\
&\quad + q_fB\left\{\frac{L_z(k_0-p_0)-k_zL_0}{L^2[(k_0-p_0)^2-\omega_k^2]^2}-\frac{R_z(k_0-p_0)-k_zR_0}{R^2[(k_0-p_0)^2-\omega_k^2]^2}\right\}\Bigg]\\
&= 12e^2\sum_f\left(\frac{q_f}{e}\right)^2 \sum\!\!\!\!\!\!\!\int_K\Bigg[\frac{(k_0-p_0)g_L^1-kg_L^2-k_zg_L^3}{L^2[(k_0-p_0)^2-\omega_k^2]}+\frac{(k_0-p_0)g_R^1-kg_R^2+k_zg_R^3}{R^2[(k_0-p_0)^2-\omega_k^2]}\\
&\quad + q_fB\frac{k_zg_L^1-(k_0-p_0)(\hat{k}_zg_L^2+g_L^3)}{L^2[(k_0-p_0)^2-\omega_k^2]^2}-q_fB\frac{k_zg_R^1-(k_0-p_0)(\hat{k}_zg_R^2-g_R^3)}{R^2[(k_0-p_0)^2-\omega_k^2]^2}\Bigg]\\
&= 12e^2\sum_f\left(\frac{q_f}{e}\right)^2 \sum\!\!\!\!\!\!\!\int_K\Bigg[\frac{k_0-p_0}{(k_0-p_0)^2-\omega_k^2}F_L^1-k\frac{1}{(k_0-p_0)^2-\omega_k^2}F_L^2-k_z\frac{1}{(k_0-p_0)^2-\omega_k^2}F_L^3\\
&\quad +\frac{k_0-p_0}{(k_0-p_0)^2-\omega_k^2}F_R^1-k\frac{1}{(k_0-p_0)^2-\omega_k^2}F_R^2+k_z\frac{1}{(k_0-p_0)^2-\omega_k^2}F_R^3\\
&\quad + q_fB\Bigg\{k_z\frac{1}{[(k_0-p_0)^2-\omega_k^2]^2}F_L^1-\hat{k}_z\frac{k_0-p_0}{[(k_0-p_0)^2-\omega_k^2]^2}F_L^2-\frac{k_0-p_0}{[(k_0-p_0)^2-\omega_k^2]^2}F_L^3\\
&\quad -k_z\frac{1}{[(k_0-p_0)^2-\omega_k^2]^2}F_R^1+\hat{k}_z\frac{k_0-p_0}{[(k_0-p_0)^2-\omega_k^2]^2}F_R^2-\frac{k_0-p_0}{[(k_0-p_0)^2-\omega_k^2]^2}F_R^3\Bigg\}\Bigg]\\
&= 12e^2\sum_f\left(\frac{q_f}{e}\right)^2 \sum\!\!\!\!\!\!\!\int_K\Bigg[f_0^{(1)}F_L^1-kf_0^{(0)}F_L^2-k_zf_0^{(0)}F_L^3+f_0^{(1)}F_R^1-kf_0^{(0)}F_R^2+k_zf_0^{(0)}F_R^3\\
&\quad + q_fB\left\{k_zf_1^{(0)}F_L^1-\hat{k}_zf_1^{(1)}F_L^2-f_1^{(1)}F_L^3-k_zf_1^{(0)}F_R^1+\hat{k}_zf_1^{(1)}F_R^2-f_1^{(1)}F_R^3\right\}\Bigg]\\
&= 12e^2\sum_f\left(\frac{q_f}{e}\right)^2\int\frac{d^3k}{(2\pi)^3}\Bigg[T\sum_{k_0}(F_L^1+F_R^1)f_1^{(0)}-kT\sum_{k_0}(F_L^2+F_R^2)f_0^{(0)}-k_zT\sum_{k_0}(F_L^3\\
&\quad -F_R^3)f_0^{(0)}+q_fB\Big\{k_zT\sum_{k_0}(F_L^1-F_R^1)f_0^{(1)}-\hat{k}_zT\sum_{k_0}(F_L^2-F_R^2)f_1^{(1)}-T\sum_{k_0}(F_L^3+F_R^3)f_1^{(1)}\Big\}\Bigg].
\end{aligned}
\tag{6.59}
$$

Here in Eq. (6.59), $\omega_k \equiv \sqrt{k^2+m_f^2}$ and we used the shorthand notation as $F^i_{(L,R)} \equiv F^i_{(L,R)}(k_0,k_\perp,k_z)$ and $f^{(0),(1)}_{0,1} \equiv f^{(0),(1)}_{0,1}\big(k_0-p_0,k\big)$. Written explicitly they are given as

$$F_L^i \equiv \frac{g_L^i}{L^2}, \qquad F_R^i \equiv \frac{g_R^i}{R^2}; \qquad\qquad i = 1,2,3$$
$$f_0^{(0)}(k_0-p_0,k) \equiv \frac{1}{(k_0-p_0)^2-\omega_k^2}, \qquad f_0^{(1)}(k_0-p_0,k) \equiv \frac{k_0-p_0}{(k_0-p_0)^2-\omega_k^2},$$
$$f_1^{(0)}(k_0-p_0,k) \equiv \frac{1}{[(k_0-p_0)^2-\omega_k^2]^2}, \qquad f_1^{(1)}(k_0-p_0,k) \equiv \frac{k_0-p_0}{[(k_0-p_0)^2-\omega_k^2]^2}. \tag{6.60}$$

We take the imaginary part of Eq. (6.59) with a decomposition as

$$\mathsf{Im}\Pi^{\mu}{}_{\mu}(p_0',\mathbf{0}) = \mathsf{Im}\Pi^{1\mu}{}_{\mu}(p_0',\mathbf{0}) - \mathsf{Im}\Pi^{2\mu}{}_{\mu}(p_0',\mathbf{0}) - \mathsf{Im}\Pi^{3\mu}{}_{\mu}(p_0',\mathbf{0}) + \mathsf{Im}\Pi^{4\mu}{}_{\mu}(p_0',\mathbf{0}) - \mathsf{Im}\Pi^{5\mu}{}_{\mu}(p_0',\mathbf{0}) - \mathsf{Im}\Pi^{6\mu}{}_{\mu}(p_0,\mathbf{0}), \tag{6.61}$$

where $p_0' = p_0 + i\epsilon$. The various terms on the R.H.S. of the above equation are defined as

$$\mathrm{Im}\Pi^{1\mu}{}_{\mu}(p_0',\mathbf{0}) = 12e^2\sum_f\left(\frac{q_f}{e}\right)^2\int\frac{d^3k}{(2\pi)^3}\mathrm{Im}\,T\sum_{k_0}\left[F_L^1(k_0,k_\perp,k_z)+F_R^1(k_0,k_\perp,k_z)\right] \times f_0^{(1)}(k_0-p_0',k), \tag{6.62}$$

$$\mathrm{Im}\Pi^{2\mu}{}_{\mu}(p_0',\mathbf{0}) = 12e^2\sum_f\left(\frac{q_f}{e}\right)^2\int\frac{d^3k}{(2\pi)^3}k\mathrm{Im}\,T\sum_{k_0}\left[F_L^2(k_0,k_\perp,k_z)+F_R^2(k_0,k_\perp,k_z)\right] \times f_0^{(0)}(k_0-p_0',k), \tag{6.63}$$

$$\mathrm{Im}\Pi^{3\mu}{}_{\mu}(p_0',\mathbf{0}) = 12e^2\sum_f\left(\frac{q_f}{e}\right)^2\int\frac{d^3k}{(2\pi)^3}k_z\mathrm{Im}\,T\sum_{k_0}\left[F_L^3(k_0,k_\perp,k_z)-F_R^3(k_0,k_\perp,k_z)\right] \times f_0^{(0)}(k_0-p_0',k), \tag{6.64}$$

$$\mathrm{Im}\Pi^{4\mu}{}_{\mu}(p_0',\mathbf{0}) = 12e^2\sum_f\left(\frac{q_f}{e}\right)^2 q_fB\int\frac{d^3k}{(2\pi)^3}k_z\mathrm{Im}\,T\sum_{k_0}\left[F_L^1(k_0,k_\perp,k_z)-F_R^1(k_0,k_\perp,k_z)\right] \times f_1^{(0)}(k_0-p_0',k), \tag{6.65}$$

$$\mathrm{Im}\Pi^{5\mu}{}_{\mu}(p_0',\mathbf{0}) = 12e^2\sum_f\left(\frac{q_f}{e}\right)^2 q_fB\int\frac{d^3k}{(2\pi)^3}\hat{k}_z\mathrm{Im}\,T\sum_{k_0}\left[F_L^2(k_0,k_\perp,k_z)-F_R^2(k_0,k_\perp,k_z)\right] \times f_1^{(1)}(k_0-p_0',k), \tag{6.66}$$

$$\mathrm{Im}\Pi^{6\mu}{}_{\mu}(p_0',\mathbf{0}) = 12e^2\sum_f\left(\frac{q_f}{e}\right)^2 q_fB\int\frac{d^3k}{(2\pi)^3}\mathrm{Im}\,T\sum_{k_0}\left[F_L^3(k_0,k_\perp,k_z)+F_R^3(k_0,k_\perp,k_z)\right] \times f_1^{(1)}(k_0-p_0',k). \tag{6.67}$$

Now, by applying the Braaten-Pisarski-Yuan prescription [216], the imaginary parts of Eqs. (6.62) -(6.67) can be obtained in terms of the spectral function of the propagators [Eqs. (5.144), (5.145), (C.1), (C.2), (C.3) and (C.4)] as

$$\mathsf{Im}\Pi^{1\mu}{}_{\mu}(p_0', \mathbf{0}) = 12e^2 \sum_f \left(\frac{q_f}{e}\right)^2 \pi \left(1 - e^{\beta p_0}\right) \int \frac{d^3k}{(2\pi)^3} \int_{-\infty}^{\infty} d\omega \int_{-\infty}^{\infty} d\omega' \left[\rho_L^1(\omega) + \rho_R^1(\omega)\right] \\ \times \rho_0^{(1)}(-\omega') \widetilde{n}(\omega) \widetilde{n}(\omega') \delta(p_0 - \omega - \omega'), \tag{6.68}$$

$$\mathsf{Im}\Pi^{2\mu}{}_{\mu}(p_0', \mathbf{0}) = 12e^2 \sum_f \left(\frac{q_f}{e}\right)^2 \pi \left(1 - e^{\beta p_0}\right) \int \frac{d^3k}{(2\pi)^3} k \int_{-\infty}^{\infty} d\omega \int_{-\infty}^{\infty} d\omega' \left[\rho_L^2(\omega) + \rho_R^2(\omega)\right] \\ \times \rho_0^{(0)}(-\omega') \widetilde{n}(\omega) \widetilde{n}(\omega') \delta(p_0 - \omega - \omega'), \tag{6.69}$$

$$\mathsf{Im}\Pi^{3\mu}{}_{\mu}(p_0', \mathbf{0}) = 12e^2 \sum_f \left(\frac{q_f}{e}\right)^2 \pi \left(1 - e^{\beta p_0}\right) \int \frac{d^3k}{(2\pi)^3} k_z \int_{-\infty}^{\infty} d\omega \int_{-\infty}^{\infty} d\omega' \left[\rho_L^3(\omega) - \rho_R^3(\omega)\right] \\ \times \rho_0^{(0)}(-\omega') \widetilde{n}(\omega) \widetilde{n}(\omega') \delta(p_0 - \omega - \omega'), \tag{6.70}$$

$$\mathsf{Im}\Pi^{4\mu}{}_{\mu}(p_0', \mathbf{0}) = 12e^2 \sum_f \left(\frac{q_f}{e}\right)^2 q_f B\pi \left(1 - e^{\beta p_0}\right) \int \frac{d^3k}{(2\pi)^3} k_z \int_{-\infty}^{\infty} d\omega \int_{-\infty}^{\infty} d\omega' \left[\rho_L^1(\omega) - \rho_R^1(\omega)\right] \\ \times \rho_1^{(0)}(-\omega') \widetilde{n}(\omega) \widetilde{n}(\omega') \delta(p_0 - \omega - \omega'), \tag{6.71}$$

$$\mathsf{Im}\Pi^{5\mu}{}_{\mu}(p_0', \mathbf{0}) = 12e^2 \sum_f \left(\frac{q_f}{e}\right)^2 q_f B\pi \left(1 - e^{\beta p_0}\right) \int \frac{d^3k}{(2\pi)^3} \hat{k}_z \int_{-\infty}^{\infty} d\omega \int_{-\infty}^{\infty} d\omega' \left[\rho_L^2(\omega) - \rho_R^2(\omega)\right] \\ \times \rho_1^{(1)}(-\omega') \widetilde{n}(\omega) \widetilde{n}(\omega') \delta(p_0 - \omega - \omega'), \tag{6.72}$$

$$\mathsf{Im}\Pi^{5\mu}{}_{\mu}(p_0', \mathbf{0}) = 12e^2 \sum_f \left(\frac{q_f}{e}\right)^2 q_f B\pi \left(1 - e^{\beta p_0}\right) \int \frac{d^3k}{(2\pi)^3} \int_{-\infty}^{\infty} d\omega \int_{-\infty}^{\infty} d\omega' \left[\rho_L^3(\omega) + \rho_R^3(\omega)\right] \\ \times \rho_1^{(1)}(-\omega') \widetilde{n}(\omega) \widetilde{n}(\omega') \delta(p_0 - \omega - \omega'). \tag{6.73}$$

As before, the rate has a pole-pole and a pole-cut part. There will also be no cut-cut part since the spectral function for a hard quark has only the pole part. Below, we compute various contributions.

6.4.0.1 Pole-Pole Part

Here, to compute the pole-pole contribution of the dilepton rate, we divide it by two parts. The contribution coming from the free part of S_F and S^* is termed as (a) magnetic field-independent part, whereas that coming from the $\mathcal{O}[(q_fB)]$ part of S_F and S^* is termed as (b) magnetic field-dependent part. Note that we neglect current quark mass m_f so that $\omega_k = k$.

(a) Magnetic Field Independent Part:

Using Eq. (C.11) in (6.68), we get,

$$\begin{aligned}
\mathrm{Im}\Pi^{1\mu}{}_{\mu} &= 12e^2 \sum_f \left(\frac{q_f}{e}\right)^2 \pi(1-e^{\beta p_0})\frac{1}{(2\pi)^3}\int_0^{2\pi} d\phi \int_0^\infty dk\, k^2 \int_{-1}^{1} d\xi \int_{-\infty}^{\infty} d\omega d\omega' \\
&\quad \left[\rho_L^1(\omega)+\rho_R^1(\omega)\right] \times \left[\frac{-\delta(\omega'+k)-\delta(\omega'-k)}{2}\right] \widetilde{n}(\omega)\widetilde{n}(\omega')\delta(p_0-\omega-\omega') \\
&= \frac{3e^2}{2\pi}(e^{\beta p_0}-1)\sum_f \left(\frac{q_f}{e}\right)^2 \int_0^\infty dk\, k^2 \int_{-1}^{1} d\xi \int_{-\infty}^{\infty} d\omega \left[\rho_L^1(\omega)+\rho_R^1(\omega)\right]\widetilde{n}(\omega) \\
&\qquad \times \left[\widetilde{n}(-k)\delta(p_0-\omega+k)+\widetilde{n}(k)\delta(p_0-\omega-k)\right].
\end{aligned} \tag{6.74}$$

Now, the spectral functions ρ_L^1 and ρ_R^1 have a pole part as well as a cut part. But here we will only use the pole part of the spectral functions. In the pole part, there are four terms in $\rho_{L(R)}^1$ [Eqs. (5.144) and (5.145)] out of which the terms with a positive sign of the pole will survive from energy conservation and we now write them as

$$
\begin{aligned}
\mathrm{Im}\Pi^{1\mu}{}_{\mu}\big|_{\text{pole-pole}} &= \frac{3e^2}{2\pi}(e^{\beta p_0}-1)\sum_f\left(\frac{q_f}{e}\right)^2\int_0^\infty dk\,k^2\int_{-1}^{1}d\xi\int_{-\infty}^{\infty}d\omega\widetilde{n}(\omega)\Big[Z^{1+}_{L(+)}\\
&\times\delta(\omega-\omega_{L(+)})+Z^{1+}_{L(-)}\delta(\omega-\omega_{L(-)})+Z^{1+}_{R(+)}\delta(\omega-\omega_{R(+)})+Z^{1+}_{R(-)}\delta(\omega-\omega_{R(-)})\Big]\\
&\times\left[\widetilde{n}(-k)\delta(p_0-\omega+k)+\widetilde{n}(k)\delta(p_0-\omega-k)\right]\\
&=\frac{3e^2}{2\pi}(e^{\beta p_0}-1)\sum_f\left(\frac{q_f}{e}\right)^2\int_0^\infty dk\,k^2\int_{-1}^{1}d\xi\Big[\widetilde{n}(\omega_{L(+)})\widetilde{n}(k)\delta\left(p_0-\omega_{L(+)}-k\right)\\
&+\widetilde{n}(\omega_{L(-)})\widetilde{n}(k)\delta(p_0-\omega_{L(-)}-k)+\widetilde{n}(\omega_{R(+)})\widetilde{n}(k)\delta(p_0-\omega_{R(+)}-k)\\
&+\widetilde{n}(\omega_{R(-)})\widetilde{n}(k)\delta(p_0-\omega_{R(-)}-k)+\widetilde{n}(\omega_{L(+)})\widetilde{n}(-k)\delta(p_0-\omega_{L(+)}+k)\\
&+\widetilde{n}(\omega_{L(-)})\widetilde{n}(-k)\delta(p_0-\omega_{L(-)}+k)+\widetilde{n}(\omega_{R(+)})\widetilde{n}(-k)\delta(p_0-\omega_{R(+)}+k)\\
&+\widetilde{n}(\omega_{R(-)})\widetilde{n}(-k)\delta(p_0-\omega_{R(-)}+k)\Big].
\end{aligned}
\tag{6.75}
$$

Now, in a similar manner and using Eq. (C.12) in Eq. (6.69), we get

$$
\begin{aligned}
\mathrm{Im}^{2\mu}{}_{\mu}\big|_{\text{pole-pole}} &= \frac{3e^2}{2\pi}\sum_f\left(\frac{q_f}{e}\right)^2\left(1-e^{\beta p_0}\right)\int_0^\infty dk\,k^2\int_{-1}^{1}d\xi\int_{-\infty}^{\infty}d\omega\,\widetilde{n}(\omega)\left[\rho^2_L(\omega)\right.\\
&\left.+\rho^2_R(\omega)\right]\left[\widetilde{n}(k)\delta(p_0-\omega-k)-\widetilde{n}(-k)\delta(p_0-\omega+k)\right]\\
&=\frac{3e^2}{2\pi}\sum_f\left(\frac{q_f}{e}\right)^2(1-e^{\beta p_0})\int_0^\infty dk\,k^2\int_{-1}^{1}d\xi\Bigg[Z^{2+}_{L(+)}\widetilde{n}(\omega_{L(+)})\widetilde{n}(k)\delta(p_0-\omega_{L(+)}-k)\\
&+Z^{2+}_{L(-)}\widetilde{n}(\omega_{L(-)})\widetilde{n}(k)\delta(p_0-\omega_{L(-)}-k)+Z^{2+}_{R(+)}\widetilde{n}(\omega_{R(+)})\widetilde{n}(k)\delta(p_0-\omega_{R(+)}-k)\\
&+Z^{2+}_{R(-)}\widetilde{n}(\omega_{R(-)})\widetilde{n}(k)\delta(p_0-\omega_{R(-)}-k)-Z^{2+}_{L(+)}\widetilde{n}(\omega_{L(+)})\widetilde{n}(-k)\delta(p_0-\omega_{L(+)}+k)\\
&-Z^{2+}_{L(-)}\widetilde{n}(\omega_{L(-)})\widetilde{n}(-k)\delta(p_0-\omega_{L(-)}+k)-Z^{2+}_{R(+)}\widetilde{n}(\omega_{R(+)})\widetilde{n}(-k)\delta(p_0-\omega_{R(+)}+k)\\
&-Z^{2+}_{L(+)}\widetilde{n}(\omega_{L(+)})\widetilde{n}(-k)\delta(p_0-\omega_{L(+)}+k)\Bigg].
\end{aligned}
\tag{6.76}
$$

Also using Eq. (C.12) in Eq. (6.70), we obtain

$$\mathrm{Im}^{3\mu}{}_{\mu}\big|_{\text{pole-pole}} = \frac{3e^2}{2\pi}\sum_f \left(\frac{q_f}{e}\right)^2 (1-e^{\beta p_0})\int_0^\infty dk\,k^2 \int_{-1}^{1} d\xi\,\xi\Big[Z^{3+}_{L(+)}\widetilde{n}(\omega_{L(+)})\widetilde{n}(k)\delta(p_0 - \omega_{L(+)} - k) + Z^{3+}_{L(-)}\widetilde{n}(\omega_{L(-)})\widetilde{n}(k)\delta(p_0-\omega_{L(-)}-k) - Z^{3+}_{R(+)}\widetilde{n}(\omega_{R(+)})\widetilde{n}(k)\delta(p_0-\omega_{R(+)} - k) - Z^{3+}_{R(-)}\widetilde{n}(\omega_{R(-)})\widetilde{n}(k)\delta(p_0-\omega_{R(-)}-k) - Z^{3+}_{L(+)}\widetilde{n}(\omega_{L(+)})\widetilde{n}(-k)\delta(p_0-\omega_{L(+)}+k) - Z^{3+}_{L(-)}\widetilde{n}(\omega_{L(-)})\widetilde{n}(-k)\delta(p_0-\omega_{L(-)}+k) - Z^{3+}_{R(+)}\widetilde{n}(\omega_{R(+)})\widetilde{n}(-k)\delta(p_0-\omega_{R(+)}+k) - Z^{3+}_{R(-)}\widetilde{n}(\omega_{R(-)})\widetilde{n}(-k)\delta(p_0-\omega_{R(-)}+k)\Big]. \quad (6.77)$$

(b) Magnetic Field Dependent Part:

We begin by stating that some terms with derivatives of Dirac δ functions are present. But after doing integration by parts, these terms will eventually get eliminated. Also, using the parity properties of the δ function and its derivatives it is easy to see that $\rho^1_{(0)}(-\omega') = -\rho^1_{(0)}(\omega')$. Using Eq. (C.16) in Eq. (6.71), we get

$$\begin{aligned}\mathrm{Im}\Pi^{4\mu}{}_{\mu}\big|_{\text{pole-pole}} &= -\frac{3e^2}{4\pi}\sum_f \left(\frac{q_f}{e}\right)^2 (1-e^{\beta p_0})q_fB\int_0^\infty dk\,k^3\int_{-1}^{1} d\xi\,\xi \\ &\qquad \int_{-\infty}^{\infty} d\omega'\widetilde{n}(\omega')\widetilde{n}(p_0-\omega')[\rho^1_L(p_0-\omega')-\rho^1_R(p_0-\omega')]\rho^{(0)}_1(\omega') \\ &= -\frac{3e^2}{4\pi}\sum_f \left(\frac{q_f}{e}\right)^2 (1-e^{\beta p_0})q_fB\int_0^\infty dk\int_{-1}^{1} d\xi\,\xi\int_{-\infty}^{\infty} d\omega'\widetilde{n}(\omega')\widetilde{n}(p_0-\omega')\left[\rho^1_L(p_0-\omega')-\rho^1_R(p_0-\omega')\right]\left[\delta(\omega'-k)-\delta(\omega'+k)+k\frac{\partial}{\partial\omega'}\left(\delta(\omega'-k)+\delta(\omega'+k)\right)\right] \\ &= -\frac{3e^2}{4\pi}\sum_f \left(\frac{q_f}{e}\right)^2 (1-e^{\beta p_0})q_fB\int_0^\infty dk\int\limits_{-1}^{1} d\xi\,\xi\Big[\widetilde{n}(k)\widetilde{n}(p_0-k)\Big\{\rho^1_L(p_0-k)-\rho^1_R(p_0-k)\Big\} - \widetilde{n}(-k)\widetilde{n}(p_0+k)\Big\{\rho^1_L(p_0+k)-\rho^1_R(p_0+k)\Big\} + k\int_{-\infty}^{\infty} d\omega\,\widetilde{n}(\omega)\widetilde{n}(p_0-\omega) \\ &\qquad \times\Big(\rho^1_L(p_0-\omega)-\rho^1_R(p_0-\omega)\Big)\Big(\delta'(\omega-k)+\delta'(\omega+k)\Big)\Big].\end{aligned} \quad (6.78)$$

At this point, we use partial fraction method to eliminate $\delta'(\omega \pm k)$, and it gives

$$
\begin{aligned}
\mathrm{Im}\Pi^{4\mu}{}_{\mu}\big|_{\text{pole-pole}} &= -\frac{3e^2}{4\pi}\sum_f\left(\frac{q_f}{e}\right)^2(1-e^{\beta p_0})q_fB\int_0^\infty dk\int_{-1}^1 d\xi\,\xi\Bigg[\widetilde{n}(k)\widetilde{n}(p_0-k)\\
&\times\Big\{\rho_L^1(p_0-k)-\rho_R^1(p_0-k)\Big\}-\widetilde{n}(-k)\widetilde{n}(p_0+k)\Big\{\rho_L^1(p_0+k)-\rho_R^1(p_0+k)\Big\}\\
&-k\int_{-\infty}^{\infty}d\omega\,\frac{\partial}{\partial\omega}\Bigg\{\widetilde{n}(\omega)\widetilde{n}(p_0-\omega)[\rho_L^1(p_0-\omega)-\rho_R^1(p_0-\omega)]\Bigg\}\Bigg(\delta(\omega-k)+\delta(\omega+k)\Bigg)\Bigg]\\
&= -\frac{3e^2}{4\pi}\sum_f\left(\frac{q_f}{e}\right)^2(1-e^{\beta p_0})q_fB\int_0^\infty dk\int_{-1}^1 d\xi\,\xi\Bigg[\widetilde{n}(k)\widetilde{n}(p_0-k)\Big\{\rho_L^1(p_0-k)\\
&-\rho_R^1(p_0-k)\Big\}-\widetilde{n}(-k)\widetilde{n}(p_0+k)\Big\{\rho_L^1(p_0+k)-\rho_R^1(p_0+k)\Big\}-k\frac{\partial}{\partial k}\Bigg(\widetilde{n}(k)\widetilde{n}(p_0-k)\\
&\times\Big\{\rho_L^1(p_0-k)-\rho_R^1(p_0-k)\Big\}-\widetilde{n}(-k)\widetilde{n}(p_0+k)\Big\{\rho_L^1(p_0+k)-\rho_R^1(p_0+k)\Big\}\Bigg)\Bigg]\\
&= -\frac{3e^2}{4\pi}\sum_f\left(\frac{q_f}{e}\right)^2(1-e^{\beta p_0})q_fB\int_0^\infty dk\int_{-1}^1 d\xi\,\xi\Bigg[2\widetilde{n}(k)\widetilde{n}(p_0-k)\Big\{\rho_L^1(p_0-k)\\
&-\rho_R^1(p_0-k)\Big\}-\widetilde{n}(-k)\widetilde{n}(p_0+k)\Big\{\rho_L^1(p_0+k)-\rho_R^1(p_0+k)\Big\}-\frac{\partial}{\partial k}\Bigg(k\widetilde{n}(k)\widetilde{n}(p_0-k)\\
&\Big\{\rho_L^1(p_0-k)-\rho_R^1(p_0-k)\Big\}-k\widetilde{n}(-k)\widetilde{n}(p_0+k)\Big\{\rho_L^1(p_0+k)-\rho_R^1(p_0+k)\Big\}\Bigg)\Bigg].
\end{aligned}
\tag{6.79}
$$

The last term, i.e., the term that contains a derivative with respect to k, when integrated out gives the boundary term and it vanishes. Also, by using the properties of the δ function, one obtains the pole-pole part as

$$\mathrm{Im}\Pi^{4\mu}{}_{\mu}\big|_{\text{pole-pole}} = -\frac{3e^2}{2\pi}\sum_f \left(\frac{q_f}{e}\right)^2 (1-e^{\beta p_0})q_f B\int_{-1}^{1} d\xi\,\xi\int_0^\infty dk\Bigg[\widetilde{n}(k)$$
$$\Bigg\{Z^{1+}_{L(+)}\widetilde{n}(\omega_{L(+)})\delta(p_0-k-\omega_{L(+)}) + Z^{1+}_{L(-)}\widetilde{n}(\omega_{L(-)})\delta(p_0-k-\omega_{L(-)}) - Z^{1+}_{R(+)}\widetilde{n}(\omega_{R(+)})$$
$$\times\,\delta(p_0-k-\omega_{R(+)}) - Z^{1+}_{R(-)}\widetilde{n}(\omega_{R(-)})\delta(p_0-k-\omega_{R(-)})\Bigg\} - \widetilde{n}(-k)\Bigg\{Z^{1+}_{L(+)}\widetilde{n}(\omega_{L(+)})$$
$$\times\,\delta(p_0+k-\omega_{L(+)}) + Z^{1+}_{L(-)}\widetilde{n}(\omega_{L(-)})\delta(p_0+k-\omega_{L(-)}) - Z^{1+}_{R(+)}\widetilde{n}(\omega_{R(+)})\delta(p_0+k-\omega_{R(+)})$$
$$- Z^{1+}_{R(-)}\widetilde{n}(\omega_{R(-)})\delta(p_0+k-\omega_{R(-)})\Bigg\}\Bigg]. \tag{6.80}$$

Using (C.15) in Eq. (6.72), we get

$$\mathrm{Im}\Pi^{5\mu}{}_{\mu}\big|_{\text{pole-pole}} = \frac{3e^2}{4\pi}\sum_f \left(\frac{q_f}{e}\right)^2 (1-e^{\beta p_0})q_f B\int_{-1}^{1} d\xi\,\xi\int_0^\infty dk\Bigg[\widetilde{n}(k)\Bigg\{Z^{2+}_{L(+)}\widetilde{n}(\omega_{L(+)})$$
$$\times\,\delta(p_0-k-\omega_{L(+)}) + Z^{2+}_{L(-)}\widetilde{n}(\omega_{L(-)})\delta(p_0-k-\omega_{L(-)}) - Z^{2+}_{R(+)}\widetilde{n}(\omega_{R(+)})\delta(p_0-k-\omega_{R(+)})$$
$$- Z^{2+}_{R(-)}\widetilde{n}(\omega_{R(-)})\delta(p_0-k-\omega_{R(-)})\Bigg\} + \widetilde{n}(-k)\Bigg\{Z^{2+}_{L(+)}\widetilde{n}(\omega_{L(+)})\delta(p_0+k-\omega_{L(+)})$$
$$+ Z^{2+}_{L(-)}\widetilde{n}(\omega_{L(-)})\delta(p_0+k-\omega_{L(-)}) - Z^{2+}_{R(+)}\widetilde{n}(\omega_{R(+)})\delta(p_0+k-\omega_{R(+)})$$
$$- Z^{2+}_{R(-)}\widetilde{n}(\omega_{R(-)})\delta(p_0+k-\omega_{R(-)})\Bigg\}\Bigg]. \tag{6.81}$$

Finally using Eq. (6.73), we get

$$\mathrm{Im}\Pi^{6\mu}{}_{\mu}\big|_{\text{pole-pole}} = \frac{3e^2}{4\pi}\sum_f\left(\frac{q_f}{e}\right)^2(1-e^{\beta p_0})q_fB\int_{-1}^{1}d\xi\int_0^\infty dk\Bigg[\widetilde{n}(k)\Bigg\{Z^{2+}_{L(+)}\widetilde{n}(\omega_{L(+)})$$
$$\times\,\delta(p_0-k-\omega_{L(+)})+Z^{2+}_{L(-)}\widetilde{n}(\omega_{L(-)})\delta(p_0-k-\omega_{L(-)})+Z^{2+}_{R(+)}\widetilde{n}(\omega_{R(+)})\delta(p_0-k-\omega_{R(+)})$$
$$+\,Z^{2+}_{R(-)}\widetilde{n}(\omega_{R(-)})\delta(p_0-k-\omega_{R(-)})\Bigg\}+\widetilde{n}(-k)\Bigg\{Z^{2+}_{L(+)}\widetilde{n}(\omega_{L(+)})\delta(p_0+k-\omega_{L(+)})+Z^{2+}_{L(-)}\widetilde{n}(\omega_{L(-)})$$
$$\times\,\delta(p_0+k-\omega_{L(-)})+Z^{2+}_{R(+)}\widetilde{n}(\omega_{R(+)})\delta(p_0+k-\omega_{R(+)})+Z^{2+}_{R(-)}\widetilde{n}(\omega_{R(-)})\delta(p_0+k-\omega_{R(-)})\Bigg\}\Bigg]. \tag{6.82}$$

(c) Dilepton rate from various processes in pole-pole part in presence of magnetic field:

We note that for numerical computation we change the integration from spherical polar to cylindrical polar through the transformation $k_\perp = k\sqrt{1-\xi^2}$, $k_z = k\xi$, where $\xi = \cos\theta$. Using (6.61) and grouping the delta functions together we get the dilepton rates in terms of the cylindrical polar coordinate from various processes discussed before as follows:

1. <u>$q_{L(+)}q \longrightarrow \gamma^*$</u>

$$\frac{dR}{d^4xd^4P}\bigg|^{q_{L(+)}q\to\gamma^*} = \frac{\alpha^2}{2p_0^2\pi^4}\sum_f\left(\frac{q_f}{e}\right)^2\int_0^\infty dk_\perp\, k_\perp\int_{-\infty}^{\infty}dk_z\widetilde{n}\Big(p_0-\sqrt{k_\perp^2+k_z^2}\Big)$$
$$\times\,\widetilde{n}\Big(\sqrt{k_\perp^2+k_z^2}\Big)\Bigg[Z^1_{L(+)}+Z^2_{L(+)}+\frac{k_z}{\sqrt{k_\perp^2+k_z^2}}Z^3_{L(+)}+\frac{q_fB}{k_\perp^2+k_z^2}\Bigg(\frac{k_z}{\sqrt{k_\perp^2+k_z^2}}Z^1_{L(+)}$$
$$+\,\frac{k_z}{2\sqrt{k_\perp^2+k_z^2}}Z^2_{L(+)}+\frac{1}{2}Z^3_{L(+)}\Bigg)\Bigg]\delta\left(p_0-\omega_{L(+)}(k_\perp,k_z)-\sqrt{k_\perp^2+k_z^2}\right). \tag{6.83}$$

2. $q_{L(-)}q \longrightarrow \gamma^*$

$$\frac{dR}{d^4xd^4P}\bigg|^{q_{L(-)}q\to\gamma^*} = \frac{\alpha^2}{2p_0^2\pi^4}\sum_f\left(\frac{q_f}{e}\right)^2\int_0^\infty dk_\perp\ k_\perp\int_{-\infty}^{\infty}dk_z\widetilde{n}\Big(p_0-\sqrt{k_\perp^2+k_z^2}\Big)$$
$$\times\,\widetilde{n}\Big(\sqrt{k_\perp^2+k_z^2}\Big)\Bigg[Z^1_{L(-)}+Z^2_{L(-)}+\frac{k_z}{\sqrt{k_\perp^2+k_z^2}}Z^3_{L(-)}+\frac{q_fB}{k_\perp^2+k_z^2}\Bigg(\frac{k_z}{\sqrt{k_\perp^2+k_z^2}}Z^1_{L(-)}$$
$$+\frac{k_z}{2\sqrt{k_\perp^2+k_z^2}}Z^2_{L(-)}+\frac{1}{2}Z^3_{L(-)}\Bigg)\Bigg]\delta\Big(p_0-\omega_{L(-)}(k_\perp,k_z)-\sqrt{k_\perp^2+k_z^2}\Big). \tag{6.84}$$

3. $q_{R(+)}q \longrightarrow \gamma^*$

$$\frac{dR}{d^4xd^4P}\bigg|^{q_{R(+)}q\to\gamma^*} = \frac{\alpha^2}{2p_0^2\pi^4}\sum_f\left(\frac{q_f}{e}\right)^2\int_0^\infty dk_\perp\ k_\perp\int_{-\infty}^{\infty}dk_z\widetilde{n}\Big(p_0-\sqrt{k_\perp^2+k_z^2}\Big)$$
$$\times\,\widetilde{n}\Big(\sqrt{k_\perp^2+k_z^2}\Big)\Bigg[Z^1_{R(+)}+Z^2_{R(+)}-\frac{k_z}{\sqrt{k_\perp^2+k_z^2}}Z^3_{R(+)}-\frac{q_fB}{k_\perp^2+k_z^2}\Bigg(\frac{k_z}{\sqrt{k_\perp^2+k_z^2}}Z^1_{R(+)}$$
$$+\frac{k_z}{2\sqrt{k_\perp^2+k_z^2}}Z^2_{R(+)}-\frac{1}{2}Z^3_{R(+)}\Bigg)\Bigg]\delta\Big(p_0-\omega_{R(+)}(k_\perp,k_z)-\sqrt{k_\perp^2+k_z^2}\Big). \tag{6.85}$$

4. $q_{R(-)}q \longrightarrow \gamma^*$

$$\frac{dR}{d^4xd^4P}\bigg|^{q_{R(-)}q\to\gamma^*} = \frac{\alpha^2}{2p_0^2\pi^4}\sum_f\left(\frac{q_f}{e}\right)^2\int_0^\infty dk_\perp\ k_\perp\int_{-\infty}^{\infty}dk_z\widetilde{n}\Big(p_0-\sqrt{k_\perp^2+k_z^2}\Big)$$
$$\times\,\widetilde{n}\Big(\sqrt{k_\perp^2+k_z^2}\Big)\Bigg[Z^1_{R(-)}+Z^2_{R(-)}-\frac{k_z}{\sqrt{k_\perp^2+k_z^2}}Z^3_{R(-)}-\frac{q_fB}{k_\perp^2+k_z^2}\Bigg(\frac{k_z}{\sqrt{k_\perp^2+k_z^2}}Z^1_{R(-)}$$
$$+\frac{k_z}{2\sqrt{k_\perp^2+k_z^2}}Z^2_{R(-)}-\frac{1}{2}Z^3_{R(-)}\Bigg)\Bigg]\delta\Big(p_0-\omega_{R(-)}(k_\perp,k_z)-\sqrt{k_\perp^2+k_z^2}\Big). \tag{6.86}$$

5. $\underline{q_{L(+)} \longrightarrow q\gamma^*}$

$$\frac{dR}{d^4xd^4P}\bigg|^{q_{L(+)}\to q\gamma^*} = \frac{\alpha^2}{2p_0^2\pi^4}\sum_f\left(\frac{q_f}{e}\right)^2\int_0^\infty dk_\perp\ k_\perp\int_{-\infty}^{\infty}dk_z\widetilde{n}\Big(p_0+\sqrt{k_\perp^2+k_z^2}\Big)$$
$$\times\,\widetilde{n}\Big(-\sqrt{k_\perp^2+k_z^2}\Big)\Bigg[Z^1_{L(+)}-Z^2_{L(+)}-\frac{k_z}{\sqrt{k_\perp^2+k_z^2}}Z^3_{L(+)}-\frac{q_fB}{k_\perp^2+k_z^2}\Bigg(\frac{k_z}{\sqrt{k_\perp^2+k_z^2}}Z^1_{L(+)}$$
$$-\frac{k_z}{2\sqrt{k_\perp^2+k_z^2}}Z^2_{L(+)}-\frac{1}{2}Z^3_{L(+)}\Bigg)\Bigg]\delta\Big(p_0-\omega_{L(+)}(k_\perp,k_z)+\sqrt{k_\perp^2+k_z^2}\Big). \tag{6.87}$$

6. $\underline{q_{L(-)} \longrightarrow q\gamma^*}$

$$\frac{dR}{d^4xd^4P}\bigg|^{q_{L(-)}\to q\gamma^*} = \frac{\alpha^2}{p_0^2\pi^4}\sum_f\left(\frac{q_f}{e}\right)^2\int_0^\infty dk_\perp\ k_\perp\int_{-\infty}^{\infty}dk_z\widetilde{n}\Big(p_0+\sqrt{k_\perp^2+k_z^2}\Big)$$
$$\times\,\widetilde{n}\Big(-\sqrt{k_\perp^2+k_z^2}\Big)\Bigg[Z^1_{L(-)}-Z^2_{L(-)}-\frac{k_z}{\sqrt{k_\perp^2+k_z^2}}Z^3_{L(-)}-\frac{q_fB}{k_\perp^2+k_z^2}\Bigg(\frac{k_z}{\sqrt{k_\perp^2+k_z^2}}Z^1_{L(-)}$$
$$-\frac{k_z}{2\sqrt{k_\perp^2+k_z^2}}Z^2_{L(-)}-\frac{1}{2}Z^3_{L(-)}\Bigg)\Bigg]\delta\Big(p_0-\omega_{L(-)}(k_\perp,k_z)+\sqrt{k_\perp^2+k_z^2}\Big). \tag{6.88}$$

7. $\underline{q_{R(+)} \longrightarrow q\gamma^*}$

$$\frac{dR}{d^4xd^4P}\bigg|^{q_{R(+)}\to q\gamma^*} = \frac{\alpha^2}{2p_0^2\pi^4}\sum_f\left(\frac{q_f}{e}\right)^2\int_0^\infty dk_\perp\ k_\perp\int_{-\infty}^{\infty}dk_z\widetilde{n}\Big(p_0+\sqrt{k_\perp^2+k_z^2}\Big)$$
$$\times\,\widetilde{n}\Big(-\sqrt{k_\perp^2+k_z^2}\Big)\Bigg[Z^1_{R(+)}-Z^2_{R(+)}+\frac{k_z}{\sqrt{k_\perp^2+k_z^2}}Z^3_{R(+)}+\frac{q_fB}{k_\perp^2+k_z^2}\Bigg(\frac{k_z}{\sqrt{k_\perp^2+k_z^2}}Z^1_{R(+)}$$
$$-\frac{k_z}{2\sqrt{k_\perp^2+k_z^2}}Z^2_{R(+)}+\frac{1}{2}Z^3_{R(+)}\Bigg)\Bigg]\delta\Big(p_0-\omega_{R(+)}(k_\perp,k_z)+\sqrt{k_\perp^2+k_z^2}\Big). \tag{6.89}$$

8. $q_{R(-)} \longrightarrow q\gamma^*$

$$\frac{dR}{d^4x d^4P}\bigg|^{q_{R(-)}\to q\gamma^*} = \frac{\alpha^2}{2p_0^2\pi^4}\sum_f \left(\frac{q_f}{e}\right)^2 \int_0^\infty dk_\perp\; k_\perp \int_{-\infty}^{\infty} dk_z \widetilde{n}\Big(p_0 + \sqrt{k_\perp^2+k_z^2}\Big)$$
$$\times\, \widetilde{n}\Big(-\sqrt{k_\perp^2+k_z^2}\Big)\Bigg[Z^1_{R(-)} - Z^2_{R(-)} + \frac{k_z}{\sqrt{k_\perp^2+k_z^2}}Z^3_{R(-)} + \frac{q_f B}{k_\perp^2+k_z^2}\Bigg(\frac{k_z}{\sqrt{k_\perp^2+k_z^2}}Z^1_{R(-)}$$
$$-\frac{k_z}{2\sqrt{k_\perp^2+k_z^2}}Z^2_{R(-)} + \frac{1}{2}Z^3_{R(-)}\Bigg)\Bigg]\delta\Big(p_0 - \omega_{R(-)}(k_\perp,k_z) + \sqrt{k_\perp^2+k_z^2}\Big). \tag{6.90}$$

From the parity symmetry of the dispersion mode, it is possible to show that

$$\begin{aligned}
\frac{dR}{d^4x d^4P}\bigg|^{\omega_{L(+)}k\to\gamma^*} &= \frac{dR}{d^4x d^4P}\bigg|^{\omega_{R(+)}k\to\gamma^*}, \\
\frac{dR}{d^4x d^4P}\bigg|^{\omega_{L(-)}k\to\gamma^*} &= \frac{dR}{d^4x d^4P}\bigg|^{\omega_{R(-)}k\to\gamma^*}, \\
\frac{dR}{d^4x d^4P}\bigg|^{\omega_{L(+)}\to k\gamma^*} &= \frac{dR}{d^4x d^4P}\bigg|^{\omega_{R(+)}\to k\gamma^*}, \\
\frac{dR}{d^4x d^4P}\bigg|^{\omega_{L(-)}\to k\gamma^*} &= \frac{dR}{d^4x d^4P}\bigg|^{\omega_{R(-)}\to k\gamma^*}.
\end{aligned} \tag{6.91}$$

Finally, the pole-pole contribution of the hard dilepton rate becomes

$$\frac{dR}{d^4x d^4P}\bigg|^{\mathrm{pp}} = 2\Bigg(\frac{dR}{d^4x d^4P}\bigg|^{\omega_{L(+)}k\to\gamma^*} + \frac{dR}{d^4x d^4P}\bigg|^{\omega_{L(-)}k\to\gamma^*} + \frac{dR}{d^4x d^4P}\bigg|^{\omega_{L(+)}\to k\gamma^*}$$
$$+ \frac{dR}{d^4x d^4P}\bigg|^{\omega_{L(-)}\to k\gamma^*}\Bigg). \tag{6.92}$$

We note that the various soft decay modes will contribute only to the soft dilepton production at low energy. Since we are interested in hard dilepton production rate, only the annihilation modes will contribute and we will omit those soft decay modes from our considerations. The resulting pole-pole contribution is plotted in Fig. 6.6. In the left panel the rate is displayed as a function of dilepton energy at $T = 200$ MeV but for different magnetic fields. In the absence of magnetic field ($eB = 0$) the annihilation between a hard and a soft quark starts when dilepton energy $E = m_{\mathsf{th}}$

and resembles that of $qq_+ \longrightarrow \gamma^* \longrightarrow l^+l^-$ as given in Fig. 6.4. As the magnetic field is turned on, all four quasiparticle modes, namely, $\omega_{L(+)}$, $\omega_{L(-)}$, $\omega_{R(+)}$, $\omega_{R(-)}$, as shown in Fig. 5.3, separately participate in annihilation with hard quark. As can be seen, the dilepton rate at finite magnetic field begins at little higher energy of the virtual photon compare to the vanishing magnetic field. This is because the presence of magnetic field contributes to the thermomagnetic mass which is lower than the thermal mass. As the energy of the dilepton increases, the rate becomes almost equal to that in absence of magnetic field. In the right panel of Fig. 6.6, the rate is displayed for various temperatures for a given magnetic filed. At energy up to the $E = p_0 \approx 2m_{\mathsf{th}}$, the rate is found to be almost independent of T as magnetic field may be the dominant scale there. At energies $E = p_0 > 2m_{\mathsf{th}}$, the rate increases with the increase of T as T is the dominant scale in the weak field approximation.

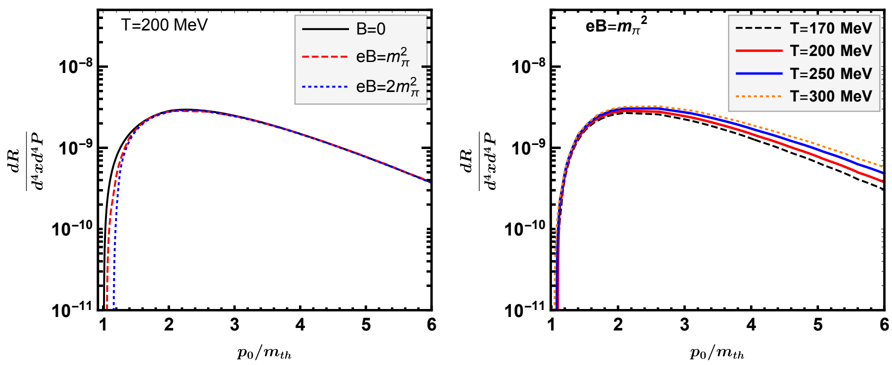

Figure 6.6: Pole-pole contribution of the dilepton production rate as a function of the energy of dilepton in the center-of-mass reference frame at $T = 200$ MeV with different magnetic field (left panel) and $eB = m_\pi^2$ with different temperature (right panel).

6.4.0.2 Pole-Cut Contribution

The presence of Θ due to spacelike momentum in the Landau cut contribution of the spectral function, $\Theta(k^2 - \omega^2)\beta^i_{L(R)}(\omega, k_\perp, k_z)$, immensely simplifies the pole-cut rate. From Eq. (6.74), we get

$$\mathrm{Im}\Pi^{1\mu}_{\mu}\Big|_{\text{pole-cut}} = \frac{3e^2}{2\pi}(e^{\beta p_0}-1)\sum_f\left(\frac{q_f}{e}\right)^2\int_0^\infty dk\,k^2\int_{-1}^{1}d\xi\int_{-\infty}^{\infty}d\omega\Theta(k^2-\omega^2)$$
$$\times\left[\beta^1_L(\omega)+\beta^1_R(\omega)\right]\widetilde{n}(\omega)\left[\widetilde{n}(-k)\delta(p_0-\omega+k)+\widetilde{n}(k)\delta(p_0-\omega-k)\right]. \tag{6.93}$$

We note that the term with $\delta(p_0-\omega+k)$ will have no contribution because $\Theta[k^2-(p_0+k)^2]=\Theta[-p_0(p_0+2k)^2]$ will never be satisfied since $k, p_0>0$. The expression to evaluate the pole-cut contribution is

$$\frac{dR}{d^4xd^4p}\Bigg|_{\text{pole-cut}} = \frac{\alpha^2}{2\pi^4p_0^2}\sum_f\left(\frac{q_f}{e}\right)^2\int_{-1}^{1}d\xi\int_0^\infty dk\ \widetilde{n}(k)\widetilde{n}(p_0-k)\Theta\left(2k-p_0\right)$$
$$\times\Bigg[k^2\Big(\beta^1_L+\beta^1_R+\beta^2_L+\beta^2_R+\xi(\beta^3_L-\beta^3_R)\Big)+q_fB\Big(\xi(\beta^1_L-\beta^1_R)+\frac{1}{2}\xi\left(\beta^2_L-\beta^2_R\right)$$
$$+\frac{1}{2}\left(\beta^3_L+\beta^3_R\right)\Big)\Bigg], \tag{6.94}$$

where $\beta^i_{(L/R)}\equiv\beta^i_{(L/R)}(p_0-k,k_\perp,k^3)$.

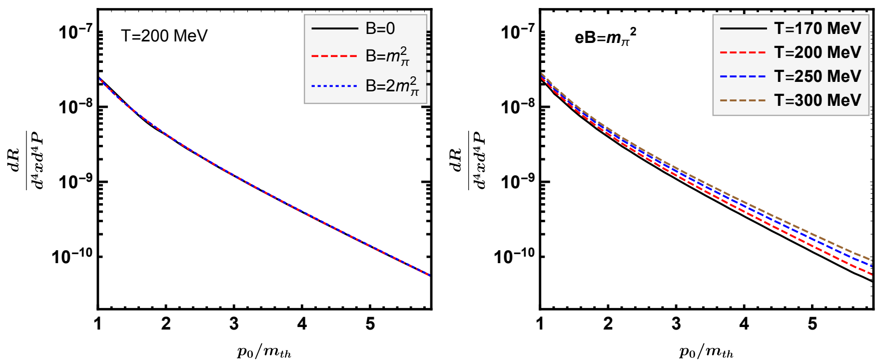

Figure 6.7: Same as Fig. 6.6 but for the pole-cut contribution.

In the left panel of Fig. 6.7, the pole-cut contribution is plotted for various magnetic fields with $T = 200$ MeV. It is found to be independent of of the magnetic field. This is because magnetic field appears as a correction in the weak field approximation and we have considered the rate up to $\mathcal{O}[(eB)]$. On the other hand, in the left panel of Fig. 6.7, it is plotted for various temperatures for a given magnetic field. The rate is found to be enhanced with the increase in temperature as the temperature is the dominant scale in the weak field approximation. Total dilepton rate is obtained by adding the pole-pole contribution from Eq. (6.92) and the pole-cut contribution from Eq. (6.94) and is plotted in Fig. (6.8) with similar behavior as in Fig. 6.6.

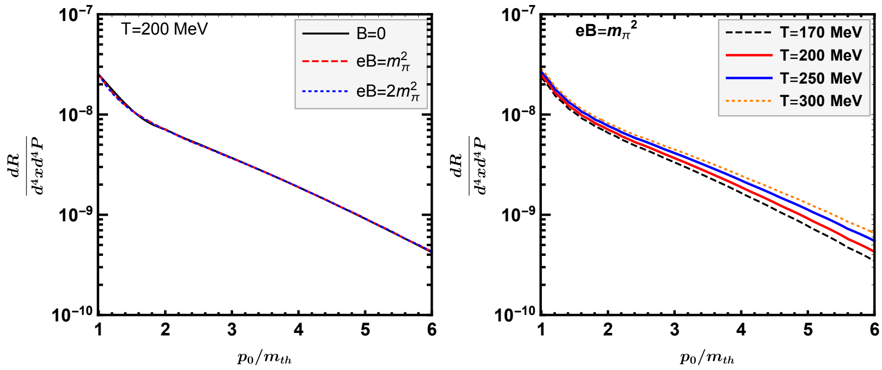

Figure 6.8: Total rate, sum of pole-pole and pole-cut contributions, of dilepton production r as a function of the energy of dilepton for various magnetic fields (left panel) and for various temperatures (right panel).

6.5 Conclusion

In conclusion, we have systematically investigated thermal dilepton production from a hot magnetized QCD medium in the weak field approximation. Since we are interested in the hard dilepton rate, it is sufficient to use just one resummed and one bare propagator in the presence of magnetic field in the photon polarization tensor diagram in Fig. 6.5. We note that the earlier works were carried out using free propagators for both the fermions in the loop in the presence of magnetic field. Since we have one resummed propagator, its spectral representation contains a pole and a (Landau) cut contribution. On the other hand, a hard spectral function corresponding to bare propagator has only pole contribution. The dilepton rate contains two types of contributions: pole-pole and pole-cut. As the magnetic field is turned on, all four quasiquark modes, namely, $\omega_{L(+)}$, $\omega_{L(-)}$, $\omega_{R(+)}$, and $\omega_{R(-)}$ individually participate in annihilation with a hard quark and contribute to the pole-pole part of the dilepton production. These annihilation processes start at higher energies as the thermomagnetic mass increases in the presence of magnetic field. The pole-cut contribution is found to dominate over those annihilation processes at low energies.

In weak field approximation, magnetic field appears as a correction to the thermal contributions. Since, for simplicity, we have considered only $\mathcal{O}[(eB)]$ correction, the effect of magnetic field on the rate is found to be very marginal here. For having a moderate effect of the magnetic field, one may need to take into account QCD corrections.

CHAPTER 7

Summary and Outlook

The phenomena of asymptotic freedom in QCD makes the theory of strong interaction distinct. It is accountable for the creation of a deconfined state of matter when the coupling constant decreases making quarks and gluons asymptotically free. In nature, QGP is believed to persist after few microseconds of Big Bang and in the core of neutron stars. But they are too unattainable for us to perform any real-time experiments. However, much to our surprise, ultra-relativistic heavy-ion collision experiments can generate a transient deconfined state of matter in a very small spatial volume. Characterization of QGP has great implication in understanding the laws of nature on another level as it acts as a bridge between the physics of early universe and neutron stars. A high anisotropic magnetic field is generated in non-central heavy ion collision in the direction perpendicular to the reaction plane. There are good reasons, based on LQCD and hydrodynamics simulations along with recent experimental observations, to believe that this magnetic field gives rise to some novel phenomena and influences QCD confinement-deconfinement and chiral phase transitions, properties of the medium and signatures of QGP. In this dissertation, we have discussed DPR in weakly magnetized medium. Dileptons are considered as one of the excellent probes as they bring least contaminated information of the medium because interact only electromagnetically with the medium. A huge amount of works were dedicated towards the production rate of dileptons from various stages of HIC. Dileptons that are produced in the QGP medium are called thermal dileptons. Thermal dileptons are the decay product of virtual photons which, in turn, are originated either from quark-antiquark anihillation or decay of radiation from quarks. Now, quarks are affected by the background magnetic field which in turn influences the production rate of dileptons.

In chapter 1, we have first discussed some prelimenaries related to QGP and HIC such as QCD phase transitions, probes of QGP, a brief timeline regarding HIC. Then we presented the impact of magnetic field followed by the mechanism involved in its generation. In chapter 2, we have took the readers on a short trip to the basics of thermal field theory. We have developed the formalism of ITF based on operational method as well as path integral method. While developing the Feynman rules in ITF, we noted that integral over the zeroth component of loop momentum is replaced by discrete sum over Matsubara frequencies owing to the fact that the topology of space-time becomes $S^1 \times \mathbb{R}^3$ from $\mathbb{R}^4$. However, any physical result should be obtained after analytic continuation from discrete frequency from continuous domain. Also HTL resummation method was also introduced and it's inevitable presence in the calculation of gauge independent observable was illustrated.

In chapter 3, we have thoroughly presented the two point green's function of a free fermion subjected to external, time-independent, homogeneous background magnetic field. We employed Schwinger's proper time method in deriving the propagator. We presented the propagator in two representation, namely integral over proper time and a summation over Landau levels., and explicity derived one representation starting from the other. Also, the analytical expression of two extreme limits,namely the strong and weak field limit, was obtained. When the scale of the magnetic field is much greater than all the involved scale of the system, the strong field approximation is relevant. On the contrary, when the strength of the magnetic field is much less, the weak field approximation can be used.

In chapter 4, we discussed the properties of collective excitations of quarks in hot deconfined medium in a nutshell. In doing so, we have used HTL approximation which is based on physics of two distinguishable scale — hard scale ($\sim T$) and soft scale ($\sim gT$). When a quark propagates in an interacting zero-temperature vacuum, it gets dressed due to the interactions. As a result, it's mass gets modified. However, while travelling in thermal medium apart from the ordinary quasi-quark mode q_+, an additional collective mode, called plasmino mode q_- appears due to the breaking of Lorentz invariance. Similar to the case in vacuum, the collective modes propagates with an effective mass. It is called thermal mass and it depends on the temperature and strong coupling constant as $m_{\mathsf{th}} \sim gT$. It is evident from the scale of the thermal mass that one needs to take into account the effect of quasi-quark modes to describe the physics at the soft scale. The effective propagator, whose poles gives us quasi-quark dispersion relation of quasi-quark mode, obeys all of the discrete symmetry of the system along with ward identity.

In chapter 5, we discussed the properties of quasi-quark excitations in hot deconfined medium in presence of external background magnetic field. The discussions in this chapter goes hand to hand with that of chapter 4. The presence of magnetic field introduces a magnetic scale $|eB|$ in the medium in addition to hard ($\sim T$) and soft scale ($\sim gT$). We have considered the scale hierarchy $m_{\mathsf{th}}^2(\sim T) < |eB| < T^2$ which is relevant for the late time in the evolution of magnetic field. Therefore it is sufficient to use weak field approximated propagator upto $\mathcal{O}\left(|eB|\right)$. The collective quasi-quark mode splits into four, namely $\omega_{L(\pm)}$ and $\omega_{R(\pm)}$, in weakly magnetised

QGP medium. All of these modes are timelike. The transverse momentum of these modes are quantised into Landau Levels as quarks carries electric charge. Also, the quasi-quark excitations acquires a thermo-magnetic mass analogous to thermal mass in hot medium. Next, we investigated discrete symmetry of the effective propagator and found out that it is invariant under parity, chirality, charge conjugation and time-reversal.

In chapter 6, we derived hard dilepton production rate in weakly magnetised medium. The DPR has two contributions — pole-pole and pole-cut contributions. The pole pole contribution gives the amplitude of the processes involved in production mechanism namely the annihilation of a hard quark with quasi-quark and decay of a quasi-quark. These processes are $\omega_{L(\pm)}q \to \gamma^* \to \ell\bar{\ell}$, $\omega_{R(\pm)}q \to \gamma^* \to \ell\bar{\ell}$, $\omega_{L(\pm)} \to q\gamma^* \to q\ell\bar{\ell}$ and $\omega_{R(\pm)} \to q\gamma^* \to q\ell\bar{\ell}$. The cut-pole contribution comes from the spacelike domain of virtual photon momenta. Physically, Landau damping is manifested through the cut-pole contribution. The magnetic field is responsible for very marginal increment of the threshold energy of annihilation process. From the parity symmetry of the dispersion mode, one can show that the annihilation and decay process involving $\omega_{L(+)}$ $\left(\omega_{L(-)}\right)$ is the same as that of $\omega_{R(+)}$ $\left(\omega_{R(-)}\right)$.

The complete determination of quasi-quark modes in magnetised media would involve the exact fermion propagator in presence of magnetic field. With this, the calculation of hard as well as soft dilepton production rate would complete the picture. However, for the soft dilepton rate, we need to replace all of the bare vertex with effective vertex and the bare prapagators with effective propagators.

APPENDIX A

Frequency Sums

The frequency sums $\mathcal{F}^{(0,0)}_{(F,B)}$ shown in Eq. (4.15) and $\mathcal{F}^{(1,0)}_{(F,B)}$ shown in Eq. (4.16) are performed in this Appendix.

We define two factors

$$\widetilde{\Delta}(k_0, E) \equiv \frac{1}{k_0^2 - E^2}, \tag{A.1}$$

with $k_0 = i(2n+1)\pi T + \mu$ related to the fermionic propagator where μ is the chemical potential of the system and

$$\Delta(k_0, E) \equiv \frac{1}{k_0^2 - E^2}, \tag{A.2}$$

with $k_0 = i2n\pi T$ related the bosonic propagator.

So the frequency sums take the following form

$$\mathcal{F}^{(0,0)}_{(F,B)} = T \sum_{n=-\infty}^{\infty} \widetilde{\Delta}(k_0, E_1)\Delta(p_0 - k_0, E_2) \tag{A.3}$$

$$\mathcal{F}^{(1,0)}_{(F,B)} = T \sum_{n=-\infty}^{\infty} k_0\widetilde{\Delta}(k_0, E_1)\Delta(p_0 - k_0, E_2) \tag{A.4}$$

Now, we can rewrite $\widetilde{\Delta}$ and Δ from Eq. (A.1) and Eq. (A.2), respectively,as

$$\Delta(k_0, E) = \sum_{s=\pm 1} \Delta_s(k_0, E), \qquad \widetilde{\Delta}(k_0, E) = \sum_{s=\pm 1} \widetilde{\Delta}_s(k_0, E), \tag{A.5}$$

where we have defined

$$\widetilde{\Delta}_s(k_0, E) \equiv \frac{s}{2E} \frac{1}{k_0 - sE}, \tag{A.6}$$

$$\Delta_s(k_0, E) \equiv \frac{s}{2E} \frac{1}{k_0 - sE}. \tag{A.7}$$

Next, we write $\widetilde{\Delta}_{s_1}(k_0, E_1)$ in Eq. (A.6) and $\Delta_{s_2}(p_0 - k_0, E_2)$ in Eq. (A.7) in mixed representation as

$$\widetilde{\Delta}_{s_1}(k_0, E_1) = \widetilde{n}_+(s_1 E_1) \int_0^\beta d\tau \, e^{-\tau(k_0 - s_1 E_1)} \tag{A.8}$$

$$\Delta_{s_2}(p_0 - k_0, E_2) = -n(s_2 E_2) \int_0^\beta d\tau \, e^{-\tau(p_0 - k_0 - s_2 E_2)} \tag{A.9}$$

A.0.1 $\mathcal{F}^{(0,0)}_{(F,B)}$

We note that term in Eq. (A.3) can be casted as

$$\mathcal{F}^{(0,0)}_{(F,B)} = \sum_{s_1=\pm 1} \sum_{s_2=\pm 1} I_{s_1,s_2}, \tag{A.10}$$

where we have defined

$$I_{s_1,s_2} \equiv T \sum_{k_0} \widetilde{\Delta}_{s_1}(k_0, s_1 E_1) \Delta_{s_2}(p_0 - k_0, s_2 E_2). \tag{A.11}$$

Now, the k_0 sum in I_{s_1,s_2} is computed as

$$\begin{aligned}
I_{s_1,s_2} &= -T\sum_{k_0}\widetilde{n}_+(s_1E_1)n(s_2E_2)\frac{s_1s_2}{4E_1E_2}\int\limits_0^\beta d\tau_1 d\tau_2 \exp\Big\{-\big[\tau_1(k_0-s_1E) \\
&\qquad + \tau_2(p_0-k_0-s_2E_2)\big]\Big\} \\
&= -T\sum_{k_0}\widetilde{n}_+(s_1E_1)n(s_2E_2)\frac{s_1s_2}{4E_1E_2}\int\limits_0^\beta d\tau_1 d\tau_2 \exp\Big\{-\big[\tau_1(i\omega_n+\mu-s_1E) \\
&\qquad + \tau_2(i\omega_l+\mu-i\omega_n-\mu-s_2E_2)\big]\Big\} \\
&= -T\sum_{k_0}\widetilde{n}_+(s_1E_1)n(s_2E_2)\frac{s_1s_2}{4E_1E_2}\int\limits_0^\beta d\tau_1 d\tau_2 \exp\left[-i\tau_2\omega_l-\tau_1\mu+s_1\tau_1E_1\right. \\
&\qquad \left.+s_2\tau_2E_2\right]\exp\left[i\omega_n\left(\tau_2-\tau_1\right)\right] \\
&= -\widetilde{n}_+(s_1E_1)n(s_2E_2)\frac{s_1s_2}{4E_1E_2}\int\limits_0^\beta d\tau_1 d\tau_2 \exp\left[-i\tau_2\omega_l-\tau_1\mu+s_1\tau_1E_1+s_2\tau_2E_2\right] \\
&\qquad T\sum_{k_0}\exp\left[i\omega_n\left(\tau_2-\tau_1\right)\right].
\end{aligned} \tag{A.12}$$

Applying the following resolution of delta function

$$T\sum_{n=-\infty}^{\infty}\exp\left[i2n\pi T(\tau_2-\tau_1)\right] = \delta(\tau_2-\tau_1), \tag{A.13}$$

we get

$$\begin{aligned}
I_{s_1,s_2} = -\widetilde{n}_+(s_1E_1)n(s_2E_2)\frac{s_1s_2}{4E_1E_2}\int\limits_0^\beta d\tau_1 d\tau_2 \exp\left[-i\tau_2\omega_l-\tau_1\mu+s_1\tau_1E_1+s_2\tau_2E_2\right] \\
e^{i\pi T(\tau_2-\tau_1)}\delta(\tau_2-\tau_1).
\end{aligned} \tag{A.14}$$

First, we integrate out τ_2 using the definition of delta-function and then we perform the remaining integration over τ_1 as follow

$$\int_0^\infty d\tau_1 e^{-\tau_1(i\omega_l+\mu-s_1E_1-s_2E_2)} = \frac{1-e^{-\beta(i\omega_l+\mu-s_1E_1-s_2E_2)}}{i\omega_l+\mu-s_1E_1-s_2E_2}. \tag{A.15}$$

We note that

$$\exp\left(-i\beta\omega_l T\right) = \exp\left(-i\omega_l\right) = \exp\left(-i(2l+1)\pi T\right) = -1 \tag{A.16}$$

Thus, Eq. (A.15) reduces to

$$\begin{aligned}\int_0^\infty d\tau_1 e^{-\tau_1(i\omega_l+\mu-s_1E_1-s_2E_2)} &= \frac{e^{\beta(s_1E_1-\mu)}e^{\beta s_2E_2}+1}{i\omega_l+\mu-s_1E_1-s_2E_2} \\ &= \frac{1-\widetilde{n}_+(s_1E_1)+n(s_2E_2)}{\widetilde{n}_+(s_1E_1)n(s_2E_2)(i\omega_l+\mu-s_1E_1-s_2E_2)}\end{aligned} \tag{A.17}$$

In the last term of the above equation, we expressed the exponentials in terms of B.E. and F.D. distribution functions. Using this and performing the analytic continuation from $i\omega_l+\mu \to p_0$, we arrive at

$$I_{s_1s_2} = T\sum_{k_0}\widetilde{\Delta}_{s_1}(k_0,E_1)\Delta_{s_2}(p_0-k_0,E_2) = -\frac{s_1s_2}{4E_1E_2}\frac{1-\widetilde{n}_+(s_1E_1)+n(s_2E_2)}{p_0-s_1E_1-s_2E_2} \tag{A.18}$$

Now , we have

$$\mathcal{F}^{(0,0)}_{(F,B)} = \sum_{s_1=\pm1}\sum_{s_2=\pm1} -\frac{s_1s_2}{4E_1E_2}\frac{1-\widetilde{n}_+(s_1E_1)+n(s_2E_2)}{p_0-s_1E_1-s_2E_2}. \tag{A.19}$$

Using $1-\widetilde{n}_+(\pm E)-\widetilde{n}_-(\mp E)=0$ and $1+n(E)+n(-E)=0$, we can write

$$\mathcal{F}^{(0,0)}_{(F,B)}=\frac{1}{4E_1E_2}\left[\frac{1-\widetilde{n}_-(E_1)+n(E_2)}{p_0+E_1+E_2}-\frac{1-\widetilde{n}_+(E_1)+n(E_2)}{p_0-E_1-E_2}+\frac{\widetilde{n}_-(E_1)+n(E_2)}{p_0+E_1-E_2}\right.$$
$$\left.-\frac{\widetilde{n}_+(E_1)+n(E_2)}{p_0-E_1+E_2}\right]. \tag{A.20}$$

We can compare this results to well known one for the $\mu=0$ case

$$\mathcal{F}^{(0,0)}_{(F,B)}\Big|_{\mu=0}=\frac{1}{4E_1E_2}\left\{[1-\widetilde{n}(E_1)+n(E_2)]\left(\frac{1}{p_0+E_1+E_2}-\frac{1}{p_0-E_1-E_2}\right)\right.$$
$$\left.+[\widetilde{n}(E_1)+n(E_2)]\left(\frac{1}{p_0+E_1-E_2}-\frac{1}{p_0+E_1-E_2}\right)\right\}. \tag{A.21}$$

A.0.2 $\mathcal{F}^{(1,0)}_{(F,B)}$

Now we go on to evaluate

$$\mathcal{F}^{(1,0)}_{(F,B)}=T\sum_{k_0}k_0\widetilde{\Delta}(k_0,E_1)\Delta(p_0-k_0,E_2). \tag{A.22}$$

Now we can see that

$$k_0\widetilde{\Delta}(k_0,E_1)=\frac{k_0}{k_0^2-E_1^2}=\sum_{s_1=\pm1}\frac{1}{2}\frac{1}{k_0-s_1E_1}. \tag{A.23}$$

Thus, we have

$$\mathcal{F}^{(1,0)}_{(F,B)}=\sum_{s_1=\pm1}\sum_{s_2=\pm1}\frac{s_2}{4E_2}T\sum_{k_0}\frac{1}{k_0-s_1E_1}\frac{1}{p_0-k_0-s_2E_2}. \tag{A.24}$$

From Eq. (A.18), we note that

$$T\sum_{k_0}\frac{1}{k_0-s_1E_1}\frac{1}{p_0-k_0-s_2E_2}=-\frac{1-\widetilde{n}_+(s_1E_1)+n(s_2E_2)}{p_0-s_1E_1-s_2E_2}. \tag{A.25}$$

Finally, we get from the last two equations

$$\mathcal{F}^{(1,0)}_{(F,B)}=\sum_{s_1=\pm1}\sum_{s_2=\pm1}-\frac{s_2}{4E_2}\frac{1-\widetilde{n}_+(s_1E_1)+n(s_2E_2)}{p_0-s_1E_1-s_2E_2}. \tag{A.26}$$

Writing the sum explicitly, we have

$$\mathcal{F}^{(1,0)}_{(F,B)}=-\frac{1}{4E_2}\left[\frac{1-\widetilde{n}_+(E_1)+n(E_2)}{p_0-E_1-E_2}+\frac{1-\widetilde{n}_-(E_1)+n(E_2)}{p_0+E_1+E_2}+\frac{\widetilde{n}_+(E_1)+n(E_2)}{p_0-E_1+E_2}\right.$$
$$\left.+\frac{\widetilde{n}_-(E_1)+n(E_2)}{p_0+E_1-E_2}\right]. \tag{A.27}$$

Now, we have for $\mu=0$

$$\mathcal{F}^{(1,0)}_{(F,B)}\Big|_{\mu=0}=-\frac{1}{4E_2}\left\{[1-\widetilde{n}(E_1)+n(E_2)]\left(\frac{1}{p_0+E_1+E_2}+\frac{1}{p_0-E_1-E_2}\right)\right.$$
$$\left.+[\widetilde{n}(E_1)+n(E_2)]\left(\frac{1}{p_0+E_1-E_2}+\frac{1}{p_0+E_1-E_2}\right)\right\}. \tag{A.28}$$

APPENDIX B

Brateen-Pisarsky-Yuan Formula

The Brateen Pisarski Yuan formula relates the imaginary part of multiplication of two function with their spectral representation.

Let $f_1(k_0)$ and $f_2(k_0)$ are two functions whose spectral representation is written as [68]

$$f_1(k_0) = \int_{-\infty}^{\infty} d\omega_1 \frac{\rho_1(\omega_1)}{\omega_1 - k_0},$$
$$f_2(k_0) = \int_{-\infty}^{\infty} d\omega_2 \frac{\rho_2(\omega_2)}{\omega_2 - k_0}. \tag{B.1}$$

Then the Bratten-Pisaski-Yuan formula reads [216]

$$\frac{1}{2i}\mathsf{Disc}\, T \sum_{n=-\infty}^{\infty} f_1(k_0) f(p_0 - k_0) = \mathsf{Im}\, T \sum_{n=-\infty}^{\infty} f_1(k_0) f(p_0 - k_0)$$
$$= \pi \left(e^{\beta p_0} - 1\right) \int_{-\infty}^{\infty} d\omega_1 d\omega_2 \rho_1(\omega_1)\rho_2(\omega_2)\widetilde{n}(\omega_1)\widetilde{n}(\omega_2)\delta(p_0 - \omega_1 - \omega_2), \tag{B.2}$$

where $k_0 = i(2n+1)\pi T + \mu$ is the fermionic Matsubara frequencies with $n = 0, 1, 2, \cdots$, ρ_i is the spectral representation of the function f_i and $\widetilde{n}(\omega) = \dfrac{1}{\exp(\beta\omega) + 1}$

is the Fermi-Dirac distribution.

So,

$$
\begin{aligned}
&\mathsf{Im}\, T\sum_n f_1(i\omega_n+\mu) f_2(i\omega - i\omega_n - \mu) \\
&= \mathsf{Im}\, T\sum_{k_0}\int_{-\infty}^{\infty} d\omega_1 d\omega_2 \frac{\rho_1(\omega_1)}{\omega_1 - i\omega_n - \mu}\frac{\rho_2(\omega_2)}{\omega_2 - i\omega + i\omega_n + \mu} \\
&= \int_{-\infty}^{\infty} d\omega_1 d\omega_2 \rho_1(\omega_1)\rho_2(\omega_2)\mathsf{Im}\, T\sum_{k_0}\frac{1}{\omega_1 - i\omega_n - \mu}\frac{1}{\omega_2 - i\omega + i\omega_n + \mu} \\
&= \int_{-\infty}^{\infty} d\omega_1 d\omega_2 \rho_1(\omega_1)\rho_2(\omega_2)\mathsf{Im}\, T\sum_{n}\frac{1}{i\omega_n + \mu - \omega_1}\frac{1}{i\omega - i\omega_n - \mu - \omega_2}
\end{aligned}
\tag{B.3}
$$

Now, we have to use the following frequency sum [179]

$$
T\sum_n \tilde{\Delta}_{s_1}(i\omega_n+\mu, E_1)\tilde{\Delta}_{s_2}(i(\omega-\omega_n)-\mu, E_2) = -\frac{s_1 s_2}{4E_1E_2}\frac{1-\widetilde{n}_+(s_1E_1)-\widetilde{n}_-(s_2E_2)}{i\omega - s_1E_1 - s_2E_2}, \tag{B.4}
$$

where

$$
\tilde{\Delta}_s(x,E) \equiv -\frac{s}{2E}\frac{1}{x-E} \qquad (\text{here} \quad s=\pm 1) \tag{B.5}
$$

and

$$
\widetilde{n}_{\pm}(y) \equiv \frac{1}{e^{\beta(y\mp\mu)}+1}. \tag{B.6}
$$

Thus, performing the frequency sum using Eq. (B.4), we obtain

$$\mathrm{Im}\, T\sum_n f_1(i\omega_n+\mu)f_2(i\omega-i\omega_n-\mu) = -\int_{-\infty}^{\infty} d\omega_1 d\omega_2 \rho_1(\omega_1)\rho_2(\omega_2) \times \mathrm{Im}\frac{1-\widetilde{n}_+(\omega_1)-\widetilde{n}_-(\omega_2)}{i\omega-\omega_1-\omega_2}. \tag{B.7}$$

Now, we perform the analytic continuation $i\omega \to p_0 + i\epsilon$ and use

$$\mathrm{Im}\, \frac{1}{x \pm i\epsilon} = \mp\pi\delta(x) \tag{B.8}$$

to get

$$\mathrm{Im}\, T\sum_n f_1(k_0)f_2(p_0-k_0) = \pi\int_{-\infty}^{\infty} d\omega_1 d\omega_2 \rho_1(\omega_1)\rho_2(\omega_2)\left[1-\widetilde{n}_+(\omega_1)-\widetilde{n}_-(\omega_2)\right] \times \delta\left(p_0-\omega_1-\omega_2\right) \tag{B.9}$$

With the help of delta function we can write

$$\left[1-\widetilde{n}_+(\omega_1)-\widetilde{n}_-(\omega_2)\right]\delta\left(p_0-\omega_1-\omega_2\right) = \left(e^{\beta p_0}-1\right)\widetilde{n}_+(\omega_1)\widetilde{n}_-(\omega_2)\delta\left(p_0-\omega_1-\omega_2\right). \tag{B.10}$$

Thus, we derived the BPY formula for non-zero μ as

$$\mathrm{Im}\, T\sum_n f_1(k_0)f_2(p_0-k_0) = \pi\left(e^{\beta p_0}-1\right)\int_{-\infty}^{\infty} d\omega_1 d\omega_2 \rho_1(\omega_1)\rho_2(\omega_2)\widetilde{n}_+(\omega_1)\widetilde{n}_-(\omega_2) \times \delta\left(p_0-\omega_1-\omega_2\right), \tag{B.11}$$

which reduces to Eq. (B.2) after setting $\mu = 0$.

APPENDIX C

Spectral Representation of Weak Field Propagator

We need to find the spectral representation of $S_B(K)$ upto $\mathcal{O}(q_fB)$. To do this we write [211]

$$
\begin{aligned}
S_B(K) &= \frac{\not{K}}{K^2-m_f^2} + i\gamma^1\gamma^2\frac{\not{K}_{\shortparallel}}{(K^2-m_f^2)^2}q_fB \\
&= \frac{\not{K}}{K^2-m_f^2} - \gamma_5\frac{k_0\gamma^3-k^3\gamma_0}{(K^2-m_f^2)^2}q_fB \\
&= \frac{k_0}{k_0^2-\omega_k^2}\gamma^0 - k\frac{1}{k_0^2-\omega_k^2}\hat{k}.\gamma - \gamma_5\left[\frac{k_0}{(k_0^2-\omega_k^2)^2}\gamma^3 - \frac{1}{(k_0^2-\omega_k^2)^2}k^3\gamma_0\right]q_fB.
\end{aligned}
$$

We define the spectral functions as follows

$$\rho_0^{(1)}(k_0,k) = \frac{1}{\pi}\mathsf{Im}\, f_0^{(1)}(k_0+i\epsilon,k) = \frac{1}{\pi}\mathsf{Im}\,\frac{k_0+i\epsilon}{(k_0+i\epsilon)^2-\omega_k^2}. \tag{C.1}$$

$$\rho_0^{(0)}(k_0,k) = \frac{1}{\pi}\mathsf{Im}\, f_0^{(0)}(k_0+i\epsilon,k) = \frac{1}{\pi}\mathsf{Im}\,\frac{1}{(k_0+i\epsilon)^2-\omega_k^2}, \tag{C.2}$$

$$\rho_1^{(1)}(k_0,k) = \frac{1}{\pi}\mathsf{Im}\, f_1^{(1)}(k_0+i\epsilon,k) = \frac{1}{\pi}\mathsf{Im}\,\frac{k_0+i\epsilon}{[(k_0+i\epsilon)^2-\omega_k^2]^2}, \tag{C.3}$$

$$\rho_1^{(0)}(k_0,k) = \frac{1}{\pi}\mathsf{Im}\, f_1^{(0)}(k_0+i\epsilon,k) = \frac{1}{\pi}\mathsf{Im}\,\frac{1}{[(k_0+i\epsilon)^2-\omega_k^2]^2}. \tag{C.4}$$

Now to prove this we need to use [178]

$$\lim_{\epsilon\to 0} \, \mathsf{Im} \, \frac{1}{x+i\epsilon} = -\pi\delta(x), \tag{C.5}$$

$$\lim_{\epsilon\to 0} \, \mathsf{Im} \, \frac{1}{(x+i\epsilon)^2} = \pi\delta'(x), \tag{C.6}$$

where $x, \epsilon \in \mathbb{R}$, $\epsilon > 0$.

To prove (C.5) and (C.6), we use the following limiting representation of Dirac delta function

$$\lim_{\epsilon\to 0} \frac{\epsilon}{x^2+\epsilon^2} = \pi\delta(x). \tag{C.7}$$

Taking derivative with respect to x on both sides of equation (C.7), we get

$$\lim_{\epsilon\to 0} \frac{2\epsilon x}{(x^2+\epsilon^2)^2} = -\pi\delta'(x). \tag{C.8}$$

Now

$$\lim_{\epsilon\to 0} \mathsf{Im} \, \frac{1}{x+i\epsilon} = \frac{1}{2i} \lim_{\epsilon\to 0} \left[\frac{1}{x+i\epsilon} - \frac{1}{x-i\epsilon}\right] = \frac{1}{2i} \lim_{\epsilon\to 0} \frac{-2i\epsilon}{x^2+\epsilon^2} = -\lim_{\epsilon\to 0} \frac{\epsilon}{x^2+\epsilon^2} = -\pi\delta(x), \tag{C.9}$$

and

$$\begin{aligned} \lim_{\epsilon\to 0} \mathsf{Im} \, \frac{1}{(x+i\epsilon)^2} &= \frac{1}{2i} \lim_{\epsilon\to 0} \left[\frac{1}{(x+i\epsilon)^2} - \frac{1}{(x-i\epsilon)^2}\right] = \frac{1}{2i} \lim_{\epsilon\to 0} \frac{-4i\epsilon x}{(x^2+\epsilon^2)^2} \\ &= -\lim_{\epsilon\to 0} \frac{2\epsilon x}{(x^2+\epsilon^2)^2} = \pi\delta'(x). \end{aligned} \tag{C.10}$$

This proves equation (C.5) and (C.6). With these it is easy to get the spectral representation for the free part:

$$\rho_0^{(1)}(k_0,k) = \frac{1}{\pi}\mathsf{Im}\,\frac{1}{2}\left(\frac{1}{k_0-\omega_k+i\epsilon}+\frac{1}{k_0+\omega_k+i\epsilon}\right) = -\frac{\delta(k_0+\omega_k)+\delta(k_0-\omega_k)}{2}, \tag{C.11}$$

$$\rho_0^{(0)}(k_0,k) = \frac{1}{\pi}\mathsf{Im}\,\frac{1}{2\omega_k}\left(\frac{1}{k_0-\omega_k+i\epsilon}-\frac{1}{k_0+\omega_k+i\epsilon}\right) = \frac{\delta(k_0+\omega_k)-\delta(k_0-\omega_k)}{2\omega_k}. \tag{C.12}$$

Now for the first order part, we need to

$$\begin{aligned}\frac{k_0}{(k_0^2-\omega_k^2)^2} &= \frac{1}{4\omega_k}\frac{4k_0\omega_k}{(k_0+\omega_k)^2(k_0-\omega_k)^2} = \frac{1}{4\omega_k}\frac{(k_0+\omega_k)^2-(k_0-\omega_k)^2}{(k_0+\omega_k)^2(k_0-\omega_k)^2}\\ &= \frac{1}{4\omega_k}\left[\frac{1}{(k_0-\omega_k)^2}-\frac{1}{(k_0+\omega_k)^2}\right],\end{aligned} \tag{C.13}$$

and

$$\begin{aligned}\frac{1}{(k_0^2-\omega_k^2)^2} &= \frac{1}{4\omega_k^2}\left[\frac{1}{k_0-\omega_k}-\frac{1}{k_0+\omega_k}\right]^2 = \frac{1}{4\omega_k^2}\left[\frac{1}{(k_0-\omega_k)^2}+\frac{1}{(k_0+\omega_k)^2}\right.\\ &\qquad\left.-\frac{2}{k_0^2-\omega_k^2}\right]\\ &= \frac{1}{4\omega_k^2}\left[\frac{1}{(k_0-\omega_k)^2}+\frac{1}{(k_0+\omega_k)^2}-\frac{1}{\omega_k}\left(\frac{1}{k_0-\omega_k}-\frac{1}{k_0+\omega_k}\right)\right].\end{aligned} \tag{C.14}$$

Thus

$$\begin{aligned}\rho_1^{(1)}(k_0,k) &= \frac{1}{\pi}\mathsf{Im}\frac{1}{4\omega_k}\left[\frac{1}{(k_0-\omega_k+i\epsilon)^2}-\frac{1}{(k_0+\omega_k+i\epsilon)^2}\right]\\ &= \frac{\delta'(k_0-\omega_k)-\delta'(k_0+\omega_k)}{4\omega_k}.\end{aligned} \tag{C.15}$$

Also

$$
\begin{aligned}
\rho_1^{(0)}(k_0,k) &= \frac{1}{\pi}\mathsf{Im}\,\frac{1}{4\omega_k^2}\left[\frac{1}{(k_0-\omega_k+i\epsilon)^2}+\frac{1}{(k_0+\omega_k+i\epsilon)^2}-\frac{1}{\omega_k}\left(\frac{1}{k_0-\omega_k+i\epsilon}\right.\right.\\
&\qquad\left.\left.-\frac{1}{k_0+\omega_k+i\epsilon}\right)\right]\\
&= \frac{1}{4\omega_k^2}\left\{\delta'(k_0-\omega_k)+\delta'(k_0+\omega_k)+\frac{1}{\omega_k}\left[\delta(k_0-\omega_k)-\delta(k_0+\omega_k)\right]\right\}.
\end{aligned}
\tag{C.16}
$$

Bibliography

[1] D. Griffiths, "Introduction to elementary particles,"

[2] M. E. Peskin and D. V. Schroeder, "An Introduction to quantum field theory,"

[3] D. J. Gross and F. Wilczek, Phys. Rev. Lett. **30**, 1343-1346 (1973)

[4] H. D. Politzer, Phys. Rev. Lett. **30**, 1346-1349 (1973)

[5] G. 't Hooft, Nucl. Phys. B **254**, 11-18 (1985)

[6] K. G. Wilson, Phys. Rev. D **10**, 2445 (1974)

[7] S. Bethke, Eur. Phys. J. C **64**, 689-703 (2009) [arXiv:0908.1135 [hep-ph]].

[8] J. Greensite, Lect. Notes Phys. **821**, 1-211 (2011)

[9] C. Ratti, Rept. Prog. Phys. **81**, no.8, 084301 (2018) [arXiv:1804.07810 [hep-lat]].

[10] P. de Forcrand, PoS **LAT2009**, 010 (2009) [arXiv:1005.0539 [hep-lat]].

[11] S. A. Chin, Phys. Lett. B **78**, 552-555 (1978)

[12] G. F. Chapline and A. K. Kerman, MIT-CTP-695.

[13] N. Cabibbo and G. Parisi, Phys. Lett. B **59**, 67-69 (1975)

[14] Y. Aoki, G. Endrodi, Z. Fodor, S. D. Katz and K. K. Szabo, Nature **443**, 675-678 (2006) [arXiv:hep-lat/0611014 [hep-lat]].

[15] J. Casalderrey-Solana, H. Liu, D. Mateos, K. Rajagopal and U. A. Wiedemann, "Gauge/String Duality, Hot QCD and Heavy Ion Collisions" [arXiv:1101.0618 [hep-th]].

[16] C. R. Allton, S. Ejiri, S. J. Hands, O. Kaczmarek, F. Karsch, E. Laermann, C. Schmidt and L. Scorzato, Phys. Rev. D **66**, 074507 (2002) [arXiv:hep-lat/0204010 [hep-lat]].

[17] C. R. Allton, M. Doring, S. Ejiri, S. J. Hands, O. Kaczmarek, F. Karsch, E. Laermann and K. Redlich, Phys. Rev. D **71**, 054508 (2005) [arXiv:hep-lat/0501030 [hep-lat]].

[18] R. V. Gavai and S. Gupta, Phys. Rev. D **78**, 114503 (2008) [arXiv:0806.2233 [hep-lat]].

[19] S. Basak *et al.* [MILC], PoS **LATTICE2008**, 171 (2008) [arXiv:0910.0276 [hep-lat]].

[20] O. Kaczmarek, F. Karsch, E. Laermann, C. Miao, S. Mukherjee, P. Petreczky, C. Schmidt, W. Soeldner and W. Unger, Phys. Rev. D **83**, 014504 (2011) [arXiv:1011.3130 [hep-lat]].

[21] P. de Forcrand and O. Philipsen, Nucl. Phys. B **642**, 290-306 (2002) [arXiv:hep-lat/0205016 [hep-lat]].

[22] M. D'Elia and M. P. Lombardo, Phys. Rev. D **67**, 014505 (2003) [arXiv:hep-lat/0209146 [hep-lat]].

[23] M. Asakawa and K. Yazaki, Nucl. Phys. A **504**, 668-684 (1989)

[24] A. Barducci, R. Casalbuoni, S. De Curtis, R. Gatto and G. Pettini, Phys. Lett. B **231**, 463-470 (1989)

[25] F. Wilczek, Int. J. Mod. Phys. A **7**, 3911-3925 (1992), [erratum: Int. J. Mod. Phys. A **7**, 6951 (1992)]

[26] J. Berges and K. Rajagopal, Nucl. Phys. B **538**, 215-232 (1999) [arXiv:hep-ph/9804233 [hep-ph]].

[27] M. G. Alford, Ann. Rev. Nucl. Part. Sci. **51**, 131-160 (2001) [arXiv:hep-ph/0102047 [hep-ph]].

[28] M. G. Alford, A. Schmitt, K. Rajagopal and T. Schäfer, Rev. Mod. Phys. **80**, 1455-1515 (2008) [arXiv:0709.4635 [hep-ph]].

[29] H. Satz, [arXiv:0903.2778 [hep-ph]].

[30] S. Borsanyi, G. Endrodi, Z. Fodor, A. Jakovac, S. D. Katz, S. Krieg, C. Ratti and K. K. Szabo, JHEP **11**, 077 (2010) [arXiv:1007.2580 [hep-lat]].

[31] J. Cleymans, K. Redlich, H. Satz and E. Suhonen, Z. Phys. C **33**, 151 (1986)

[32] H. Kouno and F. Takagi, Z. Phys. C **42**, 209 (1989)

[33] L. McLerran and R. D. Pisarski, Nucl. Phys. A **796**, 83-100 (2007) [arXiv:0706.2191 [hep-ph]].

[34] Y. Hidaka, L. D. McLerran and R. D. Pisarski, Nucl. Phys. A **808**, 117-123 (2008) [arXiv:0803.0279 [hep-ph]].

[35] E. Fermi, Prog. Theor. Phys. **5**, 570-583 (1950)

[36] L. D. Landau, Izv. Akad. Nauk Ser. Fiz. **17**, 51-64 (1953)

[37] R. Hagedorn, Nuovo Cim. Suppl. **3**, 147-186 (1965) CERN-TH-520.

[38] R. Stock and A. M. Poskanzer, Comments Nucl. Part. Phys. **7**, no.2, 41-47 (1977)

[39] S. Nagamiya, J. Randrup and T. J. M. Symons, Ann. Rev. Nucl. Part. Sci. **34**, 155-187 (1984)

[40] H. A. Gustafsson, H. H. Gutbrod, B. Kolb, H. Lohner, B. Ludewigt, A. M. Poskanzer, T. Renner, H. Riedesel, H. G. Ritter and A. Warwick, *et al.* Phys. Rev. Lett. **52**, 1590-1593 (1984)

[41] B. Muller and J. L. Nagle, Ann. Rev. Nucl. Part. Sci. **56**, 93-135 (2006) [arXiv:nucl-th/0602029 [nucl-th]].

[42] M. Gyulassy and L. McLerran, Nucl. Phys. A **750**, 30-63 (2005) [arXiv:nucl-th/0405013 [nucl-th]].

[43] F. Karsch, Lect. Notes Phys. **583**, 209-249 (2002) [arXiv:hep-lat/0106019 [hep-lat]].

[44] W. Busza, K. Rajagopal and W. van der Schee, Ann. Rev. Nucl. Part. Sci. **68**, 339-376 (2018) [arXiv:1802.04801 [hep-ph]].

[45] T. K. Nayak, Pramana **79**, 719-735 (2012) [arXiv:1201.4264 [nucl-ex]].

[46] B. Friman, C. Hohne, J. Knoll, S. Leupold, J. Randrup, R. Rapp and P. Senger, Lect. Notes Phys. **814**, pp.1-980 (2011)

[47] E. Iancu, "QCD in heavy ion collisions", [arXiv:1205.0579 [hep-ph]].

[48] F. Gelis, E. Iancu, J. Jalilian-Marian and R. Venugopalan, Ann. Rev. Nucl. Part. Sci. **60**, 463-489 (2010) [arXiv:1002.0333 [hep-ph]].

[49] T. Lappi, Acta Phys. Polon. B **40**, 1997-2012 (2009) [arXiv:0904.1670 [hep-ph]].

[50] P. F. Kolb and U. W. Heinz, [arXiv:nucl-th/0305084 [nucl-th]].

[51] C. Gale, S. Jeon and B. Schenke, Int. J. Mod. Phys. A **28**, 1340011 (2013) [arXiv:1301.5893 [nucl-th]].

[52] M. Strickland, Acta Phys. Polon. B **45**, no.12, 2355-2394 (2014) [arXiv:1410.5786 [nucl-th]].

[53] S. Jeon and U. Heinz, Int. J. Mod. Phys. E **24**, no.10, 1530010 (2015) [arXiv:1503.03931 [hep-ph]].

[54] A. Jaiswal and V. Roy, Adv. High Energy Phys. **2016**, 9623034 (2016) [arXiv:1605.08694 [nucl-th]].

[55] P. Braun-Munzinger, K. Redlich and J. Stachel, "Particle production in heavy ion collisions", [arXiv:nucl-th/0304013 [nucl-th]].

[56] J. Cleymans and H. Satz, Z. Phys. C **57**, 135-148 (1993) [arXiv:hep-ph/9207204 [hep-ph]].

[57] J. Cleymans, H. Oeschler and K. Redlich, Phys. Rev. C **59**, 1663 (1999) [arXiv:nucl-th/9809027 [nucl-th]].

[58] F. Becattini, J. Cleymans, A. Keranen, E. Suhonen and K. Redlich, Phys. Rev. C **64**, 024901 (2001) [arXiv:hep-ph/0002267 [hep-ph]].

[59] J. Cleymans, H. Oeschler, K. Redlich and S. Wheaton, Phys. Rev. C **73**, 034905 (2006) [arXiv:hep-ph/0511094 [hep-ph]].

[60] H. Satz, Lect. Notes Phys. **785**, 1-21 (2010) [arXiv:0803.1611 [hep-ph]].

[61] R. C. Hwa, "Quark - gluon plasma. Vol. 2,"

[62] P. F. Kolb, J. Sollfrank and U. W. Heinz, Phys. Rev. C **62**, 054909 (2000) [arXiv:hep-ph/0006129 [hep-ph]].

[63] J. Y. Ollitrault, Phys. Rev. D **46**, 229-245 (1992)

[64] S. Voloshin and Y. Zhang, Z. Phys. C **70**, 665-672 (1996) [arXiv:hep-ph/9407282 [hep-ph]].

[65] A. M. Poskanzer and S. A. Voloshin, Phys. Rev. C **58**, 1671-1678 (1998) [arXiv:nucl-ex/9805001 [nucl-ex]].

[66] S. A. Voloshin, A. M. Poskanzer and R. Snellings, Landolt-Bornstein **23**, 293-333 (2010) [arXiv:0809.2949 [nucl-ex]].

[67] E. L. Feinberg, Nuovo Cim. A **34**, 391 (1976) CERN-TH-2156.

[68] J. I. Kapusta, P. Lichard and D. Seibert, Phys. Rev. D **44**, 2774-2788 (1991) [erratum: Phys. Rev. D **47**, 4171 (1993)]

[69] R. Chatterjee, L. Bhattacharya and D. K. Srivastava, Lect. Notes Phys. **785**, 219-264 (2010) [arXiv:0901.3610 [nucl-th]].

[70] R. Rapp and H. van Hees, Phys. Lett. B **753**, 586-590 (2016) [arXiv:1411.4612 [hep-ph]].

[71] K. Kajantie, J. I. Kapusta, L. D. McLerran and A. Mekjian, Phys. Rev. D **34**, 2746 (1986)

[72] C. Shen, [arXiv:1511.07708 [nucl-th]].

[73] T. Matsui and H. Satz, Phys. Lett. B **178**, 416-422 (1986)

[74] F. Karsch, M. T. Mehr and H. Satz, Z. Phys. C **37**, 617 (1988)

[75] H. Satz, Rept. Prog. Phys. **63**, 1511 (2000) [arXiv:hep-ph/0007069 [hep-ph]].

[76] H. Satz, Nucl. Phys. A **783**, 249-260 (2007) [arXiv:hep-ph/0609197 [hep-ph]].

[77] J. D. Bjorken, Phys. Rev. D **27**, 140-151 (1983)

[78] D. d'Enterria, Landolt-Bornstein **23**, 471 (2010) [arXiv:0902.2011 [nucl-ex]].

[79] A. Majumder and M. Van Leeuwen, Prog. Part. Nucl. Phys. **66**, 41-92 (2011) [arXiv:1002.2206 [hep-ph]].

[80] Y. Mehtar-Tani, J. G. Milhano and K. Tywoniuk, Int. J. Mod. Phys. A **28**, 1340013 (2013) [arXiv:1302.2579 [hep-ph]].

[81] J. P. Blaizot and Y. Mehtar-Tani, Int. J. Mod. Phys. E **24**, no.11, 1530012 (2015) [arXiv:1503.05958 [hep-ph]].

[82] K. Tywoniuk, Nucl. Phys. A **1005**, 122017 (2021)

[83] J. Rafelski and B. Muller, Phys. Rev. Lett. **48**, 1066 (1982) [erratum: Phys. Rev. Lett. **56**, 2334 (1986)]

[84] P. Koch, B. Muller and J. Rafelski, Phys. Rept. **142**, 167-262 (1986)

[85] J. Letessier and J. Rafelski, Int. J. Mod. Phys. E **9**, 107-147 (2000) [arXiv:nucl-th/0003014 [nucl-th]].

[86] S. V. Afanasiev *et al.* [NA49], Phys. Rev. C **66**, 054902 (2002) [arXiv:nucl-ex/0205002 [nucl-ex]].

[87] C. Alt *et al.* [NA49], Phys. Rev. C **77**, 024903 (2008) [arXiv:0710.0118 [nucl-ex]].

[88] J. D. Jackson, “Classical Electrodynamics,”

[89] K. Tuchin, Adv. High Energy Phys. **2013**, 490495 (2013) [arXiv:1301.0099 [hep-ph]].

[90] D. E. Kharzeev, L. D. McLerran and H. J. Warringa, Nucl. Phys. A **803**, 227-253 (2008) [arXiv:0711.0950 [hep-ph]].

[91] V. Skokov, A. Y. Illarionov and V. Toneev, Int. J. Mod. Phys. A **24**, 5925-5932 (2009) [arXiv:0907.1396 [nucl-th]].

[92] S. A. Bass, M. Belkacem, M. Bleicher, M. Brandstetter, L. Bravina, C. Ernst, L. Gerland, M. Hofmann, S. Hofmann and J. Konopka, *et al.* Prog. Part. Nucl. Phys. **41**, 255-369 (1998) [arXiv:nucl-th/9803035 [nucl-th]].

[93] M. Bleicher, E. Zabrodin, C. Spieles, S. A. Bass, C. Ernst, S. Soff, L. Bravina, M. Belkacem, H. Weber and H. Stoecker, *et al.* J. Phys. G **25**, 1859-1896 (1999) [arXiv:hep-ph/9909407 [hep-ph]].

[94] A. Bzdak and V. Skokov, Phys. Lett. B **710**, 171-174 (2012) [arXiv:1111.1949 [hep-ph]].

[95] K. Tuchin, Phys. Rev. C **88**, no.2, 024911 (2013) [arXiv:1305.5806 [hep-ph]].

[96] K. Tuchin, Int. J. Mod. Phys. E **23**, 1430001 (2014)

[97] K. Tuchin, Phys. Rev. C **87**, no.2, 024912 (2013) [arXiv:1206.0485 [hep-ph]].

[98] K. Fukushima, D. E. Kharzeev and H. J. Warringa, Phys. Rev. D **78**, 074033 (2008) [arXiv:0808.3382 [hep-ph]].

[99] K. Fukushima, Lect. Notes Phys. **871**, 241-259 (2013) [arXiv:1209.5064 [hep-ph]].

[100] G. Basar and G. V. Dunne, Lect. Notes Phys. **871**, 261-294 (2013) [arXiv:1207.4199 [hep-th]].

[101] D. E. Kharzeev and J. Liao, Nature Rev. Phys. **3**, no.1, 55-63 (2021)

[102] A. Yamamoto, Phys. Rev. Lett. **107**, 031601 (2011) [arXiv:1105.0385 [hep-lat]].

[103] A. Yamamoto, PoS **LATTICE2011**, 220 (2011) [arXiv:1108.0937 [hep-lat]].

[104] V. I. Zakharov, Lect. Notes Phys. **871**, 295-330 (2013) [arXiv:1210.2186 [hep-ph]].

[105] B. I. Abelev *et al.* [STAR], Phys. Rev. Lett. **103**, 251601 (2009) [arXiv:0909.1739 [nucl-ex]].

[106] B. I. Abelev *et al.* [STAR], Phys. Rev. C **81**, 054908 (2010) [arXiv:0909.1717 [nucl-ex]].

[107] L. Adamczyk *et al.* [STAR], Phys. Rev. C **88**, no.6, 064911 (2013) [arXiv:1302.3802 [nucl-ex]].

[108] L. Adamczyk *et al.* [STAR], Phys. Rev. Lett. **113**, 052302 (2014) [arXiv:1404.1433 [nucl-ex]].

[109] L. Adamczyk *et al.* [STAR], Phys. Rev. C **89**, no.4, 044908 (2014) [arXiv:1303.0901 [nucl-ex]].

[110] D. E. Kharzeev, Prog. Part. Nucl. Phys. **75**, 133-151 (2014) [arXiv:1312.3348 [hep-ph]].

[111] D. E. Kharzeev, J. Liao, S. A. Voloshin and G. Wang, Prog. Part. Nucl. Phys. **88**, 1-28 (2016) [arXiv:1511.04050 [hep-ph]].

[112] K. Landsteiner, E. Megias and F. Pena-Benitez, Lect. Notes Phys. **871**, 433-468 (2013) [arXiv:1207.5808 [hep-th]].

[113] G. Wang and L. Wen, Adv. High Energy Phys. **2017**, 9240170 (2017) [arXiv:1609.05506 [nucl-ex]].

[114] J. Zhao, Int. J. Mod. Phys. A **33**, no.13, 1830010 (2018) [arXiv:1805.02814 [nucl-ex]].

[115] J. Zhao and F. Wang, Prog. Part. Nucl. Phys. **107**, 200-236 (2019) [arXiv:1906.11413 [nucl-ex]].

[116] Z. T. Liang and X. N. Wang, Phys. Rev. Lett. **94**, 102301 (2005) [erratum: Phys. Rev. Lett. **96**, 039901 (2006)] [arXiv:nucl-th/0410079 [nucl-th]].

[117] F. Becattini, F. Piccinini and J. Rizzo, Phys. Rev. C **77**, 024906 (2008) [arXiv:0711.1253 [nucl-th]].

[118] L. Adamczyk *et al.* [STAR], Nature **548**, 62-65 (2017) [arXiv:1701.06657 [nucl-ex]].

[119] W. T. Deng and X. G. Huang, Phys. Rev. C **93**, no.6, 064907 (2016) [arXiv:1603.06117 [nucl-th]].

[120] X. G. Huang, Nucl. Phys. A **1005**, 121752 (2021) [arXiv:2002.07549 [nucl-th]].

[121] V. P. Gusynin, V. A. Miransky and I. A. Shovkovy, Nucl. Phys. B **462**, 249-290 (1996) [arXiv:hep-ph/9509320 [hep-ph]].

[122] I. A. Shovkovy, Lect. Notes Phys. **871**, 13-49 (2013) [arXiv:1207.5081 [hep-ph]].

[123] J. Alexandre, K. Farakos and G. Koutsoumbas, Phys. Rev. D **63**, 065015 (2001) [arXiv:hep-th/0010211 [hep-th]].

[124] K. Yagi, T. Hatsuda and Y. Miake, "Quark-gluon plasma: From big bang to little bang," Camb. Monogr. Part. Phys. Nucl. Phys. Cosmol. **23**, 1-446 (2005)

[125] K. G. Klimenko, [arXiv:hep-ph/9809218 [hep-ph]].

[126] E. V. Gorbar, Phys. Lett. B **491**, 305-310 (2000) [arXiv:hep-th/0005285 [hep-th]].

[127] S. Ghosh, S. Mandal and S. Chakrabarty, Phys. Rev. C **75**, 015805 (2007) [arXiv:astro-ph/0507127 [astro-ph]].

[128] D. P. Menezes, M. Benghi Pinto, S. S. Avancini, A. Perez Martinez and C. Providencia, Phys. Rev. C **79**, 035807 (2009) [arXiv:0811.3361 [nucl-th]].

[129] D. P. Menezes, M. Benghi Pinto, S. S. Avancini and C. Providencia, Phys. Rev. C **80**, 065805 (2009) [arXiv:0907.2607 [nucl-th]].

[130] J. K. Boomsma and D. Boer, Phys. Rev. D **81**, 074005 (2010) [arXiv:0911.2164 [hep-ph]].

[131] S. Fayazbakhsh and N. Sadooghi, Phys. Rev. D **83**, 025026 (2011) [arXiv:1009.6125 [hep-ph]].

[132] B. Chatterjee, H. Mishra and A. Mishra, Phys. Rev. D **84**, 014016 (2011) [arXiv:1101.0498 [hep-ph]].

[133] K. Fukushima, M. Ruggieri and R. Gatto, Phys. Rev. D **81**, 114031 (2010) [arXiv:1003.0047 [hep-ph]].

[134] R. Gatto and M. Ruggieri, Phys. Rev. D **82**, 054027 (2010) [arXiv:1007.0790 [hep-ph]].

[135] I. A. Shushpanov and A. V. Smilga, Phys. Lett. B **402**, 351-358 (1997) [arXiv:hep-ph/9703201 [hep-ph]].

[136] N. O. Agasian, Phys. Lett. B **488**, 39-45 (2000) [arXiv:hep-ph/0005300 [hep-ph]].

[137] J. O. Andersen, JHEP **10**, 005 (2012) [arXiv:1205.6978 [hep-ph]].

[138] J. O. Andersen and R. Khan, Phys. Rev. D **85**, 065026 (2012) [arXiv:1105.1290 [hep-ph]].

[139] J. O. Andersen and A. Tranberg, JHEP **08**, 002 (2012) [arXiv:1204.3360 [hep-ph]].

[140] A. J. Mizher, M. N. Chernodub and E. S. Fraga, Phys. Rev. D **82**, 105016 (2010) [arXiv:1004.2712 [hep-ph]].

[141] D. K. Hong, Y. Kim and S. J. Sin, Phys. Rev. D **54**, 7879-7883 (1996) [arXiv:hep-th/9603157 [hep-th]].

[142] G. W. Semenoff, I. A. Shovkovy and L. C. R. Wijewardhana, Phys. Rev. D **60**, 105024 (1999) [arXiv:hep-th/9905116 [hep-th]].

[143] K. Fukushima and J. M. Pawlowski, Phys. Rev. D **86**, 076013 (2012) [arXiv:1203.4330 [hep-ph]].

[144] K. Kamikado and T. Kanazawa, JHEP **03**, 009 (2014) [arXiv:1312.3124 [hep-ph]].

[145] T. Kojo and N. Su, Phys. Lett. B **726**, 839-845 (2013) [arXiv:1305.4510 [hep-ph]].

[146] J. O. Andersen, W. R. Naylor and A. Tranberg, JHEP **04**, 187 (2014) [arXiv:1311.2093 [hep-ph]].

[147] N. Mueller, J. A. Bonnet and C. S. Fischer, Phys. Rev. D **89**, no.9, 094023 (2014) [arXiv:1401.1647 [hep-ph]].

[148] P. V. Buividovich, M. N. Chernodub, E. V. Luschevskaya and M. I. Polikarpov, Phys. Lett. B **682**, 484-489 (2010) [arXiv:0812.1740 [hep-lat]].

[149] M. D'Elia, S. Mukherjee and F. Sanfilippo, Phys. Rev. D **82**, 051501 (2010) [arXiv:1005.5365 [hep-lat]].

[150] E. S. Fraga, Lect. Notes Phys. **871**, 121-141 (2013) [arXiv:1208.0917 [hep-ph]].

[151] M. D'Elia and F. Negro, Phys. Rev. D **83**, 114028 (2011) [arXiv:1103.2080 [hep-lat]].

[152] G. S. Bali, F. Bruckmann, G. Endrodi, Z. Fodor, S. D. Katz, S. Krieg, A. Schafer and K. K. Szabo, JHEP **02**, 044 (2012) [arXiv:1111.4956 [hep-lat]].

[153] G. S. Bali, F. Bruckmann, G. Endrodi, Z. Fodor, S. D. Katz and A. Schafer, Phys. Rev. D **86**, 071502 (2012) [arXiv:1206.4205 [hep-lat]].

[154] G. Endrődi, JHEP **04**, 023 (2013) [arXiv:1301.1307 [hep-ph]].

[155] F. Preis, A. Rebhan and A. Schmitt, Lect. Notes Phys. **871**, 51-86 (2013) [arXiv:1208.0536 [hep-ph]].

[156] F. Bruckmann, G. Endrodi and T. G. Kovacs, JHEP **04**, 112 (2013) [arXiv:1303.3972 [hep-lat]].

[157] R. L. S. Farias, K. P. Gomes, G. I. Krein and M. B. Pinto, Phys. Rev. C **90**, no.2, 025203 (2014) [arXiv:1404.3931 [hep-ph]].

[158] M. Ferreira, P. Costa, O. Lourenço, T. Frederico and C. Providência, Phys. Rev. D **89**, no.11, 116011 (2014) [arXiv:1404.5577 [hep-ph]].

[159] A. Ayala, M. Loewe and R. Zamora, Phys. Rev. D **91**, no.1, 016002 (2015) [arXiv:1406.7408 [hep-ph]].

[160] A. Ayala, C. A. Dominguez, L. A. Hernandez, M. Loewe and R. Zamora, Phys. Rev. D **92**, no.9, 096011 (2015) [arXiv:1509.03345 [hep-ph]].

[161] A. Ayala, M. Loewe, A. J. Mizher and R. Zamora, Phys. Rev. D **90**, no.3, 036001 (2014) [arXiv:1406.3885 [hep-ph]].

[162] R. L. S. Farias, V. S. Timoteo, S. S. Avancini, M. B. Pinto and G. Krein, Eur. Phys. J. A **53**, no.5, 101 (2017) [arXiv:1603.03847 [hep-ph]].

[163] A. Ayala, C. A. Dominguez, L. A. Hernandez, M. Loewe, A. Raya, J. C. Rojas and C. Villavicencio, Phys. Rev. D **94**, no.5, 054019 (2016) [arXiv:1603.00833 [hep-ph]].

[164] N. Mueller and J. M. Pawlowski, Phys. Rev. D **91**, no.11, 116010 (2015) [arXiv:1502.08011 [hep-ph]].

[165] A. Bandyopadhyay and R. L. S. Farias, [arXiv:2003.11054 [hep-ph]].

[166] M. N. Chernodub, Phys. Rev. D **82**, 085011 (2010) [arXiv:1008.1055 [hep-ph]].

[167] M. N. Chernodub, Lect. Notes Phys. **871**, 143-180 (2013) [arXiv:1208.5025 [hep-ph]].

[168] M. N. Chernodub, Int. J. Mod. Phys. Conf. Ser. **14**, 27-41 (2012) [arXiv:1201.2570 [hep-ph]].

[169] D. Djukanovic, M. R. Schindler, J. Gegelia and S. Scherer, Phys. Rev. Lett. **95**, 012001 (2005) [arXiv:hep-ph/0505180 [hep-ph]].

[170] M. N. Chernodub, Phys. Rev. Lett. **106**, 142003 (2011) [arXiv:1101.0117 [hep-ph]].

[171] V. V. Braguta, P. V. Buividovich, M. N. Chernodub, A. Y. Kotov and M. I. Polikarpov, Phys. Lett. B **718**, 667-671 (2012) [arXiv:1104.3767 [hep-lat]].

[172] I. Arsene *et al.* [BRAHMS], Nucl. Phys. A **757**, 1-27 (2005) [arXiv:nucl-ex/0410020 [nucl-ex]].

[173] K. Adcox *et al.* [PHENIX], Nucl. Phys. A **757**, 184-283 (2005) [arXiv:nucl-ex/0410003 [nucl-ex]].

[174] B. B. Back *et al.* [PHOBOS], Nucl. Phys. A **757**, 28-101 (2005) [arXiv:nucl-ex/0410022 [nucl-ex]].

[175] J. Adams *et al.* [STAR], Nucl. Phys. A **757**, 102-183 (2005) [arXiv:nucl-ex/0501009 [nucl-ex]].

[176] S. Fayazbakhsh, S. Sadeghian and N. Sadooghi, Phys. Rev. D **86**, 085042 (2012) [arXiv:1206.6051 [hep-ph]].

[177] S. Fayazbakhsh and N. Sadooghi, Phys. Rev. D **88**, no.6, 065030 (2013) [arXiv:1306.2098 [hep-ph]].

[178] A. K. Das, "Finite Temperature Field Theory,"

[179] M. L. Bellac, *Thermal Field Theory* (Cambridge University Press, Cambridge, England, 1996).

[180] N. P. Landsman and C. G. van Weert, Phys. Rept. **145**, 141 (1987)

[181] M. Laine and A. Vuorinen, Lect. Notes Phys. **925**, pp.1-281 (2016) [arXiv:1701.01554 [hep-ph]].

[182] A. J. Niemi and G. W. Semenoff, Annals Phys. **152**, 105 (1984)

[183] A. J. Niemi and G. W. Semenoff, Nucl. Phys. B **230**, 181-221 (1984)

[184] Y. Fujimoto, H. Matsumoto, H. Umezawa and I. Ojima, Phys. Rev. D **30**, 1400-1403 (1984) [erratum: Phys. Rev. D **31**, 1527 (1985)]

[185] R. L. Kobes and G. W. Semenoff, Nucl. Phys. B **260**, 714-746 (1985)

[186] H. Umezawa, H. Matsumoto and M. Tachiki, "THERMO FIELD DYNAMICS AND CONDENSED STATES,"

[187] F. C. Khanna, A. P. C. Malbouisson, J. M. C. Malbouisson and A. R. Santana, "Thermal quantum field theory - Algebraic aspects and applications,"

[188] T. Matsubara, Prog. Theor. Phys. **14**, 351-378 (1955)

[189] R. D. Pisarski, Phys. Rev. Lett. **63**, 1129 (1989)

[190] E. Braaten and R. D. Pisarski, Nucl. Phys. B **337**, 569-634 (1990)

[191] E. Braaten and R. D. Pisarski, Phys. Rev. Lett. **64**, 1338 (1990)

[192] J. S. Schwinger, Phys. Rev. **82**, 664-679 (1951)

[193] V. I. Ritus, Annals Phys. **69**, 555-582 (1972)

[194] K. Bhattacharya, [arXiv:0705.4275 [hep-th]].

[195] K. Bhattacharya, Int. J. Mod. Phys. A **21**, 3151-3170 (2006) [arXiv:hep-ph/0510280 [hep-ph]].

[196] A. Chodos, K. Everding and D. A. Owen, Phys. Rev. D **42**, 2881-2892 (1990) doi:10.1103/PhysRevD.42.2881

[197] R. C. Tolman, *Relativity, thermodynamics and cosmology* (Clarendon, Oxford — 1934), pp. 152 - 160

[198] W. Pauli, *Theory of Relativity* (Pergamon, London — 1958), pp. 134 - 141

[199] H. Ott, Z. Phys, 175, 70 (1963)

[200] W. Israel, Annals Phys. **100**, 310-331 (1976)

[201] W. Israel and J. M. Stewart, Annals Phys. **118**, 341-372 (1979)

[202] A. Peshier, K. Schertler and M. H. Thoma, Annals Phys. **266**, 162-177 (1998), [arXiv:hep-ph/9708434 [hep-ph]].

[203] R. D. Pisarski, Nucl. Phys. B **309**, 476-492 (1988)

[204] H. A. Weldon, Phys. Rev. D **26**, 2789 (1982)

[205] H. A. Weldon, Phys. Rev. D **61**, 036003 (2000), [arXiv:hep-ph/9908204 [hep-ph]].

[206] P. Elmfors, D. Persson and B. S. Skagerstam, Nucl. Phys. B **464**, 153-188 (1996) [arXiv:hep-ph/9509418 [hep-ph]].

[207] N. Sadooghi and F. Taghinavaz, Phys. Rev. D **92**, no.2, 025006 (2015) [arXiv:1504.04268 [hep-ph]].

[208] K. Hattori and K. Itakura, Annals Phys. **330**, 23-54 (2013) [arXiv:1209.2663 [hep-ph]].

[209] K. Hattori and K. Itakura, Annals Phys. **334**, 58-82 (2013) [arXiv:1212.1897 [hep-ph]].

[210] A. Das, A. Bandyopadhyay, P. K. Roy and M. G. Mustafa, Phys. Rev. D **97**, no.3, 034024 (2018) [arXiv:1709.08365 [hep-ph]].

[211] T. K. Chyi, C. W. Hwang, W. F. Kao, G. L. Lin, K. W. Ng and J. J. Tseng, Phys. Rev. D **62**, 105014 (2000) [arXiv:hep-th/9912134 [hep-th]].

[212] M. H. Thoma, Article in "Quark-Gluon Plasma 2, Edited by R.C Hwa" [arXiv:hep-ph/9503400 [hep-ph]].

[213] A. Ayala, J. J. Cobos-Martínez, M. Loewe, M. E. Tejeda-Yeomans and R. Zamora, Phys. Rev. D **91**, no.1, 016007 (2015) [arXiv:1410.6388 [hep-ph]].

[214] A. Bandyopadhyay, B. Karmakar, N. Haque and M. G. Mustafa, Phys. Rev. D **100**, no.3, 034031 (2019) [arXiv:1702.02875 [hep-ph]].

[215] N. Haque, Phys. Rev. D **96**, no.1, 014019 (2017) [arXiv:1704.05833 [hep-ph]].

[216] E. Braaten, R. D. Pisarski and T. C. Yuan, Phys. Rev. Lett. **64**, 2242 (1990)

[217] J. Frenkel and J. C. Taylor, Nucl. Phys. B **334**, 199-216 (1990)

[218] P. Chakraborty, M. G. Mustafa and M. H. Thoma, Eur. Phys. J. C **23**, 591-596 (2002) [arXiv:hep-ph/0111022 [hep-ph]].

[219] F. Karsch, M. G. Mustafa and M. H. Thoma, Phys. Lett. B **497**, 249-258 (2001) [arXiv:hep-ph/0007093 [hep-ph]].

[220] C. Y. Wong, "Introduction to high-energy heavy ion collisions,"

[221] N. S. Craigie, Phys. Rept. **47**, 1-108 (1978)

[222] J. Alam, S. Sarkar, P. Roy, T. Hatsuda and B. Sinha, Annals Phys. **286**, 159-248 (2001) [arXiv:hep-ph/9909267 [hep-ph]].

[223] P. Salabura and J. Stroth, [arXiv:2005.14589 [nucl-ex]].

[224] A. Adare *et al.* [PHENIX], Phys. Rev. Lett. **104**, 132301 (2010) [arXiv:0804.4168 [nucl-ex]].

[225] A. Adare *et al.* [PHENIX], Phys. Rev. C **81**, 034911 (2010) [arXiv:0912.0244 [nucl-ex]].

[226] K. Tuchin, Phys. Rev. C **88**, 024910 (2013) [arXiv:1305.0545 [nucl-th]].

[227] N. Sadooghi and F. Taghinavaz, Annals Phys. **376**, 218-253 (2017) [arXiv:1601.04887 [hep-ph]].

[228] A. Bandyopadhyay, C. A. Islam and M. G. Mustafa, Phys. Rev. D **94**, no.11, 114034 (2016) [arXiv:1602.06769 [hep-ph]].

[229] A. Bandyopadhyay and S. Mallik, Phys. Rev. D **95**, no.7, 074019 (2017) [arXiv:1704.01364 [hep-ph]].

[230] S. Ghosh and V. Chandra, Phys. Rev. D **98**, no.7, 076006 (2018) [arXiv:1808.05176 [hep-ph]].

[231] A. Das, N. Haque, M. G. Mustafa and P. K. Roy, Phys. Rev. D **99**, no.9, 094022 (2019) [arXiv:1903.03528 [hep-ph]].

[232] L. D. McLerran and T. Toimela, Phys. Rev. D **31**, 545 (1985)

[233] H. A. Weldon, Phys. Rev. D **42**, 2384-2387 (1990)

[234] C. Greiner, N. Haque, M. G. Mustafa and M. H. Thoma, Phys. Rev. C **83**, 014908 (2011) [arXiv:1010.2169 [hep-ph]].

[235] S. Turbide, C. Gale, D. K. Srivastava and R. J. Fries, Phys. Rev. C **74**, 014903 (2006) [arXiv:hep-ph/0601042 [hep-ph]].

[236] C. A. Islam, A. Bandyopadhyay, P. K. Roy and S. Sarkar, Phys. Rev. D **99**, no.9, 094028 (2019) [arXiv:1812.10380 [hep-ph]].

Thesis Highlight

Name of the Student: Aritra Das
Name of the CI/OCC: Saha Institute of Nuclear Physics **Enrolment No.:**PHYS05201504023
Thesis Title: Effects of magnetic field in heavy-ion collision phenomenology
Discipline: Physical Science **Sub-Area of Discipline:** High Energy Physics Phenomenology in QGP
Date of Viva-Voce: 08.09.2021

In non-central high energy heavy ion collision experiments, a very strong magnetic field (up to 10^{19} Gauss in Large Hadron Collider (LHC) and unto 10^{18} Gauss in RHIC) is generated perpendicular to the reaction plane. This magnetic field gives rise to a lot of novel phenomena like chiral magnetic effects due to axial anomaly, magnetic catalysis, inverse magnetic catalysis, superconductivity of the vacuum and so on. The decay profile of the magnetic field is believed to be rapid with time from some of the studies, whereas others suggest a comparatively slow decay owing to the high electrical conductivity in the produced medium. So with time the magnetic field gets weak

When fermions traverse through hot-magnetised de-confined medium, their dispersion relations get modified or get “dressed”due to its interaction with the constituents of the medium. Now the modes of any propagating particles are obtained from quantum loop corrected effective propagator. In the first part of the thesis, the one loop effective propagator in presence of weak background magnetic field have been computed. The one loop quantum correction has been invoked through one loop quark self energy. In computing quark self energy, we have used hard thermal loop(HTL) approximation. In this approximation, the external momentum is taken as soft (i.e. of the order of gT) and the loop momentum is taken as hard (of the order of T). We have also assumed that the magnetic field is sufficiently weak. In the presence of the magnetic field the momentum component transverse to the magnetic field is quantised into different landau levels. The prime observation reported in the first part of the thesis is the emergence of four quasi-quark modes from the pole of the effective quark propagator in the weak field limit. Using the effective quark propagator, the fermion dispersion relation in a hot magnetised medium have been analysed. Apart from this, the transformation properties of the effective propagator under some of the discrete symmetries, the spinor solution of the one loop modified Dirac equation describing these dressed quark modes have also been examined in this work. The fermion spectra is found to reflect the discrete symmetries of the two-point functions.

It is well known that dileptons (lepton anti-lepton) act as a good indirect probe of QGP medium since it interacts only electromagnetically. Dileptons are produced at all stages in the evolution of the fireball throughout the entire volume and come out of the fireball with minimal final state interactions. As a result of this, they carry vital informations about the formation and evolution of the de confined medium. Owing to the presence of magnetic field in QGP phase, the dilepton spectrum is believed to be influenced. In the second part of the thesis, the production rate of hard dilepton is calculated in presence of weakly magnetised media. It consists of rates when all four quasi-quarks, originating from the poles of the propagator as computed in the first part of this thesis, individually annihilate with a bare quark to produce a virtual photon which eventually decays into lepton-antilepton pairs. Besides these, there are also contributions to dilepton production rate from the decay of quasi-quarks. In the weak field approximation, the magnetic field appears as a perturbative correction to the thermal contribution.